

Biophysical characterization of the mineral composition of seeds with varying genetic background including transgenic sorghum with reduced amounts of the storage protein kafirin

by

Roya Janeen Ndimba



Dissertation presented for the degree of
Doctor of Philosophy (Science)

at

Stellenbosch University

Institute for Plant Biotechnology, Faculty of Science

Supervisor: Prof Jens Kossmann

Co-supervisor: Dr Carlos Pineda-Vargas

December 2017

Declaration

By submitting this dissertation electronically, I declare that the entirety of the work contained therein is my own, original work, that I am the sole author thereof (save to the extent explicitly otherwise stated) that reproduction and publication thereof by Stellenbosch University will not infringe any third party rights and that I have not previously in its entirety or in part submitted it for obtaining any qualification.

Date: December 2017

Abstract

Cereals are globally recognised as a cornerstone of human nutrition, and as a result play a pivotal role in efforts to address food insecurity and malnutrition. In Africa, the highest rates of hunger and malnutrition are evident, which is often due to an over-reliance on cereals as a principal source of nutrition. To address this problem, biofortification strategies are currently underway which aim to produce improved cereal crops, particularly with enhanced grain protein and mineral nutritional profiles. Two important African cereals that have been included in such biofortification programmes are sorghum (*Sorghum bicolor* (L.) Moench) and pearl millet (*Pennisetum glaucum* (L.) R. Br.). Sorghum and millets have served as important staples for centuries, and are extensively relied on by millions of the world's poor, for nutritional sustenance, particularly in drought prone areas. Unfortunately, these grains are often nutritionally deficient in terms of their protein and/or mineral qualities, thus there is a need to produce biofortified sorghum and pearl millet.

In this study, biofortified sorghum (produced via genetic engineering) (Part 1) and biofortified pearl millet grains (produced via conventional plant breeding) (Part 2) were examined in order to assess the effect that biofortification process has had on the composition and other important quality characteristics of the grain. In the case of the genetically engineered sorghum, several independent transgenic lines, produced using RNA interference (RNAi) to suppress different subsets of kafirins were assessed in comparison to the wild-type progenitor to reveal if any unwanted changes occurred in the physico-chemical characteristics of the grain, apart from the intended change in the targeted protein profile. To carry out this comparison, an assessment of several key physical and biochemical parameters of the transgenic versus the wild-type grain were carried out. Using one way analysis of variance (ANOVA) important differences in grain weight, density, endosperm texture and lysine content were found. Ultrastructural analysis of the protein bodies of all the sorghum genotypes, using transmission electron microscopy (TEM), revealed some important differences in morphology. Kafirin suppression was confirmed in all the transgenic lines using one dimensional sodium dodecyl sulphate-polyacrylamide gel electrophoresis (1D SDS-PAGE), as well as a compensatory synthesis of other grain proteins in the fractionated protein profile. Identification of some of the compensatory proteins was done using nanoflow liquid chromatography matrix-assisted laser desorption/ionization mass spectrometry (Nano-LC/MALDI-MS). Lastly, an analysis of the mineral content in bulk (by Inductively Coupled Plasma – Atomic Emission Spectrometry (ICP-AES) and by Inductively Coupled Plasma – Mass Spectrometry (ICP-MS); and within the grain tissue, by particle induced X-ray emission with a microfocused beam (micro-PIXE), was carried out. Elemental mapping of the grain tissue, using micro-PIXE, demonstrated a significant decrease in Zn (>75%), which was localised to the outer endosperm region. In conclusion, the results of these experiments have been instrumental in highlighting important similarities and differences between the transgenic and non-transgenic sorghum, which have implications for the further development of these protein biofortified lines for enhanced nutrition.

In the second section of the work, papers are presented on work done on the elemental mapping of pearl millet cultivars involved in mineral biofortification efforts.

In the first paper, a general overview of the use of micro-PIXE to study the distribution of minerals in pearl millet is presented. Micro-PIXE was used to map the distribution of several nutritionally important minerals found in the grain tissue of two cultivars of pearl millet (*Pennisetum glaucum* (L.) R. Br.). The distribution maps revealed that the predominant localisation of minerals was within the germ (consisting of the scutellum and embryo) and the outer grain layers (specifically the

pericarp and aleurone); whilst the bulk of the endosperm tissue featured relatively low concentrations of the surveyed minerals. Within the germ, the scutellum was revealed as a major storage tissue for phosphorus (P) and potassium (K), whilst calcium (Ca), manganese (Mn) and zinc (Zn) were more prominent within the embryo. Iron (Fe) was revealed to have a distinctive distribution pattern, confined to the dorsal end of the scutellum; but was also highly concentrated in the outer grain layers. Interestingly, the hilar region was also revealed as a site of high accumulation of minerals, particularly for sulphur (S), Ca, Mn, Fe and Zn, which may be part of a defensive strategy against infection or damage.

In the second paper, the use of micro-PIXE to study differential mineral accumulation in two contrasting pearl millet genotypes is presented. Using micro-PIXE fully elemental maps were generated for each of the contrasting grain types, allowing for a comparison of the spatial distribution patterns and tissue-specific concentrations of several important minerals such as K, Ca, Fe and Zn. In the case of the high Fe/Zn phenotype, micro-PIXE analysis confirmed an approximate two-fold increase in Fe and Zn levels in both the grain endosperm and seed coat region, in comparison to the low Fe/Zn phenotype. These studies serve to highlight the utility of the micro-PIXE technique for localising and quantifying in-tissue concentration levels of important dietary minerals, such as Fe and Zn.

The presented work therefore gives several new insights into the intended and perhaps non-intended differences that can result from the biofortification of cereals grains. This information can be of some benefit to the continued effort by plant scientists to improve the nutritional quality of the important staple foods that sustain millions of the world's most poor and marginalised people.

Opsomming

Graangewasse word wêreldwyd erken as 'n hoeksteen van menslike voeding en speel gevolglik 'n sentrale rol wanneer dit kom by die aanspreek van voedselonsekerheid en wanvoeding. Die hoogste vlakke van honger en wanvoeding kom in Afrika voor, in baie gevalle as gevolg van 'n oor-afhanklikheid op graangewasse as vernaamste bron van voeding. Om hierdie probleem aan te spreek, word biofortifiseringstrategieë tans onderneem met die doel om verbeterde graangewasse te produseer, veral met verhoogde graanproteïen- en mineraalvoedingsprofiel. Twee belangrike Afrika-grane wat in sulke biofortifiseringsprogramme ingesluit is, is sorghum (*Sorghum bicolor* (L.) Moench) en pêrlmanna (*Pennisetum glaucum* (L.) R. Br.). Sorghum en manna dien reeds vir eeue as belangrike stapels en word deur miljoene van die wêreld se armes gebruik as kos, veral in gebiede wat geneig is tot droogte. Hierdie grane skiet egter in baie gevalle tekort in terme van hulle proteïen- en of mineraalgehalte, en dus is daar 'n behoefte aan die produksie van biofortifiseerde sorghum en pêrlmanna.

In hierdie studie is biofortifiseerde sorghum (geproduseer deur genetiese manipulasie) (Deel 1) en biofortifiseerde pêrlmannagrane (geproduseer deur konvensionele planteteelt) (Deel 2) ondersoek om die effek van die biofortifiseringsproses op die samestelling en ander belangrike gehaltekenmerke van die graan te assesser.

In die geval van geneties gemodifiseerde sorghum is verskeie onafhanklike transgeniese lyne wat deur die gebruik van RNA steuring (*RNA interference* – RNAi) geproduseer is om verskillende substelle van kafiriene te onderdruk, geassesseer in vergelyking met die wilde tipe stamvader om uit te vind of enige ongewenste veranderinge in die fisies-chemiese kenmerke van die graan plaasgevind het, buiten die bedoelde verandering in die geteikende proteïenprofiel. Om hierdie vergelyking uit te voer, is 'n assessering van verskeie belangrike fisiese en biochemiese parameters van die transgeniese teenoor die wilde tipe graan uitgevoer. Met gebruik van eenrigting variansie-analise (ANOVA) is belangrike verskille in graangewig, -digtheid, endospermtektuur en lisiengehalte gevind. Ultrastrukturele analise van die proteïenliggaampies van al die sorghum-genotipes m.b.v. TEM het 'n paar belangrike verskille in morfologie getoon. Kafiriën-onderdrukking is in al die transgeniese lyne met behulp van eendimensionele SDS PAGE bevestig, asook 'n kompensatoriese sintese van ander graanproteïene in die gefraksioneerde proteïenprofiel. Die identifisering van sommige van die kompenserende proteïene is gedoen met nano-LC MALDI massa spektrometrie. Laastens is 'n analise van die mineraalinhoud in grootmaat (deur ICP) en binne die graanweefsel deur mikro-PIXE uitgevoer. Elementale kartering van die graanweefsel, met gebruik van mikro-PIXE, het 'n noemenswaardige afname in Zn (> 75%) getoon wat in die buitenste endospermstreek gelokaliseer is. Ten slotte, die resultate van hierdie twee eksperimente was instrumenteel in die uitlig van belangrike ooreenkomste en verskille tussen die transgeniese en nie-transgeniese sorghum wat belangrike implikasies het vir die verdere ontwikkeling van hierdie proteïen-biofortifiseerde lyne vir verhoogde voeding.

In die tweede deel van die werk is voorleggings gedoen oor werk op die elementale kartering van pèrlmannakultivars betrokke in pogings tot minerale biofortifisering.

In die eerste voorlegging word 'n algemene oorsig aangebied van die gebruik van mikro-PIXE om die verspreiding van minerale in pèrlmanna te bestudeer. Mikro-proton geïnduseerde X-straal uitstraling (mikro-PIXE) is gebruik om die verspreiding van verskeie minerale van voedingsbelang te karteer wat in die graanweefsel van die twee kultivars van pèrlmanna (*Pennisetum glaucum* (L.) R. Br.) gevind is. Die verspreidingskaarte toon dat die oorheersende lokalisering van minerale binne die kiem (bestaande uit die saadlob en vrug) en die buitenste graanlae (spesifiek die perikarp en aleuroon) was; terwyl die meeste van die endospermweefsel redelike lae konsentrasies van die ondersoekte minerale bevat het. Binne die kiem is die saadlob gevind om die vernaamste stoorweefsel vir P en K te wees, terwyl Ca, Mn en Zn meer prominent in die vrug was. Fe het 'n kenmerkende verspreidingspatroon gehad, en is beperk tot die dorsale kant van die saadlob, maar dit was ook baie gekonsentreerd in die buitenste lae van die graan. Van belang is dat dit na vore gekom het dat die omgewing van die naeltjie (*hilar region*) 'n ligging was vir 'n groot akkumulاسie van minerale, veral S, Ca, Mn, Fe en Zn, wat moontlik deel is van 'n verdedigingstrategie teen besmetting of skade.

In die tweede voorlegging word die gebruik van mikro-PIXE om differensiële mineraalophoping in twee kontrasterende pèrlmanna-genotipes te bestudeer, aangebied. Met gebruik van mikro-PIXE is volledig kwantitatiewe elementkaarte vir elk van die kontrasterende graantipes gegenereer, wat dit moontlik gemaak het om die ruimtelike verspreidingspatrone en weefsel-spesifieke konsentrasies van verskeie belangrike minerale, soos K, Ca, Fe en Zn, te vergelyk. In die geval van die hoë Fe/Zn fenotipe het kwantitatiewe mikro-PIXE analyses 'n ongeveer tweevoudige verhoging in Fe- en Zn-vlakke in beide die endosperm en saadhuud gebied bevestig, in vergelyking met die lae Fe/Zn fenotipe. Hierdie studies dien om die bruikbaarheid van die mikro-PIXE tegniek vir die lokalisering en kwantifisering van in-weefsel konsentrasievlakke van belangrike dieetminerale, soos Fe en Zn, te beklemtoon.

Die werk wat hier aangebied word, verskaf verskeie nuwe insigte in die bedoelde en dalk onbedoelde verskille wat kan voortspruit uit die biofortifisering van graankorrels. Hierdie inligting kan van waarde wees vir die voortgesette poging deur plantwetenskaplikes om die voedingswaarde te verbeter van belangrike soorte stapelvoedsel wat miljoene van die wêreld se armste en mees gemarginaliseerde mense onderhou.

Dedication

This dissertation is dedicated to

My Parents & Grandparents

and

My children, James & MaLisa

“You may encounter many defeats but you must not be defeated. In fact, the encountering may be the very experience which creates the vitality and the power to endure.”

– Maya Angelou

Biographical sketch

Roya Ndimba is a native of the Commonwealth of the Bahamas, who studied for a BSc (Hons) degree in Natural Science, at the University of Durham in England from 1996-1999. She later took up teacher training and completed an MSc-degree in Biotechnology at the University of Teesside, Middlesborough, UK in 2004. She relocated to Cape Town South Africa in 2006 and started working at iThemba LABS in 2007. She is currently employed at the Materials Research Dept, iThemba LABS, working on the application of ion beam analysis techniques such as micro-PIXE for elemental mapping of key minerals in biofortified African seeds and grains.

Acknowledgements

I wish to express my sincere gratitude and appreciation to the following persons and institutions:

NRF: iThemba LABS for funding and continuous support throughout the study period. A special word of thanks is particularly given to Prof C Pineda-Vargas, Dr C Mtshali and the MRD accelerator operators for all the help and advice given during the micro-PIXE measurements.

University of Stellenbosch, Institute for Plant Biotechnology. Many thanks to Prof J Kossmann for accepting my study proposal and for providing much support for several aspects of this research. Special thanks is also extended to Dr S Peters for his assistance during my oral defence and for attending to all the administrative duties related to this process.

Sincere appreciation is also extended to C Van Heerden and the RNA sequencing team, at Stellenbosch University, Your time and efforts to assist me are warmly acknowledged.

Much appreciation is also extended to Ms K Vergeer, from the Faculty of AgriSciences, Stellenbosch University who was particularly kind and gracious with her time – and offered much practical assistance with the rigours involved in the final compilation of this dissertation, in accordance with Faculty requirements.

University of the Western Cape, Plant Omics Laboratory. Sincere thanks to Prof BK Ndimba, Dr A Klein, Mr A Nkomo, Mrs G Mohammed and Prof N Ludidi for allowing me to access your lab facilities and providing all the necessary assistance I needed for the protein gel work.

Council for Scientific and Industrial Research (CSIR). The input and support of Dr L Mehlo and his entire team involved in the African Biofortified Sorghum Project is gratefully acknowledged. Without your help to access the RNAi sorghum grain lines, this project would not have been successful.

Thank you to the Agricultural Research Council (ARC) for funding and assistance related to this project.

A special word of thanks is also extended to Prof A Barnabas (MRD, iThemba LABS) for his kind assistance and helpful mentorship in all aspects of the microscopy work; and to Mr M Jaffer (UCT, Physics) for his assistance with TEM analysis.

Sincere thanks to Dr J Kruger and Prof JRN Taylor, at the University of Pretoria, for their input and collaborative efforts concerning the elemental mapping of the pearl millet grains.

Many thanks to all my family and friends for their unwavering support throughout the study, especially, Dr M Khenfouch, Dr A Guesmia, Dr K Cloete, Mnr J Crafford, Sr E Jans van Rensberg and Dr R Nemutudi. Your words of encouragement really helped, when the days were darkest, and hope was nearly lost.

Lastly, to my Creator, without Your sustaining grace, I would not have made it through...Nothing is impossible, with the help of the Almighty. Thank you.

Table of Contents

Declaration	i.
Abstract	ii.
Opsomming	iv
Acknowledgements	viii
List of Abbreviations	xiii
List of Figures	xvi
List of Tables	xviii
Chapter 1. General Introduction	1
<hr/>	
1.1 The need for biofortified millets	1
1.2 Literature review I: Biofortified Sorghum and Pearl Millet	5
1.2.1 The major millets: sorghum and pearl millet	5
1.2.2 Introduction to sorghum - Origin and taxonomy	6
1.2.2.1 Sorghum growth and adaptive characteristics	6
1.2.2.2 Sorghum production and utilisation	8
1.2.2.3 Sorghum Grain – Structure	9
1.2.3 Introduction to pearl millet - Origin and taxonomy	12
1.2.3.1 Pearl millet growth and adaptive characteristics	13
1.2.3.2 Pearl millet production and utilisation	14
1.2.3.3 Pearl Millet Grain – Structure	15
1.2.4 Nutritional Composition of Sorghum and Pearl Millet Grain	17
1.2.4.1 Carbohydrates	17
1.2.4.2 Proteins	17
1.2.4.3 Fat	19
1.2.4.4 Ash	19
1.2.5 Anti-nutritional Factors in Sorghum and Pearl Millet Grain	20
1.2.5.1 Phytate	21
1.2.5.2 Phenolic compounds	22
1.2.6 The need for protein biofortified sorghum	24
1.2.6.1 Kafirin Subclasses	25
1.2.6.2 Kafirins and Protein Digestibility	25
1.2.6.3 Modifying the Protein Body	27
1.2.7 The need for mineral biofortified pearl millet	28
1.3 Study aims and research objectives	30
1.4 Dissertation organisation	31
References	32

Chapter 2. An introduction to Particle Induced X-ray Emission (PIXE) and other major analytical techniques used in this study **44**

2.1	Introduction to PIXE	44
2.1.1	Physics principles underpinning PIXE	45
2.1.2	The nuclear microprobe at iThemba LABS	47
2.1.3	Proton backscattering spectrometry (BS)	51
2.1.4	Preparation of biological samples for micro-PIXE analysis	52
2.1.5	Micro-PIXE applied to the study of mineral distribution in Millets	52
2.1.6	Advantages of the micro-PIXE method	53
2.2	Bulk Mineral Analysis by ICP-AES/MS	55
2.3	Other techniques	57
2.3.1	Sodium dodecyl sulphate-polyacrylamide gel electrophoresis (SDS-PAGE) and mass spectrometry	57
2.3.2	Transmission electron microscopy	59
2.3.3	Amino acid analysis	60
	References	61

Chapter 3. A comparative study of selected physical and biochemical traits of wildtype and transgenic sorghum to reveal differences relevant to grain quality **69**

	Abstract	69
3.1	Introduction	70
3.2	Materials and methods	73
3.2.1	Plant materials	73
3.2.2	Grain samples	74
3.2.3	Kafirin protein extraction and electrophoretic separation	75
3.2.4	Physical characteristics	76
3.2.4.1	Kernel weight	76
3.2.4.2	Grain Hardness	76
3.2.4.3	Protein Body Morphology	76
3.2.5	Biochemical characteristics	77
3.2.5.1	Amino Acid composition	77
3.2.6	Statistical Analysis	77
3.3	Results and discussion	77
3.3.1	SDS PAGE analysis of kafirin extracts	77
3.3.2	Differences in the Physical traits of the transgenic vs WT grains	81
3.3.2.1	Kernel weight and grain hardness	81
3.3.2.2	Protein body morphology	84
3.3.3	Differences in the biochemical traits of the transgenic vs WT grains	86
3.3.3.1	Amino acid analysis	86
3.4	Conclusion	90
	References	91
	Appendix: Publication	96

Chapter 4. A comparative evaluation of changes in the protein profile and the elemental composition of wild-type versus transgenic sorghum grain 104

4.1	Introduction	104
4.2	Materials and methods	105
4.2.1	Plant material	105
4.2.2	Protein extraction	105
4.2.3	One dimensional sodium dodecyl sulphate polyacrylamide gel electrophoresis (1D SDS-PAGE)	106
4.2.4	Mass fingerprinting for protein identification of isolated protein bands	106
4.2.5	Bulk mineral analysis using ICP-AES/MS	107
4.2.5.1	Sample preparation for ICP-AES/MS	107
4.2.5.2	ICP-AES/MS Analytical Procedure	108
4.2.6	Micro-PIXE analysis	109
4.2.6.1	Sample preparation for micro-PIXE	109
4.2.6.2	Micro-PIXE Analytical Procedure	109
4.2.7	Statistical Analysis	110
4.3	Results and discussion	110
4.3.1	1D SDS-PAGE and protein identification	110
4.3.2	Grain mineral composition by ICP-AES/MS	114
4.3.2.1	Bulk analysis of the Essential Major Elements	114
4.3.2.2	Bulk Analysis of the Essential Trace and Ultra-trace Elements	118
4.3.2.3	The Non-essential or Potentially Toxic Elements	119
4.3.3	Micro-PIXE analysis	120
4.4	Conclusion	129
	References	130

Chapter 5. A preliminary report of the use of RNA-seq to examine changes in the gene expression profile of wild-type versus transgenic sorghum grain 133

5.1	Introduction	133
5.1.1	Background to RNA-seq	134
5.2.	Materials and methods	135
5.2.1	Plant tissue collection	135
5.2.2	Total RNA extraction	135
5.2.3	Library construction and sequencing	137
5.3	Results and discussion	137
5.4	Conclusion	143
	References	144

Chapter 6. Micro-PIXE mapping of mineral distribution in mature grain of two pearl millet cultivars 146

Research article accepted and published in Nuclear Instruments and Methods in Physics Research B Journal

Chapter 7. A comparative study of tissue-specific differences in the mineral content of biofortified and conventional pearl millet grain using micro-PIXE analysis	153
7.1 Introduction	153
7.2 Materials and methods	155
7.2.1 Plant material	155
7.2.2 Analysis of the bulk mineral content	155
7.2.3 Sample preparation for micro-PIXE analysis	155
7.2.4 Micro-PIXE analysis	155
7.3 Results and discussion	156
7.4 Conclusion	163
References	163
Chapter 8. Summary and Future work	166
8.1 Biofortified Pearl Millet	166
8.2 Protein Biofortified Sorghum	167
References	170
APPENDIX A	
List of Peer-Reviewed published research outputs	171
APPENDIX B	
RNA-seq list of differentially expressed genes	172

LIST OF ABBREVIATIONS, ACRONYMS AND SYMBOLS

%	Percentage
°C	Degrees Celsius
α	Alpha
β	Beta
δ	Delta
γ	Gamma
μC	microCoulomb
$\mu\text{E}/\text{m}^2$	microeinstains per second per square meter
μg	Micrograms
μm	Micrometre
μL	Microlitre
1D	One-dimensional
ABS	Africa Biofortified Sorghum
ANFs	Anti-nutritional factors
ANOVA	Analysis of variance
Ba	Barium
Be	Beryllium
β -ME	β -mercaptoethanol
BS	Backscattering spectrometry
BSA	Bovine serum albumin
C	Carbon
Ca	Calcium
Cd	Cadmium
Co	Cobalt
Cr	Chromium
CSIR	Centre for Scientific and Industrial Research
Cu	Copper
Da	Dalton
DA	Dynamic analysis
DNA	Deoxyribonucleic acid
EDX	Energy dispersive X-ray
e.g.	<i>exempli gratia</i> (for example)
eV	Electronvolt
ER	Endoplasmic reticulum
<i>et al.</i>	<i>et alii</i> (and others)
FAO	Food and Agricultural Organisation
Fe	Iron
g	Gram
GE	Genetic engineering
GM	Genetically modified
h	Hour
H	Hydrogen
ha	Hectares
He	Helium
ICP-AES	Inductively coupled plasma-atomic emission spectrometry

ICP-MS	Inductively coupled plasma-mass spectrometry
ICP-OES	Inductively coupled plasma-optical emission spectrometry
ICRISAT	International Crops Research Institute for the Semi-Arid Tropics
i.e.	<i>id est</i> (that is)
K	Potassium
kDa	Kilodalton
kg	Kilogram
kg/ha	Kilograms per hectare
kV	Kilovolts
m	Metres
M	Molar
MALDI ToF	Matrix-assisted laser desorption/ionisation time-of-flight
Mbp	Million base pairs
MDL	Minimum detection limit
MeV	Mega electron Volts
mg	Milligram
mg/kg	Millogram per kilogram
Mg	Magnesium
micro-PIXE	Microbeam particle/proton induced X-ray Emission
min	Minute
mL	Millilitre
mm	Millimetre
mM	Millimolar
MV	Mega Volt
Mn	Manganese
Mo	Molybdenum
ms	Millisecond
MS	Mass spectrometry
M_w	Molecular weight
n	Number of samples
N	Nitrogen
Na	Sodium
Ni	Nickel
NIST	National Institute of Standards and Technology
nm	Nanometre
NMP	Nuclear microprobe
O	Oxygen
pA	picoAmps
P	Phosphorus
PAGE	Polyacrylamide gel electrophoresis
Pb	Lead
PEM	Protein Energy Malnutrition
PIXE	Particle/proton- Induced X-ray Emission
ppm	Parts per million
rpm	Rotations per minute
RNA	Ribonucleic acid
RNAi	RNA interference

RNA-seq	RNA sequencing
RP HPLC	Reverse-phase high performance liquid chromatography
s	Seconds
S	Sulphur
SAGL	South African Grain Laboratory
SD	Standard deviation
SDS	Sodium dodecyl sulphate
Se	Selenium
SEM	Scanning electron microscopy
Si	Silicon
Si(Li)	Silicon-Lithium
t	Tonnes
TEM	Transmission electron microscopy
TCEP	Tris (2-carboxyethyl)phosphine
TFA	trifluoroacetic acid
U	Uranium
USA	United States of America
v/v	Volume per volume
VDG	Van de Graaff
w/v	Weight per volume
WT	Wild-type
Zn	Zinc

LIST OF FIGURES

Figure 1.1	Diagrammatic depiction of a longitudinal section through a sorghum grain	10
Figure 1.2	Diagrammatic depiction of a longitudinal section through a pearl millet grain	16
Figure 1.3	Chemical structure of the phytic acid molecule	22
Figure 2.1	A schematic diagram of the Bohr model of an atom	46
Figure 2.2	An illustration of the basic principle of PIXE (A) and a representation of characteristic X-ray transitions (B)	46
Figure 2.3	Schematic diagram of the physical layout of the Van de Graaff accelerator	49
Figure 2.4	A photograph (A) of the NMP end station and (B) the inside of the NMP experimental chamber	50
Figure 2.5	An illustration of the basic steps involved in the separation of complex protein mixtures by denaturing SDS-PAGE	58
Figure 3.1	Sorghum plants (transgenic and control) being grown in the containment glasshouse at CSIR, Pretoria.	74
Figure 3.2	1D SDS-PAGE of alcohol soluble grain proteins from WT and transgenic wholegrain flour samples.	79
Figure 3.3	1D SDS-PAGE of kafirin proteins from sorghum flour (El Nour <i>et al.</i> , 1989)	80
Figure 3.4	A comparison of 100-kernel weight (A), % floaters (B), and % floury endosperm types (C) between wild-type and transgenic sorghum genotypes	83
Figure 3.5	Representative TEM images of protein bodies in the subaleurone layer of the wild-type and transgenic sorghum lines	85
Figure 4.1	Main fractions of sorghum grain proteins separated by 1D SDS-PAGE	111
Figure 4.2	A halved sorghum grain prepared for micro-PIXE analysis	120
Figure 4.3	Representative micro-PIXE element maps of wild-type and transgenic sorghum grains	122

LIST OF FIGURES, continued

Figure 4.4	Typical S distribution maps of the scanned area of the grain samples used for micro-PIXE analysis. Two main regions highlighted for region selection analysis	123
Figure 4.5	An example of the linear traverse projection rectangle used to extract concentration data spanning the regions of the grain demarcated in green	126
Figure 4.6	X-Y plots of average potassium and zinc concentration data as determined from the applied quantitative linear traverse tool in GeoPIXE	127
Figure 4.7	Schematic of typical cereal grain outer layers (left) and semi-thin resin-embedded section of sorghum (right) stained with Coomassie brilliant blue	128
Figure 5.1	An overview of the laboratory processes involved in RNA-seq analysis (A) and the subsequent data analysis pipeline (B)	134
Figure 5.2	Electrophoretic trace of total RNA extracted from immature sorghum grain samples	136
Figure 5.3	Bar chart showing the total number of differentially expressed transcripts with a false discovery rate (FDR) < 0.05 and fold change ≥ 2 or ≤ -2 , identified using RNA-seq analysis	138
Figure 7.1	Optical micrographs showing the basic morphology of bi-sectioned pearl millet grains prepared for micro-PIXE	158
Figure 7.2	Areas encircled in green represent the regions chosen for region selection analysis using GeoPIXE software. In panel A, the outer parts of the grain are encircled in green to represent the bran region. In panel B as much of the inner core of the grain endosperm is encircled to extract concentration data specific to the endosperm tissue	159
Figure 7.3	Micro-PIXE elemental maps of P, S, Zn and Fe distribution in pearl millet grain	160
Figure 7.4	Mineral element concentrations derived from region selection analysis of micro-PIXE mapping data of the grain bran layers (A) and (B) endosperm tissue of two pearl millet varieties	162

LIST OF TABLES

Table 1.1	Area, production and yield of sorghum in major producing countries	9
Table 1.2	Area, production and yield of pearl millet in major producing countries	14
Table 1.3	A comparison of the typical proximate and mineral composition of sorghum and pearl millet grains	20
Table 2.1	Comparison of the key analytical characteristics of X-ray based elemental mapping techniques	54
Table 3.1	A comparison of the protein-bound amino acid content of the wild-type and transgenic sorghum genotypes	87
Table 3.2	Detection limits calculated for each amino acid quantified by the Pico-Tag Method	89
Table 4.1	List of proteins identified from bands 1-5 in Figure 4.1	112
Table 4.2	Essential major elements in sorghum wholegrain samples	115
Table 4.3	Essential trace and ultra-trace elements found in sorghum wholegrain samples	116
Table 4.4	Non-essential trace and ultra-trace elements found in sorghum wholegrain samples	117
Table 4.5	Average concentrations (mg/kg) of P, K, S, Ca, Fe and Zn, as determined by region selection analysis of micro-PIXE data using GeoPIXE	125
Table 5.1	RNA yield and quality as assessed by the Agilent 2100 Bioanalyser	137
Table 5.2	Total number of reads and percentage of aligned reads for each sample for the RNA-seq experiment	139
Table 5.3	RNA-seq analysis data pertaining to the three kafirin genes targeted for suppression by RNAi in transgenic line 44-3.	139
Table 5.4	Top up-regulated genes in transgenic sorghum versus wild-type, identified by RNA-seq and assigned functional descriptions using the Morokoshi transcriptome database	140
Table 5.5	Top down-regulated genes in transgenic sorghum versus wild-type, identified by RNA-seq and assigned functional descriptions using the Morokoshi transcriptome database	141

LIST OF TABLES, continued

Table 7.1	Concentrations of the indicated minerals in wholegrain samples of two varieties of pearl millet.	157
-----------	--	-----

CHAPTER 1

General Introduction

1.1 The need for biofortified millets

According to recent estimates, the world's population is expected to rise from its current level of 7.1 billion people to over 9 billion by the year 2050 (United Nations, 2015). With nearly a third more mouths to feed, it is predicted that food production must increase by at least 70% over the next three decades (Gardner, 2013). In Sub-Saharan Africa, the need for increased food production is particularly critical as this region features the world's highest rates of population growth, but has consistently failed to increase per capita food output since the 1970s (Gardner, 2013). As a result, Sub-Saharan Africa has the highest proportion of undernourished people in the world, with as many as one in four Africans qualifying as chronically starved (FAO, 2015; Akombi *et al.*, 2017).

Although there many diverse socio-economic and political factors which contribute to chronic food shortages in Africa, a hostile climate is also known to play a major contributory role (Bain *et al.*, 2013). Africa is the only continent that straddles both tropics, and as such, it is characterised by a range of climatic conditions that are often highly limiting to agricultural productivity. Most notably, these conditions include periods of intense heat, erratic rainfall, unpredictable weather and nutrient-deprived soils (O'Kennedy *et al.*, 2006). Unfortunately, under the spectre of climate change, these conditions are predicted to become more severe (Masih *et al.*, 2014), as may be evidenced by the current drought crisis gripping the Sahel and Southern Africa, which is reportedly the worst experienced in decades (Akwei, 2017). Against this backdrop, stakeholders in the agricultural sector are keen to develop climate-resilient crop systems that will serve the current and future demands of a growing African population. As a result, renewed interest has been piqued in several of Africa's indigenous food crops, in particular, the millets (Sambo, 2014).

Millets are a group of highly diverse small-seeded grasses that belong to the Poaceae family, and are typically grown in the semi-arid and arid parts of Africa and Asia (Rajendrakumar, 2017). Millets are often the only crops that can survive under the harsh environmental conditions found in these regions. They can be grown at different elevations, ranging from sea level up to 3000 metres; and can further tolerate a range of unfavourable soil conditions, including acid, alkaline or saline soils (Aruna Reddy, 2017).

The millets are particularly favoured for their capacity to survive and yield grain under conditions of drought and extreme heat stress (Aruna Reddy, 2017). Amongst the cereals, millets are the only group that can survive in arid areas receiving as low as 300 mm annual rainfall (Rai *et al.*, 1999). Due to the anticipated increase in the occurrence of drought and heat stress, as a result of climate change, it is estimated that as much as 40% of the land currently used to produce maize in Sub-Saharan Africa, will no longer be able to support this crop by 2030 (Aruna Reddy, 2017). Given that maize is presently the dominant cereal food grain in Africa, there is a clear need to refocus efforts on the cultivation and improvement of millets as a superior food security crop.

The term millet is not specific to a taxonomic group, but is rather a functional or agronomic classification of a range of small-seed grass species that are grown primarily for their grain or as fodder (Aruna Reddy, 2017). The major millets are sorghum (*Sorghum bicolor* (L.) Moench) and pearl millet (*Pennisetum glaucum* (L.) R. Br.), which are respectively ranked as the world's fifth and sixth most important cereal crops under cultivation (Aruna Reddy, 2017). The minor millets are collectively ranked as the seventh most important cereals, and are comprised of eight other crop species, namely finger millet (*Eleusine coracana*), foxtail millet (*Setaria italica*), proso millet (*Panicum miliaceum*), kodo millet (*Paspalum scrobiculatum*), little millet (*Panicum miliare*), barnyard millet (*Echinochloa frumentacea*), fonio (*Digitaria exilis*) and teff (*Eragrostis tef*) (Aruna Reddy, 2017). Commonly, sorghum is distinguished from all other millets and is produced on 45 million hectares worldwide, whereas the other millets are produced on around 31 million hectares (FAO, 2014). It is reported that the millets provide a major source of energy and protein for about 1 billion people across the semi-arid parts of Africa and Asia (Belton and Taylor, 2004).

Populations that are most reliant on the millets, tend to be the rural poor who grow these crops to meet their basic subsistence needs. Unfortunately, a monotonous cereal-based diet can lead to malnutrition due to several nutritional shortcomings associated with the grain. Of significance, staple cereals tend to be constrained in terms of their overall protein quality and micronutrient content (O'Kennedy *et al.*, 2006). As a result, people that are heavily dependent on the grains of staple cereals for sustenance tend to suffer from maladies related to protein energy malnutrition (PEM) and/or micronutrient deficiency (Shivran, 2016). To address this problem, concerted global efforts have been directed towards an improvement in the protein quality and micronutrient value of several of the staple cereal food grains, by means of biofortification (Goudia and Hash, 2015).

According to Bouis *et al.*, (2011) biofortification refers to the process of increasing the content and/or bioavailability of essential nutrients in crops during plant growth through genetic and agronomic pathways. Agronomic biofortification is generally considered to be the simplest form of biofortification, and is achieved through the use of micronutrient fertilisers, which are applied directly to the soil and/or the leaves of the food crop (de Valena *et al.*, 2017). Essentially, this approach seeks to improve the micronutrient content of foods by optimising the levels of external supply. This strategy, however, will only be a success if deficiencies in the food item are reflective of low levels in the soil environment; and, furthermore, if the micronutrients are being supplied in an accessible form to the crop plant (G3mez-Galera *et al.*, 2010). Thus far, agronomic biofortification has been most effective in the case of the mineral nutrients zinc (Zn) and selenium (Se) (de Valena *et al.*, 2017). In Finland, the use of Se-enriched fertilisers increased cereal crop Se contents by an average of 15-fold (Alfthan *et al.*, 2015). In Africa, the use of Zn-enriched fertilisers increased the Zn concentration in maize, wheat and rice grains by 23%, 7% and 19% respectively (Joy *et al.*, 2015). However, in spite of these successes, the regular use of mineral fertilisers is not viewed as a sustainable option for biofortifying staple food grains, mainly due to the high economic and environmental costs associated with the application of the fertilisers (G3mez-Galera *et al.*, 2010). It is therefore proposed that for the long-term, genetic biofortification offers the most cost-effective and viable solution to the problem of nutrient deficient foods.

Genetic biofortification aims to produce superior plant genotypes that can accumulate optimal levels of essential nutrients in food, by means of plant breeding methods or by genetic engineering techniques (Farr3 *et al.*, 2011). In plant breeding, the desired outcome is achieved through accelerated mutation and forced hybridizations that introgress favourable genes from sexually compatible germplasm (Bai *et al.*, 2011). Although successful, these methods can take an excessive amount of research and development time and, furthermore, are often constrained by the limited genetic variation found within the relevant gene pool (G3mez-Galera *et al.*, 2010). In spite of these hurdles, a number of successful plant breeding programmes have been established, through the *HarvestPlus* International Consortium. Several reports of such programmes include the development of mineral-enriched pearl millet (Rai *et al.*, 2013), rice (Neelamraju *et al.*, 2012), wheat (Calderini and Ortiz-Monasterio, 2003) and maize (Ortiz-Monasterio *et al.*, 2007).

In comparison to plant breeding methods, it is generally agreed that genetic engineering (GE) offers a faster and much simpler route to the development of biofortified food. Within this context, researchers use recombinant DNA technology to improve the levels of important nutrients in the edible parts of the targeted crop plant. Importantly, the recombinant genes used in GE can be derived from any source (including animals and microbes) and, furthermore, can be stacked in the same plant to obtain the simultaneous biofortification of a range of valuable nutrients (Zhu *et al.*, 2007, 2008). As a result, GE is touted as the only technology available that can produce nutritionally complete staple foods (Gómez-Galera *et al.*, 2010). Important recent examples of the genetic engineering approach to biofortification include the work of Naqvi *et al.*, (2009), which significantly increased the amount of carotene, ascorbate and folate in transgenic maize; and the work of Masuda *et al.*, (2008; 2013) which significantly increased the iron content in rice grain using genes involved in mugineic acid biosynthesis and the soybean ferritin gene.

In the case of millets, both genetic and plant breeding techniques have been used to produce biofortified millet grains, with the majority of efforts focused on the development of biofortified sorghum and pearl millet lines (O'Kennedy *et al.*, 2006). In the case of sorghum, the main impetus has been to produce transgenic sorghum with improved protein digestibility and essential amino acid content; whereas for pearl millet, researchers have been focused on its mineral biofortification with improved levels of iron (Fe) and zinc (Zn) mainly via a plant breeding approach (Taylor *et al.*, 2014). Although there are published reports indicating the initial success of these efforts, it is of interest to investigate more fully the intended and perhaps non-intended effects that biofortification may have had on certain quality characteristics of the targeted grains. In the case of the transgenic biofortified sorghum, it is of interest to know if the genetic modification has had other unexpected or unintended effects on the grain characteristics that may be of biological or nutritional importance. Additionally, in the case of the mineral biofortified pearl millet, it is important to interrogate if the intended enrichment of minerals is localised within the most nutritionally relevant tissues, such as the endosperm. It is therefore the aim of this present study to address these two concerns related to the biofortification of sorghum and pearl millet, using a range of different conventional techniques related to grain quality assessment, and the non-conventional technique, known as micro Particle-Induced X-ray Emission (micro-PIXE) spectrometry.

1.2 Literature review I: Biofortified Sorghum and Pearl Millet

The sections outlined in this literature review serve two main objectives. The first objective is to provide a comprehensive review of the scientific literature related to the development of protein-biofortified sorghum and mineral-biofortified pearl millet. This involves a basic introduction to sorghum and pearl millet, highlighting details related to their origin, taxonomy and the general utilisation of each grain type. Next, a review will be given of the physical and biochemical properties of each grain, along with a basic assessment of each grain's nutritional quality. Following this, an overview of the research efforts that have been made to date to produce the biofortified sorghum and millet varieties of interest to the present study will be presented. As a conclusion to this section, the overall study aims and research objectives will be presented.

1.2.1 The major millets: sorghum and pearl millet

The two most widely grown species of millet are sorghum (*Sorghum bicolor* (L.) Moench) and pearl millet (*Pennisetum glaucum* (L.) R. Br.), which are collectively referred to as the major millets (Rajendrakumar, 2017). Both species are classed together in the second largest subfamily of the grasses – the Panicoideae, which includes other major crop species such as maize (*Zea mays*) and sugarcane (*Saccharum officinarum*) (Sánchez-Ken and Clark, 2010). Both sorghum and pearl millet are C₄ species, with high photosynthetic efficiency and dry matter production capacity, which favours their use as subsistence crops in semi-arid and arid areas (Rai *et al.*, 1999). Across Africa and Asia, sorghum and pearl millet grains are predominantly used as staple foods which supply a major proportion of the calories, protein and micronutrients to the poor (O'Kennedy *et al.*, 2006). Traditionally the grains are used to make a diverse range of foods, which include breads, porridges and couscous, as well as a range of alcoholic and non-alcoholic beverages (Rai *et al.*, 1999). In developed countries the grains are principally used as feed ingredients, but amongst health-food enthusiasts there is a burgeoning interest in the use of these grains for their nutraceutical value. It is well known for example, that sorghum and millet grains are rich in health-promoting phytochemicals, such as phenolics, which have beneficial effects against common health problems such as cardiovascular disease, hypertension, type II diabetes and some types of cancer (Aruna Reddy, 2017). Additionally, these cereals, are gluten-free, and are therefore sought after by people suffering from coeliac disease or wheat intolerances (Taylor and Duodu, 2017).

1.2.2 Introduction to sorghum - Origin and taxonomy

Sorghum (*Sorghum bicolor* (L.) Moench) is the fifth most important cereal in the world agricultural economy, after rice, wheat, maize, and barley, and the second (after maize) in sub-Saharan Africa (Proietti *et al.*, 2015). Archaeological evidence from near the Egyptian-Sudanese border support the notion that the crop was first cultivated in this region around 8000 years ago (Dahlberg and Wasylkowa, 1996). The genus *Sorghum* as currently proscribed consists of 25 recognised species (Price *et al.*, 2005). All domesticated or cultivated varieties of sorghums are classified under the subgenera *Eu-Sorghum*, and conform to the following taxonomical description (Sanjana Reddy, 2017a):

Family:	<i>Poaceae</i>
Subfamily:	Panicoideae
Tribe:	Andropogoneae
Subtribe:	<i>Sorghinae</i>
Subgenera:	<i>Eu-Sorghum</i>
Genus:	<i>Sorghum</i>
Species:	<i>bicolor</i>

Cultivated sorghum has a diploid genome of 735 Mbp, which has recently been fully sequenced (Paterson *et al.*, 2009). Although this is nearly twice the size of rice (389 Mbp), the sorghum genome is much smaller than other important cereals, such as wheat (16 900 Mbp) and maize (2600 Mbp) (Dillon *et al.*, 2007).

Around the world, sorghum is further referred to by a variety of different common names which include great millet, guinea corn, mtama, jowar, mabele, dura, kaoliang and milo (Taylor and Duodu, 2017; Sanjana Reddy, 2017a).

1.2.2.1 Sorghum growth and adaptive characteristics

S. bicolor is an erect plant with a solid stem, which can grow from 0.8 m to 5 m high (Vara Prasad and Staggenborg, 2011). It is predominantly an annual, self-pollinated crop with 2-20% outcrossing (Rai *et al.*, 1999); but, there are some species characterised as perennials, which can be harvested many times (Aruna Reddy, 2017). Sorghum varieties are grown over a wide range of agro-ecologies, from the equator to over 50° N and 40° S (Vara Prasad and Staggenbord, 2011), and at altitudes from sea level up to 2300 m

(Doggett, 1988). Amongst the cereals, sorghum is uniquely tolerant of some of the worst abiotic stress factors, which include heat, drought, salinity, nutrient-poor soils and even water-logging stress (Vara Prasad and Staggenbord, 2011). Its remarkable stress tolerance is linked to several inherent features of its biochemistry and structure. Firstly, it is a C₄ plant with high photosynthetic capacity, which becomes enhanced under conditions of high heat and light intensity (Byrt *et al.*, 2011). This makes sorghum very efficient at converting sunlight energy into biomass, which contributes to its rapid growth and high potential yields (Mullet *et al.*, 2014). Secondly, sorghum has an extensive root system, which, in comparison to other grain crops, has been found to penetrate a greater volume of soil, resulting in better water and nutrient absorption for the plant (Vara Prasad and Staggenbord, 2011). To tolerate heat and drought stress, sorghum has a thick waxy cuticle that reduces water loss through evaporation and also reflects away radiant heat energy from the sun (Shepherd and Wynne Griffiths, 2006). Leaves further contribute to the conservation of water by readily closing their stomata and rolling up along the midrib when moisture-stressed, so as to reduce evapo-transpiration rates (Singh and Lohithaswa, 2006). Lastly, certain sorghum varieties are particularly well known for their 'stay green' genes, which allow the plants to maintain a green leaf area and photosynthetic capability under severe drought stress during the post-flowering phase (Xu *et al.*, 2000).

In terms of its cultivation, sorghum is typically propagated by seed. Its inflorescence (the panicle or head) has both male and female organs, and therefore the plant is mostly self-pollinating (Saballos, 2008). Flowering occurs between 55 – 70 days post-germination, and gives rise to seeds that reach physiological maturity 30 – 40 days post anthesis (Dillon *et al.*, 2007). These seeds or kernels are the plants' edible fruit, which serve as food grain. Across the various cultivars, grain size, shape and colour is reported to differ greatly (Dillon *et al.*, 2007). However, commercial sorghum grains are generally 4 mm long, 2 mm wide and about 2.5 mm thick (Rooney and Miller, 1982), with a spherical shape that is flattened on one end and with the embryo situated at the base (Vara Prasad and Staggenbord, 2011). At physiological maturity, all grains are distinguished by a darkened hilum area, which signifies the end of nutrient delivery to the seed and the beginning of senescence and desiccation (Dicko *et al.*, 2006). A well-developed sorghum panicle produces about 3000 - 4000 seeds (Hamilton *et al.*, 1982; Arnon, 1972); which range in weight from 1 – 6 grams per hundred seeds (Upadhaya *et al.*, 2008).

1.2.2.2 Sorghum production and utilisation

Globally, more than 68 million tonnes of sorghum is produced over an area of about 45 million hectares (ha) (FAO, 2014). The world's top ten sorghum producers (Table 1.1) are responsible for more than three-quarters of the total sorghum output, with the biggest harvests located in USA, Mexico, Nigeria, Sudan and India. Sudan, India and Nigeria have the largest land areas devoted to sorghum cultivation, but experience relatively low production yields. In industrialised countries, like USA, Mexico, China and Argentina, sorghum is mainly produced in a commercial context to provide feed and fodder for the livestock sector. Production is therefore highly mechanised and modern, and is further focused on the utilisation of only high-yielding hybrid cultivars (Taylor and Duodu, 2017). In developing countries, sorghum production tends to be dominated by small-scale subsistence farming methods, with traditional sorghum landraces and no modern farming aids to boost production. As a result, yields tend to be low. It is reported that in the last 35 years, the area devoted to sorghum production in Africa has nearly doubled, but yields averaging 800 kg/ha have not increased (Sanjana Reddy, 2017a). In recent years, sorghum research in Sub-Saharan Africa has been directed towards the development and release of high-yielding cultivars to benefit production for local farmers (Taylor and Duodu, 2017; Ahmed *et al.*, 2000).

Sorghum is regarded as one of the world's most versatile crops, and is valued not only for its grain, but also for its stalks and leaves (Proietti *et al.*, 2015). The grain or the whole plant can be used to provide forage, hay or silage (Woods, 2001). Additionally, the fibrous material collected from sorghum can be used for building material, fencing and a variety of paper/cardboard products (Woods, 2001). With increasing interest in the development of renewable fuels, sweet stemmed varieties of sorghum have also been exploited to produce bioethanol (Wu *et al.*, 2010). These sweet-stemmed sorghums are of particular significance for future sustainability, as bioethanol can be produced from the stalk's sweet juice, whilst the grain can still be harvested for food.

It is estimated that about 50% of sorghum is grown directly for human consumption, with more than 500 million people relying on it as a dietary staple (Ratnavathi and Komala, 2016). The consumption of sorghum as food is particularly high in areas where the climate does not allow the economic production of other cereals and where per capita incomes are relatively low, such as in the African Sahel, and parts of India and China (Ratnavathi and

Komala, 2016). Most sorghum produced for food is consumed as unleavened/leavened breads, porridge, couscous or noodles (Singh and Lohithaswa, 2006). Additionally, it is also used to produce a variety of snack foods and an assortment of malted alcoholic and non-alcoholic beverages (Ratnavathi and Komala, 2016). In Western markets, interest in sorghum food products is increasing due to its gluten-free status, and neutral flavour, which make it an attractive alternative for people afflicted with coeliac disease or other forms of wheat intolerance (de Mesa Stonestreet *et al.*, 2010). Moreover, sorghum is rich in fibre and highly resistant starches which makes it an ideal food for diabetics and the obese (Ratnavathi and Komala, 2016). Additionally, sorghum exhibits antioxidant, anticancer and cholesterol-lowering properties which are credited to the phenolic compounds found in its grain (Pasha *et al.*, 2014).

Table 1.1 Area, production and yield of sorghum in major producing countries (FAO, 2014).

Country	Sorghum		
	Area (million ha)	Production (million t)	Yield (kg/ha)
USA	2.59	11	4242
Mexico	2.01	8.4	4168
Nigeria	5.44	6.7	1240
Sudan	8.38	6.3	750
India	5.82	5.4	926
Ethiopia	1.83	4.3	2365
Argentina	0.79	3.5	4400
China	0.62	2.9	4659
Brazil	0.84	2.3	2713
Burkina Faso	1.55	1.7	1103
Total	29.87	52.5	
World	44.96	68.9	1533

1.2.2.3 Sorghum Grain – Structure

The structure and chemical composition of cereal grains are important determinants of overall nutritional quality; therefore, it is useful to review these characteristics in relation to this study on sorghum grain. According to strict botanical terms, the sorghum grain is defined as a naked caryopsis (Earp *et al.*, 2004) consisting of three major parts: (i) bran (pericarp-testa, 7%), (ii) germ (embryo, 9%) and (iii) endosperm (storage tissue, 84%) (Serna-Saldivar and Rooney, 1995). The major anatomical features of the sorghum grain are depicted in Figure 1.1 and subsequently discussed in more detail in the following subsections.

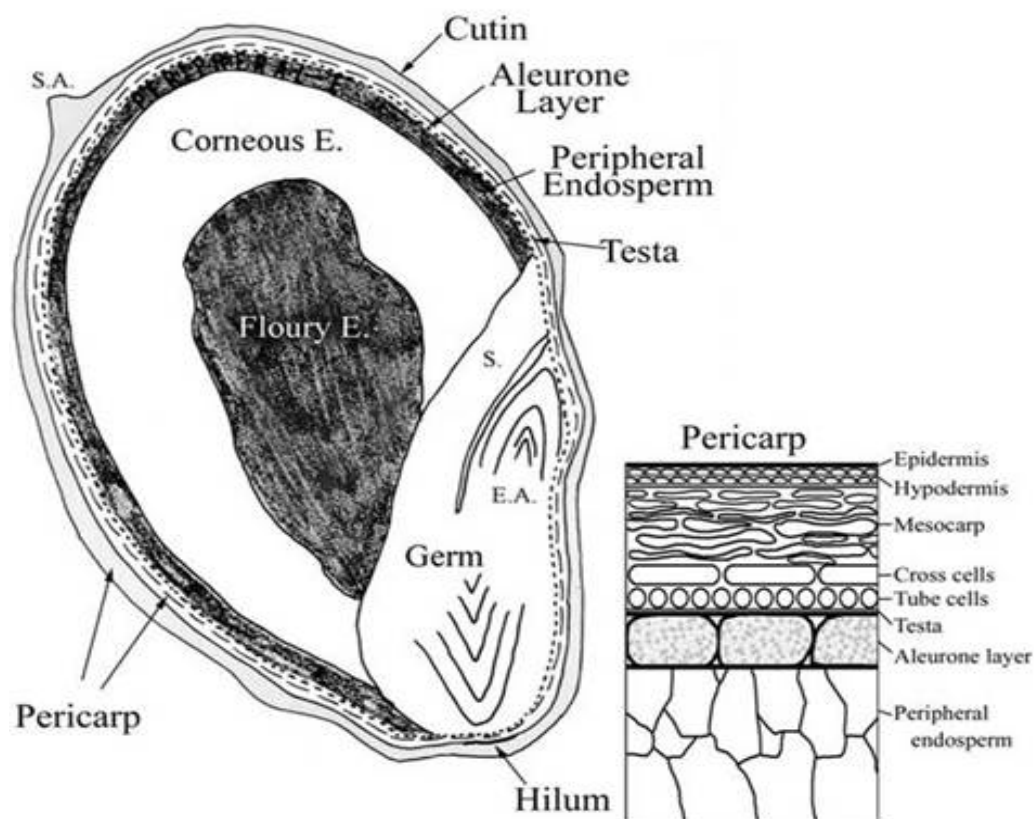


Figure 1.1 Diagrammatic depiction of a longitudinal section through a sorghum grain, depicting the three major anatomical parts: the pericarp, germ (scutellum (S) and embryonic axis (EA)) and endosperm E. SA refers to the stylar area of the pericarp (Earp *et al.*, 2004).

The Bran (Pericarp-Testa)

The bran refers to the outer layers of the grain, which include the pericarp and seed coat (testa) (Hwang *et al.*, 2002). This fraction is known to be rich in phytochemicals, fibre, vitamins, minerals and some nutrients (Slavin, 2004). The pericarp is derived from the ovary wall and can be subdivided into three distinct tissue types: the epicarp, mesocarp and endocarp (Earp *et al.*, 2004). The outermost layer, the epicarp, usually comprises two to three layers of cells, which are thick-walled, rectangular in shape and contain wax (Rooney and Murty, 1982). Additionally, the epicarp may contain pigmented compounds that strongly influence the grain's overall colour (Serna-Salvidar and Rooney, 1995). The innermost part of the pericarp is known as the endocarp, which is divided into two distinct layers of outer cross cells and inner tube cells. The tube cells are implicated in conducting water during germination, whereas the cross cells serve to form an impervious layer around this network to curtail moisture loss (Rooney and Murty, 1982; Waniska, 2000).

The mesocarp makes up the middle section of the pericarp and is characterised by several layers of thin-walled parenchyma cells, which can contain starch granules (Serna-Salvidar and Rooney, 1995). According to Earp *et al.*, (2004), the amount of starch located within the mesocarp may be a determinative factor of the overall pericarp thickness. This thickness is highly variable, with reported values ranging from 8 μm – 160 μm , depending on the cultivar and the area of the grain being investigated (Waniska, 2000). For individual grains, the pericarp is typically thickest at the stylar area (the point at which the style was attached during pollination) and at the hilum (the placenta scar tissue resulting from the detachment of the seed from the ovary wall), whilst at the sides of the grain, the pericarp is at its thinnest (Waniska, 2000). The thickness of the pericarp has important implications for the milling of the grain (Earp *et al.*, 2004) and is also positively linked to the overall polyphenol content found in sorghum (Beta *et al.*, 1999).

Directly beneath the pericarp is the testa or seed coat layer, which is derived from the maternal ovule integuments (Waniska, 2000). Like the pericarp, the testa varies in thickness across different sorghum lines and also within different areas of the grain (Rooney and Murty, 1982). However, in some varieties of sorghum, the testa layer is completely absent (Hoseney *et al.*, 1974). A pigmented testa is a notable feature of several sorghum varieties, and is indicative of the presence of condensed tannins (proanthocyanins) (Earp *et al.*, 2004).

The Germ

The germ area of the sorghum grain may be divided into two main parts: the embryonic axis and the scutellum. The embryonic axis refers to the nascent plant, which is comprised of a radicle (early root) and a plumule (early shoot). The scutellum refers to the seed cotyledon, which serves as a major nutrient reserve for the germ, and also acts as a link between the germ and the major storage reserves of the endosperm tissue (Waniska, 2000). The germ is made up mostly of parenchymatous cells and is rich in lipids, proteins and minerals (Serna-Saldivar and Rooney, 1995), whilst almost completely devoid of starch (Rooney and Miller, 1982).

The Endosperm

The main reservoir for starch in sorghum grain is the endosperm, which may be subdivided into the aleurone layer, the peripheral endosperm and the floury and corneous

endosperm. The aleurone layer, which may be described as the outer coat of the endosperm (Hwang *et al.*, 2002), is a single layer of thick walled rectangular cells, which contain large amounts of proteins, phytic acid and oil, but is virtually free of starch (Waniska, 2000). Directly beneath the aleurone layer is the peripheral endosperm (or sub-aleurone), which is a compacted region of 2 – 6 cell layers (15 – 30 µm wide) that contains very small starch granules and a denser protein matrix in comparison to the endosperm proper (Dillon *et al.*, 2007). The rest of the endosperm is made up of varying proportions of corneous and flourey endosperm types, which serve as the grain's main storage centres for starch.

In general, the flourey endosperm is concentrated within the central portion of the grain and consists of loosely packed spherical starch granules surrounded by a discontinuous protein matrix (Waniska, 2000; Rooney and Murty, 1982). The presence of large intergranular air spaces is a distinguishing feature of the flourey endosperm, which diffuses light and results in the characteristic chalky or opaque appearance of the flourey endosperm (Serna-Saldivar and Rooney, 1995; Hoseneey *et al.*, 1974). In contrast, the corneous outer endosperm has a translucent or vitreous appearance, due to a compact structure that is devoid of air spaces (Waniska, 2000). The starch granules within the corneous endosperm are typically polygonal in shape and are tightly packed within a continuous protein matrix that harbours many protein bodies (Hoseneey *et al.*, 1974; Waniska, 2000). The relative proportions of corneous and flourey endosperm have a significant impact on grain texture and overall quality, and are influenced by both genetic and environmental factors (Serna-Saldivar and Rooney, 1995; Rooney and Murty, 1982).

1.2.3 Introduction to pearl millet - Origin and taxonomy

Pearl millet (*Pennisetum glaucum* (L.) R. Br.) is the world's sixth most important cereal crop, which follows after sorghum (Aruna Reddy, 2017). The greatest diversity of pearl millet is found in the Sahel zone of western Africa (Sanjana Reddy, 2017b). It is presumed that the species originated in this area about 4500 years ago, most likely in the region of present day Mali (Manning *et al.*, 2011). The genus *Pennisetum* contains about 140 different species (Upadhyaya *et al.*, 2008), with different basic chromosome numbers, ploidy levels and life cycles (annual, biennial, or perennial) (Martel *et al.*, 1997). The current taxonomical classification for the main cultivated form of pearl millet is as follows (Sanjana Reddy *et al.*, 2017b):

Family:	<i>Poaceae</i>
Subfamily:	Panicoideae
Tribe:	Paniceae
Subtribe:	Panicinae
Subgenera:	Penicillaria
Genus:	Pennisetum
Species:	<i>glaucum</i>

Cultivated pearl millet has a 2530 Mbp genome and a diploid chromosome number of 7, $2n=14$ (Bennet *et al.*, 2000). The genome size of pearl millet is more than six times larger than that of rice (389 Mbp), three times larger than that of sorghum (735 Mbp) and almost equal to that of maize (2600 Mbp) (Dillon *et al.*, 2007). Common names used for pearl millet include bulrush millet, candle millet, cattail millet, sanio, bajra, babala and cumbu (Mathur, 2012; Aruna Reddy, 2017).

1.2.3.1 Pearl millet growth and adaptive characteristics

P. glaucum is a predominantly cross-pollinating, diploid grass species that is most commonly grown in arid and semi-arid regions of Africa and Asia (Vadez *et al.*, 2012). As a C_4 plant, pearl millet has very high photosynthetic efficiency and dry matter production capacity (Yadav and Rai, 2013). Plants can vary in stature from 0.5 to 4.5 m tall (Mason *et al.*, 2015) and are principally grown for food grain and dry fodder (Yadav and Rai, 2013). Pearl millet is described as a central component of food security for the rural poor in dry and hot areas (Vadez *et al.*, 2012). It typically grows under the most adverse agro-climatic conditions, where other crops like maize and sorghum cannot grow. Pearl millet exhibits a number of characteristics which confer upon it exceptional adaptation to arid conditions. For example it has a short life cycle, with a tendency to flower early as part of an in-built drought escape mechanism (Vadez *et al.*, 2012). Additionally, it has a deep and extensive root system to actively seek out nutrients and moisture from the soil; as well as a high tillering capacity, which allows for a measure of developmental plasticity during times of heightened environmental stress (Andrews *et al.*, 1993).

The inflorescence or panicle of a pearl millet plant is a compound terminal spike that is generally cylindrical or conical (Sanjana Reddy, 2017b). Seed set can be seen in the panicle about a week after fertilisation (Sanjana Reddy, 2017b). Grain weight is known to

vary from 0.5 to over 2.0 g per hundred grains; whilst each panicle can bear between 500 to 3,000 grains (Andrews *et al.*, 1993).

1.2.3.2 Pearl millet production and utilisation

Pearl millet is produced on approximately 30 million hectares of land, in 30 countries, spread across Africa, Asia, the Americas and Australia (Yadav *et al.*, 2012). Reporting authorities, such as the FAO, combine production statistics of pearl millet with other millet crops (such as finger millet, foxtail millet etc.), therefore it is difficult to obtain accurate up to date data for pearl millet alone. However, it is generally accepted that pearl millet accounts for about 50% of global millet production, with total harvests exceeding 24 million tonnes per year (Taylor and Duodu, 2017). According to one source, the total global production of pearl millet at the end of 2013 was about 28 million tonnes, with the largest harvests found in India, Niger, Nigeria and China (Table 1.2).

Table 1.2 Area, production and yield of pearl millet in major producing countries (Dyakar Rao *et al.*, 2016).

Country	Pearl millet		
	Area (million ha)	Production (million t)	Yield (kg/ha)
India	9.66	11.4	1184.3
Niger	7.08	3.3	460.7
Nigeria	2.72	2.5	925.3
China	0.74	1.7	2316.7
Mali	1.86	1.5	783.5
Chad	0.90	0.6	648.2
Tanzania	0.31	0.3	989.4
Total	23.3	21.3	
World	32.2	27.9	867.7

In Sub-Saharan Africa, pearl millet ranks as the third major cereal crop (after maize and sorghum) and is principally grown in two regions: west/central Africa (Nigeria, Niger, Chad, Mali and Senegal) and east/southern Africa (Sudan, Ethiopia, Uganda and Tanzania) (Jukanti *et al.*, 2016; Moreta *et al.*, 2015). In Asia, pearl millet cultivation is mainly centred in India and China, which are the leading countries in terms of production yield (Dyakar Rao *et al.*, 2016). Outside of Africa and Asia, pearl millet is also grown in Australia, Canada, Mexico, Brazil and USA, where it serves as a forage crop for livestock production (Moreta *et al.*, 2015; Taylor and Duodu, 2017).

It is currently estimated that about 95% of pearl millet grain is used for human consumption, with the remainder serving as animal or poultry feed (Pahoja, 2012). Several food preparations are made from pearl millet, which include thick and thin porridges, fermented and unfermented breads, boiled and steam-cooked products, alcoholic and non-alcoholic beverages, as well as a variety of snacks (Taylor *et al.*, 2010). Pearl millet consumption is also being encouraged, due to several health-promoting properties that are associated with the grain. For example it is gluten-free, has a low glycaemic index and has a favourable phytochemical composition. The polyphenols found in pearl millet are known to be important for the prevention and treatment of cardiovascular disease, diabetes, arthritis and certain types of cancer (Nambiar *et al.*, 2011).

1.2.3.3 Pearl Millet Grain – Structure

Pearl millet grains are about one-third the size of sorghum grains and are generally described as cono-spherical or tear-shaped (Jain and Bai, 1997). The grain dimensions vary substantially according to variety type and cultivation practice, but on average have a length (mm), width (mm) and weight (mg) of 1.5, 1.5 and 8.5 (Matz, 1991). The overall structure of the pearl millet kernel is quite similar to that of sorghum. The kernel is also described as a naked caryopsis, and is comprised of three major components: the pericarp, endosperm and germ, with a distribution of 7.2 to 10.6%, 15.5 to 21% and 71 to 76% respectively (Abdelrahman *et al.*, 1984).

The pericarp of pearl millet can be of variable thickness, depending on the variety and is comprised of three layers: the epicarp, mesocarp and endocarp (Sehgal *et al.*, 2004). The epicarp is one to two cell layers thick, whilst the mesocarp can vary in thickness and may contain some starch granules (Taylor, 2016). The innermost section of the pericarp is the endocarp, which is characterised by the presence of cross and tube cells (Zeleznaek and Varriano-Martson, 1982). Beneath the pericarp is the seed coat, which may contain considerable amounts of pigments (Taylor, 2016). These pigments influence the colour of the kernel, which can be predominantly white, grey, yellow, brown or purple (Taylor and Emmambux, 2008).

The next layer underneath the seed coat is the aleurone. It is a single layer of cells that forms the first layer of the endosperm (Zeleznaek and Varriano-Marston, 1982). The aleurone cells have thick cell walls and contain protein bodies, enzymes, mineral deposits and oil in the form of spherosomes within their cytoplasm (Serna-Saldivar and Rooney,

1995). The rest of the endosperm is characterised by two distinctive areas: the outer corneous (also referred to as vitreous or hard) endosperm and the inner floury (also referred to as soft) endosperm (Taylor, 2016). The corneous endosperm contains few starch granules and is dominated by an airspace-free continuous matrix of proteins, comprising protein bodies and matrix protein (Taylor, 2016). In contrast, the floury endosperm has many air spaces, with comparatively larger starch granules and much fewer protein bodies, embedded in a discontinuous protein matrix (McDonough and Rooney, 1989).

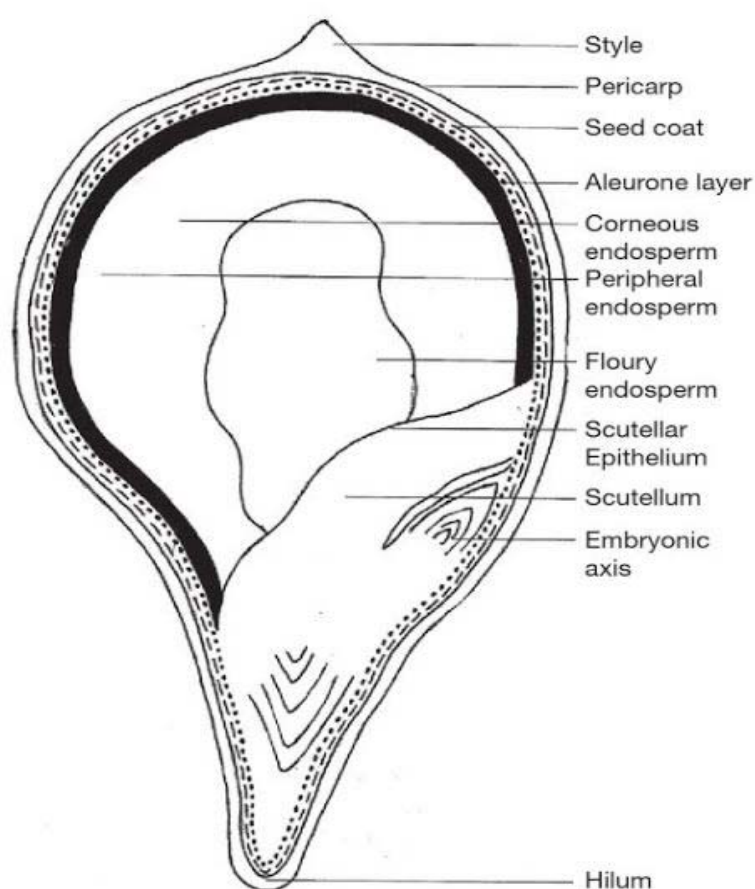


Figure 1.2 Diagrammatic depiction of a longitudinal section through a pearl millet grain (Barrion, 2008).

The remaining major structural component of pearl millet is the germ. The germ is proportionately large for pearl millet, comprising about 16.5% of the kernel compared to an average of 9.4% for sorghum (Abdelrahman *et al.*, 1984). The germ is comprised of two parts: the scutellum and the embryonic axis. The scutellum serves as a major storage

tissue for lipids, proteins and minerals that are important for the early growth of the embryo (FAO, 1995).

1.2.4 Nutritional Composition of Sorghum and Pearl Millet Grain

The overall nutritional value of a cereal is commonly assessed in terms of its main dietary components, which typically includes an analysis of the macro- and micronutrients, as well as the antinutrients or toxins present within the grain. In the subsections that follow, a review of the main nutritional components of sorghum and pearl millet grain will be presented.

1.2.4.1 Carbohydrates

Starch is the dominant form of carbohydrate in cereal grains, which serves as the main energy storage compound (Ratnavathi and Komala, 2016). It is mainly present in the form of granules that are localised in the endosperm cells (Serna-Saldivar and Rooney, 1995). These granules range in size from 2 - 30 μm in diameter in sorghum; and from 6 – 12 μm in diameter in pearl millet (Taylor and Duodu, 2017). The starch granules are made up of two glucose polymers: amylose and amylopectin (Ratnavathi and Komala, 2016). In normal (i.e. non-waxy) sorghum cultivars, amylose and amylopectin contribute 20-30% and 70%, respectively, of the total starch found in the grain (Serna-Saldivar and Rooney, 1995). In pearl millet, the percentage of amylose is in the range of 17 – 21.5% (Taylor, 2016). Waxy type sorghums contain about 95% amylopectin and 5% amylose (Serna-Saldivar and Rooney, 1995). There are no reports of a waxy-type pearl millet (Taylor, 2016).

The next major group of carbohydrates are the non-starch polysaccharides (NSP). The NSP mainly refer to the hemicellulose, cellulose and pectin components of the pericarp and endosperm cell walls that contribute to dietary fibre, along with lignin (Dicko *et al.*, 2006). The dietary fibre content of both sorghum and pearl millet is mainly of the insoluble (water inextractable) type (Taylor, 2016). The other carbohydrates found in the grain are primary sugars. These make up about 1 - 2% of the grain dry weight and are mainly present in the form of sucrose, glucose, fructose, maltose and raffinose (Ratnavathi and Komala, 2016; Taylor, 2016).

1.2.4.2 Proteins

The amount of protein found in both sorghum and pearl millet grains can vary widely, with reported values ranging from 8.1 – 16.8% for sorghum (Sehgal *et al.*, 2004); and 8.6 – 19.4% for pearl millet (Taylor, 2016). This variation may be due to differences in the method of cultivation (such as the use of fertilisers) or, it may be the result of other environmental influences that can have an impact on the total protein content (Bean *et al.*, 2011; Serna-Saldivar and Rooney, 1995). The average grain protein content of sorghum is typically ~10 – 11%, which is comparable to the levels found in other major cereals such as maize and wheat (Bean *et al.*, 2011; de Mesa Stonestreet *et al.*, 2010). However, in comparison, pearl millet tends to be richer in protein content, with an average level of ~14.5% (Taylor, 2016).

In general, sorghum and pearl millet grain proteins may be categorised as either prolamin or non-prolamin in type. The prolamins are the dominant storage proteins found in both grains, which account for 70 – 80% of the total protein content in sorghum (Hamaker *et al.*, 1995); and about 22 – 35% of total protein content in pearl millet (Nambiar *et al.*, 2011). The prolamins are alcohol soluble proteins which are rich in glutamic acid and nonpolar amino acids (such as proline, leucine and alanine), but are limited in the essential amino acid lysine (de Mesa Stonestreet *et al.*, 2010). The prolamin proteins of sorghum are referred to as kafirins (de Mesa Stonestreet *et al.*, 2010); whereas the prolamins of pearl millet are known as pennisitens (Taylor, 2016). The prolamin proteins are generally known as endosperm-specific, and are typically stored in the form of protein bodies in the grain endosperm (Taylor, 2016).

The non-prolamin proteins make up the minority fraction of sorghum and pearl millet grain protein and consist of albumins, globulins and glutelins (Bean *et al.*, 2011; Taylor, 2016). The albumins and globulins are principally located in the germ and are mainly saline soluble proteins (Taylor, 2016). In sorghum, they collectively make up about 23% of the total protein content (Taylor and Belton, 2002); whilst in pearl millet they are somewhat higher, contributing up to 35% of the total protein content (Nambiar *et al.*, 2011). These proteins are chiefly involved in metabolic processes linked to the development of the embryo and thus include bioactive species such as enzymes, nucleoproteins, glycoproteins and pathogenesis-related compounds (Bean *et al.*, 2011). The relatively higher albumin/globulin content of pearl millet is likely a consequence of its large germ which also leads to a more favourable amino acid composition (Taylor, 2016). For

example, pearl millet is richer in the essential amino acids, lysine, cysteine and methionine in comparison to other grains such as sorghum and maize (Sehgal *et al.*, 2004).

The remainder of the non-prolamin grain proteins are glutelins, which tend to be alkali or acid extractable proteins (Shewry and Casey, 1999). The glutelins mainly function as endosperm matrix proteins (Serna-Saldivar and Rooney 1995) and as a source of enzymes linked to reserve starch and protein hydrolysis (Taylor *et al.*, 1984). In sorghum grain, glutelins make up 23.5 – 45% of the total protein content (Sehgal *et al.*, 2004); whereas, in pearl millet, glutelins make up 28 – 32% of the total protein content (Taylor, 2016). In general, the non-prolamin proteins (i.e. albumins, globulins and glutelins) are considered to have a higher nutritional value in comparison to the prolamins because they contain higher concentrations of the essential amino acid lysine (Taylor and Schüssler, 1986).

1.2.4.3 Fat

Reports on the total fat or lipid content of sorghum and pearl millet grains can vary considerably, (principally due to differences related to the extraction method applied), however, it is generally accepted that sorghum grains contain about 3.4% crude fat (Sehgal *et al.*, 2004); and pearl millet has a much higher level at around 5.1% (Taylor, 2016). The crude fat content of other major cereals such as wheat, barley and rice is comparatively much less, at 1.9%, 1.5% and 1.8% respectively (Ratnavathi and Komala, 2016). The fat content of maize however is more or less comparable to that of sorghum and pearl millet, as it is cited to be 4.8 – 5.2% of the total grain weight (Kent and Evers, 1994). The relatively high levels of fat in pearl millet and maize are attributed to the proportionately large germ found in these grains (Taylor, 2016). Both sorghum and pearl millet grains are rich in the essential polyunsaturated fatty acids oleic, linoleic and linolenic acids, which are critical for good nutrition (Stefoska-Needham *et al.*, 2015; Taylor, 2016).

1.2.4.4 Ash

The ash content of food refers to the inorganic residue that remains after the removal of water and organic matter, and as such it provides a measure of the total mineral content of the food sample (Sathe, 1999). Both sorghum and pearl millet are reputed to be good sources of several dietary minerals (Taylor, 2016; Dicko *et al.*, 2006). The minerals found in sorghum and pearl millet are primarily concentrated in the pericarp, aleurone and germ tissues (O'Kennedy *et al.*, 2006; Taylor, 2016). Decortication and milling processes which

remove these tissues significantly reduce the mineral content of the resultant refined flour (Taylor, 2016). In general, the total mineral (ash) content of the millets is often found to be higher than that of sorghum and other cereals (Klopfenstein and Hosney, 1995). However, it is noted that different cultivation practices, weather conditions, soil mineral levels and genetic factors also play a significant role in establishing the final mineral content of different cereal grains (Shegro *et al.*, 2012).

Table 1.3 A comparison of the typical proximate and mineral composition of sorghum and pearl millet grains (per 100 g dry weight, whole grain).

	Sorghum	Pearl millet
Proximates		
Starch (g)	72.1	71.6
Protein (g)	10.6	14.5
Fat (g)	3.4	5.1
Dietary Fiber (g)	6.7	8.5
Ash (g)	1.6	2.0
Minerals		
Calcium, Ca (mg)	15	46
Iron, Fe (mg)	4.2	8.0
Magnesium, Mg (mg)	171	137
Phosphorus, P (mg)	352	379
Potassium, K (mg)	363	460
Sodium, Na (mg)	2	17
Manganese, Mn (mg)	1.2	0.8
Copper, Cu (mg)	0.4	0.5
Zinc, Zn (mg)	2.5	3.1

Sources: Sehgal *et al.*, 2004; Sankara Rao *et al.*, 1983; FAO (1995); Taylor, 2016; Stefoska-Needham *et al.*, 2015

1.2.5 Anti-nutritional Factors in Sorghum and Pearl Millet Grain

In spite of the good balance of macro- and micronutrients present in sorghum and pearl millet grains, these cereals are generally viewed as nutritionally inferior, because of the presence of anti-nutritional factors (ANFs) which tend to have a detrimental effect on the grains' overall nutritional value. ANFs are broadly defined as substances present in foodstuffs that exert effects contrary to optimum nutrition (Gumede and Ratta, 2014). In sorghum and pearl millet grains, the most widely recognised ANFs include phytate, and the polyphenols (Ogbonna *et al.*, 2012). These substances act as ANFs because they have the capacity to interfere with the digestion or the absorption of other important nutrients. Interestingly however, it would be erroneous to view ANFs as intrinsically

harmful. The ANFs are simply a subset of the vast range of plant secondary metabolites, which, depending on the situation could have either a deleterious or advantageous effect on the consumer (Soetan and Oyewole, 2009). From an evolutionary standpoint, the toxic, unpalatable or anti-nutritive features of ANFs are an important part of a seed's survival strategy, because these compounds elicit a potent deterrent effect on herbivory and microbial/viral attack (Enneking and Wink, 2000). It is therefore evident that ANFs exhibit both protective and toxic functions within biological systems, and for this reason, there is much scientific interest in understanding how these compounds contribute to overall nutrition and health (Enneking and Wink, 2000; Soetan and Oyewole, 2009).

1.2.5.1 Phytate

Phytic acid (*myo*-inositol hexakisphosphate or IP₆), and its salts, known as phytates, collectively refer to a range of naturally-occurring phosphorus storage compounds found in all seeds and possibly all cells of plants (Oomah *et al.*, 2008). Its chemical structure (Figure 1.3) consists of a ring of six carbon atoms esterified with reactive phosphate groups that are predominantly negatively charged at physiological pH (Coulibaly *et al.*, 2011). As a result, phytate has strong chelative (or binding) properties and will readily form insoluble complexes with minerals and proteins, leading to reduced bioavailability and absorption of these important nutrients in the gut (Pontoppidan *et al.*, 2007). In particular, phytic acid displays a strong affinity for complexing multi-charged metal ions, such as Zn (II), Ca (II) and Fe (III), and as such can aggravate conditions of mineral malnutrition in both humans and animals (Bohn *et al.*, 2008). In sorghum, phytate levels range from 170 to 380 mg/100 g and account for over 85% of the total phosphorus in the whole grain (Doherty *et al.*, 1982). In pearl millet, phytate levels appear to be much higher, and reportedly range from 350 to 800 mg/100g (Taylor, 2016).

Most of the phytate in sorghum and pearl millet is located within the germ and bran layers of the seed, with minimal amounts found in the endosperm (Taylor, 2016). To limit the anti-nutritional effect of phytate, a range of strategies may be adopted, which include soaking, fermentation, germination or blanching of the seed (Afify *et al.*, 2011; Gupta *et al.*, 2015; Archana and Kawatra, 1998). These processes stimulate endogenous phytases, which break down the phytate molecule, and thereby decrease its chelating capacity (Pontoppidan *et al.*, 2007). Although many historical reports focus on the negative impact of dietary phytate, there are now several alternative studies which focus instead on the protective or beneficial effects that may be derived from phytate's strong chelating

capacity. Of note, there are reports which highlight phytate's role in the reduction of serum cholesterol levels (Onomi *et al.*, 2004), the inhibition of coronary artery calcification (Grases *et al.*, 2008) and as a possible treatment against colon cancer development (Norazalina *et al.*, 2010).

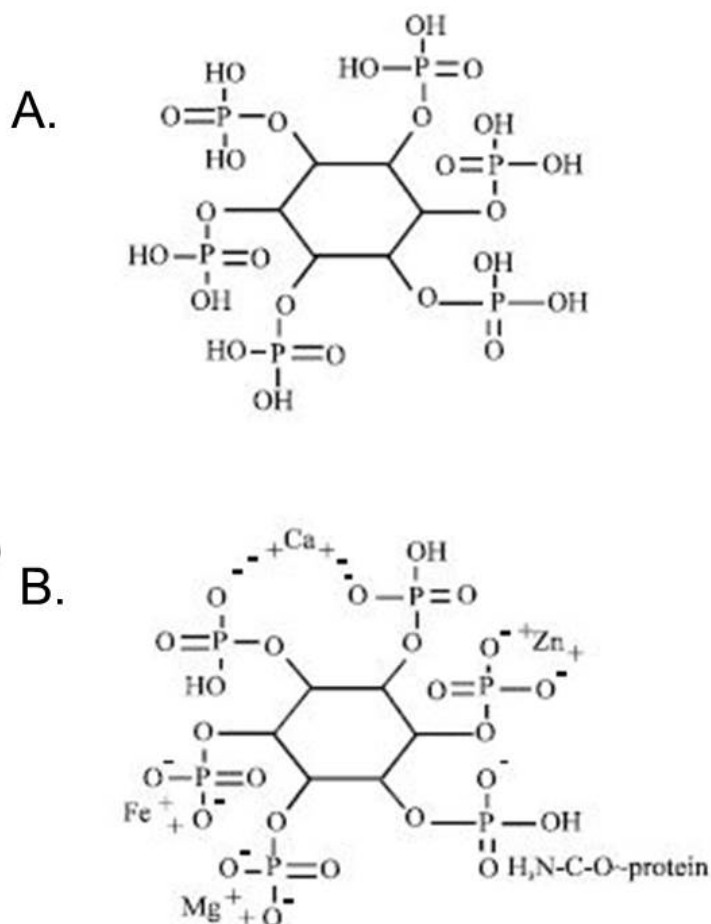


Figure 1.3 (A) Chemical structure of the phytic acid molecule; (B) a depiction of the phytic acid molecule with different possible interaction partners such as metal cations (minerals) and protein residues (Coulibaly *et al.*, 2011).

1.2.5.2 Phenolic compounds

Phenolic compounds are a large and important class of secondary metabolites, which are ubiquitously found throughout the plant kingdom (Bravo, 1998). Nearly 10,000 individual plant phenolic compounds have been identified, which range in complexity, from simple phenols, to highly polymerised compounds, such as tannins (Fürstenberg-Hägg *et al.*, 2013). All phenolic compounds are characterised by one or more aromatic ring structures, with varying numbers of hydroxyl groups attached (Pereira *et al.*, 2009) and are biogenetically derived from the shikimic acid and/or the malonic acid synthetic pathways

(Fürstenberg-Hägg *et al.*, 2013). In general, the phenolics are viewed as plant defensive compounds, because they serve to protect the plant from various forms of abiotic and biotic stress factors which include pathogen attack, predation and even ultraviolet radiation (Lattanzio *et al.*, 2009).

Sorghum is generally regarded to have high levels of phenolics, which can account for as much as 10% of the total dry weight in certain cultivars (Bravo, 1998). These compounds can be grouped into three main categories: phenolic acids, flavonoids and tannins, and are often referred to as polyphenols (Chung *et al.*, 1998). Strictly speaking, the phenolic acids are monophenols (given that they feature only one phenol ring), however because they share many of their properties with the flavonoids and tannins, they are described as “functional polyphenols” (Dixon, 2004). The phenolic acids are present in both free and bound forms and are principally found in the outer layers of the grain (Dykes and Rooney, 2006), where they are thought to inhibit the growth of microorganisms (FAO, 1995). The major flavonoids in sorghum, the anthocyanins, contribute mainly to the colour of the grain, and further function as phytoalexins, which are produced in response to fungal attack or other stresses (Dykes and Rooney, 2006). The tannins are high-molecular weight polyphenols, derived from the condensation of flavan-3-ols, and are the major phenolic compounds in Type II and Type III sorghums (FAO, 1995; Dykes and Rooney, 2006). The tannins are known to protect the grain from predation, fungal infestation and weathering and are chemically responsible for imparting a bitter/astringent taste to the grain (Waniska, 2000). The tannins are widely regarded as anti-nutrients because of their capacity to bind dietary proteins, carbohydrates and minerals into indigestible complexes (Dykes and Rooney, 2006). This binding behaviour can lead to reduced feed efficiencies of up to 30% (Dykes and Rooney, 2006). For this reason, various methods are used to reduce tannin levels in sorghum, which include decortication, soaking and fermentation (Falmata *et al.*, 2013; Dlamini *et al.*, 2007).

In spite of some nutritional problems associated with tannins, there is much widespread interest in the antioxidant and other health promoting effects of sorghum polyphenols in the diet (Dlamini *et al.*, 2007). With the understanding that harmful free radicals are often at the source of many human diseases (such as cancer, asthma, diabetes and cardiovascular problems) and the ageing process (Kumar *et al.*, 2012), antioxidant-rich foods are increasingly being sought after for their medicinal or nutraceutical value (Varzakas *et al.*, 2016). According to a number of studies, certain sorghum varieties

display higher antioxidant capacities than some fruits. This was found to be the case for high tannin varieties, as well as for sorghum types with high flavonoid levels (Awika *et al.*, 2003; Awika and Rooney, 2004). Impressively, several studies have already been conducted which highlight the role of sorghum polyphenols in anti-carcinogenic (Turner *et al.*, 2006), anti-microbial (Kil *et al.*, 2009), anti-diabetic (Kim and Park, 2012) and cholesterol-lowering activities (Kim *et al.*, 2015).

Unlike sorghum, pearl millet does not contain condensed tannins (Dykes and Rooney, 2006; Berwal *et al.*, 2016), but is known to be rich in other phenolics, which are highly concentrated in the grain bran layers (Nambiar *et al.*, 2012). According to several studies, pearl millet ecotypes can vary widely in their phenolic composition, due to both genetic and environmental factors (Berwal *et al.*, 2016; Radhouane *et al.*, 2013). In general however, the total phenolic content of pearl millet grains has been found to range from 0.5 to about 0.8% of the total grain weight (Khetarpaul and Chauhan, 1990). Using high performance liquid chromatography (HPLC), a recent study identified several of the most abundant phenolic acids found in pearl millet grains (Radhouane *et al.*, 2013). According to the HPLC profiles, the major peaks revealed the dominance of three main types of phenolic acids: trans-cinnamic, protocatechic and hydroxybenzoic acids; whilst several of the minor peaks were identified as gallic, catechin, ferulic, coumaric or vanillic acid (Radhouane *et al.*, 2013). In another study, several important flavonoids were identified in pearl millet, which include tricetin, acacetin and luteolin (Nambiar *et al.*, 2012). Several of these phenolic compounds have been noted for their antioxidant, chemopreventive, and antidiabetic effect in both *in vitro* and *in vivo* studies (Kasala *et al.*, 2016; Vinayagam *et al.*, 2016; Ghasemzadeh and Ghasemzadeh, 2011). The nutraceutical value of pearl millet is therefore an important area of research that is steadily gaining momentum in the health and wellness sector (Radhouane *et al.*, 2013; Berwal *et al.*, 2016).

1.2.6 The need for protein biofortified sorghum

Despite being relied upon as a staple grain for millions of people, sorghum is generally viewed as an inferior cereal, because of nutritional deficiencies associated with its dominant storage proteins, the kafirins. The kafirins make-up 70-80% of the total proteins found in sorghum wholegrain flour (Hamaker *et al.*, 1995), and are problematic from a nutritional perspective, because of their low lysine content and poor digestibility (Shewry, 2007). The kafirins were first isolated in 1916, and were so named because they were

extracted from the sorghum variety “Dwarf kafir” (Johns and Brewster, 1916). Due to their solubility in aqueous alcohol and their high proline and glutamine content, kafirins naturally fall under the larger protein classification of prolamins (Shewry and Tatham, 1990). Interestingly, it is noted that sorghum kafirins share a high degree of sequence and structural homology with prolamins from other related cereals, in particular the zeins (from maize), the caneins (from sugarcane) and the coixins (from Coix, commonly known as Job’s tears) (Laidlaw *et al.*, 2010).

During seed development, kafirins are synthesised on rough endoplasmic reticulum (ER), and thereafter transported to the ER lumen, where they are stored as discrete protein bodies inside endosperm cells (Taylor *et al.*, 1985; Krishnan *et al.*, 1989). Here they serve as repositories of carbon, nitrogen and sulphur for seed germination (Saito *et al.*, 2010). Protein bodies in sorghum are mostly found in the peripheral regions of the endosperm, where they are “glued” into place by an embedding glutelin matrix and a surrounding complex of starch granules (de Mesa-Stonestreet *et al.*, 2010). Tight packing of the protein bodies into this matrix contributes to important grain attributes, such as hardness, overall digestibility and post-harvest processing qualities (Laidlaw *et al.*, 2010).

1.2.6.1 Kafirins Subclasses

Based on molecular weight and DNA sequence, the kafirins are typically grouped into four subclasses, namely, α -, β -, γ - and δ -kafirins (Wu *et al.*, 2013; Laidlaw *et al.*, 2010). The δ -kafirins are the least abundant of the four, are rich in methionine and have a molecular weight (M_w) of about 13 kDa (Belton *et al.*, 2006). It is proposed that δ -kafirins contribute to less than 1% of the total seed storage protein in mature sorghum grains (Laidlaw *et al.*, 2010). In contrast to the almost negligible contribution of the δ -kafirins, the α -, β -, γ - types make up the bulk of the kafirin proteins found in sorghum seed. Of these, the α -kafirins are the most dominant form. The α -kafirins constitute between 66 – 84% of the total protein found in the sorghum endosperm and are divided into two polypeptide forms of molecular weights 25 and 23 kDa, respectively named α_1 and α_2 -kafirins (de Mesa-Stonestreet *et al.*, 2010). The remainder of the kafirin proteins are either β - or γ -kafirins, which account for up to 20% of the total protein found in the sorghum grain endosperm (Wong *et al.*, 2009). The β -kafirins are approximately 18 kDa and abound in the amino acids methionine and cysteine. The γ -kafirins, on the other hand, are dominated by the amino acids proline, cysteine and histidine and have a molecular weight of about 28 kDa (Wong *et al.*, 2009; de Mesa-Stonestreet *et al.*, 2010).

1.2.6.2 Kafirins and Protein Digestibility

In 1981, MacLean *et al.*, conducted a study which showed that the level of protein digestibility in cooked sorghum porridge was only about 46% (MacLean *et al.*, 1981). This was significantly lower than the digestibility levels of 81%, 73% and 66% that were found in comparable cooked samples of wheat, maize and rice respectively. The low digestibility of sorghum protein is largely related to the type of microstructures that are formed as a result of the inter- and intramolecular bonding that takes place between the kafirins. Using a range of microscopy techniques, which have included scanning electron microscopy (SEM), transmission electron microscopy (TEM) and confocal laser microscopy, it has been resolved that the protein body structure (which is mostly comprised of kafirins) is maintained throughout most cooking methods (Choi *et al.*, 2008). These protein bodies are 0.5 to 3.5 μm in diameter (Taylor *et al.*, 1985) and are internally organised in such a way that the abundant and more digestible α -kafirins are completely encapsulated by an outer “shell” of highly crosslinked β - and γ -kafirins (de Mesa-Stonestreet *et al.*, 2010). The α -kafirins are therefore shielded away from exposure to hydrolytic enzymes, whilst the outer β - and γ -kafirins, which are rich in cysteines, form extensive disulphide bonds, which strongly resist proteolysis (Laidlaw *et al.*, 2010). As a result, the problem of protein digestibility in sorghum mainly arises from the nature of the kafirins and their organisation within the protein bodies (Wong *et al.*, 2009).

An extensive review of the factors that impact sorghum protein digestibility has been presented by Duodu *et al.*, (2003), and is divided into two main categories: endogenous or exogenous factors. The endogenous factors concern protein-to-protein interactions and as discussed above mainly involve considerations of disulphide crosslinking between the kafirins. The exogenous factors on the other hand, refer to the interactions of proteins with non-protein entities such as polyphenols, phytates, starch, lipids and cell wall components (de Mesa-Stonestreet *et al.*, 2010; Duodu *et al.*, 2003). The kafirins are known to form complexes with these components, which has the overall effect of reducing protein digestibility. Moreover, it has been shown that cooking further enhances this interaction, thereby compromising further the overall levels of protein digestibility. Amongst the exogenous factors, polyphenols (e.g. tannins) have a marked negative effect on the digestibility of sorghum kafirins because they are known to bind strongly to these proteins via hydrogen bonding and hydrophobic interactions (Butler *et al.*, 1984). In a report by Taylor *et al.*, (2007), it was found that protein digestibility was reduced by 50% due to the complexation of sorghum tannins with kafirins. Of the three main kafirin types, the γ -

kafirins were found to be most affected by tannin binding and this was suggested to be chiefly related to the high proline content of the γ -kafirins (Taylor *et al.*, 2007; de Mesa-Stonestreet *et al.*, 2010).

Phytic acid reacts in a similar way to the tannins, and has also been found to form insoluble complexes with sorghum kafirins (Ryden and Selvendran, 1993). However, because phytic acid is reduced in sorghum upon cooking, this helps to limit its effect on protein digestibility (de Mesa-Stonestreet *et al.*, 2010). Although much research has been centred on the inhibitory effect that protein has on starch digestibility (Ezeogu *et al.*, 2008), the converse has also been demonstrated in other studies (Duodu *et al.*, 2003; Wong *et al.*, 2009). Lastly, the interaction of sorghum proteins with various cell wall components is another important exogenous factor which reduces protein digestibility by limiting the accessibility of these cell-wall bound proteins to enzymatic breakdown (Bach Knudsen and Munck, 1985).

1.2.6.3 Modifying the Protein Body

With 80% of sorghum proteins locked in rigid spherical bodies, there is keen interest in understanding how these structures can be modified so as to release the nutritional potential of the bulk of the proteinaceous matter found in sorghum grain. In 2000, a study that analysed the microstructure of protein bodies from a highly digestible mutant, found that the protein bodies had a completely different shape in comparison to the normal cultivars (Oria *et al.*, 2000). The protein bodies from the mutant exhibited a highly irregular shape with deep invaginations or folds that reached into the central area of the protein body structure, thus giving rise to different haphazardly shaped lobes (Oria *et al.*, 2000). It was therefore theorised that the altered morphology of the protein bodies aided increased protein digestibility because the many invaginations increased the surface area and thereby facilitated improved enzymatic access for proteolytic activity to occur. Additionally, it was found that the localisation of the γ -kafirins in the mutant protein bodies had shifted. Instead of their normal position at the periphery of the protein body, in the highly digestible mutants, γ -kafirins were found at the base of the folded areas. This change therefore allowed the easily digestible α -kafirins to be more exposed to the action of digestive enzymes.

With the knowledge gained from the Oria *et al.*, (2000) study, genetic engineering techniques were soon developed which aimed to improve sorghum protein quality through

the suppression of the γ -kafirins. In 2007, as part of the Africa Biofortified Sorghum (ABS) Project, Zhao (2007) reported the use of RNA interference (RNAi) technology to reduce the synthesis of γ -kafirins in sorghum. The transgenic lines produced by this study were confirmed to have improved *in vitro* protein digestibility and also dramatically improved lysine content (Henley and Taylor, 2010). Further work on the suppression of kafirin synthesis in sorghum was achieved at the Centre for Scientific and Industrial Research (CSIR) in Pretoria, South Africa, as reported in the study of Da Silva *et al.*, (2011). In this study, the co-suppression of the α -, β - and γ -kafirin sub-classes resulted in transgenic sorghum lines with improved protein digestibility and essential amino acid scores. Later, the work of Grootboom *et al.*, (2014) pinpointed a minimal set of kafirin proteins that can be suppressed to obtain both improved digestibility and increased levels of the essential amino acid lysine. From Grootboom's study a selection of independent transgenic lines of interest were identified. An interest was piqued in these specific lines because of the results of Western Blot analyses that indicated a complete suppression of certain targeted kafirins. The findings published by Grootboom *et al.*, (2014) proposed that a combined suppression of γ -kafirins and α -kafirins is needed to bring about a marked increase in protein digestibility in sorghum; and furthermore that this improvement is attributable to changes in the protein body microstructure which render the available proteins more susceptible to proteolytic digestion.

According to the research studies outlined above, genetic engineering (GE) technology has proven to be a useful tool for improving the nutritive value of sorghum, through the suppression of certain kafirins. However, the uptake of such technology continues to face fierce opposition in the public sphere due to concerns over the safety of genetically modified (GM) crops and food products. In order to bring the transgenic sorghum lines into commercial production, extensive testing and further study is needed to ensure that there are no unintended changes in the grains that may constitute a risk to consumers or the environment.

1.2.7 The need for mineral biofortified pearl millet

Pearl millet plays a critical role as a nutritional source in dry and impoverished areas of the developing world. In major pearl millet growing areas of India, it is reported that the grain accounts for 19 – 63% of the total Fe intake and 16 – 56% of the total Zn intake from all food sources (Parthasarathy Rao *et al.*, 2006). The grain is also recognised as one of the

cheapest sources of dietary Fe and Zn compared to other cereals and vegetables (Rai *et al.*, 2013). Various reports indicate that about half of the world's population suffers from Fe and/or Zn deficiencies (Meenakshi *et al.*, 2010; Goudia and Hash, 2015). The consequences of Fe and Zn deficiency include: poor growth and compromised psychomotor development in children, reduced immunity, muscle wasting, sterility, increased morbidity and in acute cases even death (Rawat *et al.*, 2013). Given that Fe and Zn deficiencies rank high as major causes of mineral malnutrition amongst human populations, it is important to increase the cultivation of pearl millet varieties with high grain Fe and Zn densities (Rai *et al.*, 2013).

Importantly, a substantial amount of variability for Fe and Zn density in pearl millet germplasm has been reported (Velu *et al.*, 2007, 2008; Rai *et al.*, 2013, 2015). Initial screening of available accessions revealed ranges of 30 – 76 mg/kg for Fe and 25- 65 mg/kg for Zn, with the highest levels found in the *Injadi* germplasm (a group of landraces from Togo, Burkina Faso, Ghana and Benin) (Rai *et al.*, 2015). The *Injadi* germplasm has therefore been used extensively to develop high yielding breeding lines with target levels > 75 mg/kg Fe and > 55 mg/kg Zn in the pearl millet grain (Rai *et al.*, 2013). Thus far, several biofortified lines for high Fe and Zn densities have been developed, mainly as a result of the pearl millet improvement programme in place at the International Crops Research Institute for the Semi-Arid Tropics (ICRISAT), based in Patancheru, India (Rai *et al.*, 2013; Andersson *et al.*, 2017). These lines have been wholly developed using conventional breeding rather than transgenic approaches, with a major emphasis on improving the Fe content as a first priority, because of the more serious nature of Fe deficiency in comparison to Zn (Rai *et al.*, 2013). Fortunately, a high degree of correlation has been found between Fe and Zn grain content in pearl millet, which has allowed for the simultaneous selection of both traits in the pearl millet biofortification programme (Andersson *et al.*, 2017).

In any attempt to increase the Fe and Zn concentration in pearl millet, however, it is important to have a thorough understanding of how these minerals may be distributed and stored within the grain tissues. This knowledge is particularly valuable because pearl millet is often consumed decorticated, and therefore it is vital that an increased concentration of essential minerals is not only limited to the bran layers, but is also evident within the bulk of the starchy endosperm. Additionally, it is also of vital importance to consider the factors that increase the bioavailability of the minerals that are present. According to Hunt (2003)

it is often the inhibitors of mineral adsorption (such as anti-nutrients) and not poor dietary levels, which are at the root cause of mineral deficiencies. As a result, mineral biofortification strategies are also focused on the reduction of anti-nutrient factors that may be present in targeted food grains (Shahzad *et al.*, 2014).

1.3 Study aims and research objectives

The development of improved food resources, such as biofortified sorghum and pearl millet, is an important part of a global strategy to reduce the scourge of food insecurity and malnutrition. Although much scientific work has been done to produce protein biofortified sorghum and minerally enriched pearl millet lines, it is not always clear if the results of such biofortification efforts are as originally intended. This concern is of particular significance when genetic engineering technology forms part of the biofortification process. The present study was therefore initiated to examine some of the intended and perhaps non-intended effects that may arise as a result of grain biofortification.

Specifically, the research objectives of this study were:

1. To characterise differences between the parental control and transgenic protein biofortified sorghum grains (featuring kafirin suppression) in terms of several conventional physical and biochemical quality traits.
2. To evaluate the impact of targeted kafirin suppression on the transgenic sorghum grain protein profile, using one dimensional polyacrylamide gel electrophoresis (1D PAGE) and nanoflow liquid chromatography matrix-assisted laser desorption/ionization mass spectrometry (Nano-LC/MALDI-MS).
3. To interrogate differences in the mineral composition of the transgenic and non-transgenic grains using the bulk technique of inductively coupled plasma-atomic emission spectrometry (ICP-AES) or inductively coupled plasma-mass spectrometry (ICP MS), and using elemental mapping by micro-PIXE analysis.
4. To identify and explore significant differences in gene expression in the immature transgenic and non-transgenic control grains by means of RNAseq analysis and bioinformatics tools.

5. To evaluate differences in the mineral composition of pearl millet grains involved in mineral biofortification, using ICP- based methods and micro-PIXE analysis.

1.4 Dissertation organisation

This dissertation is organised into eight main chapters and is based on a compilation of research papers that were published or prepared for publication during the study period.

The outline of the chapters is as follows:

Chapter 1: General Introduction and Literature Review I: Biofortified Millets

Chapter 2: Literature Review II: An Introduction to Particle Induced X-ray Emission (PIXE) and other major analytical techniques used in this study

Chapter 3: A comparative study of selected physical and biochemical traits of wild-type and transgenic sorghum to reveal differences relevant to grain quality.

Chapter 4: A comparative evaluation of changes in the protein profile and the elemental composition of wild-type versus transgenic sorghum grain.

Chapter 5: A preliminary report of the use of RNA seq to examine changes in the gene expression profile of wild-type versus transgenic sorghum grains.

Chapter 6: Micro-PIXE mapping of mineral distribution in the mature grain of two pearl millet cultivars.

Chapter 7: A comparative study of tissue-specific differences in the mineral content of biofortified and conventional pearl millet grain using micro-PIXE analysis.

Chapter 8: Conclusions and Future work.

References

- Abdelrahman A, Hosene RC, Varriano-Marston E. 1984. The proportion of chemical compositions of hand dissected anatomical parts. *Journal of Cereal Science* 2: 127-133.
- Afify AE-MMR, El-Beltagi HS, Abd El-Salam SM, Omran AA. 2011. Bioavailability of iron, zinc, phytate and phytase activity during soaking and germination of white sorghum varieties. *PLoS ONE* 6(10): e25512. URL: <https://doi.org/10.1371/journal.pone.0025512>.
- Ahmed MM, Sanders JH, Nell WT. 2000. New sorghum and millet cultivar introduction in Sub-Saharan Africa: impacts and research agenda. *Agricultural Systems* 64: 55–65.
- Akwei I. 2017. Reality of the worst drought since 1945 peaking in parts of Africa. *Africanews.com*; URL <http://www.africanews.com/2017/03/17/depth-of-the-worst-drought-since-1945-peaking-in-parts-of-africa/>. Accessed 22/07/2017.
- Akombi BJ, Agho KE, Merom D, Renzaho AM, Hall JJ. 2017. Child malnutrition in Sub-Saharan Africa: A meta-analysis of demographic and health surveys (2006-2016). *PLoS ONE* 12(5): e0177338. <https://doi.org/10.1371/journal.pone.0177338>.
- Alfthan G, Eurola M, Ekholm P, Venäläinen ER, Root T, Korkalainen K, Hartikainen H, Salminen P, Hietaniemi V, Aspila P, Aro A. 2015. Effects of nationwide addition of selenium to fertilizers on foods, and animal and human health in Finland: from deficiency to optimal selenium status of the population. *Journal of Trace Elements in Medicine and Biology* 31: 142-147.
- Andersson MS, Saltzman A, Virk PS, Pfeiffer WH. 2017. Progress update: Crop development of biofortified staple food crops under HarvestPlus. *African Journal of Food, Agriculture, Nutrition and Development* 17(2): 11905-11935.
- Andrews DJ, Rajewski JF, Kumar KA. 1993. Pearl millet: New Feed Grain Crop. In: Janick J, Simon JE (Eds). *New Crops*. pp 198-208. Wiley, New York, USA.
- Archana SS, Kawatra A. 1998. Reduction of polyphenol and phytic acid content of pearl millet grains by malting and blanching. *Plant Foods for Human Nutrition* 53: 93–98.
- Arnon I. 1972. Crop production in dry regions. Volume II Systematic treatment of the principal crops. pp 92-145. Leonard Hill, London, UK.
- Aruna Reddy C. 2017. Millets – The Miracle Grains. In: Patil JV (Ed) *Millets and Sorghum: Biology and Genetic Improvement*. pp xxi-xxxvi. John Wiley and Sons Ltd, West Sussex, UK.
- Awika JM, Rooney LW. 2004. Sorghum phytochemicals and their potential impact on human health. *Phytochemistry* 65: 1199-1221.
- Awika JM, Rooney LW, Wu X, Prior RL, Cisneros-Zevallos L. 2003. Screening methods to measure antioxidant activity of sorghum (*Sorghum bicolor*) and sorghum products. *Journal of Agricultural and Food Chemistry* 51: 6657-6662.
- Bach Knudsen KE, Munck L. 1985. Dietary fibre contents and compositions of sorghum and sorghum-based foods. *Journal of Cereal Science* 3(2): 153-164.
- Bai C, Twyman RM, Farre G, Sanahuja G, Christou P, Capell T, Zhu C. 2011. A golden era-pro-vitamin A enhancement in diverse crops. *In Vitro Cellular and Developmental Biology – Plant* 47(2): 205–221.

- Bain LE, Awah PK, Geraldine N, Kindong NP, Sigal Y, Bernard N, Tanjeko AT. 2013. Malnutrition in Sub – Saharan Africa: burden, causes and prospects. *Pan African Medical Journal* 15:120, <http://doi:10.11604/pamj.2013.15.120.2535>.
- Barrion SC. 2008. Pearl millet milling. Comparison between traditional Namibian fermentation-, semi-wet milling and dry milling. MSc (Agric) Dissertation, University of Pretoria, Pretoria.
- Bean SR, Ioerger BP, Blackwell DL. 2011. Separation of kafirins on surface porous reverse-phase high performance liquid chromatography columns. *Journal of Agricultural and Food Chemistry* 59(1): 85-91.
- Belton PS, Delgado I, Halford NG, Shewry PR. 2006. Kafirin structure and functionality. *Journal of Cereal Science* 44: 272-286.
- Belton PS, Taylor JRN. 2004. Sorghum and millets: protein sources for Africa. *Trends in Food Science & Technology* 15: 94–98.
- Bennett MD, Bhandol P, Leitch IJ. 2000. Nuclear DNA amounts in angiosperms and their modern uses – 807 new estimates. *Annals of Botany* 86: 859-909.
- Berwal MK, Chugh LK, Goyal P, Kumar R. 2016. Variability in total phenolic content of pearl millet genotypes: inbreds and designated B-lines. *Journal of Agriculture and Ecology* 1: 41-49.
- Beta T, Rooney LW, Marovatsanga LT, Taylor JRN. 1999. Phenolic compounds and kernel characteristics of Zimbabwean sorghums. *Journal of the Science of Food and Agriculture* 79: 1003-1010.
- Bohn L, Meyer AS, Rasmussen. 2008. Phytate: impact on environment and human nutrition: a challenge for molecular breeding. *Journal of Zhejiang University Science B* 9(3): 165-191.
- Bouis HE, Hotz C, McClafferty B, Meenakshi JV, Pfeiffer WH. 2011. Biofortification: a new tool to reduce micronutrient malnutrition. *Food and Nutrition Bulletin* 32: S31-S40.
- Bravo L. 1998. Polyphenols: chemistry, dietary sources, metabolism and nutritional significance. *Nutrition Reviews* 56:317–333.
- Butler LG, Riedl DJ, Lebyk DG, Blytt HJ. 1984. Interaction of proteins with sorghum tannin: mechanism, specificity and significance. *Journal of the American Oil Chemists Society* 61: 916-920.
- Byrt CS, Grof CPL, Furbank RT. 2011. C4 plants as biofuel feedstocks: optimising biomass production and feedstock quality from a lignocellulosic perspective. *Journal of Integrative Plant Biology* 53: 120–135.
- Calderini DF, Ortiz-Monasterio I. 2003. Are synthetic hexaploids a means of increasing grain element concentrations in wheat? *Euphytica* 134: 169-178.
- Coulibaly A, Kouakou B, Chen J. 2011. Phytic acid in cereal grains: structure, healthy or harmful ways to reduce phytic acid in cereal grains and their effects on nutritional quality. *American Journal of Plant Nutrition and Fertilization Technology* 1: 1-22.
- Choi SJ, Woo HD, Ko SH, Moon TW. 2008. Confocal laser scanning microscopy to investigate the effect of cooking and sodium bisulfite on in vitro digestibility of waxy sorghum flour. *Cereal Chemistry* 85(1): 65-69.
- Chung K-T, Tit YW, Cheng IW, Yao-Wen H, Yuan L. 1998. Tannins and human health: a review. *Critical Reviews in Food Science and Nutrition* 38 (6): 421–464.

- Dahlberg J, Wasylikowa K. 1996. Image and statistical analyses of early sorghum remains (8000 BP) from the Nabta Playa archaeological site in the Western Desert, Southern Egypt. *Vegetation History and Archaeobotany* 5(4): 293-299.
- Da Silva LS, Jung R, Zhao Z, Glassman K, Taylor J, Taylor JRN. 2011. Effect of suppressing the synthesis of different kafirin sub-classes on grain endosperm texture, protein body structure and protein nutritional quality in improved sorghum lines. *Journal of Cereal Science* 54(1): 160-167.
- de Mesa-Stonestreet NJ, Alavi S, Bean SR. 2010. Sorghum proteins: the concentration, isolation, modification and food applications of kafirins. *Journal of Food Science* 75(5): 90-104.
- de Valença AW, Bake A, Brouwer ID, Giller KE. 2017. Agronomic biofortification of crops to fight hidden hunger in sub-Saharan Africa. *Global Food Security* 12: 8-14.
- Dicko MH, Gruppen H, Traore AS, Voragen AGJ, van Berkel WJH. 2006. Sorghum grain as human food in Africa: relevance of content of starch and amylose activities. *African Journal of Biotechnology* 5(5): 384-395.
- Dillon SL, Shapter FM, Henry RJ, Cordeiro G, Izquierdo L, Lee LS. 2007. Domestication of crop improvement: genetic resources for Sorghum and Saccharum (Andropogoneae). *Annals of Botany* 100(5): 975-989.
- Dixon RA. 2004. Phytoestrogens. *Annual Review of Plant Physiology and Plant Molecular Biology* 55: 225-261.
- Dlamini NR, Taylor JRN, Rooney LW. 2007. The effect of sorghum type and processing on the antioxidant properties of African sorghum-based foods. *Food Chemistry* 105: 1412-1419.
- Doggett E. 1988. Sorghum. John Wiley & Sons, New York, USA.
- Doherty C, Faubion JM, Rooney LW. 1982. Semiautomated determination of phytate in sorghum and sorghum products. *Cereal Chemistry* 59: 373 – 377.
- Duodu KG, Taylor JRN, Belton PS, Hamaker BR. 2003. Factors affecting sorghum protein digestibility. *Journal of Cereal Science* 38: 117-131.
- Dyakar Rao B, Malleshi NG, Annor GA, Patil JV. 2016. Production and utilisation of millets. In: Dyakar Rao B, Malleshi NG, Annor GA, Patil JV (Eds). *Millet Value Chain for Nutritional Security*. pp 1-17. CABI publishers, Oxfordshire, UK.
- Dykes L, Rooney LW. 2006. Sorghum and millet phenols and antioxidants. *Journal of Cereal Science* 44: 236–251.
- Earp CF, McDonough CM, Rooney LW. 2004. Microscopy of pericarp development in the caryopsis of *Sorghum bicolor* (L.) Moench. *Journal of Cereal Science* 39: 21- 27.
- Enneking D, Wink M. 2000. Towards the elimination of antinutritional factors in grain legumes. In: Knight R. (Ed.) *Linking Research and Marketing Opportunities for Pulses in the 21st Century*. Proceedings of the Third International Food Legume Research Conference, Adelaide 1997. *Current Plant Science and Biotechnology in Agriculture*. 34: 375- 384.
- Ezeogu LI, Duodu KG, Emmambux MN, Taylor JRN. 2008. Influence of cooking conditions on the protein matrix of sorghum and maize endosperm flours. *Cereal Chemistry* 85(3): 397-402.

- Falmata AS, Modu S, Zainab MA, Bintu BP, Yagana S. 2013. The soaking and dehulling effects on chemical composition, tannins and mineral elements content of five local varieties of sorghum. *Scholarly Journal of Agricultural Science* 3(4): 126-131.
- Farré G, Twyman RM, Zhu C, Capell T, Christou P. 2011. Nutritionally enhanced crops and food security: scientific achievements versus political expediency. *Current Opinion in Biotechnology* 22: 245-251.
- Food and Agricultural Organisation of the United Nations (FAO). 2015. The State of Food Insecurity in the World 2015. Meeting the 2015 international hunger targets: taking stock of uneven progress, Rome. [Internet document] URL <http://www.fao.org/3/a-i4671e.pdf>. Accessed 22/06/2017.
- FAO. 2014. URL <http://www.fao.org/faostat/en/#data/QC>. Accessed 23/06/2017.
- FAO. 1995. Sorghum and Millet in Human Nutrition. FAO Food and Nutrition Series, No. 27, Rome. URL <http://www.fao.org/docrep/T0818E/T0818E0b.htm>. Accessed 9/08/2017.
- Fürstenberg-Hägg J, Zagrobelny M, Bak S. 2013. Plant defence against insect herbivores. *International Journal of Molecular Sciences* 14: 10242-10297.
- Gardner, B. 2013. *Global Food Futures: Feeding the World in 2050*, London, Bloomsbury, 2013.
- Ghasemzadeh A, Ghasemzadeh N. 2011. Flavonoids and phenolic acids: role and biochemical activity in plants and humans. *Journal of Medicinal Plants Research* 5(31): 6697-6703.
- Gómez-Galera S, Rojas E, Sudhakar D, Zhu C, Pelacho AM, Capell T, Christou P. 2010. Critical evaluation of strategies for mineral fortification of staple crops. *Transgenic Research* 19:165–180.
- Goudia BD, Hash CT. 2015. Breeding for high grain Fe and Zn levels in cereals. *International Journal of Innovation and Applied Studies* 12(2): 342-354.
- Grases F, Sanchis P, Perello J, Isern B, Prieto RM, Fernandez-Palomeque C, Saus C. 2008. Phytate reduces age-related cardiovascular calcification. *Frontiers in Bioscience* 13:7115-7122.
- Grootboom AW, Mkhonza NL, Mbambo Z, O’Kennedy MM, da Silva LS, Taylor J, Taylor JRN, Chikwamba R, Mehlo L. 2014. Co-suppression of synthesis of major α -kafirin sub-class together with γ -kafirin-1 and γ -kafirin-2 required for substantially improved protein digestibility in transgenic sorghum. *Plant Cell Reports* 33: 521-537.
- Gumede HF, Ratta N. 2014. Antinutritional factors in plant foods: potential health benefits and adverse effects. *Global Advanced Research Journal of Food Science and Technology* 3(4): 103-117.
- Gupta RK, Singh Gagoliya S, Kumar Singh N. 2015. Reduction of phytic acid and enhancement of bioavailable micronutrients in food grains. *Journal of Food Science and Technology* 52(2): 676-684.
- Hamaker BR, Mohamed AA, Habben JE, Huang CP, Larkins BA. 1995. Efficient procedure for extracting maize and sorghum kernel proteins reveals higher prolamin contents than conventional method. *Cereal Chemistry* 72: 583–588.
- Hamilton RI, Subramanian B, Narayana Reddy M, Hanumantha Rao C. 1982. Compensation in grain yield components in a panicle of rainfed sorghum. *Annals of Applied Biology* 101: 119-125.

- Henley EC, Taylor JRN. 2010. The importance of dietary protein in human health: combating protein deficiency in Sub-Saharan Africa through transgenic biofortified sorghum. *Advances in Food and Nutrition Research* 60: 21-52.
- Hoseney RC, Davis AB, Herbers LH. 1974. Pericarp and endosperm structure of sorghum grain shown by scanning electron microscopy. *Cereal Chemistry* 51: 552–558.
- Hunt JR. 2003. Bioavailability of iron, zinc and other trace minerals from vegetarian diets. *American Journal of Clinical Nutrition* 78: 633-639.
- Hwang KT, Cuppett SL, Weller CL, Hanna MA. 2002. Properties, composition and analysis of grain sorghum wax. *Journal of the American Oil Chemists Society* 79(6): 521-527.
- Jain RK, Bai S. 1997. Properties of pearl millet. *Journal of Agricultural Engineering Research* 66(2): 85-91.
- Johns CO, Brewster JF. 1916. Kafirin, an alcohol-soluble protein from Kafir and *Andropogon sorghum*. *Journal of Biological Chemistry* 28: 59-65.
- Joy EJM, Stein AJ, Young SD, Ander EL, Watts MJ, Broadley MR. 2015. Zinc-enriched fertilisers as a potential public health intervention in Africa. *Plant Soil* 389(1-2): 1-24.
- Jukanti AK, Laxmipathi Gowda CL, Rai KN, Manga VK, Bhatt RK. 2016. Crops that feed the world 11. Pearl Millet (*Pennisetum glaucum* L.): an important source of food security, nutrition and health in the arid and semi-arid tropics. *Food Security* [Internet document] URL <http://www.bashanfoundation.org/gowda/2016.-Gowda-FS.pdf>. Accessed 6/06/2017.
- Kasala ER, Bodduluru LN, Baria CC, Gogoi R. 2016. Antioxidant and antitumor efficacy of luteolin, a dietary flavone on benzo(a)pyrene-induced experimental lung carcinogenesis. *Biomedicine and Pharmacotherapy* 82: 568-577.
- Kent NL, Evers AD. 1994. *Technology of Cereals: An introduction for students of Food Science and Agriculture*, 4th Ed. pp 129- 169. Pergamon, Oxford, UK.
- Khetarpaul N, Chauhan BM. 1990. Effects of germination and pure culture fermentation by yeasts and Lactobacilli on phytic acid and polyphenol content of pearl millet. *Journal of Food Science* 55:1180-1182.
- Krishnan HB, White JA, Pueppke SG. 1989. Immunocytochemical analysis of protein body formation in seeds of *Sorghum bicolor*. *Canadian Journal of Botany* 67: 2850-2856.
- Kil HY, Seong ES, Ghimire BK, Chung IM, Kwon SS, Goh EJ, Heo K, Kim HM, Lim JD, Lee D, Yu CY. 2009. Antioxidant and antimicrobial activities of crude sorghum extract. *Food Chemistry* 115(4): 1234-1239.
- Kim E, Kim S, Park Y. 2015. Sorghum extract exerts cholesterol-lowering effects through the regulation of hepatic cholesterol metabolism in hypercholesterolemic mice. *International Journal of Food Sciences and Nutrition* 66(3): 308-313.
- Kim J, Park Y. 2012. Anti-diabetic effect of sorghum extract on hepatic gluconeogenesis of streptozotocin-induced diabetic rats. *Nutrition and Metabolism* 9: 106. URL <https://doi.org/10.1186/1743-7075-9-106>.
- Klopfenstein CF, Hoseney RC .1995. Nutritional properties of sorghum and millet. In: Dendy DAV (Ed) *Sorghum and Millets: Chemistry and Technology*. pp 125-168. AACC International: St. Paul, MN, USA.

- Kumar H, Lim H-W, More SV, Kim B-W, Koppula S, Kim IS, Choi D-K. 2012. The role of free radicals in the aging brain and Parkinson's disease: convergence and parallelism. *International Journal of Molecular Sciences* 13(8): 10478-10504.
- Laidlaw HK, Mace ES, Williams SB, Sakrewski K, Mudge AM, Prentis PJ, Jordan DR, Godwin ID. 2010. Allelic variation of the β -, γ - and δ -kafirin genes in diverse sorghum genotypes. *Theoretical and Applied Genetics* 121: 1227-1237.
- Lattanzio V, Kroon PA, Quideau S, Treutter D. 2009. Plant phenolics – secondary metabolites with diverse functions. In: Daayf F, Lattanzio V (Eds). *Recent advances in polyphenol research Vol 1*. pp 1-35. Wiley-Blackwell Publishing, Oxford, UK.
- MacLean WC, Lopez de Romana G, Placko RP. 1981. Protein quality and digestibility of sorghum in preschool children: balances studies and plasma free amino acids. *Journal of Nutrition* 111: 1928-1936.
- Manning K, Pelling R, Higham T, Schwenniger J-L, Fuller DQ. 2011. 4500-Year old domesticated pearl millet (*Pennisetum glaucum*) from the Tilemsi Valley, Mali: New insights into an alternative cereal domestication pathway. *Journal of Archaeological Science* 38: 312-322.
- Martel E, De Ney D, Silijak-Yakovlev S, Brown S, Sarr A. 1997. Genome size variation and basic chromosome number in pearl millet and fourteen related *Pennisetum* species. *Journal of Heredity* 88: 139-143.
- Masih I, Maskey S, Mussa F, Trambauer P. 2014. A review of droughts on the African continent: a geospatial and long-term perspective. *Hydrology and Earth Systems Sciences* 18(9): 3635–3649.
- Mason SC, Maman N, Pale S. 2015. Pearl millet production practices in semi-arid West Africa: a review. *Experimental Agriculture* 51(4): 501-521.
- Masuda H, Suzuki M, Morikawa KC, Kobayashi T, Nakanishi H, Takahashi M, Saigusa M, Mori S, Nishizawa NK. 2008. Increase in iron and zinc concentrations in rice grains via the introduction of barley genes involved in phyto siderophore synthesis. *Rice* 1:100–108.
- Masuda H, Kobayashi T, Ishimaru Y, Takahashi M, Aung MS, Nakanishi H, Mori S, Nishizawa NK. 2013. Iron-biofortification in rice by the introduction of three barley genes participated in mugineic acid biosynthesis with soybean ferritin gene. *Frontiers in Plant Science* 4:132. doi: 10.3389/fpls.2013.00132.
- Mathur PN. 2012. Global strategy for the ex situ conservation of pearl millet and its wild relatives. Strategy Document of the Global Crop Diversity Trust. [Internet document] URL www.croptrust.org. Accessed 29/06/2017.
- Matz SA. 1991. *Cereals as Food and Feed*. Vam Nostrand Reinhold Publishers, New York.
- McDonough CM, Rooney LW. 1989. Structural characteristics of *Pennisetum americanum* (pearl millet) using scanning electron and fluorescence microscopy. *Food Structure* 8(1): Article 16. URL <http://digitalcommons.usu.edu/foodmicrostructure/vol8/iss1/16>
- Meenakshi JV, Johnson NL, Manying VM, DeGroot H, Javelosa J, Yanggen DR, Naher F, Gonzalez C, Garcia J, Meng E. 2010. How cost-effective is biofortification in combating micronutrient malnutrition? An Ex ante assessment. *World Development* 38(1): 64-75.
- Moreta DE, Mathur PN, van Zonneveld M, Amaya K, Arango J, Gomez Selvaraj M, Dedicova B. 2015. Current issues in cereal crop biodiversity. *Advances in Biochemical Engineering/ Biotechnology* 147: 1-36.

- Mullet J, Morishige D, McCormick R, Truong S, Hilley J, McKinley B, Anderson R, Olson SN, Rooney W. 2014. Energy Sorghum—a genetic model for the design of C4 grass bioenergy crops. *Journal of Experimental Botany* 65(13): 3479-3489.
- Nambiar VS, Sareen N, Daniel M, Gallego EB. 2012. Flavonoids and phenolic acids from pearl millet (*Pennisetum glaucum*) based foods and their functional implications. *Functional Foods in Health and Disease* 2(7): 251-264.
- Nambiar VS, Dhaduk JJ, Sareen N, Shahu T, Desai R. 2011. Potential functional implications of pearl millet (*Pennisetum glaucum*) in health and disease. *Journal of Applied Pharmaceutical Science* 1(10): 62-67.
- Naqvi S, Zhu C, Farré G, Ramessar K, Bassie L, Breitenbach J, Perez Conesa D, Ros G, Sandmann G, Capell T, Christou P. 2009. Transgenic multivitamin corn through biofortification of endosperm with three vitamins representing three distinct metabolic pathways. *Proceedings of the National Academy of Sciences USA* 106:7762–7767.
- Neelamraju S, Mallikarjuna Swamy BP, Kaladhar K, Anuradha K, Venkateshwar Rao Y, Batchu AK. 2012. Increasing iron and zinc in rice grains using deep water rices and wild species – identifying genomic segments and candidate genes. *Quality Assurance and Safety Assurance of Crops and Foods* 4(3): 138-138.
- Norazalina S, Mohd.-Esa N, Hairuszah I, Norashareena MS. 2010. Anticarcinogenic efficacy of phytic acid extracted from rice bran on azoxymethane-induced colon carcinogenesis in rats. *Experimental and Toxicological Pathology* 62: 259-268.
- Ogbonna AC, Abuajah CI, Ide EO, Udofia US. 2012. Effect of malting conditions on the nutritional and anti-nutritional factors of sorghum grist. *Food Technology* 36: 64-72.
- O’Kennedy MM, Grootboom A, Shewry PR. 2006. Harnessing sorghum and millet biotechnology for food and health. *Journal of Cereal Science* 44: 224-235.
- Onomi S, Okazaki Y, Katayama T. 2004. Effect of dietary level of phytic acid on hepatic and serum lipid status in rats fed a high-sucrose diet. *Bioscience Biotechnology and Biochemistry* 68(6):1379–1381.
- Oomah BD, Blanchard C, Balasubramanian P. 2008. Phytic acid, phytase, minerals, and antioxidant activity in Canadian dry bean (*Phaseolus vulgaris* L.) cultivars. *Journal of Agricultural and Food Chemistry* 56(23): 11312-11319.
- Oria MP, Hamaker BR, Axtell JD, Huang CP. 2000. A highly digestible sorghum mutant cultivar exhibits a unique folded structure of endosperm protein bodies. *Proceedings of the National Academy of Sciences, USA* 97: 5065-5070.
- Ortiz-Monasterio JI, Palacios-Rojas N, Meng E, Pixley K, Trethowan R, Peña RJ. 2007. Enhancing the mineral and vitamin content of wheat and maize through plant breeding. *Journal of Cereal Science* 46(3): 293-307.
- Pahoja VM. 2012. Properties of lipase from pearl millet seedling. *Pakistan Journal of Biochemistry and Molecular Biology* 45(1): 26-30.
- Paterson AH, Bowers JE, Bruggmann R, Dubchak I, Grimwood J, Gundlach H, Haberler G, Hellsten U, Mitros T, Poliakov A, Schmutz J, Spannagl M, Tang H, Wang X, Wicker T, Bharti AK, Chapman J, Feltus FA, Gowik U, Grigoriev IV, Lyons E, Maher CA, Martis M, Narechania A, Otiillar RP, Penning BW, Salamov AA, Wang Y, Zhang L, Carpita NC, Freeling M, Gingle AR, Hash CT, Keller B, Klein P, Kresovich S, McCann MC, Ming R,

- Peterson DG, ur-Rahman M, Ware D, Westhoff P, Mayer K, Messing J, Rokhsar DS. 2009. The *Sorghum bicolor* genome and the diversification of grasses. *Nature* 457: 551-556.
- Parthasarathy Rao P, Birthal PS, Reddy BVS, Rai KN, Ramesh S. 2006. Diagnostics of sorghum and pearl millet grains-based nutrition in India. *International Sorghum and Millets Newsletter* 46: 93-96.
- Pasha I, Riaz A, Saeed M, Randhawa MA. 2014. Exploring the antioxidant perspective of sorghum and millet. *Journal of Food Processing and Preservation* 39(6): 1089-1097.
- Pereira DM, Valentão P, Pereira JA, Andrade PB. 2009. Phenolics: from Chemistry to Biology. *Molecules* 14: 2202-2211.
- Pontoppidan K, Pettersson D, Sandberg AS. 2007. The type of thermal feed treatment influences the inositol phosphate composition. *Animal Feed Science and Technology* 132(1-2): 137-147.
- Price HJ, Dillon SL, Hodnett G, Rooney WL, Ross L, Johnston JS. 2005. Genome evolution in the genus *Sorghum* (Poaceae). *Annals of Botany* 95(1): 219-227.
- Proietti I, Frazzoli C, Mantovani A. 2015. Exploiting the nutritional value of staple foods in the world's semi-arid areas: risks, benefits, challenges and opportunities of sorghum. *Healthcare* 3(2): 172-193.
- Radhouane L, Fattouch S, Tlili I, Ilahy R. 2013. Antioxidant and polyphenol oxidase activity of some Tunisian pearl millet (*Pennisetum glaucum* (L.) R.Br.) ecotypes. *Food (Global Science Books)* 7: 36-40.
- Rai KN, Velu G, Govindaraj M, Upadhyaya HD, Rao AS, Shivade H, Reddy KN. 2015. *Iniadi* pearl millet germplasm as a valuable genetic resource for high grain iron and zinc densities. *Plant Genetic Resources C* 13(1):75-82.
- Rai KN, Yadav OP, Rajpurohit BS, Patil HT, Govindaraj M, Khairwal IS, Rao AS, Shivade H, Pawar VY, Kulkarni MP. 2013. Breeding pearl millet cultivars for high iron density with zinc density as an associated trait. *Journal of Semi-Arid Tropical Agricultural Research* 11: 1-7.
- Rai KN, Murty DS, Andrews DJ, Bramel-Cox PJ. 1999. Genetic enhancement of pearl millet and sorghum for the semi-arid tropics of Asia and Africa. *Genome* 42(4): 617-628.
- Rajendrakumar P. 2017. Molecular markers for the genetic improvement of millets. In: Patil JV (Ed) *Millets and Sorghum: Biology and Genetic Improvement*. pp 341-394. John Wiley and Sons Ltd, West Sussex, UK. doi: 10.1002/9781119130765.ch13
- Ratnavathi CV, Komala VV. 2016. Sorghum Grain Quality. In: Ratnavathi CV, Patil JV, Chavan UD (Eds) *Sorghum Biochemistry: An industrial perspective*. pp 1-62. Academic Press, London, UK.
- Rawat N, Neelam K, Tiwari VK, Dhaliwal HS. 2013. Biofortification of cereals to overcome hidden hunger. *Plant Breeding* 132: 437-445.
- Rooney LW, Miller FR. 1982. Variation in the structure and kernel characteristics of sorghum. In: Mertin JV (Ed) *Proceedings of the International Symposium on Sorghum Grain Quality*. pp 143-162. ICRISAT, Patancheru, India.
- Rooney LW, Murty DS. 1982. Evaluation of sorghum food quality. In: House LR, Mughogho LK, Peacock JM, Mertin JV (Eds). *Sorghum in the Eighties. Proceedings of an International Symposium on Sorghum*. pp 571-588. ICRISAT, Patancheru, India.

- Ryden P, Selvendran RR. 1993. Phytic acid: properties and determination. In: Macrae R, Robinson RK, Sadler MJ (Eds) Encyclopedia of Food Science, Food Technology and Nutrition. pp 3582-3587. Academic Press, London, UK.
- Saballos A. 2008. Development and utilisation of sorghum as a bioenergy crop. In: Vermerris W (Ed) Genetic Improvement of Bioenergy Crops. pp 211-248. Springer Verlag, New York, USA.
- Saito Y, Shigemitsu T, Tanaka K, Morita S, Satoh S, Masumura T. 2010. Ultrastructure of mature protein body in the starchy endosperm of the dry cereal grain. Bioscience, Biotechnology and Biochemistry 74(7): 1485-1487.
- Sambo BE. 2014. Endangered, neglected indigenous resilient crops: a potential against climate change impact for sustainable crop productivity and food security. IOSR Journal of Agriculture and Veterinary Science 7: 34-41.
- Sánchez-Ken JG, Clark LG. 2010. Phylogeny and a new tribal classification of the Panicoideae s.l. (Poaceae) based on plastid and nuclear sequence data and structural data. American Journal of Botany 97(10):1732-1748.
- Sanjana Reddy P. 2017a. Sorghum, *Sorghum bicolor* (L.) Moench. In: Patil JV (Ed) Millets and Sorghum: Biology and Genetic Improvement. pp 1-48. John Wiley and Sons Ltd, West Sussex, UK.
- Sanjana Reddy P. 2017b. Pearl millet, *Pennisetum glaucum* (L.) R. Br. In: Patil JV (Ed) Millets and Sorghum: Biology and Genetic Improvement. pp 49-86. John Wiley and Sons Ltd, West Sussex, UK.
- Sankara Rao DS, Deosthale YG. 1983. Mineral composition, ionizable iron and soluble zinc in malted grains of pearl millet and *ragi*. Food Chemistry 11:217–223.
- Sathe AY. 1999. A First Course in Food Analysis. pp 5-19. New Age International Publishers, New Delhi, India.
- Shahzad Z, Rouached H, Rakha A. 2014. Combating mineral malnutrition through iron and zinc biofortification of cereals. Comprehensive Reviews in Food Science and Food Safety 13: 329-346.
- Shegro A, Shargie NG, Van Biljon A, Labuschagne MT. 2012. Diversity in starch, protein and mineral composition of sorghum landrace accessions from Ethiopia. Journal of Crop Science and Biotechnology 15: 275-280.
- Shepherd T, Wynne Griffiths D. 2006. The effects of stress on plant cuticular waxes. New Phytologist 171(3): 469-499.
- Shewry PR. 2007. Improving the protein content and composition of cereal grain. Journal of Cereal Science 46: 239-250.
- Shewry PR, Casey R. 1999. Seed proteins. Kluwer Academic Publishers, Dordrecht, The Netherlands.
- Shewry PR, Tatham AS. 1990. The prolamin proteins of cereal seeds: structure and evolution. Biochemical Journal 267: 1-12.
- Shivran AC. 2016. Biofortification for nutrient rich millets. In: Singh U, Praharaj CS, Singh SS, Singh NP (Eds) Biofortification of Food Crops. pp 409-420. Springer, New Delhi, India.

- Sehgal S, Kawatra A, Singh G. 2004. Recent technologies in pearl millet and sorghum processing and food product development. *Alternative uses of sorghum and pearl millet in Asia: Proceedings of an expert meeting, 1-4 July, 2003.* pp 60-92. ICRISAT, Patancheru, India.
- Serna-Saldivar S, Rooney LW. 1995. Structure and Chemistry of Sorghum and Millets. In: Dendy DA (Ed) *Sorghum and the Millets—Chemistry and Technology.* pp 69-124. American Association of Cereal Chemists, St. Paul, MN, USA.
- Singh HP, Lohithaswa HC. 2006. Genome mapping and molecular breeding in plants, cereals and millets. In: Kole C. (Ed.), *Sorghum.* pp 257-302. Springer Verlag, Berlin, Germany.
- Slavin J. 2004. Whole grains and human health. *Nutrition Research Reviews* 17 doi: 10.1079/NRR200374.
- Soetan K, Oyewole O. 2009. The need for adequate processing to reduce the antinutritional factors in plants used as human foods and animal feeds: A review. *African Journal of Food Science* Vol. 3 (9): 223-232.
- Stefoska-Needham A, Beck EJ, Johnson SK, Tapsell LC. 2015. Sorghum: An Underutilized Cereal Whole Grain with the Potential to Assist in the Prevention of Chronic Disease. *Food Reviews International* 31(4): 401-437.
- Taylor JRN. 2016. Pearl millet: Overview. In: Wrigley CW, Corke H, Seetharaman K, Faubion J (Eds). *Encyclopedia of Food Grains, Second Edition.* pp 190-198. Academic Press, Oxford, UK.
- Taylor JRN, Duodu KG. 2017. Sorghum and millets: grain quality characteristics and management of quality requirements. In: Wrigley C, Batey I, Miskelly D (Eds) *Cereal grains: assessing and managing quality.* pp 317-352. Woodhead Publishing, Duxford, UK.
- Taylor JRN, Emmambux MN. 2008. Products containing other specialty grains: sorghum, the millets and pseudocereals. In: Hamaker BR (Ed) *Technology of Functional Cereal Products.* pp 281-225. Woodhead Publishers, Cambridge, UK.
- Taylor JRN, Belton PS. 2002. Sorghum. In: Belton PS, Taylor JRN (Eds) *Pseudocereals and less common cereals: grain properties and utilization potential.* pp 25-82. Springer-Verlag: Berlin, Germany.
- Taylor JRN, Schüssler L. 1986. The protein compositions of the different anatomical parts of sorghum grain. *Journal of Cereal Science* 4: 361-369.
- Taylor JRN, Belton PS, Beta T, Duodu KG. 2014. Increasing the utilisation of sorghum, millets and pseudocereals: developments in the science of their phenolic phytochemicals, biofortification and protein functionality. *Journal of Cereal Science* 59(3): 257-275.
- Taylor JRN, Barrion SC, Rooney LW. 2010. Pearl millet – new developments in ancient food grain. *Cereal Food World* 55(1): 16-19.
- Taylor JRN, Schüssler L, Liebenberg N. 1985. Protein body formation in the starchy endosperm of developing Sorghum bicolor (L.) Moench seeds. *South African Journal of Botany* 51: 35-40.
- Taylor JRN, Novellie L, Liebenberg N.v.d.W. 1984. Sorghum protein body composition and ultrastructure. *Cereal Chemistry* 61: 69-73.
- Taylor J, Bean SR, Ioerger BP, Taylor JRN. 2007. Preferential binding of sorghum tannins with gamma-kafirin and the influence of tannin binding on kafirin digestibility and biodegradation. *Journal of Cereal Science* 46: 22-31.

- Turner ND, Diaz A, Taddeo SS, Vanamala J, McDonough CM, Dykes L, Murphy ME, Carroll RJ, Rooney LW. 2006. Bran from black or brown sorghum suppresses colon carcinogenesis. *Federation of American Societies for Experimental Biology* 20: A599
- Upadhyaya HD, Reddy KN, Sastry D. 2008. Regeneration guidelines: pearl millet. In: Dulloo ME, Thormann I, Jorge MA, Hanson J (Eds) *Crop specific regeneration guidelines*, CGIAR System-wide Genetic Resource Programme, Rome, Italy. [Internet document] URL http://cropgenebank.sgrp.cgiar.org/images/file/other_crops/Pearl_millet_ENG.pdf. Accessed 06/06/2017.
- United Nations, Department of Economic and Social Affairs, Population Division (2015). *World Population Prospects: The 2015 Revision, Key Findings and Advance Tables*. Working Paper No. ESA/P/WP.241. [Internet document] URL https://esa.un.org/unpd/wpp/publications/files/key_findings_wpp_2015.pdf. Accessed 22/06/2017.
- Vadez V, Hash T, Bidinger FR, Kholova J. 2012. Phenotyping pearl millet for adaptation to drought. *Frontiers in Physiology Methods* 3: 386 doi:10.3389/fphys.2012.00386.
- Vara Prasad PV, Staggenborg SA. 2011. Growth and production of sorghum and millets. *Soils, Growth and Crop Production Vol II*. [Internet document]. URL https://www.researchgate.net/profile/P_V_Vara_Prasad/publication/260392531_Growth_and_Production_of_Sorghum_and_Millets/links/0c9605311770e75b1b000000/Growth-and-Production-of-Sorghum-and-Millets.pdf. Accessed 29/06/2017.
- Varzakas T, Zakyntinos G, Verpoort F. 2016. Plant food residues as a source of nutraceuticals and functional foods. *Foods* 5: 88 doi.org/10.3390/foods5040088.
- Velu G, Rai KN, Sahrawat KL. 2008. Variability for grain iron and zinc content in a diverse range of pearl millet populations. *Crop Improvement* 35(2): 186-191.
- Velu G, Rai KN, Muralidharan V, Kulkarni VN, Longvah T, Raveendran TS. 2007. Prospects of breeding biofortified pearl millet with high grain iron and zinc content. *Plant Breeding* 126: 182-185.
- Vinayagam R, Jayachandran M, Xu B. 2016. Antidiabetic effects of simple phenolic acids: a comprehensive review. *Phytotherapy Research* 30: 184-199.
- Waniska RD. 2000. Structure, phenolic compounds and antifungal proteins of sorghum caryopses. In: Chandrashekar A, Bandyopadhyay R, Hall AJ (Eds) *Technical and institutional options for sorghum mould management: Proceedings of an International Consultation*, pp 72-106. ICRISAT, Patancheru, India.
- Wong JH, Lau T, Cai N, Singh J, Pedersen JF, Vensel W, Hurkman WJ, Wilson JD, Lemaux PG, Buchanan BB. 2009. Digestibility of protein and starch from sorghum (*Sorghum bicolor*) is linked to biochemical and structural features of grain endosperm. *Journal of Cereal Science* 49: 73-82.
- Woods J. 2001. The potential for energy production using sweet sorghum in Southern Africa. *Energy for Sustainable Development* 5(1): 31-38.
- Wu X, Staggenborg S, Propheter JL, Rooney WL, Yu J, Wang D. 2010. Features of sweet sorghum juice and their performance in ethanol fermentation. *Industrial Crops and Products* 31: 164-170.

- Wu Y, Yuan L, Guo X, Holding DR, Messing J. 2013. Mutation in the seed storage protein kafirin creates a high-value food trait in sorghum. *Nature Communications* 4: 2217 doi10.1038/ncomms3217.
- Xu WW, Subudhi PK, Crasta OR, Rosenow DT, Mullet JE, Nguyen HT. 2000. Molecular mapping of QTLs conferring stay-green in grain sorghum (*Sorghum bicolor* L. Moench). *Genome* 43: 461-469.
- Yadav OP, Rai KN. 2013. Genetic improvement of pearl millet in India. *Agricultural Research* 2(4): 275-292.
- Yadav OP, Rai KN, Rajpurohit BS, Hash CT, Mahala RS, Gupta SK, Shetty HS, Bishnoi HR, Rathore MS, Kumar A, Sehgal S, Raghvani KL. 2012. Twenty-five years of pearl millet improvement in India. In: All India Coordinated Pearl Millet Improvement Project, Jodhpur, India.
- Zeleznak K, Varriano-Marston E. 1982. Pearl millet (*Pennisetum americanum* (L.) Leeke) and grain sorghum (*Sorghum bicolor* (L.) Moench) ultrastructure. *American Journal of Botany* 69: 1306-1312.
- Zhao Z. 2007. The Africa Biofortified Sorghum Project – applying biotechnology to develop nutritionally improved sorghum for Africa. In: Xu Z, Li J, Xue Y, Yang W. (Eds) *Biotechnology and Sustainable Agriculture 2006 and beyond*. pp 273-277. Springer, Dordrecht.
- Zhu C, Naqvi S, Breitenbach J, Sandmann G, Christou P, Capell T. 2008. Combinatorial genetic transformation generates a library of metabolic phenotypes for the carotenoid pathway in corn. *Proceedings of the National Academy of Sciences USA* 105: 18232–18237.
- Zhu C, Naqvi S, Gómez-Galera S, Pelacho AM, Capell T, Christou P. 2007. Transgenic strategies for the nutritional enhancement of plants. *Trends in Plant Science* 12: 548–555.

CHAPTER 2: LITERATURE REVIEW II

An Introduction to Particle Induced X-ray Emission (PIXE) and other major analytical techniques used in this study

The purpose of this chapter is to provide important background information on several major analytical techniques used in this dissertation. Although much emphasis will be given to the technique of micro-PIXE (due to its extensive use throughout the study); a brief introduction to some of the other important analytical methods, will also be of value. Of primary concern here will be to introduce the methods used to analyse the bulk mineral content of the grain samples (such as, inductively coupled plasma-atomic emission spectrometry (ICP-AES) and inductively coupled plasma-mass spectrometry (ICP-MS)); as well as some of the methods used to interrogate aspects of the grain protein quality (such as, one dimensional polyacrylamide gel electrophoresis (1D PAGE); nanoflow liquid chromatography matrix-assisted laser desorption/ionization mass spectrometry (nano-LC/MALDI-MS), transmission electron microscopy (TEM), and amino acid analysis). A formal introduction to RNA sequencing (RNAseq) is reserved for a separate chapter that utilises this technique to discern differences between wild-type and transgenic sorghum grains at the level of gene expression (see Chapter 5).

2.1 Introduction to PIXE

Much of the novelty in the work described in this dissertation is related to the application of the nuclear microscopy technique of PIXE to study the distribution and concentration of mineral elements within cereal grain tissues. Although this technique is renowned amongst nuclear analytical methods for its multi-elemental capacity to quantitatively map trace elements in biological samples, it is often limited in application due to the relative scarcity of accelerated proton beam research centres (Szökefalvi-Nagy, 1994). iThemba LABS is one of the few laboratories for accelerator based sciences on the African continent. For the past 40 years the PIXE technique has been an instrumental part of the research activities at iThemba LABS (Cape Town, South Africa) and has been applied across several research disciplines, including, materials science, geology, archaeology, biomedicine, agriculture and plant biology.

PIXE is an atomic microscopy technique that can simultaneously detect elements from sodium (Na) to uranium (U) in various samples with a spatial resolution down to 1-3 μm (Pongrac *et al.*, 2013a; Mesjasz-Przybyłowicz and Przybyłowicz, 2002). In biology, PIXE has been successfully used in a wide variety of studies for the quantification of essential elements and contaminants in different plant and animal tissues (Pongrac *et al.*, 2013a; Safaverdi *et al.*, 2009). Most notably, the technique has been found useful for mapping trace elements at spatial scales that are relevant to seed biology (Lombi *et al.*, 2011). As a result, several important food grains, such as wheat (Singh *et al.*, 2013), rice (Lombi *et al.*, 2009), soybean (Malan *et al.*, 2012), buckwheat (Pongrac *et al.*, 2013b) and the common bean (Cvitanich *et al.*, 2011) have been successfully analysed by PIXE.

The research work presented in this dissertation reports the use of PIXE for the first time, as a tool to map elemental distributions in biofortified millet grains. The information provided is useful for interrogating the effect that biofortification strategies may have on the localisation and tissue concentrations of important minerals within biofortified food grains. In the sections that follow, more details of some of the basic physics principles involved in the PIXE technique (including an introduction to the experimental set-up for PIXE that is situated at the Materials Research Department, iThemba LABS), will be presented. This information will provide important background context to the results reported in subsequent research chapters that involve micro-PIXE analysis.

2.1.1 Physics principles underpinning PIXE

An understanding of the PIXE technique begins with a fundamental appreciation of the structure of an atom, as depicted by Bohr's atomic theory. According to the Bohr model (Bohr, 1913) the electronic structure of an atom consists of a central nucleus that is surrounded by one or more orbiting electrons (Figure 2.1). The orbiting electrons occupy discrete energy shells that are stationary and arranged in order of increasing energy identified by the letters, *K*, *L*, *M*, *N* and *O* (Agrawal, 2016). In the event that an electron from an inner orbiting shell is removed, a vacancy is created, which is then immediately filled by another electron from an outer shell. When such a transition occurs, a quantum of energy equal to the energy difference between the two shells is released in the form of an X-ray (Figure 2.2). Since each atom has its own unique structure, the emission of X-rays that results from the creation of inner shell electron vacancies, is characteristic of the particular atom. The characteristic X-ray spectrum can therefore be used as a signature to

identify the atoms of a particular element. Elements with atomic numbers up to $Z=50$ are principally detected through their K X-rays, whilst heavier elements are measured using their L X-ray lines (Rihawy, 2007). The emitted X-rays are identified as K or L according to the electronic shell being filled by an outer orbiting electron.

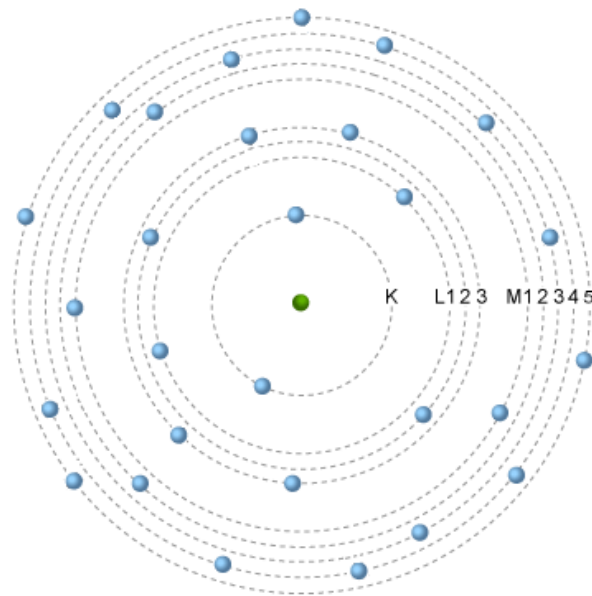


Figure 2.1 A schematic diagram of the Bohr model of an atom, showing the nucleus surrounded by the K , L and M electron shells (<http://www.ammrf.org.au>).

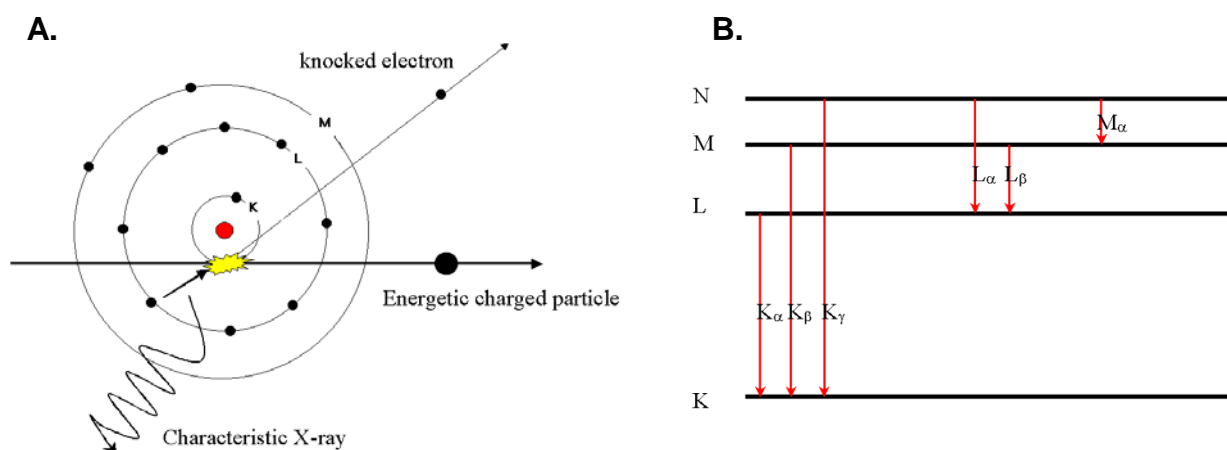


Figure 2.2 (A) An illustration of the basic principle of PIXE; (B) A representation of the characteristic X-ray transitions that may be created as a result of particle bombardment. The characteristic X-rays lines are identified as K , L , M according to the electron shell being filled. The subscript α , β , or γ refers to the outer shell origin of the transiting electron (Rihawy, 2007).

When a beam of accelerated particles is used to induce X-ray emission this is known as Particle induced X-ray Emission (PIXE). Most frequently in PIXE, the beam of accelerated particles are ions with no remaining electrons, such as protons ($^1\text{H}_1^+$) or alphas (He^{2+}), with energies of 2 – 4 mega-electron Volts (MeV) (Garman and Grime, 2005). When protons are used as the beam of accelerated particles, the PIXE technique may also be referred to as Proton-Induced X-ray Emission. The first reported use of PIXE as an analytical method was documented by Johansson *et al.*, (1970), in Lund, Sweden. A comprehensive treatment of the nuclear physics that underpins PIXE is presented by Johansson and Campbell (1988) in their authoritative text on this particular subject.

In essence, there are two main approaches to PIXE analysis, which are distinguished on the basis of the size of the incident particle beam. Broad-beam PIXE uses a millimetre sized beam, whereas micro-PIXE utilises a particle beam focused to micrometre dimensions (Pallon *et al.*, 2017). Focused ion beams of 1- 10 μm , are particularly useful for carrying out investigations related to the elemental composition of biological cells with the possibility to reveal trace element distributions within single cells (Tapper, 1989). The focused ion beam set-up required for micro-PIXE analysis is often referred to as a nuclear microprobe.

2.1.2 The nuclear microprobe at iThemba LABS

Micro-PIXE measurements used for this study were carried out at the nuclear microprobe (NMP) facility situated at the Materials Research Department, iThemba LABS. For micro-PIXE analysis, specimens were typically bombarded with a 3.0 MeV focused proton beam that was supplied by a single ended 6 MV Van de Graaff (VDG) accelerator. A schematic diagram depicting the layout of the beam line (from the analysing magnet to the point of ion-target interaction in the target chamber) and key optics components is shown in Figure 2.3; whilst a more detailed photograph of the NMP system is shown in Figure 2.4. The proton beam required for micro-PIXE, is generated by an ion source, located in the 6 MV terminal. Along the acceleration flight path, a number of quadrupole magnets and collimators are positioned to facilitate beam focusing. The final destination of the focused beam is to impinge on the target located in the centre of the NMP experimental chamber, where the pressure is kept at $\sim 10^{-6}$ Torr during micro-PIXE analysis (Prozesky *et al.*, 1995).

Specimens are mounted in the NMP experimental chamber using a motorised sample ladder with three degrees of freedom (X, Y, Z) that precisely positions the analytical surface of the target-specimen in the focal point of the ion beam probe. This manoeuvring of the target-specimen is facilitated by means of an optical microscope, with 60x magnification (see Figure 2.4). Induced X-rays from the specimen are detected by a Silicon – Lithium (Si(Li)) drifted X-ray detector, which features an active area of 30 mm² and a typical resolution of 150 eV per channel. The Si(Li) detector is positioned at a working distance of 22 - 25 mm away from the specimen at an angle of 135° to the incidental beam direction. The Si(Li) crystal of the detector is maintained at -175°C using liquid nitrogen by means of a copper (Cu) cold finger. Scattered energetic protons produced during the analysis are prevented from hitting the detector window by interposing a beryllium (Be) absorber of 125 µm thickness. An annular silicon (Si) surface barrier detector, positioned at ~6 cm in front of the target, and 176° from the direction of the incident ion beam is mounted in the chamber to detect proton backscattering (BS) spectra. All X-ray data signals, including the yield, pixel position and charge collected are acquired in event-by-event mode by the data acquisition system. Signals are processed electronically for amplification and digitisation and stored as event-by-event data files (Prozesky *et al.*, 1995). Calibration of the system is carried out before each experimental run using permanently mounted ASTIMEX[®] standards, which include 44 pure metals and 53 minerals (Prozesky *et al.*, 1995). Charge normalisation of the results proceeds by using the integrated beam charge collected from the insulated specimen holder mounted onto the specimen ladder and a Faraday cup placed behind the specimen.

Offline processing of the event-by-event data and the raw PIXE spectral data is conveniently carried out using the GeoPIXE II software package (Ryan, 2000) featuring the dynamic analysis (DA) method (Ryan and Jamieson, 1993; Ryan *et al.*, 1995). The DA method enables the projection of event-by-event data directly onto quantitative elemental images, with both background subtraction and deconvolution of spectra using accurate X-ray relative intensity values from databases, particularly for the case of 3.0 MeV incident ions. Other spectral artefacts such as escape peaks from the Si(Li) detector and pile-up peaks (including coincidences) are also taken into account for the accurate deconvolution of the spectra (Ryan and Jamieson, 1993; Ryan *et al.*, 1995, 1996; Ryan, 2001). The results of this analysis lead to the generation of fully quantitative elemental maps, with colour intensity scales indicating the localised variations in elemental concentration, within the selected scanned area, with typical minimum detection limits (MDL) down to the part

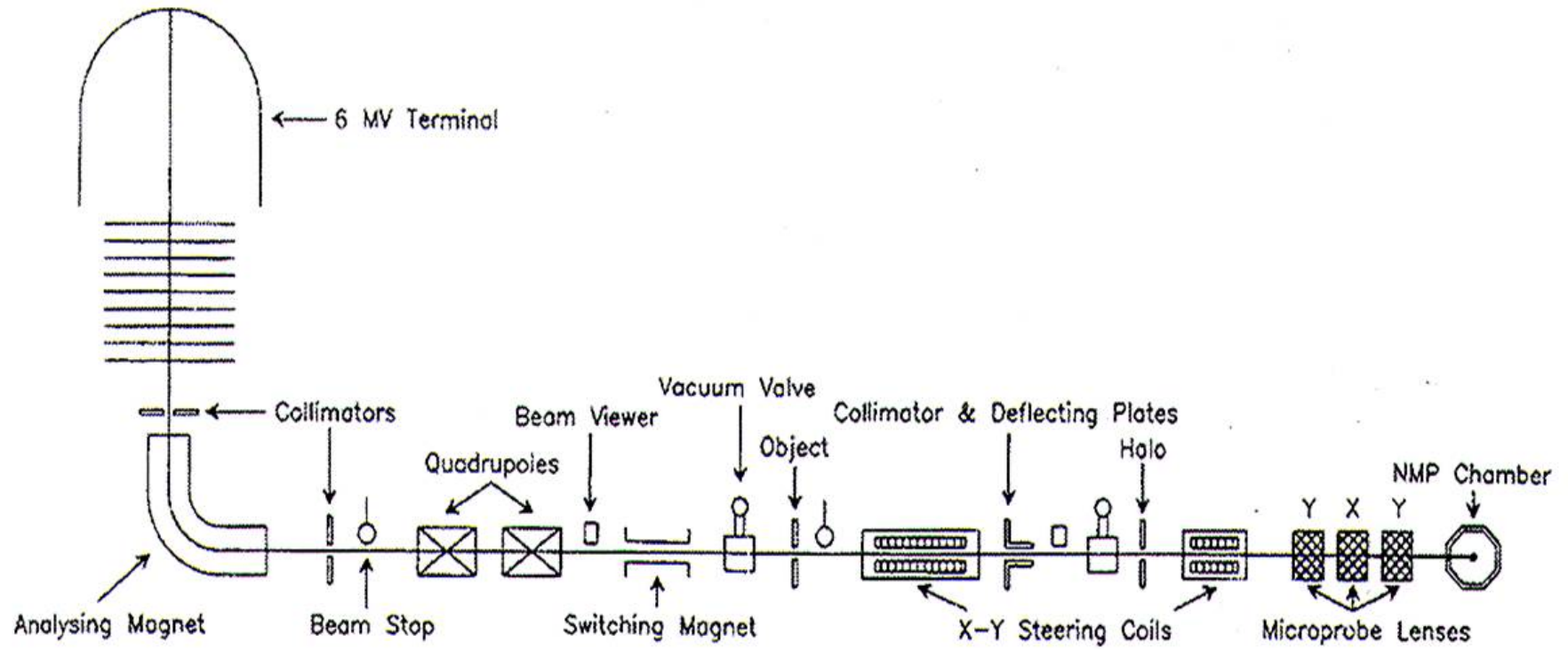


Figure 2.3 Schematic diagram of the physical layout of the Van de Graaff accelerator and servicing beam line for the nuclear microprobe (NMP) situated at the Materials Research Dept, iThemba LABS (Prozesky *et al.*, 1995).

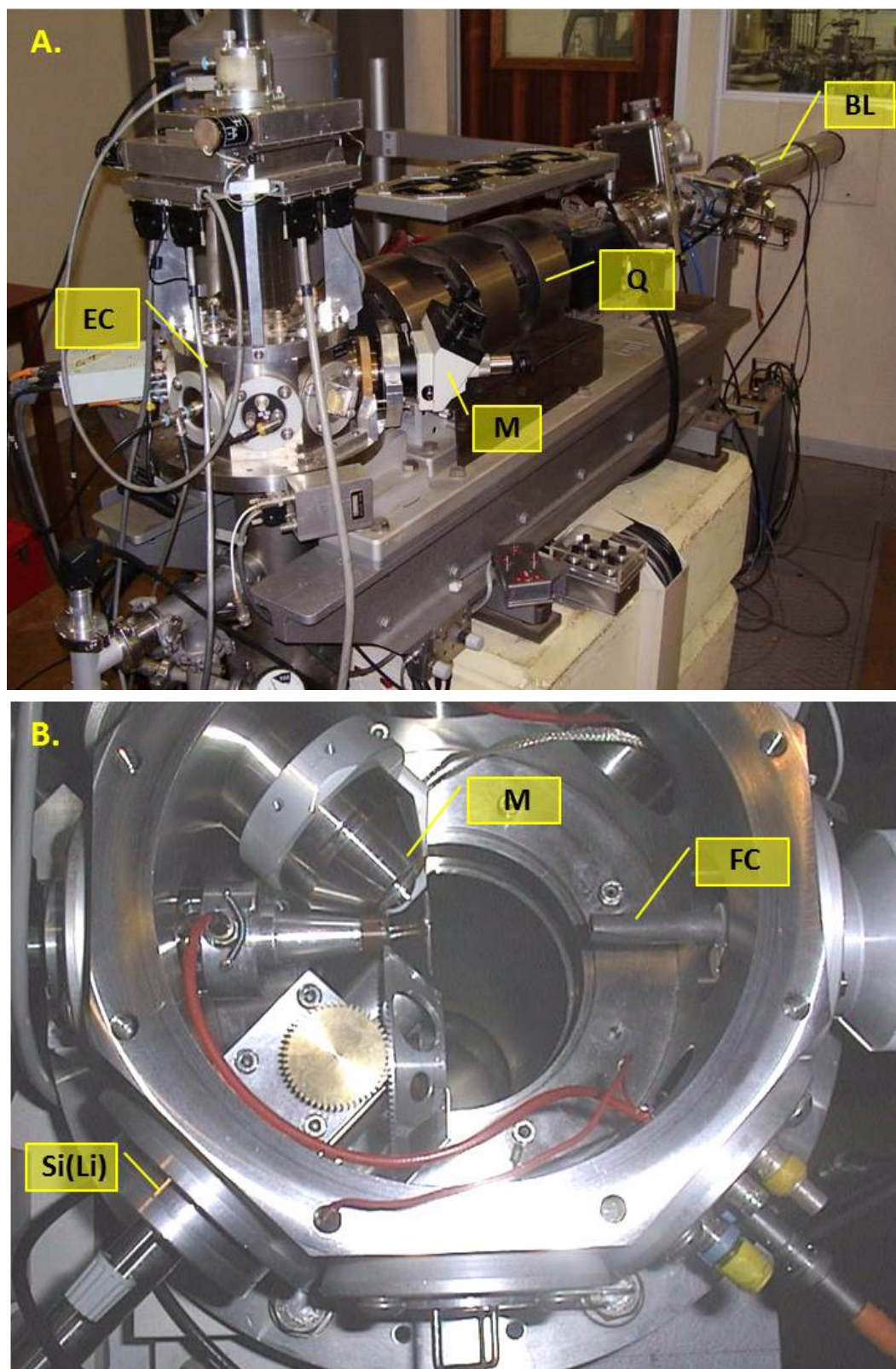


Figure 2.4 (A) A photograph of the NMP end station at iThemba LABS. For PIXE analysis, the proton beam is accelerated along the beam line (BL), focused using a set of quadrupole lenses (Q) and directed to impinge on the target-specimen in the centre of the high vacuum experimental chamber (EC). (B) A photograph of the inside of the experimental chamber, indicating the position of the microscope objective lens (M), the Faraday Cup (FC) and the X-ray detector (Si(Li)).

per million level (Lombi *et al.*, 2011; Pineda-Vargas *et al.*, 2001). Interestingly, if micro-PIXE is carried out with a highly focused proton beam, quantitative elemental mapping of specimens can be achieved at the microscopic or even sub-microscopic level (Garman and Grime, 2005; Carmona *et al.*, 2008; Cloete *et al.*, 2010).

To accurately determine elemental concentrations by micro-PIXE analysis, computer fitting codes, such as GeoPIXE are indispensable for handling the X-ray spectral data (Vogel-Mikuš *et al.*, 2014). However in general, fully quantitative results are much easier to obtain for thin targets than for thick targets. This is because for thick targets, there are additional matrix effects that must be taken into consideration, which include beam energy loss within the target and the attenuation of X-rays leaving the target. These complicating factors are mainly determined by the elements in the sample with the largest concentrations (i.e. the matrix composition). In the case of thick biological specimens, such as bisected seeds/grains, it is appropriate to treat such samples as “infinitely thick”, with a sample matrix approximated to that of cellulose (Witkowski *et al.*, 1997; Przybylowicz *et al.*, 1999). Validation for this approach is based on the study of Pineda and Peisach (1988), which verified that trace element analysis of biological specimens by PIXE can be based on an assumed matrix composition of cellulose, particularly for elements with an atomic number ≥ 19 , such as Fe and Zn, where the maximum relative standard deviation for a number of biological standards was less than 10%.

2.1.3 Proton backscattering spectrometry (BS)

During micro-PIXE measurements at the NMP, proton backscattering spectrometry (BS) is also usually performed simultaneously as a complementary technique to PIXE. The BS method is based on the physics associated with the energy loss phenomena that results from the collision between the incident ion beam and the nuclei of the target sample (Chu *et al.*, 1978). The technique consists of measuring the energy spectrum of the incident ions, which are backscattered along certain angles after a collision with the targeted sample atoms. The resultant energy spectrum is measured using a sensitive solid state detector, and provides a means of analysing not only the elemental composition of the sample, but also the sample thickness (Mulware, 2015). When applied to biological samples, the BS method is

particularly useful for determining the organic composition of such samples, due to its capability to detect elements such as carbon (C), nitrogen (N) and oxygen (O). In this way, it serves as a complementary technique to PIXE, because these elements cannot be measured using PIXE. BS is also particularly useful because the technique provides important information about the incoming beam current and the cumulative charge that occurs during sample irradiation. These details are essential for the correct fitting and normalisation of the PIXE spectrum, which allows for the accurate determination of elemental concentrations within the target sample (Grime, 1996; Carmona *et al.*, 2008).

2.1.4 Preparation of biological samples for micro-PIXE analysis

Micro-PIXE usually involves the use of high vacuum and, as a result, most biological specimens would require careful sample preparation before analysis. For biological tissues containing a significant amount of water, sample preparation typically involves chemical or cryofixation followed by freeze drying (Vogel-Mikuš *et al.*, 2010). These treatments, however, have been known to cause some undesired changes in the sample, such as the shrinkage of cellular membranes and changes to intracellular structures, as well as a loss and redistribution of elements (Vogel-Mikuš *et al.*, 2010; Kachenko *et al.*, 2008). As an alternative, Tylko *et al.*, (2007) developed an advanced technique of biological sample preparation that allows for the micro-PIXE analysis in the frozen hydrated state. This is now considered the technique of choice for advanced methods of nuclear nanoprobe analysis, with sub-500 nm beams (Vogel-Mikuš *et al.*, 2010). Fortunately, in the case of mature dried seed material, there is no need for an elaborate sample preparation procedure, as the sample has minimal water content (< 10%); and therefore can be analysed 'as-is' (Vogel-Mikuš *et al.*, 2009).

2.1.5 Micro-PIXE applied to the study of mineral distribution in Millets

For the present study, micro-PIXE has provided a unique opportunity to interrogate spatial differences in mineral concentration that can have a significant impact on the nutritional or biological quality of biofortified millet grains. In the investigations related to transgenic sorghum, micro-PIXE was used to find out if kafirin suppression had an

unintentional effect on the mineral composition of the grain. In the case of the mineral biofortified pearl millet, the rationale behind the use of micro-PIXE was to assess tissue-specific concentration differences in various parts of the grain in order to gain knowledge that can assist future biofortification strategies. Because the millets are not considered high profile crops, very little research involving quantitative elemental mapping of these grains had been done. As a result of this present work and other allied projects, several studies that feature micro-PIXE elemental mapping in millet grains have been published. Notably, these include studies on finger millet (Kruger *et al.*, 2014); pearl millet (Minnis-Ndimba *et al.*, 2015) and sorghum (Mbambo *et al.*, 2014; Ndimba *et al.*, 2015; Ndimba *et al.*, 2017). Given the vast diversity of millet species that exist, there are many more opportunities in the future to investigate spatial differences in mineral concentrations that relate to the nutritional value of these important food grains.

2.1.6 Advantages of the micro-PIXE method

Although there are several different techniques that are available for *in situ* elemental analyses (van der Ent *et al.*, 2017; Lombi *et al.*, 2011), micro-PIXE is noted to be the technique of choice for mapping elemental distribution in biological tissues, where high elemental sensitivity, high lateral resolution and full quantification capabilities are required simultaneously (Vogel-Mikuš *et al.*, 2014). The leading techniques for elemental mapping may be categorised as either X-ray or non-X-ray based, and a comparison of some of their most relevant analytical features are presented in Table 2.1. Importantly, micro-PIXE is amongst the few techniques that qualify as fully quantitative. It features elemental sensitivities that are approximately two-orders of magnitude higher than energy-dispersive X-ray analysis (EDX), and are more-or-less comparable to that of X-ray fluorescence (XRF) spectroscopy (Vogel-Mikuš *et al.*, 2014). The capabilities of XRF and micro-PIXE are frequently compared, with both techniques highlighted as sharing important advantages such as being non-destructive, multi-elemental and capable of parts-per-million (ppm) detection limits with no standards (Willis, 1988; Ali, 2004).

Table 2.1. Comparison of the key analytical characteristics of X-ray based and non-X-ray based elemental mapping techniques (van der Ent *et al.*, 2017; Lombi *et al.*, 2011).

	Technique	Excitation source	Element range	Spatial resolution (μm)	Limit of detection (ppm)	Quantification
X-ray based	Laboratory micro-XRF	X-rays	Multi-element (Al – U)	30-50	< 50	Semi-quantitative
	X-ray fluorescence microscopy	X-rays	Multi-element (Al – U, but poor 2 nd row Z >42)	0.05-1	< 0.1 at best, (varies 1 - 1000)	Quantitative
	Particle induced X-ray Emission (PIXE)	Protons	Multi-element (Na – U)	1-3	1-10	Quantitative
	Electron microscopy with energy-dispersive X-ray spectroscopy (SEM/TEM-EDX)	Electrons	Multi-element (O – U)	1-5	< 5000	Semi-quantitative
Non-X-ray based	Secondary ion mass spectrometry (SIMS)	Ions	Multi-element (Al – U)	0.05	< 1	Semi-quantitative
	Confocal microscopy with fluorophores	UV and visible light	Single-element	0.01	< 1	Semi-quantitative
	Autoradiography	Isotopes	Single-element (isotope dependant)	0.01	< 1	Quantitative
	Laser ablation inductively coupled mass spectrometry (LA-ICP-MS)	Laser	Multi-element (Al – U)	0.1	< 1	Semi-quantitative

In terms of cost and accessibility, XRF is often viewed as preferable to PIXE; however, the fact that PIXE analysis can be run in parallel with other ion beam techniques (such as Rutherford backscattering spectroscopy (RBS)), unique data related to the thickness and composition of the sample, can be ascertained, which leads to more accurate and precise quantification of target elemental profiles (Mesjasz-Przybyłowicz and Przybyłowicz, 2002; Vogel-Mikuš *et al.*, 2014). Another important advantage of micro-PIXE is that it can simultaneously acquire spectral data of nearly all the elements from Na to U (Mesjasz-Przybyłowicz and Przybyłowicz, 2002; Vogel-Mikuš *et al.*, 2014). Other techniques, such as synchrotron-radiation-micro-X-ray fluorescence (SR-micro-XRF), which are far more sensitive than micro-PIXE, often operate in X-ray energy regimes that do not allow for the simultaneous detection of the full range of elements that are of relevance for plant tissue elemental analysis (Vogel-Mikuš *et al.*, 2014).

2.2 Bulk Mineral Analysis by Inductively coupled plasma-atomic emission spectrometry (ICP-AES) or inductively coupled plasma-mass spectrometry (ICP-MS)

The bulk mineral content of biological samples is most frequently analysed by either ICP-AES or ICP-MS (Hansen *et al.*, 2009, 2013). In general, this approach relies on the decomposition of samples (solids or liquids) into ions followed by the spectroscopic determination of their concentrations (Laursen *et al.*, 2014). In comparison to other analytical methods, such as atomic absorption spectroscopy (AAS) or X-ray fluorescence spectroscopy (XRF), ICP-based techniques are lauded for their superior multi-elemental capacity, in addition to excellent precision and sensitivity (Hansen *et al.*, 2009, 2013). The advantage of ICP-based methods lies in the superior ionisation capacity of the excitation source – the plasma - which is due to its very high temperature (6000 – 10 000K) (Zhang and Cresswell, 2016). The plasma excites atoms within the target sample, which leads to photon emission and ionization. The emitted radiation from the plasma is then used for the qualitative and quantitative elemental analysis of the target sample.

The two main types of ICP-based techniques are: inductively-coupled plasma atomic emission spectrometry (ICP-AES) (which is also referred to as ICP-optical emission spectrometry (ICP-OES) and ICP-mass spectrometry (ICP-MS). Using ICP-AES, up to 60 elements can be screened per sample, with moderate-to-low limits of detection (LODs) (Drivelos and Georgiou, 2012). ICP-MS in comparison, is far more sensitive, providing LODs for more than 70 elements at low concentrations, typically at the level of parts-per-billion or -trillion (ppb or ppt) (Drivelos and Georgiou, 2012). The cost of ICP-AES is however significantly lower than ICP-MS, and therefore it tends to be a more popular choice (Hansen *et al.*, 2009; 2013). However, to adequately detect several important trace elements such as cadmium (Cd), lead (Pb) and mercury (Hg), the superior sensitivity of ICP-MS is deemed indispensable (Hansen *et al.*, 2009; 2013).

Although ICP-based methods are recognised for their leading analytical capabilities, it must be noted that these techniques require the complete destruction of the plant organic matrix, so that the sample can be introduced into the plasma as a homogenous aqueous solution (Szymczycha-Madeja, 2014). Typically, the decomposition of the organic matrix is based on high-temperature-oxidation (dry ashing) or wet digestion using strong acids with or without the addition of oxidising solvents (Hansen *et al.*, 2009). Although effective, these methods make use of several concentrated reagents, which can lead to the loss of analytes and/or the contamination of samples (Szymczycha-Madeja, 2014). Additionally, the use of bulk analysis excludes a spatial comprehension of mineral accumulation patterns, which can be incisive for analysing the distribution of important elements across the main compartments of the grain. It is therefore appropriate to complement bulk mineral content analysis by ICP-AES/MS, with an elemental mapping technique, such as micro-PIXE.

2.3 Other techniques used specifically to assess differences between transgenic and wild-type sorghum grains

2.3.1 Sodium dodecyl sulphate-polyacrylamide gel electrophoresis (SDS-PAGE) and mass spectrometry

SDS-PAGE is cited as one of the most useful analytical tools available to study protein molecules (Marchesi, 2008). The method is used in almost every molecular biology and biochemistry laboratory to evaluate protein heterogeneity and molecular weight; and, enjoys immense popularity due to its relative simplicity, affordability and ability to yield rapid results (Rath *et al.*, 2013). The most common approach to SDS-PAGE is based on the discontinuous electrophoresis method that was first described by Laemmli (1970). In this method, proteins are resolved on the basis of their molecular weight (MW) due to differential rates of migration through the sieving matrix of a polyacrylamide gel, under the influence of an applied electric field (Roy and Kumar, 2014). To successfully resolve native proteins in this manner, it is first necessary to impart a uniform geometry and a constant charge/mass ratio to the proteins (Khan, 2016). This is accomplished by denaturing the native proteins by heating the samples with the anionic detergent sodium dodecyl sulphate (SDS) and reducing agents such as dithiothreitol (DTT) or 2-mercaptoethanol. This denaturing and reducing treatment, disrupts the inter- and intramolecular bonds, which allow the proteins to unfold into a linearised polypeptide chain. In this denatured form, SDS binds strongly to the protein molecules, imparting a near uniform negative charge along the entire length of the polypeptide chain (Khan, 2016). This uniform negative charge ensures that the protein's electrophoretic mobility is a function only of its molecular weight. Thus, when SDS-treated proteins are loaded onto a gel and placed in an electric field, they differentially migrate towards the positive anode depending only on their size, and thus become separated due to the sieving effect of the gel matrix environment (Roy and Kumar, 2014). After electrophoretic separation, the proteins can be visualised on the gel using protein-specific staining, and the size of a protein can be estimated by comparing its migration distance with that of a known molecular weight marker (Roy and Kumar, 2014; Ndimba and Ngara, 2013).

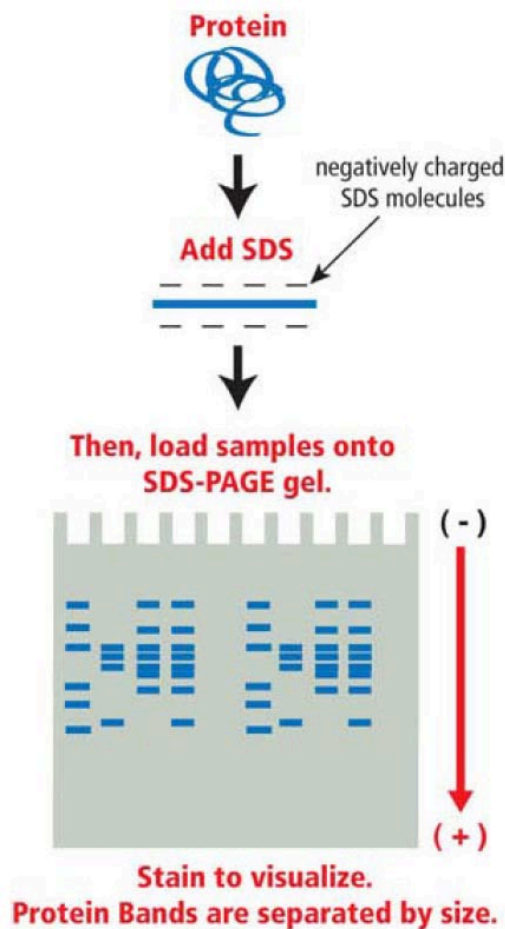


Figure 2.5 An illustration of the basic steps involved in the separation of complex protein mixtures by denaturing SDS-PAGE (<http://www.edvotek.com/SDS-PAGE>).

After separation by SDS-PAGE, protein bands localised in the gel matrix, may be further analysed to obtain protein identities using advanced methods, such as nanoflow liquid chromatography matrix-assisted laser desorption/ionization mass spectrometry (nano-LC/MALDI-MS). In brief, the basic steps in this procedure include the excision of the gel slice containing the protein of interest, followed by the digestion of the proteins into peptide fragments, typically using the restriction enzyme trypsin. The peptide fragments are then subjected to chromatographic separation using nanoflow liquid chromatography (nano-LC). Nano-LC, features a reduced sample flow rate (nanolitres per minute), which results in greater analytical sensitivity and higher signal-to-noise ratio, in comparison to standard liquid chromatography approaches (Cutillas, 2005; Gobom *et al.*, 1999). Once separated,

the peptide fractions, can then be analysed using matrix-assisted laser desorption/ionization mass spectrometry (MALDI-MS).

In MALDI-MS, the peptides are ionised by applying laser pulse UV light to the sample, which has been deposited onto a special MALDI target plate along with a concentrated mixture of matrix solution. Aromatic groups belonging to the matrix chemicals absorb the laser pulse UV light (desorption), whilst the acidic groups donate protons to the sample peptides (ionisation), leading to a process of sublimation, which brings the peptide ions into a gaseous phase (Karas *et al.*, 1990). Subsequently, the analyte molecules are accelerated into a fieldless vacuum, wherein time-of-flight (TOF) analysis is used to determine their unique mass-to-charge ratio, and hence give yield to high resolution mass spectrometry (MS) data (Lewis *et al.*, 2000). To analyse the large amount of data generated by MS, bioinformatics tools are needed to match the sample mass spectra to reference spectra captured in protein sequence databases. This process can lead to precise peptide/protein identifications, which are classically determined using the molecular weight search (MOWSE) score (Thiede *et al.*, 2005; Pappin *et al.*, 1993).

MS has now become an indispensable tool for protein analysis in cereals, thanks to the advanced performance of mass spectrometers and the increasing availability of gene and genomic sequence databases (Cunsolo *et al.*, 2012). Using the combination of gel electrophoresis, mass spectrometry and bioinformatics, the identities of thousands derived from major cereal grains have been resolved thus far (Du Pont *et al.*, 2011; Lesage *et al.*, 2012, Zhang *et al.*, 2012).

2.3.2 Transmission electron microscopy

Transmission electron microscopy (TEM) represents a considerable advance over light microscopy techniques, and is credited with revolutionising the biologists' view of the sub-microscopic world of cells (Bozzola and Russell, 1999). TEM can achieve sub-nanometer resolution, which is well below that of the highest-resolution light microscopes (Winey *et al.*, 2014). The reason for this dramatic increase in resolving power is due to the use of electrons as the source of illuminating radiation. The wavelengths of electrons are much shorter than those of photons (~100,000-fold

shorter), and consequently the resolving power is far greater (up to 10 Angstrom versus approximately 200 nm) (Winey *et al.*, 2014; Frankl *et al.*, 2015). TEM is one of the most commonly used forms of electron microscopy for biological samples and is typically used for the morphological characterisation of subcellular structures and organelles (Frankl *et al.*, 2015). To successfully examine biological specimens using TEM, sample preparation is key and usually involves the generation of very thin sections (~60 – 80 nm) (Winey *et al.*, 2014). For relatively hard biological samples, like cereal grains this can be a distinct technical challenge. Cereal grains tend to be difficult to thin-section for several reasons related to the large amount of dense material compacted in the grain, the low levels of moisture and the lack of intercellular air spaces (Bechtel, 1990). These factors inhibit the penetration of the embedding resin which acts as a support during the sectioning process. To overcome these challenges, specimens typically must be small (<1 mm³); chemically fixed and dehydrated well; followed by extended impregnation times in a low viscosity resin (Saito *et al.*, 2010). Once the thin sections of the desired samples are obtained, a double staining procedure involving uranyl acetate followed by lead citrate is used to enhance contrast prior to imaging with the electron microscope (Winey *et al.*, 2014). TEM has been used in this study principally to compare differences in the size and shape of the protein bodies (that are mainly composed of kafirins) found in different transgenic sorghum lines and their non-transgenic parental counterpart. TEM has also been used to characterise the morphology of protein bodies in maize (Yao *et al.*, 2016), rice (Ashida *et al.*, 2011) and in early studies of wheat (Bechtel, 1985).

2.3.3 Amino Acid Analysis

The nutritional quality of cereal proteins is mainly dictated by their amino acid composition (Otter, 2012). The amino acids are the monomeric building blocks of proteins, and are usually classified nutritionally, as either essential or non-essential. The essential amino acids cannot be synthesised by the body and therefore must be sourced from food. For humans, there are ten essential amino acids that must be supplied in the diet. These are namely arginine, valine, histidine, isoleucine, leucine, lysine, methionine, phenylalanine, threonine and tryptophan (Kim *et al.*, 2009). Among this group, arginine and histidine may be further distinguished as semi-essential amino acids, because although they can be partly synthesised in adults,

this is not the case for young children. The non-essential amino acids, on the other hand, can be synthesised by the body, and include alanine, asparagine, aspartic acid, cysteine, glutamic acid, glycine, proline, serine and tyrosine (Kim *et al.*, 2009).

To evaluate the amino acid content of food proteins, several different approaches such as amino acid analysers (Ohtsuki *et al.*, 1987), capillary electrophoresis (Hsieh and Chen, 2007) and high-performance liquid chromatography (Tan *et al.*, 2011) have been employed. In the specific case of cereal proteins, the most common approach involves the use of high performance liquid chromatography, particularly in combination with reversed-phase columns and pre-column derivatisation. Amino acid analysis by reverse-phase high performance liquid chromatography (RP-HPLC) and ultraviolet (UV) detection following pre-column derivatization is prevalent, mainly because of the greater versatility, sensitivity and speed of the method in comparison to traditional ion-exchange amino acid analyses (Woo, 2003). Although several different options for pre-column derivatisation may exist, the most popular derivatisation reagent for amino acid analysis is phenylisothiocyanate (PITC). In brief, the derivatisation procedure involves the hydrolysis of sample proteins/peptides with PITC under alkaline conditions, which gives rise to phenylthiocarbamyl (PTC-) amino acids. The PTC amino acids are then separated by reverse-phase liquid chromatography and quantified from their UV absorbance at 254 nm (Irvine and Davidson, 2003). The full details of the application of this method was first published in 1984 (Bidlingmeyer *et al.*, 1984), and has subsequently been developed into a commercial system by the Millipore Corporation, known as the Waters™ Pico-Tag workstation. Importantly, the Pico-Tag method, was recently used to analyse the total amino acid content of gamma-irradiated (Mehlo *et al.*, 2013) and transgenic sorghum grain (Grootboom *et al.*, 2014).

References

- Agrawal HM. 2016. Nuclear Physics: Problems based approach including MATLAB. PHI Learning Private Ltd, Delhi, India.
- Ali M. 2004. PIXE and RIXRF comparison for applications to biological sample analysis, Nuclear Instruments and Methods in Physics Research B 222: 567-576.

- Ashida K, Saito Y, Masumura T, Iida S. 2011. Ultrastructure of protein bodies in mutant rice (*Oryza sativa* L.) with altered storage protein composition. *Breeding Science* 61: 201-207.
- Bechtel DB. 1990. Preparation of cereals and grain products for transmission electron microscopy. *Food structure* 9(3): 241-251.
- Bechtel DB. 1985. The microstructure of wheat: its development and conversion into bread. *Food structure* 4(1): 125-133.
- Bidlingmeyer BA, Cohen SA, Tarvin TL. 1984. Rapid analysis of amino acids using pre-column derivatization. *Journal of Chromatography - Biomedical Applications* 336(1): 93-104.
- Bohr N. 1913. On the constitution of atoms and molecules, Part I. *Philosophical Magazine* 26(151):1-24.
- Bozzola JJ, Russell LD. 1999. *Electron microscopy: Principles and techniques for Biologists*. Jones and Bartlett Publishers, Sudbury, Massachusetts, USA.
- Carmona A, Deves G, Ortega R. 2008. Quantitative micro-analysis of metal ions in subcellular compartments of cultured dopaminergic cells by combination of three ion beam techniques. *Analytical and Bioanalytical Chemistry* 390: 1585-1594.
- Chu WK, Mayer JW, Nicolet MA. 1978. *Backscattering spectrometry*. Academic Press, Orlando FL, USA.
- Cloete KJ, Przybylowicz WJ, Mesjasz-Przybyłowicz J, Barnabas AD, Valentine AJ, Botha A. 2010. Micro-particle-induced X-ray emission mapping of elemental distribution in roots of a Mediterranean-type sclerophyll, *Agathosma betulina* (Berg.) Pillans, colonised by *Cryptococcus laurentii*. *Plant, Cell and Environment* 33: 1005-1015.
- Cutillas PR. 2005. Principles of nanoflow liquid chromatography and applications to proteomics. *Current Nanoscience* 1(1): 65-71.
- Cunsolo V, Muccilli V, Saletti R, Foti S. 2012. Mass spectrometry in the proteome analysis of mature cereal kernels. *Mass Spectrometry Reviews* 31(4): 448-465.
- Cvitanich C, Przybylowicz WJ, Mesjasz-Przybyłowicz J, Blair MW, Astudillo C, Orlowska E, Jurkiewicz AM, Jensen EO, Stougaard J. 2011. Micro-PIXE investigation of bean seeds to assist micronutrient biofortification. *Nuclear Instruments and Methods in Physics Research B* 269: 2297-2302.
- Drivelos SA, Georgiou CA. 2012. Multi-element and multi-isotope-ratio analysis to determine the geographical origin of foods in the European Union. *Trends in Analytical Chemistry* 40: 38-51.
- Du Pont FM, Vensel WH, Tanaka CK, Hurkman WJ, Altenbach SB. 2011. Deciphering the complexities of the wheat flour proteome using quantitative two-dimensional electrophoresis, three proteases and tandem mass spectrometry. *Proteome Science* 9:10 doi: 10.1186/1477-5956-9-10.
- Frankl A, Mari M, Reggiori F. 2015. Electron microscopy for ultrastructural analysis and protein localisation in *Saccharomyces cerevisiae*. *Microbial Cell* 2(11): 412-428.

- Garman EF, Grime GW. 2005. Elemental analysis of proteins by micro-PIXE. *Progress in Biophysics and Molecular Biology* 89(2): 173-205.
- Gobom J, Nordhoff E, Mirgorodskaya E, Ekman R, Roepstorff P. 1999. Sample purification technique based on nano-scale reverse phase columns for the sensitive analysis of complex peptide mixtures by matrix assisted laser desorption/ionisation mass spectrometry. *Journal of Mass Spectrometry* 34: 105-116.
- Grime GW. 1996. The “Q factor” method: quantitative microPIXE analysis using RBS normalisation. *Nuclear Instruments and Methods in Physics Research B* 109: 170-174.
- Grootboom AW, Mkhonza NL, Mbambo Z, O’Kennedy MM, da Silva LS, Taylor J, Taylor JRN, Chikwamba R, Mehlo L. 2014. Co-suppression of synthesis of major α -kafirin sub-class together with γ -kafirin-1 and γ -kafirin-2 required for substantially improved protein digestibility in transgenic sorghum. *Plant Cell Reports* 33: 521-537.
- Hansen TH, de Bang TC, Laursen KH, Pedas P, Husted S, Schjoerring JK. 2013. Multielement plant tissue analysis using ICP spectrometry. In: Maathuis F (Ed.) *Plant Mineral Nutrients. Methods in Molecular Biology (Methods and Protocols)*, Vol 953. Humana Press, Totowa, New Jersey.
- Hansen TH, Laursen KH, Persson DP, Pedas P, Husted S, Schjoerring JK. 2009. Micro-scaled high-throughput digestion of plant tissue samples for multi-elemental analysis. *Plant Methods* 5:12. doi:10.1186/1746-4811-5-12.
- Hsieh MM, Chen SM. 2007. Determination of amino acids in tea leaves and beverages using capillary electrophoresis with light-emitting diode-induced fluorescence detection. *Talanta* 73: 326-331.
- Irvine GB, Davidson I. 2003. Amino acid analysis. Precolumn derivatisation methods. In: Smith BJ (Ed.) *Protein sequencing protocols, Second Edition*, Humana Press, Totowa, New Jersey, pp 123-131.
- Karas M, Bahr U, Ingendoh A, Nordhoff E, Stahl B, Strupat K, Hillenkamp F. 1990. Principles and applications of matrix-assisted UV-laser desorption/ionisation mass spectrometry. *Analytica Chimica Acta* 241(2): 175-185.
- Kim MY, Chung IM, Lee SJ, Ahn JK, Kim EH, Kim MJ, Kim SL, Moon HI, Ro HM, Kang EY, Seo SH, Song MJ. 2009. Comparison of free amino acid, carbohydrates concentrations in Korean edible and medicinal mushrooms. *Food Chemistry* 113: 386-393.
- Johansson TB, Akselsson R, Johansson SAE. 1970. X-ray analysis: elemental trace analysis at the 10^{-12} g level. *Nuclear Instruments and Methods in Physics Research* 84: 141-143.
- Johansson SAE, Campbell JL. 1988. *PIXE – A novel technique for elemental analysis*. John Wiley & Sons Ltd, Chichester, UK.
- Kachenko AG, Siegele R, Bhatia NP, Singh B, Ionescu M. 2008. Evaluation of specimen preparation techniques for micro-PIXE localisation of elements in hyperaccumulating plants. *Nuclear Instruments and Methods in Physics Research B* 266:1598–1604.

- Khan FA. 2016. *Biotechnology Fundamentals*, 2nd Edition. CRC Press, Boca Raton, FL, USA.
- Kruger J, Pineda-Vargas CA, Minnis-Ndimba R, Taylor JRN. 2014. Visualisation of the distribution of minerals in red non-tannin finger millet using PIXE microanalysis. *Journal of Cereal Science* 60: 1-3.
- Laemmli, UK. 1970. Cleavage of structural proteins during the assembly of the head of bacteriophage T4. *Nature* 227(5259): 680-685.
- Laursen K, Schjoerring JK, Kelly SD, Husted S. 2014. Authentication of organically grown plants – advantages and limitations of atomic spectroscopy for multi-element and stable isotope analysis. *Trends in Analytical Chemistry* 59: 73-82.
- Lesage VS, Merlino M, Chambon C, Bouchet B, Marion D, Branlard G. 2012. Proteomes of hard and soft near-isogenic wheat lines reveal that kernel hardness is related to the amplification of a stress response during endosperm development. *Journal of Experimental Botany* 63: 1001–1011.
- Lewis JK, Wei J, Siuzdak G. 2000. Matrix-assisted laser desorption/ionisation mass spectrometry in peptide and protein analysis. In: Meyers RA (Ed.) *Encyclopedia of Analytical Chemistry*, pp 5880-5894, John Wiley & Sons Ltd, Chichester, UK.
- Lombi E, KG Scheckel, Kempson IM. 2011. In situ analysis of metal(loid)s in plants: State of the art and artefacts. *Environmental and Experimental Botany* 72: 3-17.
- Lombi E, Scheckel KG, Pallon J, Carey AM, Zhu YG, Meharg AA. 2009. Speciation and distribution of arsenic and localisation of nutrients in rice grains. *New Phytologist* 184: 193-201.
- Malan HL, Mesjasz-Przybyłowicz J, Przybyłowicz WJ, Farrant JM, Linder PW. 2012. Distribution patterns of the metal pollutants Cd and Ni in soybean seeds. *Nuclear Instruments and Methods in Physics Research B* 273: 157-160.
- Marchesi VT. 2008. The relevance of research on red cell membranes to the understanding of complex human disease: a personal perspective. *Annual Review of Pathology* 3: 1-9.
- Mbambo Z, Minnis-Ndimba R, Pineda C, Ndimba B, Bado S, Lin J, Chikwamba R, Mehlo L. 2014. Proton-induced X-ray emission and electron microscopy analysis of induced mutants of sorghum. In: Tomlekova N, Kozgar I, Wani R (Eds.) *Mutagenesis: exploring novel genes and pathways*. Wageningen Academic Publishers, Netherlands, pp 181-196.
- Mehlo L, Mbambo Z, Bado S, Lin J, Moagi SM, Buthelezi S, Stoychev S, Chikwamba R. 2013. Induced protein polymorphisms and nutritional quality of gamma irradiation mutants of sorghum. *Mutation Research* 749: 66-72.
- Mesjasz-Przybyłowicz J, Przybyłowicz WJ. 2002. Micro-PIXE in plant sciences: Present status and perspectives. *Nuclear Instruments and Methods in Physics Research B* 189:470-481.
- Minnis-Ndimba R, Kruger J, Taylor JRN, Mtshali C, Pineda-Vargas CA. 2015. Micro-PIXE mapping of mineral distribution in mature grain of two pearl millet cultivars. *Nuclear Instruments and Methods in Physics Research B* 363: 177-182.

- Mulware SJ. 2015. The review of nuclear microscopy techniques: an approach for non-destructive trace elemental analysis and mapping of biological materials. *Journal of Bophysics*, Article ID 740751 <http://dx.doi.org/10.1155/2015/740751>
- Ndimba BK, Ngara R. 2013. Sorghum and Sugarcane Proteomics. In: Paterson AH (Ed.) *Genomics of the Saccharine, Plant Genetics and Genomics: Crops and Models*, Springer Science, New York, pp 141-168.
- Ndimba R, Grootboom AW, Mehlo L, Mkhonza NL, Kossmann J, Barnabas AD, Mtshali C, Pineda-Vargas C. 2015. Detecting changes in the nutritional value and elemental composition of transgenic sorghum grain. *Nuclear Instruments and Methods in Physics Research B* 363: 183-187.
- Ndimba R, Cloete K, Mehlo L, Kossmann J, Mtshali C, Pineda-Vargas C. 2017. Using ICP and micro-PIXE to investigate possible differences in the mineral composition of genetically modified versus wild-type sorghum grain. *Nuclear Instruments and Methods in Physics Research B* 404: 121-124.
- Ohtsuki K, Kawabata M, Kokura H, Taguchi K. 1987. Simultaneous determination of S-methylmethionine, vitamin U and free amino acids in extracts of green tea with an HPLC-Amino Acid Analyzer. *Agricultural and Biological Chemistry* 51(9): 2479-2484.
- Otter DE. 2012. Standardised methods for amino acid analysis of food. *British Journal of Nutrition* 108: S230-S237.
- Pallon J, De La Rosa N, Elfman M, Kristiansson P, Charlotta Nilsson EJ, Ros L. 2017. A new quantitative X-ray system for micro-PIXE analysis. *X-ray Spectrometry* doi: 10.1002/xrs.2779.
- Pappin DJ, Hojrup P, Bleasby AJ. 1993. Rapid identification of proteins by peptide-mass fingerprinting. *Current Biology* 3(6): 327-332.
- Pineda CA, Peisach M. 1988. Matrix corrections for the determination of trace elements in thick biological samples by PIXE. *Nuclear Instruments and Methods in Physics Research B* 35: 344-348.
- Pineda-Vargas CA, Prozesky VM, Przybyłowicz WJ, Mayer JE. 2001. Correspondence analysis evaluation of linear nutrient distribution in root tips of the tropical forage *Brachiaria brizantha*. *Nuclear Instruments and Methods in Physics Research B* 181: 493-498.
- Pongrac P, Kreft I, Vogel-Mikuš K, Regvar M, Germ M, Vavpetič P, Grlj N, Jeromel L, Eichert D, Budic B, Pelicon P. 2013a. Relevance for food sciences of quantitative spatially resolved element profile investigation in wheat (*Triticum aestivum*) grain. *Journal of the Royal Society Interface* 10: 20130296.
- Pongrac P, Vogel-Mikuš K, Jeromel L, Vavpetič P, Pelicon P, Kaulich B, Gianoncelli A, Eichert D, Regvar M, Kreft I. 2013b. Spatially resolved distributions of the mineral elements in the grain of tartary buckwheat (*Fagopyrum tataricum*). *Food Research International* 54: 125-131.
- Prozesky VM, Przybyłowicz WJ, van Achterbergh E, Churms CL, Pineda CA, Springhorn KA, Pilcher JV, Ryan CG, Kritzing J, Schmitt H, Swart T. 1995. The NAC nuclear microprobe facility. *Nuclear Instruments and Methods in Physics Research B* 104: 36-42.

- Przybyłowicz WJ, Pineda CA, Barnabas AD, Mesjasz- Przybyłowicz. 1999. Micro-PIXE mapping of sodium and chlorine in selected sea grasses. *Nuclear Instruments and Methods in Physics Research B* 150: 282-290.
- Rath A, Cunningham F, Deber CM. 2013. Acrylamide concentration determines the direction and magnitude of helical membrane protein gel shifts. *Proceedings of the National Academy of Sciences* 110(39): 15668-15673.
- Rihawy, MS. 2007. In-vacuum and in-air ion beam analysis techniques for the investigation of diffusion in materials. PhD dissertation, Dept of Physics, University of Surrey, UK.
- Roy S, Kumar V. 2014. A practical approach on SDS PAGE for separation of protein. *International Journal of Science and Research* 3(8): 955-960.
- Ryan CG. 2001. Developments in Dynamic Analysis for Quantitative PIXE True Elemental Imaging. *Nuclear Instruments and Methods in Physics Research B* 181: 170-179.
- Ryan CG. 2000. Quantitative Trace Element Imaging using PIXE and the Nuclear Microprobe. *International Journal of Imaging Systems and Technology* 11: 219-230.
- Ryan CG, Jamieson DN. 1993. Dynamic Analysis: On-line quantitative PIXE microanalysis and its use in overlap-resolved elemental mapping. *Nuclear Instruments and Methods in Physics Research B* 77: 203-214.
- Ryan CG, van Achterbergh E, Jamieson DN, Churms CL. 1996. Overlap corrected on-line PIXE imaging using the Proton Microprobe. *Nuclear Instruments and Methods in Physics Research B* 109/110: 154-160.
- Ryan CG, Jamieson DN, Churms CL, Pilcher JV. 1995. A new method for on-line true-elemental imaging using PIXE and the proton microprobe. *Nuclear Instruments and Methods in Physics Research B* 104: 157-165.
- Safaverdi S, Roshani F, Lamehi Rashti M, Golkhoo Sh, Hassan ZM, Langroudi L. 2009. Micro-PIXE analysis in invasive ductal carcinoma tissues after treatment of astaxanthin. *Iranian Journal of Radiation Research* 7(1): 33-39.
- Saito Y, Shigemitsu T, Tanaka K, Morita S, Satoh S, Masumura T. 2010. Ultrastructure of mature protein body in the starchy endosperm of dry cereal grain. *Bioscience, Biotechnology and Biochemistry* 74(7): 1485-1487.
- Singh SP, Vogel-Mikuš K, Arčon I, Vavpetič P, Jeromel L, Pelicon O, Kumar J, Tuli R. 2013. Pattern of iron distribution in maternal and filial tissues in wheat grains with contrasting levels of iron. *Journal of Experimental Botany* 64(11): 3249-3260.
- Szökefalvi-Nagy Z. 1994. Applications of PIXE in the life sciences. *Biological Trace Element Research* 43-45: 73-78.
- Szymczycha-Madeja A. 2014. A simple and rapid method for the multi-element analysis of wheat crispbread products by Inductively Coupled Plasma-Optical Emission Spectrometry. *Journal of AOAC International* 97(6): 1656-1661.
- Tan F, Tan C, Zhao A, Li M. 2011. Simultaneous determination of free amino acid content in tea infusions by using high-performance liquid chromatography with fluorescence

- detection coupled with alternating penalty trilinear decomposition algorithm. *Journal of Agricultural and Food Chemistry* 59(20): 10839-10847.
- Tapper S. 1989. Development of a nuclear microprobe and its applications to neurobiology. Doctoral Dissertation, Department of Nuclear Physics, Lund University, Sweden.
- Thiede B, Höhenwarter W, Krah A, Mattow J, Schmid M, Schmidt F, Jungblut PR. 2005. Peptide mass fingerprinting. *Methods* 35(3): 237-247.
- Tylko G, Mesjasz-Przybyłowicz J, Przybyłowicz WJ. 2007. X-ray microanalysis of biological material in the frozen-hydrated state by PIXE. *Microscopy Research and Techniques* 70:55–68
- van der Ent A, Przybyłowicz WJ, de Jonge MD, Harris HH, Ryan CG, Tylko G, Paterson DJ, Barnabas AD, Kopittke PM, Mesjasz-Przybyłowicz J. 2017. X-ray elemental mapping techniques for elucidating the ecophysiology of hyperaccumulating plants. *New Phytologist* doi: 10.1111/nph.14810.
- Vogel-Mikuš K, Pongrac, P, Pelicon P. 2014. Micro-PIXE elemental mapping for ionome studies of crop plants. *International Journal of PIXE* 24: 217-233.
- Vogel-Mikuš K, Arcon I, Kodre A 2010. Complexation of cadmium in seeds and vegetative tissues of the cadmium hyperaccumulator *Thlaspi praecox* as studied by X-ray absorption spectroscopy. *Plant Soil* 331: 439–451.
- Vogel-Mikuš K, Pelicon P, Vavpetic P, Kreft I, Regvar M. 2009. Elemental analysis of edible grains by micro-PIXE: common buckwheat case study. *Nuclear Instruments and Methods in Physics Research B* 267: 2884–2889.
- Willis JP. 1988. XRFS and PIXE: Are they complementary or competitive techniques - a critical comparison. *Nuclear Instruments and Methods in Physics Research B* 35: 378-387.
- Winey M, Meehl JB, O'Toole ET, Giddings TH. 2014. Conventional transmission electron microscopy. *Molecular Biology of the Cell* 25(3): 319-323.
- Witkowski ETF, Weiersbye-Witkowski IM, Przybyłowicz WJ, Mesjasz- Przybyłowicz. 1997. Nuclear microprobe studies of elemental distributions in dormant seeds of *Burkea africana*. *Nuclear Instruments and Methods in Physics Research B* 130: 381-387.
- Woo K-L, 2003. Determination of amino acids in foods by reversed-phase HPLC with new precolumn derivatives, butylthiocarbamyl, and benzylthiocarbamyl derivatives compared to the phenylthiocarbamyl derivative and ion exchange chromatography. *Molecular Biotechnology* 24(1): 69-88.
- Yao D, Qi W, Li X, Yang Q, Yan S, Ling H, Wang G, Wang G, Song R. 2016. Maize *opaque10* encodes a cereal-specific protein that is essential for the proper distribution of zeins in endosperm protein bodies. *PLoS Genetics* 12(8): e1006270. <https://doi.org/10.1371/journal.pgen.1006270>.
- Zhang C, Yin Y, Zhang A, Lu Q, Wen X, Zhu Z, Zhang L, Lu C. 2012. Comparative proteomic study reveals dynamic proteome changes between superhybrid rice LYP9 and its parents at different developmental stages. *Journal of Plant Physiology* 169: 387–398.

Zhang X, Cresswell M. 2016. Materials characterisation of inorganic controlled release technology. In: Inorganic Controlled Release Technology, Elsevier Ltd, Oxford, UK, pp 1-16.

CHAPTER 3

A comparative study of selected physical and biochemical traits of wild-type and transgenic sorghum to reveal differences relevant to grain quality*

Abstract

Sorghum (*Sorghum bicolor* (L.) Moench) is an important African food security crop that is grown in many hot and arid regions around the world. The nutritional quality of sorghum grain is however less favourable in comparison to other major cereal grains due to the poor digestibility of its major storage proteins, the kafirins. Improved protein digestibility types were recently developed using RNA interference (RNAi) technology to suppress selected kafirin subsets, however, it was not firmly established if other important quality parameters were adversely affected by this genetic intervention. The main objective of the present study was therefore to carry out a comparative assessment of the transgenic lines versus the wild-type (WT), to reveal significant differences in selected physicochemical traits that play an important role in grain quality. After confirming the suppression of kafirin proteins in the transgenic lines (via 1D SDS-PAGE), a number of important physical and biochemical differences that serve to differentiate the wild-type from the transgenic lines were detected. Importantly, the transgenic grains were found to be much less dense and characterised by a floury endosperm texture in comparison to WT. Some transgenic lines also featured protein bodies with a lobed structure, indicative of the high digestibility trait. The highest increase in grain lysine content was observed in the transgenic lines with the most drastically changed protein body morphology, in comparison to WT.

* Published in part as: Ndimba R, Kruger J, Mehlo L, Barnabas AD, Kossmann J, Ndimba BK. 2017. A comparative study of selected physical and biochemical traits of wild-type and transgenic sorghum to reveal differences relevant to grain quality. *Frontiers in Plant Science* 8:952. doi: 10.3389/fpls.2017.00952.

3.1 Introduction

In spite of the significant progress made in the last few decades to reduce global hunger, nearly 800 million of the world's people suffer from undernourishment, with the highest levels (~23%) found in Sub-Saharan Africa (FAO, IFAD and WFP, 2015). Here, dramatic rates of population growth coupled with severe climatic conditions often result in a heightened demand for food resources, which cannot always be met by the current supply (Ezeagu and Ibegbu, 2010). Grain sorghum (*Sorghum bicolor* (L.) Moench), is one of Africa's most prized indigenous cereals, which has been relied upon for centuries as a major food security crop. Approximately 43% of all major staple foods produced on the continent are known to incorporate some aspect of sorghum grain (Etuk *et al.*, 2012), and as a result, the crop is frequently cited as Africa's second most important cereal, following after maize (Hasan, 2015).

It is currently estimated that about 500 million people depend on grain sorghum to satisfy their daily dietary requirements (Lindsay, 2010). Although nutritionists would generally agree that sorghum is a healthy and nutritious wholegrain product, an over-reliance on it for complete sustenance is not recommended, due to certain nutritional shortcomings associated with its grain. Of primary concern are sorghum's dominant grain proteins, the kafirins. The kafirins are alcohol soluble proteins which are ranked low in nutritional quality, because they are notoriously difficult to digest (Wong *et al.*, 2009), and are furthermore deficient in several essential amino acids, such as lysine, methionine and tryptophan (Shewry, 2007). To compound this problem, sorghum grain is also known to feature significant levels of certain phytochemicals, such as tannins and phytate, which can act as anti-nutrients.

A lack of quality proteins and minerals in the diet is frequently cited as the most prevalent and important forms of malnutrition to plague humankind (Ezeagu and Ibegbu, 2010; Igwe *et al.*, 2012). Protein energy malnutrition (PEM) is particularly singled out as the most lethal form of hunger (Jamabo and Onwukwe, 2010); whilst deficiencies in certain mineral nutrients, like iron (Fe) and zinc (Zn) are known to affect more than half of the world's population (Welch and Graham, 2004). Poor communities subsisting on monotonous cereal-based diets, like sorghum, are especially vulnerable to these forms of malnutrition. Hence, within the past decade, several notable research projects focused on improving the nutritional value of sorghum grain have been initiated (Reddy *et al.*, 2010; Zhao, 2008). Of

specific interest here, is the recent work of Grootboom *et al.*, (2014), wherein RNAi technology was used to suppress the expression of select kafirin subclasses, which resulted in transgenic sorghum grain with improved protein digestibility levels of up to 53%. Although this approach has been recognised as an effective strategy for increasing the protein digestibility (and hence the nutritional value) of sorghum grain, these “improved” transgenic lines have not yet found their way to market. This is likely a consequence of the strict legislative requirements involved in the pre-approval of genetically modified (GM) food crops before general or commercial release (Shepherd *et al.*, 2006; García-Villalba *et al.*, 2008). Undoubtedly, a key concern is to ensure that the transgenic food item is as safe and nutritious as its non-transgenic counterpart, and poses no potential new risks to the consumer or the environment (Chassy, 2010; Jiang and Xiao, 2010). To this end, rigorous testing and safety evaluations must be pursued, which are principally aimed at establishing the “substantial equivalence” of the transgenic food item to its non-transgenic counterpart.

The concept of substantial equivalence (SE) was originally formulated by the Organisation for Economic Co-operation and Development (OECD) in 1993, and was further expounded upon by the Food and Agriculture Organisation of the United Nations (FAO) and the World Health Organization (WHO) in 2000 and 2002, respectively (Li *et al.*, 2007). It is based on the idea that world’s major food crops have been consumed over millennia and are thus regarded as safe (Shepherd *et al.*, 2006). Therefore, if the composition of a genetically engineered (GE) product is within the range of variation shown by the conventional or non-modified product grown under the same conditions, then the GE food is regarded as substantially equivalent and thus safe (Cellini *et al.*, 2004; Shewry *et al.*, 2007). With GE foods, it is common for substantial equivalence testing to follow a targeted approach, which focuses on a comparative analysis of key nutrients, anti-nutrients and toxicants that are known to be essential, beneficial or harmful to health (Cellini *et al.*, 2004). Additionally, because transgenesis has the potential to introduce non-desirable phenotypic traits, it is important to also include a comparative assessment of various agronomic or morphological features of the GE crop that may have an impact on yield or post-harvest processing qualities (Pons *et al.*, 2012).

The need for a comprehensive characterisation of transgenic crops/foods is warranted because the process of genetic transformation can give rise to a range of different effects which are not always predictable (Connor and Jacobs, 1999). For example, the products of the transgene or its regulatory elements may interact with the host genome in unexpected

ways, leading to altered biochemical pathways in the host plant (Pons *et al.*, 2012). Alternatively, the transgene insertion event could be mutagenic in nature, leading to the silencing or activation of native genes, with possible toxic, allergenic or other unsuitable effects (Uzogara, 2000). Moreover, unintended effects may also arise due to somaclonal variation, which are changes that are unrelated to the transgene itself, but instead are a consequence of both genetic and epigenetic factors at play during the process of transforming and regenerating transgenic plants (Connor and Jacobs, 1999; Stamova *et al.*, 2009).

Although it is evident that there are many avenues by which transgenic plants/foods may sustain undesirable or unintended changes which go beyond the primary expected effect of the introduced transgene, the phenomenon of unintended effects in food crops is not confined to GE variants only. This phenomenon also frequently occurs during conventional plant breeding and is brought about by mechanisms related to point mutations or chromosomal recombination (Mohan Jain, 2001). Inferior lines characterised by unintended effects are often readily identified and eliminated during early screening procedures, which is a process that is similarly replicated with GE lines (Cellini *et al.*, 2004; Pons *et al.*, 2012). For this reason, the significance of unintended effects is often categorised as negligible (Pons *et al.*, 2012). However, even after selection, there are incidences of apparently normal transgenic plants exhibiting peculiar behavioural or biochemical traits upon further analysis, which include occurrences of lower yield (Zeller *et al.*, 2010); enhanced allergenicity (Chen *et al.*, 2009) and higher susceptibility to pest attack (Birch *et al.*, 2002). It is therefore of great importance to carry out SE testing on a wide range of different parameters, in order to pinpoint where unintended differences may exist. Once these differences can be identified, the biological significance and/or the health and safety risks posed by the unintended change in the GE product can be more thoroughly investigated (Pons *et al.*, 2012; Modirroosta *et al.*, 2014).

Several studies have been conducted which compare transgenic and conventionally bred lines of major food crops such as maize (Ridley *et al.*, 2002; George *et al.*, 2004; Levandi *et al.*, 2008; Barros *et al.*, 2010), wheat (Baker *et al.*, 2006; Baudo *et al.*, 2006), rice (Li *et al.*, 2007; Jiang and Xiao, 2010; Gayen *et al.*, 2013), potatoes (Shepherd *et al.*, 2006; El-Khishin *et al.*, 2009), and soybean (García-Villalba *et al.*, 2008; Zhu *et al.*, 2008). Thus far, however, no such comparable studies have been completed on transgenic sorghum. In the present work an attempt will be made to investigate aspects of substantial equivalence

between transgenic sorghum grain and its non-transgenic parental counterpart. The approach will involve a comparative analysis of key physical and biochemical characteristics of the grains that have an important impact on grain quality and/or nutritional value. The key physical grain quality traits that will be analysed include a comparative evaluation of kernel weight, grain hardness and protein body morphology. For assessing differences in the biochemical composition, a comparative study of the amino acid profile will be evaluated. The results of this study will be important for highlighting some of the key differences that distinguish the transgenic grain from their wild-type counterpart, and further, whether or not these differences may have significant biological or nutritional consequences.

3.2 Materials and methods

3.2.1 Plant materials

Six independent transgenic sorghum lines developed using RNAi to effect kafirin suppression, and their non-transgenic parental counterpart, P898012, were used as the subject material for the present study. The transgenic lines can be separated into two groups, based on the different genetic constructs used for the original genetic transformations (described fully in Grootboom *et al.*, 2014). The first group consists of three lines, which were originally transformed with the pABS042 construct. This construct targets the suppression of γ -kafirin-1 (27 kDa) and γ -kafirin-2 (50 kDa) proteins. The three independent transgenic lines transformed with the pABS042 construct, are herein designated as 42-1, 42-2 and 42-4. The second group of transgenic lines, also includes three independently transformed lines, but were originally developed using the pABS044 construct. The pABS044 construct targets the suppression of γ -kafirin-1 (27 kDa), γ -kafirin-2 (50 kDa) and α -kafirin A1 (25 kDa), and the resultant independent transgenic lines are herein designated as 44-1, 44-2 and 44-3. All of the transgenic lines were chosen on the basis of previous analyses by Western Blot, which indicated that there was complete suppression of the targeted kafirin proteins, as a result of the intended RNAi silencing (Grootboom *et al.*, 2014).

All of the chosen independent transgenic lines represent the fifth generation of self-crossing progenies from T₀ sorghum transformants, which were originally produced using particle bombardment, as described by Grootboom *et al.*, (2014). Plants from each

independent transgenic line and the parental control cultivar P898012 (hereafter referred to as wild-type, WT), were grown in pots in a containment glasshouse located at the Centre for Scientific and Industrial Research (CSIR) Bioscience Division (Pretoria, South Africa) (Figure 3.1). Environmental conditions were controlled (12-h photoperiod, 25°C/20°C day/night, ~50% humidity, 800 $\mu\text{E}/\text{m}^2$ irradiance), with a minimum of three biological replicates per line. In this study, a biological replicate refers to an individual plant of a specific genotype. At each occasion of watering, the plant arrangement in the glasshouse was randomised to counter any possible positional effects due to microhabitat; and, at anthesis, the panicle of each plant was bagged to prevent outcrossing. This was done to ensure that each plant produced selfed seeds. At full maturity, the grains were hand-harvested from each plant, and manually cleaned to remove all glumes, damaged grains, and other extraneous matter.

3.2.2 Grain samples

For the physical characterisation of the grain, whole kernels, separately derived from individual plants of each genotype were used to make up the sample. However, for the biochemical and protein analyses, the whole kernels had to be ground into fine flour. To reduce biological variation and to maximise the limited amount of sample material available, equal portions of grain from individual plants from each genotype were pooled and homogenised to fine flour, using a standard laboratory mill. Milled grain flour was used immediately for the intended analysis or stored at -20°C in airtight containers until analysed.

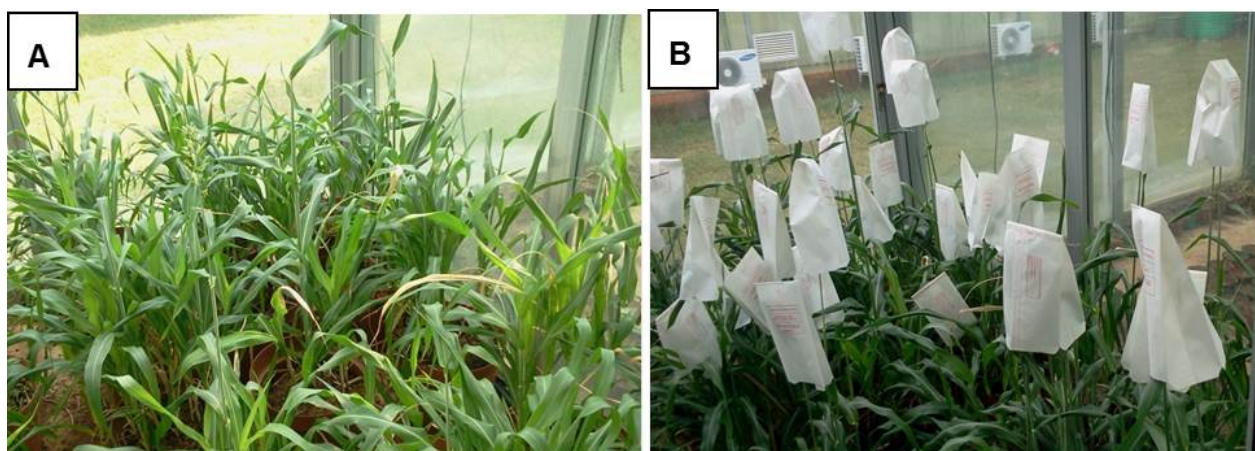


Figure 3.1 Sorghum plants (transgenic and control) being grown in the containment glasshouse at CSIR, Pretoria. Panel A shows plants just before flowering. Panel B shows the plants with their individual panicles bagged to prevent outcrossing.

3.2.3 Kafirin protein extraction and electrophoretic separation

The extraction of kafirin proteins from the different sorghum wholegrain flour samples was performed using two different methods. For method I, approximately 200 mg of grain flour from each sample, was extracted in 1 mL of 70% (v/v) aqueous ethanol, with vigorous shaking for a period of 24h at 37°C, according to Krishnan *et al.*, (1989). In Method II, a modified version of the procedure described in Bean *et al.*, 2011, was followed. In brief, albumins and globulins were pre-extracted using a 50 mM Tris-HCl buffer (pH 7.8) containing 100mM KCl, and discarded prior to extracting the kafirins. Kafirins were then extracted from 200 mg of the wholegrain flour samples using 1 mL of solution containing 60% (v/v) tert-butanol, 2% (v/v) β -mercaptoethanol (β -ME) and 0.5% (w/v) sodium acetate, with vigorous shaking for 4 hours at room temperature. For both methods, the sample extracts were then centrifuged at 15 000 x *g* for 10 minutes, at room temperature to produce a clear supernatant containing the soluble proteins. The supernatants were transferred to fresh tubes before mixing with 5 x volume of ice-cold methanol containing 0.1 M ammonium acetate, and incubated for a minimum of 12 hours at -20°C, for protein precipitation. The precipitated proteins were then recovered after centrifugation as before, and solubilised in 250 μ L of Bio-Rad's IEF sample buffer. The protein concentration of each extract was then determined using the Bio-Rad Bradford Protein Assay solution, with bovine serum albumin (BSA) as the protein standard (Bradford, 1976). For each sample, an aliquot equating to 10 μ g of extracted protein was resuspended in loading buffer (10% (v/v) glycerol, 5% (v/v) β -ME, 2% (w/v) SDS, 0.01% (w/v) bromophenol blue in 0.125 M Tris-HCl, pH 6.8) and heated at 95°C for 5 minutes, before separation by one dimensional sodium dodecyl sulphate polyacrylamide gel electrophoresis (1D SDS-PAGE). The electrophoretic separation was performed using pre-cast 12% Bis-Tris Bio-Rad gels, essentially according to the Laemmli method (1970). After electrophoresis, gels were stained with Coomassie Blue R250 for six hours to visualise the polypeptide bands. Destaining was achieved by gently shaking the gels in an aqueous solution containing 40% (v/v) methanol and 10% (v/v) acetic acid until the bands were visible against the background.

3.2.4 Physical characteristics

3.2.4.1 Kernel weight

For each line, the mass of 100 randomly selected kernels was determined using a 10⁻⁴ precision balance. This measurement was repeated for three biological replicates per line, to obtain the mean 100-kernel weight \pm standard deviation (SD).

3.2.4.2 Grain hardness

To evaluate differences in grain hardness, the floater test (Hallgren and Murthy, 1983) was used, where 100 randomly selected kernels from each line (replicated across three biological individuals) were placed in a solution of sodium nitrate with a specific gravity of 1.250 g/mL (as measured with a hydrometer) and the percentage of floating kernels (low density) was determined. As a complement to this test, a visual inspection of the grain endosperm texture was also carried out. Individual kernels (20 randomly selected from each line, replicated across 3 biological individuals) were longitudinally sectioned through the middle and subjectively categorised as a floury (i.e. completely opaque) or an intermediate phenotype using ICC Standard No.176 (ICC, 2008). The percentage of floury endosperm phenotypes found for each line was then tabulated and compared.

3.2.4.3 Protein Body Morphology

Transmission electron microscopy (TEM) was used to investigate the morphology of the sorghum grain protein bodies. In brief, segments of the peripheral endosperm (~1-2 mm³ pieces) were sectioned from randomly selected mature grains ($n \geq 3$) of each line, and fixed in a 0.1 M sodium cacodylate buffer containing 3% (v/v) glutaraldehyde (pH 7.2) for 24 h at room temperature. The samples were then postfixed in 2% (v/v) osmium tetroxide at 4°C for 24 h, dehydrated in a graded ethanol series and embedded in Agar Low Viscosity Resin for 16 h at 70°C. Ultrathin (60-90 nm) sections of resin embedded samples were cut using an ultramicrotome (Leica EM UC7) fitted with a Diatome diamond knife and double stained with 2% (w/v) uranyl acetate (8 minutes) and 0.1% (w/v) lead citrate (5 minutes). Protein bodies located in the sub-aleurone layer of the grain endosperm tissue were imaged using a FEI Tecnai™ G2 transmission electron microscope, operating at an accelerating voltage of 200 kV (Electron Microscope Unit, University of Cape Town).

3.2.5 Biochemical characteristics

3.2.5.1 Amino Acid composition

The protein-bound amino acid content was measured according to the Pico-Tag reverse – phase high performance liquid chromatography (RP-HPLC) procedure (Bidlingmeyer *et al.*, 1984) at the South African Grain Laboratory (SAGL) (Pretoria, South Africa). In brief, 400 mg of each sorghum sample was hydrolysed in 6N HCl for 24 h, after performic acid oxidation (for the analysis of cysteine and methionine) or without previous oxidation (for all other amino acids, except for tryptophan). The liberated amino acids were then derivatised, before separation and quantification by RP-HPLC using a WatersTM Pico-Tag C18 column (3.9 mm x 150 mm) and the relevant amino acid standards. For each sorghum sample, three independent determinations of the amino acid content were made. The derivatised amino acids were detected by their ultraviolet (UV) absorbance at 254 nm. The detection limit of each amino acid was calculated in accordance with American Chemical Society (ACS) guidelines (ACS, 1980) and was found to range from 0.06 to 0.30 mMol/100g (wholegrain flour, dry weight) (Table 3.2).

3.2.6 Statistical Analysis

Unless otherwise stated, investigated parameters were analysed in triplicate and the results expressed as the mean \pm SD. Data were subjected to analyses of variance (ANOVA) and means compared by Fisher's Least Significant Difference (LSD) test ($p < 0.05$) using *Statistica* for Windows Version 13.0 (StatSoft Inc., USA).

3.3 Results and discussion

3.3.1 SDS-PAGE analysis of kafirin extracts

The alcohol soluble proteins in sorghum are mainly kafirins, which are often analysed in terms of their pattern of separation by 1D SDS-PAGE. In this study, two established methods of kafirin extraction were utilised to extract and compare the kafirin protein profiles of the wild-type (WT) and transgenic samples. In Method I (Krishnan *et al.*, 1989), 70% aqueous ethanol was used as the extracting solvent; whilst in Method II, the main extracting solvent was 60% tert-butanol (Bean *et al.*, 2011). For both extraction methods, distinctive electrophoretic patterns were observed (Figure 3.2) that appeared to correspond well to the profile of kafirin proteins previously described in the literature

(Hamaker *et al.*, 1995; Mokrane *et al.*, 2009; Mehlo *et al.*, 2013; Soares Correa de Souza *et al.*, 2015).

One example of the sorghum kafirin profile, is shown in Figure 3.3 which depicts the separation of the major subclasses of these proteins by 1D SDS-PAGE (El Nour *et al.*, 1989). According to the characterisation of this profile (Figure 3.3), the kafirin monomers are typically separated into 4 bands, spanning a molecular weight range of ~17- 30 kDa. These bands are identified as γ -kafirin (~28 kDa), α 1- and α 2-kafirin (~26 and 23 kDa) and β -kafirin (~20 kDa) (El Nour *et al.*, 1989; Mokrane *et al.*, 2009). Oligomeric forms of the kafirins are instead resolved at much higher molecular weights, with kafirin dimers present at ~45 kDa; kafirin trimers at ~66 kDa, and other polymeric forms at > 92 kDa.

The results obtained in the present study (Figure 3.2), showed a similar electrophoretic profile to the characterisation described by El Nour *et al.*, 1989. This suggested that both approaches for kafirin extraction performed in this study were effective. The main purpose of the electrophoretic separation of the alcohol-soluble extracts from the WT and transgenic lines was to visualise aspects of the targeted kafirin suppression amongst the transgenic lines in comparison to the WT. Although definitive protein identities are not possible by analysing the electrophoretic pattern alone, some important inferences may be made. Firstly, given constant protein loading (10 μ g/lane), there were some clear indications, as pointed out by the red dashed arrows (Figure 3.2 A and B) of reduced band intensity or complete absence in the transgenic lines in comparison to the WT. It is plausible that these highlighted areas reflect the targeted suppression of kafirins in the transgenic lines. For example, across all the transgenic lines there is an expected targeted suppression of γ -kafirin-1 (27 kDa) and γ -kafirin-2 (50 kDa) proteins; whilst in transgenic lines 44-1, 44-2 and 44-3, the α -kafirin A1 (25 kDa) protein is also expected to be suppressed (Grootboom *et al.*, 2014). Accordingly, the electrophoretic pattern of the alcohol-soluble protein extracts (Figure 3.2 A and B) appear to confirm the suppression of these proteins, in view of the reduced band intensities resolved at ~ 25 and 45 kDa, in the transgenic samples (lanes 3-8) in comparison to the WT (lane 2). In the case of the tert-butanol extracts (Figure 3.2 B), there appeared to be complete suppression in the transgenic lines of the band that is resolved at ~ 42 kDa in the WT sample (Figure 3.2B). The band that is resolved at ~46 kDa in the WT sample however, seemed to be upshifted in most of the transgenic lines. The suppression of this 42 and 46 kDa band that is present

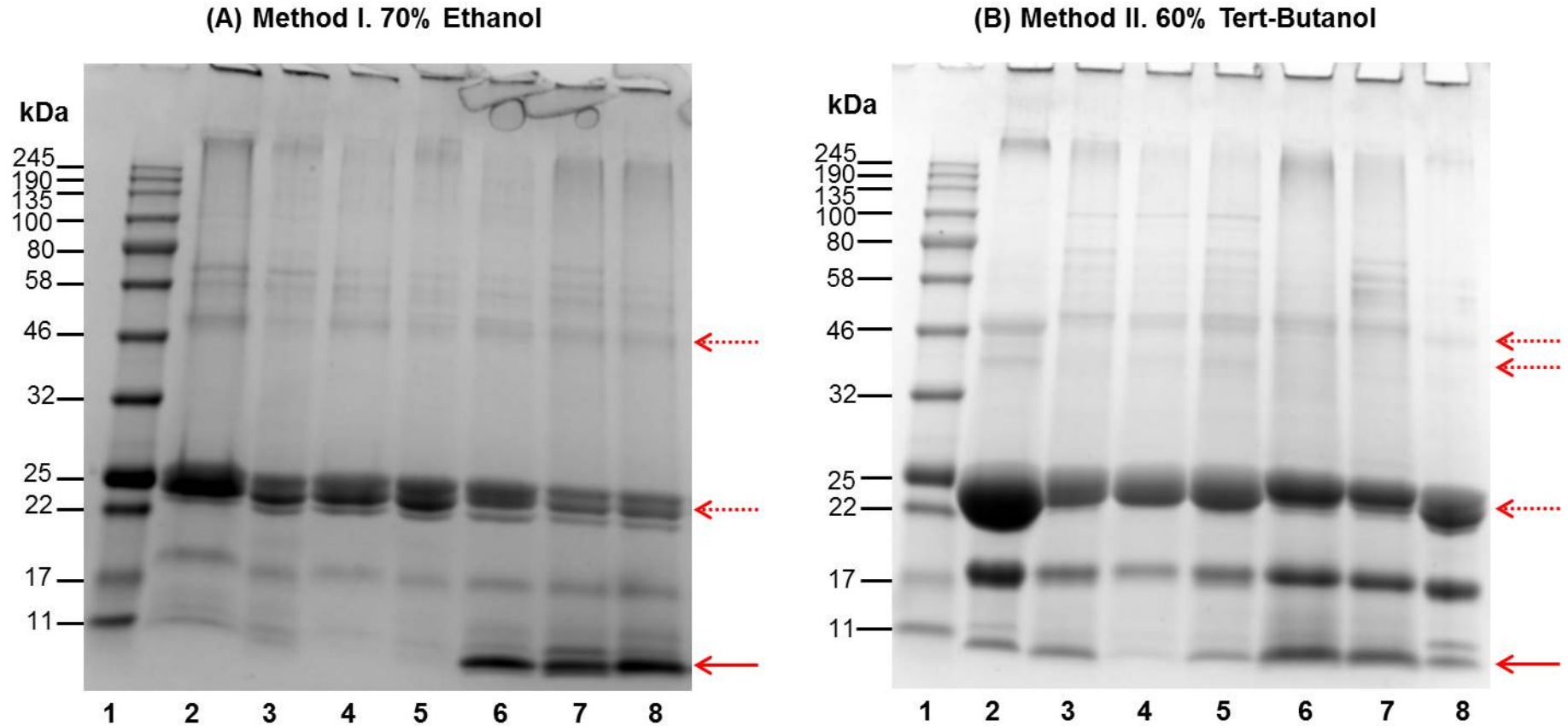


Figure 3.2 1D SDS-PAGE of alcohol soluble grain proteins extracted using 70% ethanol (A) or 60% tert-butanol (B) from WT and transgenic wholegrain flour samples. Lane 1: molecular weight markers (kDa); lane 2: WT; lane 3: 42-1; lane 4: 42-2; lane 5: 42-4; lane 6: 44-1; lane 7: 44-2; lane 8: 44-3 with loading at constant protein 10 μ g/ lane (in (A) and (B)). Red arrows indicate areas of key difference between the protein profiles of the WT versus the transgenic samples. Dashed arrows show areas of reduced band intensity/ or absence in the transgenic lines in comparison to WT. Solid arrows indicate areas of increased band intensity for some of the transgenic lines in comparison to WT.

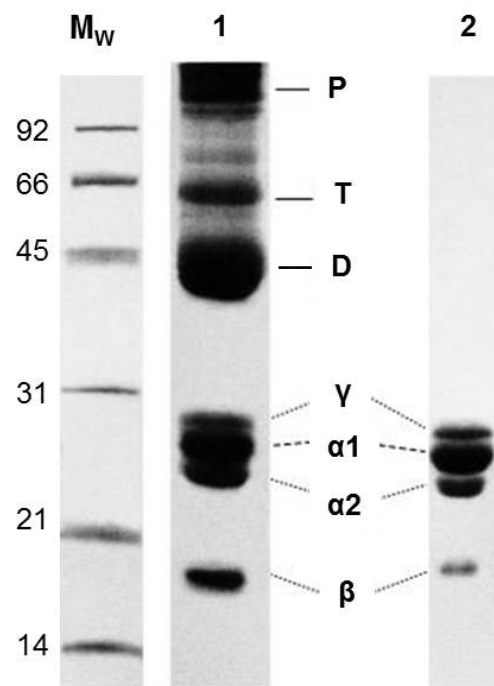


Figure 3.3 1D SDS PAGE of kafirin proteins from sorghum grain flour, M_w : protein markers indicating molecular weight in kDa, Lane 1: unreduced 60% (v/v) tert-butanol extract; Lane 2: reduced 60% (v/v) tert-butanol extract. Positions of the alpha- (α_1 , α_2), gamma- (γ) and beta- (β) kafirin subclasses are indicated, as well as kafirin dimers (D), trimers (T) and kafirin polymers (P) (El Nour *et al.*, 1989).

in the WT appeared to be most severe in the transgenic line 44-3 (Figure 3.2 B, lane 8). The banding pattern in the ethanol extracts at around 46kDa (Figure 3.2 A) appeared much simpler in comparison to what was found for the tert-butanol extracts (Figure 3.2 B). In the ethanol extract, only 1 band was present in the WT that also appeared in all the transgenic lines, but at a lower intensity. It may be that this banding pattern is reflective of the targeted suppression of the γ -kafirin-2 (50 kDa) in all the transgenic lines.

The second main area of difference between the WT and transgenic samples that was revealed by 1D SDS-PAGE, likely corresponds to the known positions of the γ -, α_1 - and α_2 -kafirins, at ~22 – 25 kDa, as depicted by El Nour *et al.*, 1989 (Figure 3.3). In the ethanol extracts (Figure 3.2 A) this banding pattern appears clearer in comparison to the tert-butanol extracts (Figure 3.2 B). In both extracts however, it is evident that there is a suppression of protein resolved in the molecular weight range of ~22 – 25 kDa for all the transgenic lines, in comparison to the WT. It is likely that the reduced band intensity is due to the suppression of the targeted kafirin proteins. Interestingly, the banding pattern of proteins resolved within this narrow molecular weight range (i.e. ~22 – 25 kDa), is

somewhat different for the transgenic lines transformed with the ABS042 construct (Figure 3.2, lanes 3-5) in comparison to the transgenic lines transformed with the ABS044 construct (Figure 3.2, lanes 6-8). This is likely reflective of the fact that whereas only γ -kafirin-1 is targeted for suppression in transgenic lines 42-1, 42-2 and 42-4, both γ -kafirin-1 and α -kafirin A1 are targeted for suppression in transgenic lines 44-1, 44-2 and 44-3.

The last key area of difference that was apparent from the 1D SDS-PAGE analysis of the alcohol soluble extracts was the change in the number and intensity of bands of low molecular weight (~11 kDa or less) in some of the transgenic lines in comparison to WT. In the ethanol extracts (Figure 3.2 A) the appearance of an intense low molecular weight band stood out starkly for transgenic lines 44-1, 44-2 and 44-3 (Figure 3.2 A, lanes 6-8) in comparison to WT and the other transgenic samples. In the tert-butanol extracts (Figure 3.2B) similar intense bands of low molecular weight (< 11 kDa) appear in the transgenic samples, that is again particularly prominent in transgenic lines 44-1, 44-2 and 44-3 (Figure 3.2 B, lanes 6-8). In a different study, that also investigated the protein profile of transgenic sorghum lines with suppressed kafirin synthesis, a similar finding of an increased presence of low molecular weight proteins (< 14.4 and 6 kDa) was made (Da Silva *et al.*, 2011). It is speculated that these low molecular weight proteins may be kafirins, kafirin fragments or other types of alcohol-soluble grain proteins that are synthesised as a result of a compensatory response to the imposed kafirin suppression (Da Silva *et al.*, 2011).

3.3.2 Differences in the Physical traits of the transgenic vs WT grains

3.3.2.1 Kernel weight and grain hardness

The results pertaining to differences in the physical traits of grain from the six transgenic lines and their non-transgenic parental counterpart (WT) are presented in Figure 3.4. For the mean 100-kernel weight, all the transgenic lines were observed to have a lower weight in comparison to WT, but a statistically significant reduction could only be ascribed to the grains in line 42-2 and 44-1 (Figure 3.4 A). In the case of the percentage of floating kernels (Figure 3.4 B) and the proportion of floury endosperm types (Figure 3.4 C), all the transgenic lines were observed to have significantly increased levels of these characteristics in comparison to WT.

According to the literature, physical traits such as the kernel weight, density and endosperm texture are important indicators of quality for sorghum because of their impact on grain hardness. Hard grains tend to be heavy (> 2.0 g 100-kernel weight) with a low percentage of floaters ($< 40\%$), and a corneous to intermediate endosperm texture (Gomez *et al.*, 1997). For large scale production and processing, hard grains are generally preferred because of their association with reduced post-harvest losses (due to breakage and/or spoilage) and enhanced milling yields (Jambunathan *et al.*, 1992; Simonyan *et al.*, 2007).

The high percentage of floating grains amongst the transgenic lines (ranging from 77 – 98%) indicated a significant decrease in the grain density in comparison to WT. The rationale informing the use of the sodium nitrate solution with a specific gravity of 1.25 g/mL is that this value is approximately equal to the average density of a wide range of sorghum kernels (Kirleis and Crosby, 1981). Thus, in this solution, kernels of lower density than average will float, while those of greater density will sink (Gomez *et al.*, 1997). From the results (Figure 3.4 B) it is clear that the transgenic grains are not only less dense than the WT, but are also less dense than the average known in general for sorghum grain. The reason for this decreased density is likely attributable to the significant increase in the percentage of floury endosperm types. The floury endosperm phenotype is associated with loosely packed starch granules that accommodate more air spaces (Rooney and Miller, 1982; Hosney, 1994). It is therefore likely that the reduced density on the transgenic grain is attributable to the inclusion of more air spaces within the grain endosperm, which results in the characteristic opaque or floury visual appearance of this endosperm structure.

The increased percentage of floury endosperm phenotypes in the transgenic lines was commensurate with similar findings reported previously (Da Silva *et al.*, 2011; Grootboom *et al.*, 2014). Amongst the transgenic lines, a significant difference in the average number of floury endosperm types was observed, with the highest percentage found in line 42-1 at 85%. The lowest percentage of floury endosperm types was found in transgenic lines 42-2 and 44-1, at 47% and 38% respectively. Despite being low in comparison to other transgenic lines, these values indicated that number of floury endosperm types was more than 3 times the value found for the WT, which was observed to have only 12% floury endosperm types amongst its grains. The floury endosperm phenotype is generally associated with improved nutritional qualities, such as improved protein digestibility and,

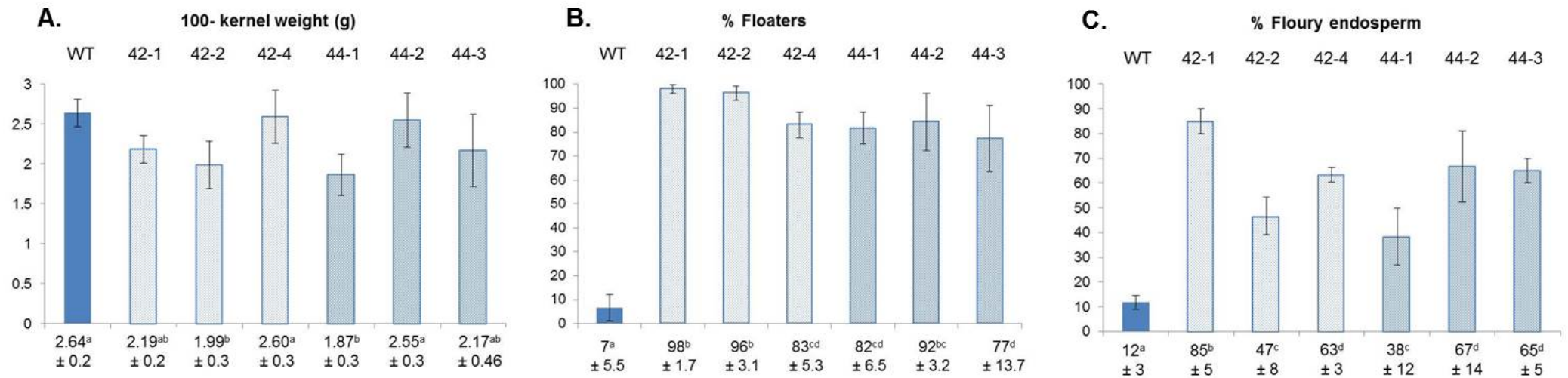


Figure 3.4 A comparison of 100-kernel weight (A), % floaters (B) and % floury endosperm types (C) between the wild-type (WT) and transgenic sorghum genotypes. Values below the bars on the charts correspond to the mean \pm SD. Means sharing the same superscript are not significantly different at $p < 0.05$.

essential amino acid content (Singh and Axtell, 1973; Tesso *et al.*, 2006; Da Silva *et al.*, 2011). However these nutritional gains are often overshadowed by the increased susceptibility of these softer floury grains to post-maturity losses and damage due to moulding and insect infestation (Waniska and Rooney, 2002).

3.3.2.2 Protein body morphology

Another physical trait of the grains that was studied was the morphology of grain protein bodies using TEM analysis. This was considered an important line of investigation because kafirins are stored within these protein body structures, particularly in the grain subaleurone layer (Shull *et al.*, 1992). Representative TEM images of the grain protein bodies for each of the sorghum lines are shown in Figure 3.5. In the earlier work of Grootboom *et al.*, (2014), the protein bodies of the transgenic lines transformed with the ABS042 construct did not reportedly deviate much in terms of the overall shape and size, as compared to the protein bodies found in the grain of the non-transgenic parent, P898012. In contrast the protein bodies of the transgenic lines transformed with the ABS044 construct were reported to have a changed morphology, with an irregular overall shape and deep invaginations present at the periphery. In the present study, the protein bodies found in grains of the ABS042 lines (Figure 3.5 b-d) and ABS044 lines (Figure 3.5 e-g) did not conform in each case to what was previously reported by Grootboom *et al.*, (2014). For the ABS042 group, line 42-2 (Figure 3.5 c) featured protein bodies that were most similar in shape and size to that of the WT (Figure 3.5 a). The 42-2 protein bodies exhibited a regular overall polygonal shape, with some distinctive patterns of the internal concentric ring structure that is present in the protein bodies of the WT. The other two ABS042 lines however, displayed some major distinguishing features. Line 42-1, exhibited protein bodies that were drastically changed in morphology in comparison to WT. These protein bodies (Figure 3.5 b) were irregularly shaped, with deep invaginations at the periphery. The protein bodies of line 42-4, also displayed an amorphous morphology that contrasted greatly with the ordered polygonal structure of protein bodies in the WT. A proliferation of much smaller protein bodies (< 0.5 μm diameter) were also found in this line (Figure 3.5 d).

Two of the ABS044 transgenic lines (44-2 and 44-3) conformed to the expected change in protein body morphology as was reported in Grootboom *et al.*, (2014). In these lines

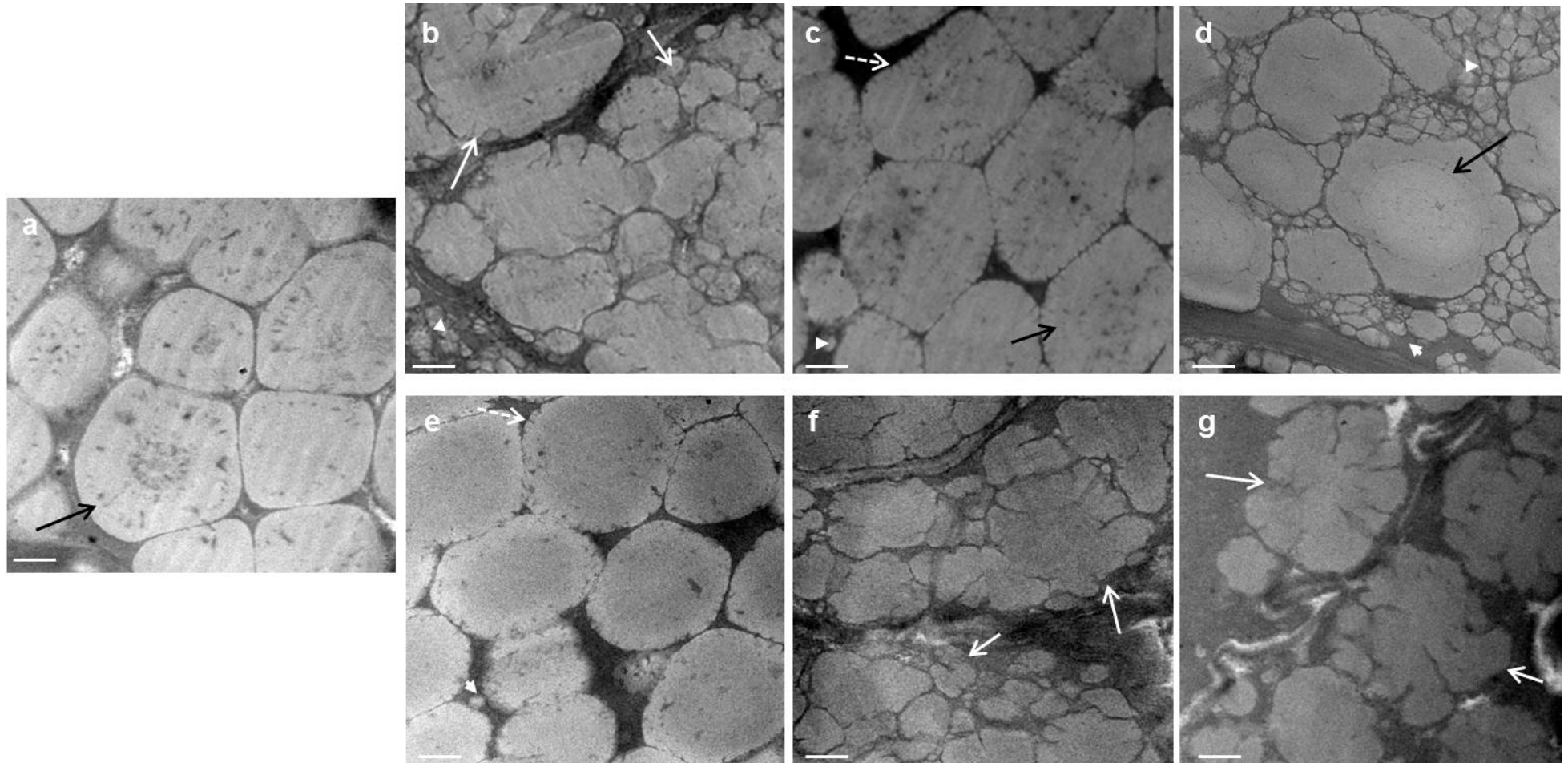


Figure 3.5 Representative TEM images of protein bodies in the subaleurone layer of the wild-type (WT) and transgenic sorghum lines; a: WT, b: 42-1; c: 42-2; d: 42-4; e: 44-1; f: 44-2; g: 44-3. Black arrows point to internal concentric ring structure present in WT and some transgenic protein bodies. White arrows point to irregularly shaped protein bodies with invaginations at the periphery. “Cracked” peripheral structure of transgenic protein bodies, pointed out with a white dotted arrow. White arrowheads point out the presence of small protein bodies (< 0.5 μm diameter) in the transgenic lines. Scale bar represents 0.5 μm .

(Figure 3.5 f,g) it was clear that the protein bodies were misshapen, with a lobed overall structure. No internal concentric ring structures were observed in the protein bodies of these two lines. Line 44-1 of this group however, was different. The protein bodies in this line (Figure 3.5 e) conformed instead to the regular polygonal shape that is typical of the WT protein bodies. At the periphery of the protein bodies however, line 44-1 differed from WT, in that the edges were characterised by a cracked appearance, due to a number of small fissures.

From the TEM analyses, it was apparent that complete uniformity in terms of the change to protein body morphology was not exhibited across all the transgenic lines that have been transformed with the same construct. In the ABS042 group, line 42-1 featured protein bodies with an overall structure that was similar to what was found in line 44-2 and 44-3. This highly misshapen protein body type is commensurate with the structural changes found in protein bodies of high-lysine Ethiopian landraces (Singh and Axtell, 1973; Oria *et al.*, 2000) and other transgenic lines featuring both γ - and α -kafirin suppression (Da Silva *et al.*, 2011). In the ABS044 group, line 44-1 featured protein bodies that were more aligned to the WT morphology, with much resemblance to the protein bodies found in line 42-2. These results therefore indicated that a range of responses to kafirin suppression may be exhibited by the protein bodies in transgenic lines. In the most extreme cases (42-1, 44-2, 44-3) a misshapen protein body, with deep invaginations may be evident; whilst in other cases, the polygonal structure to the protein body may persist, with only some signs of peripheral “cracking” at the boundaries (42-2; 44-1). The size and shape of the protein bodies play a critical role in determining the degree of protein digestibility for sorghum grains. Large, rigidly shaped protein bodies, readily resist proteolytic digestion, whereas smaller, lobed-shaped protein bodies are far easier to digest, due to the more favourable surface to volume ratio, which makes the protein body more susceptible to enzymatic attack (Da Silva *et al.*, 2011; Grootboom *et al.*, 2014).

3.3.3 Differences in the biochemical traits of the transgenic vs WT grains

3.3.3.1 Amino Acids Analysis

Data depicting the protein-bound amino acid content of the WT and the six transgenic sorghum lines is presented in Table 3.1. The concentration levels of 17 different amino

Table 3.1 A comparison of the protein-bound amino acid content of the wild-type (WT) and transgenic sorghum genotypes, presented on a dry weight basis in mMol/100 g wholegrain flour. Amino acids that differed significantly between WT and the transgenic lines are highlighted yellow.

Amino Acids	WT	42-1	42-2	42-4	44-1	44-2	44-3	p-value
MET*	2.10 ^a ± 0.16	2.06 ^a ± 0.23	1.99 ^a ± 0.24	1.97 ^a ± 0.25	1.58 ^a ± 0.24	2.12 ^a ± 0.19	2.05 ^a ± 0.37	0.1960
CYS*	3.16 ^a ± 0.70	2.39 ^a ± 0.38	2.99 ^a ± 0.58	2.54 ^a ± 0.24	2.22 ^a ± 0.46	2.59 ^a ± 0.51	2.38 ^a ± 0.28	0.2272
ASX	9.29 ^a ± 0.20	10.14 ^a ± 0.08	9.46 ^a ± 0.70	9.53 ^a ± 0.86	9.22 ^a ± 0.88	9.41 ^a ± 0.27	9.42 ^a ± 0.76	0.6487
GLX	25.53 ^a ± 0.74	23.22 ^{bc} ± 0.43	25.69 ^a ± 0.60	23.56 ^{bc} ± 1.70	24.76 ^{ab} ± 0.95	22.05 ^c ± 1.54	22.03 ^c ± 1.01	0.0029
SER	7.94 ^a ± 0.51	7.15 ^a ± 0.13	7.71 ^a ± 0.23	7.41 ^a ± 0.64	7.61 ^a ± 0.58	7.02 ^a ± 0.69	6.89 ^a ± 0.60	0.2067
GLY	7.63 ^a ± 1.00	7.77 ^a ± 0.36	7.52 ^a ± 0.57	7.46 ^a ± 0.64	7.37 ^a ± 0.60	7.89 ^a ± 0.78	7.18 ^a ± 0.63	0.8822
HIS**	3.25 ^a ± 0.09	2.76 ^b ± 0.17	3.22 ^{ac} ± 0.05	3.04 ^{abcd} ± 0.07	3.11 ^{acd} ± 0.05	2.96 ^{bcd} ± 0.26	2.84 ^{bd} ± 0.25	0.0154
ARG**	5.09 ^{abc} ± 0.35	6.38 ^d ± 0.27	4.49 ^a ± 0.02	5.36 ^{bc} ± 0.68	4.87 ^{ab} ± 0.57	5.66 ^{cd} ± 0.44	5.14 ^{abc} ± 0.42	0.0034
THR*	5.22 ^a ± 0.36	5.24 ^a ± 0.18	5.26 ^a ± 0.12	5.11 ^a ± 0.45	5.08 ^a ± 0.47	5.43 ^a ± 0.17	5.05 ^a ± 0.20	0.7640
ALA	16.13 ^a ± 0.68	14.77 ^a ± 0.36	16.21 ^a ± 0.19	15.60 ^a ± 1.47	16.23 ^a ± 0.73	14.13 ^a ± 1.23	14.28 ^a ± 1.33	0.0567
PRO	12.39 ^{ab} ± 0.36	10.57 ^{bc} ± 1.67	13.07 ^a ± 1.14	11.12 ^{bc} ± 1.23	12.35 ^{ab} ± 0.80	10.07 ^c ± 0.99	9.75 ^c ± 0.73	0.0106
TYR*	3.49 ^a ± 0.17	2.60 ^b ± 0.27	2.92 ^b ± 0.29	2.86 ^b ± 0.25	2.92 ^b ± 0.16	2.99 ^b ± 0.37	2.93 ^b ± 0.17	0.0276

Table 3.1 continued.

Amino Acids	WT	42-1	42-2	42-4	44-1	44-2	44-3	p-value
VAL*	8.25 ^a ± 0.41	8.24 ^a ± 0.23	8.30 ^a ± 0.10	8.03 ^a ± 0.55	8.17 ^a ± 0.48	7.96 ^a ± 0.25	8.05 ^a ± 0.84	0.9593
ILE*	5.64 ^a ± 0.29	5.06 ^{cd} ± 0.20	5.21 ^{bcd} ± 0.11	5.38 ^{abc} ± 0.25	5.58 ^{ab} ± 0.25	5.27 ^{abcd} ± 0.20	4.91 ^d ± 0.17	0.0103
LEU*	16.42 ^a ± 1.13	14.27 ^a ± 0.44	16.06 ^a ± 0.32	15.59 ^a ± 1.16	15.22 ^a ± 1.94	14.20 ^a ± 1.49	13.93 ^a ± 1.50	0.1683
PHE*	5.58 ^a ± 0.15	4.65 ^c ± 0.18	5.30 ^{ab} ± 0.06	4.97 ^{bc} ± 0.39	4.85 ^{bc} ± 0.42	4.88 ^{bc} ± 0.27	4.79 ^c ± 0.18	0.0097
LYS*	2.38 ^a ± 0.24	3.59 ^b ± 0.07	2.34 ^a ± 0.15	3.11 ^c ± 0.18	2.40 ^a ± 0.17	3.15 ^c ± 0.19	3.31 ^{bc} ± 0.39	0.00001

Values are means ± SD of three independent determinations. Means in rows sharing the same superscript are not significantly different at $p < 0.05$. Essential amino acids are marked with an asterisk (*). Conditionally essential amino acids are marked with a double asterisk (**).

Table 3.2 Detection limits calculated for each amino acid quantified by the Pico Tag Method, presented on a dry weight basis in mMol/100g wholegrain flour.

Amino Acid	Detection limit (mMol/100g)	Amino Acid	Detection limit (mMol/100g)
MET	0.11	ALA	0.11
CYS	0.30	PRO	0.09
ASX	0.08	TYR	0.06
GLX	0.07	VAL	0.09
SER	0.10	ILE	0.08
GLY	0.13	LEU	0.08
HIS	0.06	PHE	0.06
ARG	0.06	LYS	0.07
THR	0.08		

acids were determined and for the purpose of a meaningful comparison were expressed in terms of the molar amount per 100g of the wholegrain flour sample. According to the calculated detection limits (Table 3.2), all of the quantified amino acids were above the detection limit of the analysis method. Eight amino acids were found to differ significantly ($p < 0.05$) between the WT and one or more of the transgenic lines. These were glutamic acid (GLX), histidine (HIS), arginine (ARG), proline (PRO), tyrosine (TYR), isoleucine (ILE), phenylalanine (PHE) and lysine (LYS). The majority of the amino acids that were found to be statistically different between the WT and transgenic lines were significantly decreased. These were namely six amino acids: glutamic acid, proline, tyrosine, phenylalanine, histidine and isoleucine, which are all associated with kafirins. According to a recent study of the amino acid profile of extracted sorghum kafirins, glutamic acid is the most abundant amino acid present in kafirins, accounting for about 28.2 % of the total amino acids; whilst the nonpolar neutral amino acids, such as proline, isoleucine, tyrosine and phenylalanine contribute up to 60.1% (Xiao *et al.*, 2015). Given that these amino acids are prominent amongst the kafirins, it is likely that the significant reduction of the five amino acids glutamic acid, proline, tyrosine, phenylalanine and isoleucine, is due to kafirin

suppression. Notably, a reduction in tyrosine was consistent across all of the transgenic lines in comparison to WT. The other four amino acids were found to be significantly reduced in at least three or more of the transgenic sorghum lines. Histidine is the remaining amino acid that was found to be significantly reduced in some of the transgenic lines. Although histidine content is relatively low in kafirins in general (Xiao et al., 2015), it is one of the amino acids that is more prominent in the γ -kafirins (Taylor and Belton, 2002). It is therefore likely that the reduced level of histidine in some of the transgenic sorghum lines is reflective of the targeted suppression of the γ -kafirins.

Arginine and lysine are the remaining two amino acids that were found to be significantly increased in some of the transgenic lines in comparison to WT. Both of these amino acids tend to be associated with non-kafirin type proteins (Lasztity, 1996; Belton *et al.*, 2006). The increase in lysine content for transgenic lines 42-1, 42-4, 44-2 and 44-3 is especially notable. This is because lysine is the most limiting amino acid in sorghum and most other cereals (Ferreira *et al.*, 2005). Therefore, an increase in lysine content is indicative of an increase in the overall protein quality of the grain. In comparison to WT, lysine was significantly increased in the transgenic lines 42-1, 42-4, 44-2 and 44-3, by 50.8%, 30.7%, 32.4% and 39.1% respectively. In the original study of these transgenic lines by Grootboom *et al.*, (2014), a significant increase in the lysine content of the ABS042 lines was not found. However, in the present study, the greatest increase in lysine was observed for line 42-1 of the ABS042 group. It is therefore of great interest to study these lines more extensively, to gain a fuller understanding of the nature of the kafirin suppression that has led to the observed phenotypes.

3.4 Conclusion

This study has revealed a number of important differences in quality characteristics amongst and between transgenic sorghum lines (featuring kafirin suppression) and their wild-type counterpart. In terms of consistent trends, transgenic grains were found to have a higher proportion of floury endosperm types in comparison to WT and were conspicuously less dense. A consistent change in the protein body morphology however was not observed across all lines. Some lines featured protein bodies that were highly irregular in shape; whereas others retained a polygonal shape that was similar to that of the WT. The amino acid profile revealed further significant changes in some lines that

likely reflected the suppression of kafirins and a compensatory synthesis of other more lysine-rich proteins.

References

- American Chemical Society (ACS). 1980. Sub-committee on environmental analytical chemistry. Guidelines for data acquisition and data quality evaluation in environmental chemistry. *Analytical Chemistry* 52: 2242-2280.
- Baker JM, Hawkins ND, Ward JL, Lovegrove A, Napier JZ, Shewry PR, Beale MH. 2006. A metabolomics study of substantial equivalence of field-grown genetically modified wheat. *Plant Biotechnology Journal* 4: 381-392.
- Barros E, Lezar S, Anttonen MJ, van Dijk JP, Röhlig RM, Kok EJ, Engel K-H. 2010. Comparison of two GM maize varieties with a near isogenic non-GM variety using transcriptomics, proteomics and metabolomics. *Plant Biotechnology Journal* 8: 436-451.
- Baudo MM, Lyons R, Powers S, Pastori GM, Edwards KJ, Holdsworth MJ, Shewry PR. 2006. Transgenesis has less impact on the transcriptome of wheat grain than conventional breeding. *Plant Biotechnology Journal* 4: 369-380.
- Bean SR, Ioerger BP, Blackwell DL. 2011. Separation of kafirins on surface porous reverse phased-high performance liquid chromatography columns. *Journal of Agricultural and Food Chemistry* 59: 85-91.
- Belton PS, Delgadillo I, Halford NG, Shewry PR. 2006. Kafirin structure and functionality. *Journal of Cereal Science* 44: 272-286.
- Bidlingmeyer BA, Cohen SA, Tarvin TL. 1984. Rapid analysis of amino acids using pre-column derivatization. *Journal of Chromatography* 336: 93-104.
- Birch ANE, Geoghegan IE, Griffiths DW, McNichol JW. 2002. The effect of genetic transformations for pest resistance on foliar solanidine-based glycoalkaloids of potato (*Solanum tuberosum*). *Annals of Applied Biology* 140: 143-149.
- Bradford MM. 1976. A rapid and sensitive method for the quantitation of microgram quantities of protein utilizing the principle of protein-dye binding. *Analytical Biochemistry* 72: 248-254.
- Cellini F, Chesson A, Colquhoun I, Constable A, Davies HV, Engel KH, Gatehouse AMR, Kärenlampi S, Kok EJ, Leguay JJ, Lehesranta S, Noteborn HPJM, Pedersen J, Smith M. 2004. Unintended effects and their detection in genetically modified crops. *Food and Chemical Toxicology* 42: 1089-1125.
- Chassy BM. 2010. Food safety risks and consumer health. *New Biotechnology* 27: 534-544.
- Chen H, Bodulovic G, Hall PJ, Moore A, Higgins TJV, Djordjevic MA, Rolfe BG. 2009. Unintended changes in protein expression revealed by proteomic analysis of seeds from transgenic pea expressing a bean α -amylase inhibitor gene. *Proteomics* 9: 4406-4415.
- Conner AJ, Jacobs JME. 1999. Genetic engineering of crops as potential source of genetic hazard in the human diet. *Mutation Research* 443: 223-234.
- Da Silva LS, Taylor J, Taylor JRN. 2011. Transgenic sorghum with altered kafirin synthesis: kafirin solubility, polymerisation and protein digestion. *Journal of Agricultural and Food Chemistry* 59: 9265-9270.

- El-Khishin DA, Hamid AA, El-Moghazy G, Metry A. 2009. Assessment of genetically modified potato lines resistant to potato virus Y using compositional analysis and molecular markers. *Research Journal of Agriculture and Biological Science* 5: 261-271.
- El Nour INA, Peruffo ADB, Curioni A. 1998. Characterisation of sorghum kafirins in relation to their cross-linking behaviour. *Journal of Cereal Science* 28: 197 – 208.
- Ezeagu EI, Ibegbu MD. 2010. Biochemical composition and nutritional potential of ukpa: a variety of tropical Lima beans (*Phaseolus lunatus*) from Nigeria. *Polish Journal of Food and Nutrition Sciences* 60 (3): 231-235.
- Ferreira RR, Varisi VA, Meinhardt LW, Lea PJ, Azevedo RA. 2005. Are high-lysine cereal crops still a challenge? *Brazilian Journal of Medical and Biological Research* 38(7): 985-994. <https://dx.doi.org/10.1590/S0100-879X2005000700002>.
- García-Villalba R, León C, Dinelli G, Segura-Carretero A, Fernández-Gutiérrez A, Garcia-Cañas V, Cifuentes A. 2008. Comparative metabolomics study of transgenic versus conventional soybean using capillary electrophoresis-time-of-flight mass spectrometry. *Journal of Chromatography A* 1195: 164-173.
- Gayen D, Nath Sarkar S, Datta SK, Datta K. 2013. Comparative analysis of nutritional compositions of transgenic high iron rice with its non-transgenic counterpart. *Food Chemistry* 138: 835-840.
- George C, Ridley WP, Obert JC, Nemeth MA, Breeze ML, Astwood JD. 2004. Composition of grain and forage from corn rootworm-protected corn event MON 863 is equivalent to that of conventional corn (*Zea mays* L.). *Journal of Agricultural and Food Chemistry* 52: 4149-4158.
- Gomez MI, Obilarra AB, Martin DE, Madzvamuse M, Monyo ES. 1997. Manual of laboratory procedures for quality evaluation of sorghum and pearl millet. Technical Manual No.2 Patancheru 502 324, Andhra Pradesh, India: International Crops Research Institute for the Semi-Arid Tropics.
- Grootboom AW, Mkhonza NL, Mbambo Z, O’Kennedy MM, da Silva LS, Taylor J, Taylor JRN, Chikwamba R, Mehlo L. 2014. Co-suppression of synthesis of major α -kafirin sub-class together with γ -kafirin-1 and γ -kafirin-2 required for substantially improved protein digestibility in transgenic sorghum. *Plant Cell Reports* 33: 521-537.
- Hallgren L, Murthy DS. 1983. A screening test for grain hardness in sorghum employing density grading in sodium nitrate solution. *Journal of Cereal Science* 1: 265-274.
- Hamaker BR, Mohamed AA, Habben JE, Huang CP, Larkins BA. 1995. Efficient procedure for extracting maize and sorghum kernel proteins reveals higher prolamin contents than conventional method. *Cereal Chemistry* 72: 583–588.
- Hoseney RC. 1994. *Principles of Cereal Science and Technology*. 2nd Edition. American Association of Cereal Chemists. St. Paul, MN, USA. pp. 1-28.
- Igwe CU, Ojiako AO, Anugweje KC, Nwaogu LA, Ujowundu CO. 2012. Amino acid profile of raw and locally processed seeds of *Prosopis africana* and *Ricinus communis*: Potential antidotes to protein malnutrition. *Functional Foods in Health and Disease* 2(4): 107-119.
- Jamabo T, Onwukwe AO. 2010. The incidence of marasmic-kwashiokor among children in Port Harcourt, Nigeria. *Nigerian Journal of Agriculture, Food and Environment* 6: 96-100.

- Jambunathan R, Kherdekar MS, Stenhouse JW. 1992. Sorghum grain hardness and its relationship to mold susceptibility and mold resistance. *Journal of Agricultural and Food Chemistry* 40: 1403–1408.
- Jiang X, Xiao G. 2010. Detection of unintended effect in genetically modified herbicide-tolerant (GMHT) rice in comparison with non-target phenotypic characteristics. *African Journal of Agricultural Research* 5(10): 1082-1088.
- Kirleis AW, Crosby KD. 1981. Sorghum hardness: comparison of methods for its evaluation. In: *Proceedings of the International Symposium on Sorghum Grain Quality*. LW Rooney and DS Murty (Eds) ICRISAT (International Crops Research Institute for the Semi-Arid Tropics) Patancheru, India, pp. 231-241.
- Krishnan HB, White JA, Pueppke SG. 1989. Immunocytochemical analysis of protein body formation in seeds of *Sorghum bicolor*. *Canadian Journal of Botany* 67: 2850-2856.
- Lasztity R. 1996. *The Chemistry of cereal proteins*. Boca Raton FL, CRC Press.
- Levandi T, Leon C, Kaljurand M, Garcia-Cañas, Cifuentes A. 2008. Capillary Electrophoresis Time-of-Flight Mass Spectrometry for comparative metabolomics of transgenic versus conventional maize. *Analytical Chemistry* 80: 6329-6335.
- Laemmli UK. 1970. Cleavage of structural proteins during the assembly of the head of bacteriophage T4. *Nature* 227: 680-685.
- Li X, Huang K, He X, Zhu B, Liang Z, Li H, Luo Y. 2007. Comparison of nutritional quality between Chinese Indica Rice with *sck* and *cry1Ac* genes and its non-transgenic counterpart. *Journal of Food Science* 72(6): S420-S424.
- Mehlo L, Mbambo Z, Bado S, Lin J, Moagi SM, Buthelezi S, Stoychev S, Chikwamba R. 2013. Induced protein polymorphisms and nutritional quality of gamma irradiation mutants of sorghum. *Mutation Research/Fundamental and Molecular Mechanisms of Mutagenesis* 749(1): 66-72.
- Modirroosta BH, Tohidfar M, Saba J, Moradi F. 2014. The substantive equivalence of transgenic (Bt and Chi) and non-transgenic cotton based on metabolite profiles. *Functional and Integrative Genomics* 14: 237-244.
- Mohan Jain S. 2001. Tissue culture-derived variation in crop improvement. *Euphytica* 118: 153-166.
- Mokrane H, Lagrain B, Gebruers K, Courtin CM, Brijs K, Proost P, Delcour JA. 2009. Characterisation of kafirins in Algerian sorghum cultivars. *Cereal Chemistry* 86(5): 487-491.
- Pons E, Peris JE, Peña L. 2012. Field performance of transgenic citrus trees: Assessment of the long-term expression of *uidA* and *nptII* transgenes and its impact on relevant agronomic and phenotypic characteristics. *BMC Biotechnology* 12(41):1-15.
- Ratnavathi CV, Komala VV. 2016. Sorghum Grain Quality. In: Ratnavathi CV, Patil JV, Chavan UD (Eds) *Sorghum Biochemistry: An industrial perspective*. Academic Press, London, UK. pp 1-62.
- Reddy BVS, Kumar AA, Reddy PS. 2010. Recent advances in sorghum improvement research at ICRISAT. *Kasetsart Journal Natural Science* 44: 499-506.

- Ridley WP, Sidhu RS, Pyla PD, Nemeth MA, Breeze ML, Astwood JD, 2002. Comparison of the nutritional profile of glyphosphate-tolerant corn event NK603 with that of conventional corn (*Zea mays* L.). *Journal of Agricultural and Food Chemistry* 50: 7235-7243.
- Rooney LW, Miller FR. 1982. Variations in the structure and kernel characteristics of sorghum. In: *Proceedings of the International Symposium on Sorghum Grain Quality*. LW Rooney, DS Murty (Eds) ICRISAT (International Crops Research Institute for the Semi-Arid Tropics) Patancheru, India, pp. 143-162.
- Shepherd LVT, McNicol JW, Razzo R, Taylor MA, Davies HV. 2006. Assessing the potential for unintended effects in genetically modified potatoes perturbed in metabolic and developmental processes. Targeted analysis of key nutrients and anti-nutrients. *Transgenic Research* 15: 409-425.
- Shewry PR. 2007. Improving the protein content and composition of cereal grain. *Journal of Cereal Science* 46: 239-250.
- Shull JM, Watterson JJ, Kirleis AW. 1992. Purification and immunocytochemical localization of kafirins in *Sorghum bicolor* (L. Moench) endosperm. *Protoplasma* 171: 64-74.
- Simonyan KJ, El-Okene AM, Yiljep YD. 2007. Some Physical Properties of Samaru Sorghum 17 Grains. *Agricultural Engineering International: the CIGR eJournal manuscript FP 07008*. Vol. IX. <https://core.ac.uk/download/files/205/4909156.pdf>.
- Singh R, Axtell LD. 1973. High lysine mutant gene (hl) that improves protein quality and biochemical value of grain sorghum. *Crop Science* 13: 535-539.
- Soares Correa de Souza R, Santana Balbuena T, Arruda P. 2015. Structure, organisation and expression of the alpha prolamin multigenic family bring new insights into the evolutionary relationships among grasses. *The Plant Genome* 8(1): 1-11.
- Stamova BS, Roessner U, Suren S, Laudencia-Chingcuanco D, Bacic A, Beckles DM. 2009. Metabolic profiling of transgenic wheat over-expressing the high-molecular-weight Dx5 glutenin subunit. *Metabolomics* 5: 239-252.
- Taylor JRN, Belton PS. 2002. Sorghum. In: Belton PS, Taylor JRN (Eds) *Pseudocereals and less common cereals: grain properties and utilization potential*. pp 25-82. Springer-Verlag: Berlin, Germany.
- Tesso T, Ejeta G, Chandrashekar A, Huang CP, Tandjung A, Lewamy M, Axtell JD, Hamaker BR. 2006. A novel modified endosperm texture in a mutant high-protein digestibility/high-lysine grain sorghum (*Sorghum bicolor* (L.) Moench). *Cereal Chemistry* 83: 194-201.
- Uzogara SG. 2000. The impact of genetic modification of human foods in the 21st century: A review. *Biotechnology Advances* 18: 179-206.
- Waniska RD, Rooney LW. 2002. Sorghum grain quality for increased utilisation. In: *Sorghum and Millet Diseases*, JF Leslie (Ed). Iowa State Press, pp. 327-338.
- Welch RM, Graham RD. 2004. Breeding for micronutrients in staple food crops from a human nutrition perspective. *Journal of Experimental Botany* 55(396): 353-364.
- Wong JH, Lau T, Cai N, Singh J, Pedersen JF, Vensel W, Hurkman WJ, Wilson JD, Lemaux PG, Buchanan BB. 2009. Digestibility of protein and starch from sorghum (*Sorghum bicolor*) is linked to biochemical and structural features of grain endosperm. *Journal of Cereal Science* 49: 73-82.

- Xiao J, Li Y, Li J, Gonzalez AP, Xia Q, Huang Q. 2015. Structure, morphology, and assembly behaviour of kafirin. *Journal of Agricultural and Food Chemistry* 63: 216–224.
- Zeller SL, Kalinina O, Brunner S, Keller B, Schmid B. 2010. Transgene x environment interactions in genetically modified wheat. *PLoS One* 5, e11405.
- Zhao Z. 2007. The Africa Biofortified Sorghum Project – applying biotechnology to develop nutritionally improved sorghum for Africa. In: Xu Z, Li J, Xue Y, Yang W. (Eds) *Biotechnology and Sustainable Agriculture 2006 and beyond*. Springer, Dordrecht. pp 273-277.
- Zhu J, Patzoldt WL, Shealy RT, Vodkin LO, Clough SJ, Tranel PJ. 2008. Transcriptome response to glyphosate in sensitive and resistant soybean. *Journal of Agricultural and Food Chemistry* 56: 6355-6363.

CHAPTER 3

Appendix: Published Article



A Comparative Study of Selected Physical and Biochemical Traits of Wild-Type and Transgenic Sorghum to Reveal Differences Relevant to Grain Quality

Roya J. Ndimba^{1,2*}, Johanita Kruger³, Luke Mehlo⁴, Alban Barnabas¹, Jens Kossmann² and Bongani K. Ndimba^{5,6}

¹ iThemba LABS, National Research Foundation, Cape Town, South Africa, ² Institute for Plant Biotechnology, University of Stellenbosch, Matieland, South Africa, ³ Department of Food Science and Institute for Food Nutrition and Well-Being, University of Pretoria, Pretoria, South Africa, ⁴ Enterprise Creation for Development Unit, Council for Scientific and Industrial Research, Pretoria, South Africa, ⁵ Agricultural Research Council, Infruitec-Nietvoorbij, Stellenbosch, South Africa, ⁶ Proteomics Unit, Department of Biotechnology, University of the Western Cape, Bellville, South Africa

OPEN ACCESS

Edited by:

Soren K. Rasmussen,
University of Copenhagen, Denmark

Reviewed by:

Godfrey Akpan Iwo,
University of Calabar, Nigeria
Tian-Qing Zheng,
Institute of Crop Sciences/National
Key Facility for Crop Gene Resources
and Genetic Improvement, Chinese
Academy of Agricultural Sciences,
China

*Correspondence:

Roya J. Ndimba
minnis@tlabs.ac.za

Specialty section:

This article was submitted to
Crop Science and Horticulture,
a section of the journal
Frontiers in Plant Science

Received: 09 December 2016

Accepted: 22 May 2017

Published: 07 June 2017

Citation:

Ndimba RJ, Kruger J, Mehlo L,
Barnabas A, Kossmann J and
Ndimba BK (2017) A Comparative
Study of Selected Physical and
Biochemical Traits of Wild-Type and
Transgenic Sorghum to Reveal
Differences Relevant to Grain Quality.
Front. Plant Sci. 8:952.
doi: 10.3389/fpls.2017.00952

Transgenic sorghum featuring RNAi suppression of certain kafirins was developed recently, to address the problem of poor protein digestibility in the grain. However, it was not firmly established if other important quality parameters were adversely affected by this genetic intervention. In the present study several quality parameters were investigated by surveying several important physical and biochemical grain traits. Important differences in grain weight, density and endosperm texture were found that serve to differentiate the transgenic grains from their wild-type counterpart. In addition, ultrastructural analysis of the protein bodies revealed a changed morphology that is indicative of the effect of suppressed kafirins. Importantly, lysine was found to be significantly increased in one of the transgenic lines in comparison to wild-type; while no significant changes in anti-nutritional factors could be detected. The results have been insightful for demonstrating some of the corollary changes in transgenic sorghum grain, that emerge from imposed kafirin suppression.

Keywords: sorghum, transgenic, amino acid profile, protein body, grain quality traits

INTRODUCTION

Nearly 800 million of the world's population suffer from undernourishment, with the highest levels (~23%) found in Sub-Saharan Africa (FAO, IFAD, and WFP, 2015). Here, high rates of population growth coupled with severe climatic conditions often result in a chronic supply-demand mismatch (Knox et al., 2012). Grain sorghum [*Sorghum bicolor* (L) Moench], is one of Africa's most prized indigenous cereals that has been relied upon for centuries as a major food security crop (Dicko et al., 2006). Approximately 43% of all major staple foods produced on the continent are known to incorporate some aspect of sorghum grain (Etuk et al., 2012), and as a result, the crop is frequently cited as Africa's second most important cereal, after maize (Hassan, 2015). However, an over-reliance on sorghum as a basic staple is not recommended due to several nutritional shortcomings associated with its grain. Firstly, sorghum's dominant storage proteins, the kafirins, are difficult to

digest and are moreover deficient in the essential amino acids lysine, methionine and tryptophan (Shewry, 2007; Wong et al., 2009). Secondly, some sorghum grain types contain high levels of anti-nutrients such as tannins and phytate (Reddy et al., 1982; Gilani et al., 2012), which are known to strongly bind proteins and essential minerals, leading to reduced bioavailability, and hence compromised levels of nutrient uptake.

Given that poor communities subsisting on monotonous cereal-based diets, like sorghum, are vulnerable to malnutrition, significant research has been directed toward improving the nutritional value of sorghum grain (Zhao, 2008; Reddy et al., 2010). Grootboom et al. (2014), used RNA interference (RNAi) technology to suppress the expression of select kafirin subclasses, which resulted in transgenic sorghum grain with improved protein digestibility levels of up to 53%. Although, this approach has been recognized as an effective strategy for increasing the protein digestibility (and hence the nutritional value) of sorghum grain, these “improved” transgenic lines have not yet been commercialized or cultivated. This is likely a consequence of the strict legislative requirements involved in the pre-approval of genetically modified (GM) food crops before general or commercial release (Shepherd et al., 2006; García-Villalba et al., 2008). Undoubtedly, a key concern is to ensure that the transgenic food item is as safe and nutritious as its non-transgenic counterpart, and poses no potential new risks to the consumer or the environment (Chassy, 2010; Jiang and Xiao, 2010).

Several studies have been conducted which compare transgenic and conventionally bred lines of major food crops such as maize (Ridley et al., 2002; George et al., 2004; Levandi et al., 2008; Barros et al., 2010), wheat (Baker et al., 2006; Baudo et al., 2006), rice (Li et al., 2007; Jiang and Xiao, 2010; Gayen et al., 2013), potatoes (Shepherd et al., 2006; El-Khishin et al., 2009), and soybean (García-Villalba et al., 2008; Zhu et al., 2008). Thus, far, however, no such comparable studies have been completed on transgenic sorghum. In the present work an attempt will be made to investigate aspects of substantial equivalence between transgenic sorghum grain and its non-transgenic parental counterpart. The approach will involve a comparative analysis of key physical and biochemical characteristics of the grains that have an important impact on grain quality and/or nutritional value. The key physical grain quality traits that will be analyzed include a comparative evaluation of grain weight, grain hardness, and protein body morphology. For assessing differences in the biochemical composition, a comparative study of the amino acid composition and key anti-nutrients (such as condensed tannins and phytate) will be carried out. The results of this study will be important for highlighting some of the key differences that distinguish the transgenic grain from the wild-type and further, whether or not these differences have significant biological or nutritional consequences.

MATERIALS AND METHODS

Plant Materials

Two independent transgenic sorghum lines, featuring the pABS042 construct, for the targeted suppression of γ -kafirin-1

(27 kDa) and γ -kafirin-2 (50 kDa) were assessed in the present study. Previous analyses found complete suppression of the targeted kafirin proteins and a significant improvement (of up to 37%) in the *in vitro* protein digestibility of the transgenic grains (Grootboom et al., 2014). The transgenic lines represent the fifth generation of self-crossing progenies from T₀ sorghum transformants, which were originally produced using particle bombardment as described in Grootboom et al. (2014). Plants from each independent transgenic line (hereafter referred to as 42-1 and 42-2) and the parental control cultivar P898012 (hereafter referred to as WT), were grown in pots in a containment glasshouse located at the Centre for Scientific and Industrial Research (CSIR) Biosciences Division (Pretoria, South Africa). Environmental conditions were controlled (12-h photoperiod, 25°C/20°C day/night, ~50% humidity, 800 μ E/s/m² irradiance), with a minimum of three biological replicates per line. At each occasion of watering, the plant arrangement in the glasshouse was randomized to counter any possible positional effects due to the microhabitat, and at anthesis, the panicle of each plant was bagged to prevent outcrossing. At full maturity, the grains were hand-harvested from each plant, and manually cleaned to remove all glumes, damaged grains, and other extraneous matter. For the physical characterization of the grain, whole kernels, separately derived from individual plants of each genotype were used to make up the sample. However, for the chemical analyses, the whole kernels had to be ground into fine flour. To reduce biological variation and to maximize the limited quantity of sample material available, equal portions of grain from individual plants from each genotype were pooled and homogenized to fine flour, using a standard laboratory mill. Milled grain flour was used immediately for the intended analysis or stored at -20°C in airtight containers until analyzed.

Physical Characteristics

Kernel Weight

For each line, the mass of 100 randomly selected kernels was determined using a 10⁻⁴ precision balance. This measurement was repeated three times for three biological replicates per line, to obtain the mean 100-kernel weight \pm SD.

Grain Hardness

To evaluate differences in grain hardness, the floater test (Hallgren and Murthy, 1983) was used, where 100 randomly selected kernels from each line (replicated 3 times) were placed in a solution of sodium nitrate with a specific gravity of 1.250 g/mL (as measured with a hydrometer) and the percentage of floating kernels (low density) was determined. As a complement to this test, a visual inspection of the grain endosperm texture was also carried out. Individual kernels (20 randomly selected from each line, replicated 3 times) were longitudinally sectioned through the middle and subjectively categorized as a floury (completely opaque) or an intermediate (partly corneous/partly opaque) phenotype using ICC Standard No.176 (ICC, 2008). The percentage of floury endosperm phenotypes found for each line was then tabulated and compared.

Protein Body Morphology

Transmission electron microscopy (TEM) was used to investigate the morphology of the grain protein bodies. In brief, segments of the peripheral endosperm ($\sim 1\text{--}2\text{ mm}^3$ pieces) were sectioned from randomly selected mature grains of each line, and fixed in a 0.1 M sodium cacodylate buffer containing 3% (v/v) glutaraldehyde (pH 7.2) for 24 h at room temperature. The samples were then postfixed in 2% (v/v) osmium tetroxide at 4°C for 24 h, dehydrated in a graded ethanol series and embedded in Agar Low Viscosity Resin for 16 h at 70°C. Ultrathin (60–90 nm) sections of resin embedded samples were cut using an ultramicrotome (Leica EM UC7) fitted with a Diatome diamond knife and double stained with 2% (w/v) uranyl acetate (8 min) and 0.1% (w/v) lead citrate (5 min). Protein bodies located in the sub-aleurone layer of the grain endosperm tissue were imaged using a FEI Tecnai™ G2 transmission electron microscope, operating at an accelerating voltage of 200 kV (Electron Microscope Unit, University of Cape Town).

Biochemical Characteristics

Total Amino Acid Composition

The protein-bound amino acid content was measured according to the Pico-Tag reverse-phase high performance liquid chromatography (RP-HPLC) procedure (Bidlingmeyer et al., 1984) at the South African Grain Laboratory (SAGL) (Pretoria, South Africa). In brief, sorghum samples were hydrolysed in 6N HCl for 24 h, after performic acid oxidation (for the analysis of cysteine and methionine) or without previous oxidation (for all other amino acids). The liberated amino acids were then derivatized before separation and quantification by means of RP-HPLC using a Waters™ Pico-Tag C18 column (3.9×150 mm) and the relevant amino acid standards.

Anti-nutrient Levels

The condensed tannins and phytate content were measured in duplicate for two independent samples of each sorghum genotype. To determine the condensed tannin contents, a modified vanillin-HCl method was followed (Price et al., 1978), where the tannins were extracted with acidified methanol. For each sample, the absorbance of sample blanks were subtracted to compensate for non-tannin pigments related to grain color. The final concentration of condensed tannins in each sample was determined against a gallic catechin standard, and expressed in mg catechin equivalents (CE) per g of wholegrain sorghum flour. The phytate levels were determined using an indirect quantitative assay based on anion-exchange chromatography (Frubeck et al., 1995) following extraction with 2.4% conc. HCl. The final phytate content was expressed in terms mg/g wholegrain sorghum flour.

Statistical Analysis

Unless otherwise stated, investigated parameters were analyzed in triplicate and the results expressed as the mean \pm SD. Data were subjected to analyses of variance (ANOVA) and means compared by the Fisher Least Significant Difference (LSD) test ($p < 0.05$) using *Statistica* for Windows Version 13.0 (StatSoft Inc., USA).

RESULTS AND DISCUSSION

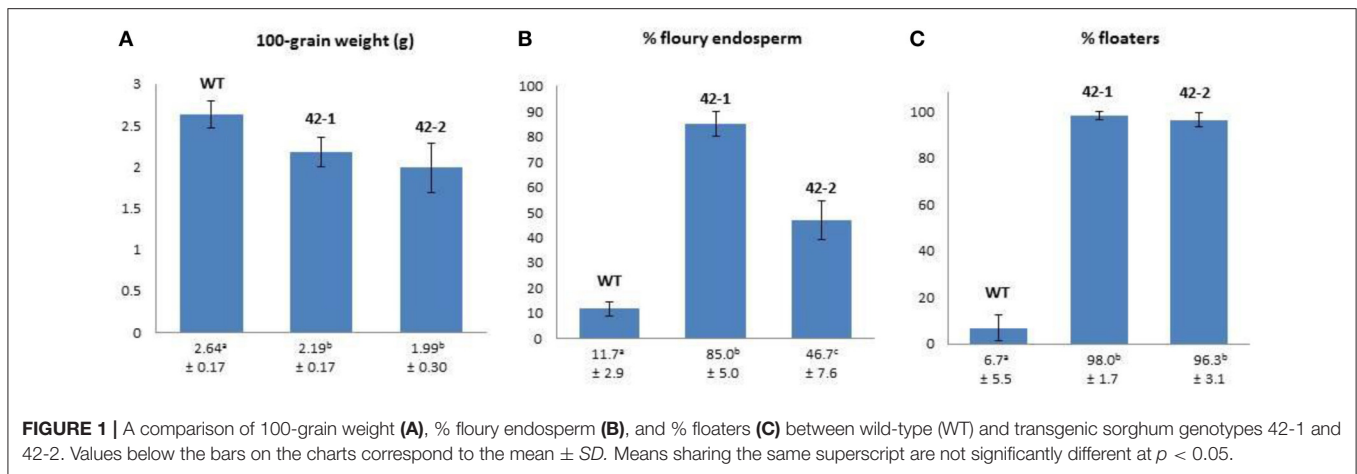
Differences in the Physical Traits of the Transgenic vs. WT Grains

The results pertaining to differences in the physical traits of grain from the two transgenic lines (42-1, 42-2) and their non-transgenic parental counterpart (WT) are presented in **Figure 1**. For the mean 100-grain weight, both transgenic lines were observed to have a lower weight in comparison to WT, but a statistically significant reduction could only be ascribed to the grains in line 42-2. In the case of the proportion of floury endosperm types and the percentage of floating kernels, both transgenic lines were found to have significantly increased levels of these characteristics in comparison to WT.

According to the literature, physical traits such as grain weight, density, and endosperm texture are important indicators of quality for sorghum because of their impact on grain hardness. Hard grains tend to be heavy (>2.0 g 100-grain weight) with a low percentage of floaters ($<40\%$), and a corneous to intermediate endosperm texture (Gomez et al., 1997). For large scale production and processing, hard sorghum grains are generally preferred because of their association with reduced post-harvest losses (due to breakage and/or spoilage) and enhanced milling yields (Jambunathan et al., 1992; Simonyan et al., 2007).

The high percentage of floating grains amongst the transgenic lines ($>96\%$) indicated a significant decrease in the grain density in comparison to the WT. The rationale informing the use of the sodium nitrate solution with a specific gravity of 1.25 g/mL is that this value is approximately equal to the average density of a wide range of sorghum kernels (Kirleis and Crosby, 1981). Thus, in this solution, kernels of lower density than average will float, while those of greater density will sink (Gomez et al., 1997). It is therefore clear that the transgenic grains are not only less dense than the WT, but are also less dense than the average known for sorghum grain. The reason for this decreased density is likely attributable to the significant increase in the percentage of floury endosperm types. The floury endosperm phenotype is associated with loosely packed starch granules that accommodate more air spaces (Rooney and Miller, 1982; Hosene, 1994). It is therefore likely that the reduced density in the transgenic grain is attributable to the inclusion of more air spaces within the grain endosperm, which results in the characteristic opaque or floury visual appearance of this endosperm structure.

The increased percentage of floury endosperm phenotypes in the transgenic lines was commensurate with similar findings reported previously (Da Silva et al., 2011; Grootboom et al., 2014). Amongst the transgenic lines, a significant difference in the average number of floury endosperm types, was observed, with the highest percentage found in line 42-1 (85%), which was close to twice the value of that found in line 42-2 (47%). The floury endosperm phenotype is generally associated with improved nutritional qualities, such as improved protein digestibility and essential amino acid content (Singh and Axtell, 1973; Tesso et al., 2006; Da Silva et al., 2011). However, these nutritional gains are often overshadowed by the increased susceptibility of these softer floury grains to post-maturity losses



and damage due to molding and insect infestation (Waniska and Rooney, 2002).

Morphological features of the grain protein bodies were studied using TEM analysis, the results of which are shown in **Figure 2**. In the earlier work of Grootboom et al. (2014), the protein bodies of the transgenic lines transformed with the ABS042 construct did not deviate much in terms of overall shape and size, as compared to the protein bodies found in the grain of the non-transgenic parent, P898012. This finding is consistent with similar studies featuring transgenic sorghum with targeted γ -kafirin suppression, such as the ABS 149 line (Da Silva et al., 2011) and the TX430 line (Kumar et al., 2012). In the present work, however, some important deviations in the morphology of the protein bodies in the transgenic lines were detected. Firstly in terms of size, no protein bodies of less than 0.5 μm diameter were found in the WT. In contrast, both transgenic lines were found to have protein bodies (of varying number) that were diminutive in size (<0.5 μm) in comparison to the WT. The reduced size of the protein bodies translate to a reduced surface to volume ratio, which would favor enhanced proteolytic digestion. Secondly in terms of shape, the most extreme change of morphology was evident in transgenic line 42-1. WT protein bodies conformed to the expected highly-ordered polygonal structure, with internal concentric rings, that is typical of normal sorghum. In contrast the protein bodies of line 42-1, were highly irregular in shape, with no internal concentric ring structures, and with deep invaginations present at the periphery. In line 42-2, the protein bodies were closer in morphology to the WT, exhibiting a regular overall polygonal shape, with some distinctive patterns of internalized concentric rings. The only features that served to differentiate the protein bodies of transgenic lines 42-2 from WT, were the small peripheral indentations that gave the boundary region a cracked appearance. The highly misshapen protein body morphology of line 42-1 is commensurate with the structural changes found in protein bodies of high-lysine Ethiopian landraces (Singh and Axtell, 1973; Oria et al., 2000) and transgenic lines featuring both γ - and α -kafirin suppression (Da Silva et al., 2011; Grootboom et al., 2014). It may therefore be speculated that the intended

γ -kafirin suppression in line 42-1 manifests itself in a unique way that is aligned to the genetic programming in the floury endosperm phenotypes, but is distinctly different from other “related” transgenic lines with targeted γ -kafirin suppression only. This result warrants further investigation, particularly into the storage protein expression profile of 42-1 grain, which may provide vital clues into the determining factors that may underlie this “novel” phenotype.

Comparative Differences in the Biochemical Traits of the Transgenic vs. WT Grains

Amino Acids Analysis

Data depicting the protein-bound amino acid content of the WT and two transgenic sorghum lines is presented in **Table 1**. A number of important variations that serve to distinguish the transgenic lines from the WT were observed. Firstly, in comparison to WT, transgenic line 42-1 featured more significant changes in amino acid composition compared to line 42-2. In line 42-1 the concentration of 9 out of 17 amino acids were determined to be significantly different from the WT, whereas for line 42-2 this was the case for only 4 amino acids. Three amino acids that were determined to be significantly reduced in both transgenic lines in comparison to WT were tyrosine, isoleucine, and phenylalanine. The sorghum kafirins are known to contain relatively higher amounts of tyrosine, isoleucine and phenylalanine in comparison to other grain storage proteins (Virupaksha and Sastry, 1968). It may therefore be suggested that the reduction in these three amino acids is reflective of the intended targeted suppression of kafirins in the transgenic grains by RNAi. Interestingly, in the case of arginine, a significant increase (25.3%) in comparison to WT was found for line 42-1; whereas, a significant decrease (11.8%) in comparison to WT was found for line 42-2. This important difference may be indicative of a shift in the relative amounts of non-kafirins that may be present in the grains, as non-kafirins tend to have high amounts of arginine (Lasztity, 1996). An increase in the relative amount of non-kafirin grain protein in line 42-1 seems

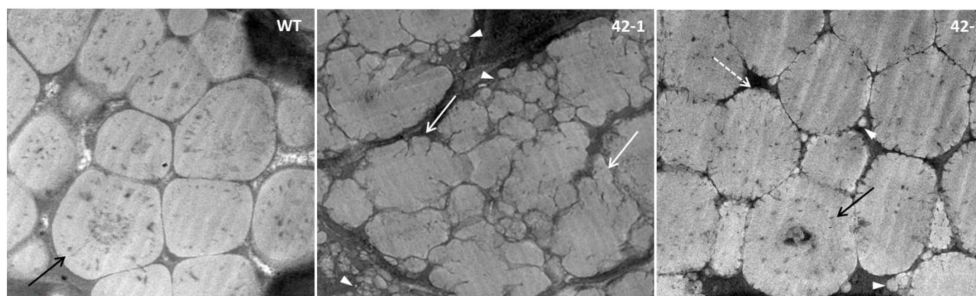


FIGURE 2 | Representative TEM images of protein bodies in the subaleurone layer of the wild-type (WT) and transgenic sorghum lines (42-1, 42-2). Black arrow points to internal concentric ring structure present in WT and some transgenic protein bodies. White arrows point to irregularly shaped protein bodies with invaginations at the periphery. “Cracked” peripheral structure of transgenic protein bodies, pointed out with white dotted arrow. White arrowheads point out the presence of small protein bodies (<0.5 μm diameter) in the transgenic lines. Scale bar represents 0.5 μm.

TABLE 1 | A comparison of the protein-bound amino acid content of the wild-type (WT) and transgenic sorghum genotypes 42-1 and 42-2, presented on a dry weight basis in mMol/100 g wholegrain flour.

Amino acids	WT	42-1	42-2	p-value
MET*	2.10 ^a ± 0.16	2.06 ^a ± 0.23	1.99 ^a ± 0.24	0.804
CYS*	3.16 ^a ± 0.70	2.39 ^a ± 0.38	2.99 ^a ± 0.58	0.290
ASX	9.29 ^a ± 0.20	10.14 ^a ± 0.08	9.46 ^a ± 0.70	0.102
GLX	25.53 ^a ± 0.74	23.22 ^b ± 0.43	25.69 ^a ± 0.60	0.004
SER	7.94 ^a ± 0.51	7.15 ^a ± 0.13	7.71 ^a ± 0.23	0.062
GLY	7.63 ^a ± 1.00	7.77 ^a ± 0.36	7.52 ^a ± 0.57	0.903
HIS**	3.25 ^a ± 0.09	2.76 ^b ± 0.17	3.22 ^a ± 0.05	0.003
ARG**	5.09 ^a ± 0.35	6.38 ^b ± 0.27	4.49 ^c ± 0.02	0.0003
THR*	5.22 ^a ± 0.36	5.24 ^a ± 0.18	5.26 ^a ± 0.12	0.974
ALA	16.13 ^a ± 0.68	14.77 ^b ± 0.36	16.21 ^a ± 0.19	0.014
PRO	12.39 ^a ± 0.36	10.57 ^a ± 1.67	13.07 ^a ± 1.14	0.094
TYR*	3.49 ^a ± 0.17	2.60 ^b ± 0.27	2.92 ^b ± 0.29	0.013
VAL*	8.25 ^a ± 0.41	8.24 ^a ± 0.23	8.30 ^a ± 0.10	0.962
ILE*	5.64 ^a ± 0.29	5.06 ^b ± 0.20	5.21 ^b ± 0.11	0.038
LEU*	16.42 ^a ± 1.13	14.27 ^b ± 0.44	16.06 ^a ± 0.32	0.023
PHE*	5.58 ^a ± 0.15	4.65 ^b ± 0.18	5.30 ^c ± 0.06	0.005
LYS*	2.38 ^a ± 0.24	3.59 ^b ± 0.07	2.34 ^a ± 0.15	0.000

Values are means (±SD) of three independent determinations. Means in rows sharing the same superscript are not significantly different at p < 0.05; Essential amino acids marked with asterisk (*). Conditionally essential amino acids are marked with double asterisk (**).

particularly evident due to the significantly increased level of lysine (50.8%) in comparison to WT. Given that kafirins are virtually lysine-free (Belton et al., 2006), the improved lysine content of line 42-1, is likely due to an increased abundance of the more lysine-rich grain proteins, such as the albumins, globulins, and glutelins (Da Silva et al., 2011). The amino acid results have confirmed the distinctiveness of line 42-1 in comparison to its sister transgenic line (42-2), as well as to WT. Of key importance from a nutritional point of view, is the significant increase of lysine in line 42-1 grain. An increase in lysine serves as one of the most important indicators of improved nutritional value since this amino acid is most limiting in sorghum and

TABLE 2 | A comparison of selected anti-nutritional factors present in wild-type (WT) and transgenic sorghum genotypes 42-1 and 42-2 wholegrain flour, on a dry weight basis.

Anti-nutritional factor	WT	42-1	42-2
Tannin (mg CE/g)	3.96 ± 0.42 ^a	4.31 ± 0.72 ^a	3.54 ± 0.47 ^a
Phytate (mg/g)	8.74 ± 0.33 ^a	8.43 ± 0.43 ^a	8.34 ± 0.73 ^a

Values are means (±SD) of duplicate samples measured twice. Means in rows sharing the same superscript are not significantly different at p < 0.05.

most other cereals. Given that the observed increase in lysine for line 42-1 was not found before in the original study of Grootboom et al. (2014), it would be of interest to study this line more extensively to determine the long-term stability and precise molecular mechanisms underpinning this desirable trait.

Anti-nutritional Factors

A statistical comparison of tannin and phytate content revealed no significant differences between the transgenic samples and WT (Table 2). The genetic intervention therefore had no substantial impact on the levels of these anti-nutritional factors in the grain.

CONCLUSION

This study has revealed a number of important differences in quality characteristics amongst and between two independent transgenic sorghum lines (featuring gamma kafirin suppression) and their wild-type counterpart. Importantly, transgenic grains were found to have a higher proportion of floury endosperm types, were conspicuously less dense and featured smaller protein body structures in comparison to wild-type grains. In terms of amino acid content, a significant increase in lysine was only found in transgenic line 42-1, which coincidentally also exhibited an extreme change in protein body morphology in comparison to that of WT. Many of the significant differences highlighted in this study were found to be consistent with observations made by other investigators interested in the high protein

digestibility phenotype in sorghum varieties. A concern therefore remains that the softer endosperm phenotype may mean that the transgenic grains are more susceptible to abiotic and biotic stress in the field. Further studies are therefore needed to evaluate the field performance of these modified lines in conjunction with more extensive analysis of key grain quality traits, such as the significant increase in lysine in line 42-1 over a multi-year multi-location large-scale trial.

AUTHOR CONTRIBUTIONS

RN: Carried out the bulk of the experimental work, compiled the results, drafted the manuscript. JoK: Responsible for

the anti-nutrient experiments, gave scientific input on the structure and form of the manuscript, edited as necessary. LM: Provided access to the GM material, grew the plants at the containment facility, collected the samples, prepared material for the experiments, gave scientific input into the structure and form of the manuscript. AB: Instrumental in the preparation of samples for TEM analysis. JeK: provided lab infrastructure and funding in support of the experimental work performed at Stellenbosch. BN: provided lab infrastructure and funding in support of the experimental work performed, in particular the amino acid analyses costs, and extensive editing and scientific input into the preparation of the final manuscript.

REFERENCES

- Baker, J. M., Hawkins, N. D., Ward, J. L., Lovegrove, A., Napier, J. Z., Shewry, P. R., et al. (2006). A metabolomics study of substantial equivalence of field-grown genetically modified wheat. *Plant Biotechnol. J.* 4, 381–392. doi: 10.1111/j.1467-7652.2006.00197.x
- Barros, E., Lezar, S., Anttonen, M. J., van Dijk, J. P., Röhlig, R. M., Kok, E. J., et al. (2010). Comparison of two GM maize varieties with a near isogenic non-GM variety using transcriptomics, proteomics and metabolomics. *Plant Biotechnol. J.* 8, 436–451. doi: 10.1111/j.1467-7652.2009.00487.x
- Baudo, M. M., Lyons, R., Powers, S., Pastori, G. M., Edwards, K. J., Holdsworth, M. J., et al. (2006). Transgenesis has less impact on the transcriptome of wheat grain than conventional breeding. *Plant Biotechnol. J.* 4, 369–380. doi: 10.1111/j.1467-7652.2006.00193.x
- Belton, P. S., Delgadillo, I., Halford, N. G., and Shewry, P. R. (2006). Kafirin structure and functionality. *J. Cereal Sci.* 44, 272–286. doi: 10.1016/j.jcs.2006.05.004
- Bidlingmeyer, B. A., Cohen, S. A., and Tarvin, T. L. (1984). Rapid analysis of amino acids using pre-column derivatization. *J. Chromatogr.* 336, 93–104. doi: 10.1016/S0378-4347(00)85133-6
- Chassy, B. M. (2010). Food safety risks and consumer health. *New Biotechnol.* 27, 534–544. doi: 10.1016/j.nbt.2010.05.018
- Da Silva, L. S., Jung, R., Zhao, Z., Glassman, K., Taylor, J., and Taylor, J. R. N. (2011). Effect of suppressing the synthesis of different kafirin subclasses on grain endosperm texture, protein body structure and protein nutritional quality in improved sorghum lines. *J. Cereal Sci.* 54, 160–167. doi: 10.1016/j.jcs.2011.04.009
- Dicko, M. H., Gruppen, H., Traore, A. S., Voragen, A. G. J., and Van Berkel, W. J. H. (2006). Sorghum grain as human food in Africa: relevance of content of starch and amylase activities. *Afr. J. Biotechnol.* 5, 384–395. doi: 10.5897/AJB05.060
- El-Khishin, D. A., Hamid, A. A., El-Moghazy, G., and Metry, A. (2009). Assessment of genetically modified potato lines resistant to potato virus Y using compositional analysis and molecular markers. *Res. J. Agric. Biol. Sci.* 5, 261–271.
- Etuk, E. B., Ifeduba, A. V., Okata, U. E., Chiaka, I., Okoli, I. C., Okeudo, N. J., et al. (2012). Nutrient composition and feeding value of sorghum for livestock and poultry: a review. *J. Anim. Sci. Adv.* 2, 510–524.
- Frubeck, G., Alonso, R., Marzo, F., and Santidrian, S. (1995). A modified method for the indirect quantitative analysis of phytate in foodstuffs. *Anal. Biochem.* 225, 206–212. doi: 10.1006/abio.1995.1145
- García-Villalba, R., León, C., Dinelli, G., Segura-Carretero, A., Fernández-Gutiérrez, A., García-Cañas, V., et al. (2008). Comparative metabolomics study of transgenic versus conventional soybean using capillary electrophoresis-time-of-flight mass spectrometry. *J. Chromatogr. A* 1195, 164–173. doi: 10.1016/j.chroma.2008.05.018
- Gayen, D., Nath Sarkar, S., Datta, S. K., and Datta, K. (2013). Comparative analysis of nutritional compositions of transgenic high iron rice with its non-transgenic counterpart. *Food Chem.* 138, 835–840. doi: 10.1016/j.foodchem.2012.11.065
- George, C., Ridley, W. P., Obert, J. C., Nemeth, M. A., Breeze, M. L., and Astwood, J. D. (2004). Composition of grain and forage from corn rootworm-protected corn event MON 863 is equivalent to that of conventional corn (*Zea mays* L.). *J. Agric. Food Chem.* 52, 4149–4158. doi: 10.1021/jf035023m
- Gilani, G. S., Xiao, C. W., and Cockell, K. A. (2012). Impact of antinutritional factors in food proteins on the digestibility of protein and the bioavailability of amino acids and on protein quality. *Br. J. Nutr.* 108, S315–S332. doi: 10.1017/S0007114512002371
- Gomez, M. I., Obilarra, A. B., Martin, D. E., Madzvamuse, M., and Monyo, E. S. (1997). *Manual of Laboratory Procedures for Quality Evaluation of Sorghum and Pearl Millet*. Technical Manual No.2 Patancheru 502 324. International Crops Research Institute for the Semi-Arid Tropics, Andhra Pradesh.
- Grootboom, A. W., Mkhonza, N. L., Mbambo, Z., O'Kennedy, M. M., da Silva, L. S., Taylor, J., et al. (2014). Co-suppression of synthesis of major α -kafirin sub-class together with γ -kafirin-1 and γ -kafirin-2 required for substantially improved protein digestibility in transgenic sorghum. *Plant Cell Rep.* 33, 521–537. doi: 10.1007/s00299-013-1556-5
- Hallgren, L., and Murthy, D. S. (1983). A screening test for grain hardness in sorghum employing density grading in sodium nitrate solution. *J. Cereal Sci.* 1, 265–274. doi: 10.1016/S.0733-5210(83)80014-9
- Hassan, T. A. (2015). Economics of sorghum production under traditional farming system in Nyala Governate of South Darfur State, Sudan. *ARPN J. Sci. Technol.* 5, 74–79.
- Hoseney, R. C. (1994). *Principles of Cereal Science and Technology, 2nd Edn.* St. Paul, MN: American Association of Cereal Chemists.
- FAO, IFAD, and WFP (2015). *The State of Food Insecurity in the World 2015. Meeting the 2015 International Hunger Targets: Taking Stock of Uneven Progress*. Rome: FAO. Available online at: <http://www.fao.org/3/a-i4671e.pdf> (Accessed August 13, 2015).
- International Association for Cereal Science and Technology (ICC) (2008). *Estimation of Sorghum Grain Endosperm Texture, ICC Standard 176*. Vienna: ICC.
- Jambunathan, R., Kherdekar, M. S., and Stenhouse, J. W. (1992). Sorghum grain hardness and its relationship to mold susceptibility and mold resistance. *J. Agric. Food Chem.* 40, 1403–1408. doi: 10.1021/jf00020a023
- Jiang, X., and Xiao, G. (2010). Detection of unintended effect in genetically modified herbicide-tolerant (GMHT) rice in comparison with non-target phenotypic characteristics. *Afr. J. Agric. Res.* 5, 1082–1088.
- Kirleis, A. W., and Crosby, K. D. (1981). "Sorghum hardness: comparison of methods for its evaluation," in *Proceedings of the International Symposium on Sorghum Grain Quality*, eds L. W. Rooney and D. S. Murty (Patancheru: ICRISAT, International Crops Research Institute for the Semi-Arid Tropics), 231–241.
- Knox, J., Hess, T., Daccache, A., and Wheeler, T. (2012). Climate change impacts on crop productivity in Africa and South Asia. *Environ. Res. Lett.* 7:034032. doi: 10.1088/1748-9326/7/3/034032
- Kumar, T., Dweikat, I., Sato, S., Ge, Z., Nersesian, N., Chen, H., et al. (2012). Modulation of kernel storage proteins in grain sorghum

- (*Sorghum bicolor* (L.) Moench). *Plant Biotechnol. J.* 10, 533–544. doi: 10.1111/j.1467-7652.2012.00685.x
- Laszti, R. (1996). *The Chemistry of Cereal Proteins*. Boca Raton, FL: CRC Press.
- Levandi, T., Leon, C., Kaljurand, M., Garcia-Cañas, V., and Cifuentes, A. (2008). Capillary electrophoresis time-of-flight mass spectrometry for comparative metabolomics of transgenic versus conventional maize. *Anal. Chem.* 80, 6329–6335. doi: 10.1021/ac8006329
- Li, X., Huang, K., He, X., Zhu, B., Liang, Z., Li, H., et al. (2007). Comparison of nutritional quality between Chinese Indica Rice with *sck* and *cry1Ac* genes and its non-transgenic counterpart. *J. Food Sci.* 72, S420–S424. doi: 10.1111/j.1750-3841.2007.00416.x
- Oria, M. P., Hamaker, B. R., Axtell, J. D., and Huang, C.-P. (2000). A highly digestible sorghum mutant cultivar exhibits a unique folded structure of endosperm protein bodies. *Proc. Natl. Acad. Sci. U.S.A.* 97, 5065–5070. doi: 10.1073/pnas.080076297
- Price, M. L., Van Scoyoc, S., and Butler, L. G. (1978). A critical evaluation of the vanillin reaction as an assay for tannin in sorghum grain. *J. Agric. Food Chem.* 26, 1214–1218. doi: 10.1021/jf60219a031
- Reddy, B. V. S., Kumar, A. A., and Reddy, P. S. (2010). Recent advances in sorghum improvement research at ICRISAT. *Kasetsart J. Nat. Sci.* 44, 499–506.
- Reddy, N. R., Sathe, S. K., and Salunkhe, D. K. (1982). Phytates in legumes and cereals. *Adv. Food Res.* 28, 1–92. doi: 10.1016/S0065-2628(08)60110-X
- Ridley, W. P., Sidhu, R. S., Pyla, P. D., Nemeth, M. A., Breeze, M. L., and Astwood, J. D. (2002). Comparison of the nutritional profile of glyphosate-tolerant corn event NK603 with that of conventional corn (*Zea mays* L.). *J. Agric. Food Chem.* 50, 7235–7243. doi: 10.1021/jf0205662
- Rooney, L. W., and Miller, F. R. (1982). “Variations in the structure and kernel characteristics of sorghum,” in *Proceedings of the International Symposium on Sorghum Grain Quality*, eds L. W. Rooney and D. S. Murty (Patancheru: ICRISAT, International Crops Research Institute for the Semi-Arid Tropics), 143–162.
- Shepherd, L. V. T., McNicol, J. W., Razzo, R., Taylor, M. A., and Davies, H. V. (2006). Assessing the potential for unintended effects in genetically modified potatoes perturbed in metabolic and developmental processes. Targeted analysis of key nutrients and anti-nutrients. *Transgenic Res.* 15, 409–425. doi: 10.1007/s11248-006-0012-5
- Shewry, P. R. (2007). Improving the protein content and composition of cereal grain. *J. Cereal Sci.* 46, 239–250. doi: 10.1016/j.jcs.2007.06.006
- Simonyan, K. J., El-Okene, A. M., and Yiljep, Y. D. (2007). *Some Physical Properties of Samaru Sorghum 17 Grains*. Agricultural Engineering International: the CIGR eJournal manuscript FP 07008. Available online at: <https://core.ac.uk/download/files/205/4909156.pdf>
- Singh, R., and Axtell, L. D. (1973). High lysine mutant gene (hl) that improves protein quality and biochemical value of grain sorghum. *Crop Sci.* 13, 535–539. doi: 10.2135/cropsci1973.0011183X001300050012x
- Tesso, T., Ejeta, G., Chandrashekar, A., Huang, C. P., Tandjung, A., Lewamy, M., et al. (2006). A novel modified endosperm texture in a mutant high-protein digestibility/high-lysine grain sorghum (*Sorghum bicolor* (L.) Moench). *Cereal Chem.* 83, 194–201. doi: 10.1094/CC-83-0194
- Virupaksha, T. K., and Sastry, L. V. S. (1968). Studies on the protein content and amino acid composition of some varieties of grain sorghum. *J. Agric. Food Chem.* 16, 199–203. doi: 10.1021/jf60156a022
- Waniska, R. D., and Rooney, L. W. (2002). “Sorghum grain quality for increased utilisation,” in *Sorghum and Millet Diseases*, ed J. F. Leslie (Ames, IA: Iowa State Press), 327–338.
- Wong, J. H., Lau, T., Cai, N., Singh, J., Pedersen, J. F., Vensel, W. H., et al. (2009). Digestibility of protein and starch from sorghum (*Sorghum bicolor*) is linked to biochemical and structural features of grain endosperm. *J. Cereal Sci.* 49, 73–82. doi: 10.1016/j.jcs.2008.07.013
- Zhao, Z. Y. (2008). “The Africa Biofortified Sorghum Project – Applying Biotechnology to develop nutritionally improved sorghum for Africa,” in *Biotechnology and Sustainable Agriculture 2006 and Beyond*, eds Z. Xu, J. Li, Y. Xue, and W. Yang (Dordrecht: Springer), 273–277.
- Zhu, J., Patzoldt, W. L., Shealy, R. T., Vodkin, L. O., Clough, S. J., and Tranel, P. J. (2008). Transcriptome response to glyphosate in sensitive and resistant soybean. *J. Agric. Food Chem.* 56, 6355–6363. doi: 10.1021/jf801254e

Conflict of Interest Statement: The authors declare that the research was conducted in the absence of any commercial or financial relationships that could be construed as a potential conflict of interest.

Copyright © 2017 Ndimba, Kruger, Mehlo, Barnabas, Kossmann and Ndimba. This is an open-access article distributed under the terms of the Creative Commons Attribution License (CC BY). The use, distribution or reproduction in other forums is permitted, provided the original author(s) or licensor are credited and that the original publication in this journal is cited, in accordance with accepted academic practice. No use, distribution or reproduction is permitted which does not comply with these terms.

CHAPTER 4

A comparative evaluation of changes in the protein profile and the elemental composition of wild-type versus transgenic sorghum grain

4.1 Introduction

Amongst the diverse range of factors that impact grain nutritional quality, protein and mineral content rank as highly important (Syltje and Dahnke, 1983). This is mainly because of the critical role that proteins and minerals play in the diet. Sorghum is one important food security crop that is currently being developed to produce biofortified transgenic lines with improved protein quality. In the study of Grootboom *et al.*, (2014) RNAi was used to suppress certain subclasses of kafirins in sorghum grain, which resulted in a number of transgenic lines with improved protein digestibility characteristics and some improvement to the lysine content. In the previous chapter, three of these transgenic lines were identified to have a significantly improved lysine content that was increased by up to 50% in comparison to the wild-type (WT) grain. Although it is speculated that the increase in lysine is due to a compensatory synthesis of other lysine-rich grain proteins, no direct evidence of this change in the protein profile has been provided thus far. Additionally, because proteins and minerals are known to share a close association in biological systems (Garman and Grime, 2005; Distelfeld *et al.*, 2007) it may be plausible that the genetic intervention that was aimed at the suppression of kafirin protein, may have an inadvertent detrimental effect on the localisation and/or concentration of certain minerals in the grain. To address these two main concerns, the present study was initiated to evaluate changes in the protein and mineral profile of the transgenic sorghum versus the wild-type (WT) sorghum grain. To study changes in the grain protein profile, a proteomics approach was adopted, which involved a sequential extraction of the three major protein fractions of the grain, followed by 1D SDS-PAGE and a final identification of differentially expressed proteins by matrix-assisted laser desorption/ionisation time-of-flight mass spectrometry (MALDI TOF MS). For the assessment of possible changes in the grain mineral profile, a bulk characterisation of the grain mineral content was made using ICP-AES/MS; whilst in-tissue concentration differences were analysed using the nuclear microscopy technique of micro-PIXE. Prior to this study, no similar report evaluating changes in the protein and mineral profile of these transgenic sorghum grains was completed. The current study therefore represents a new approach to characterising differences between these transgenic lines and their wild-type counterpart, and therefore could provide new and

valuable insights into the effect that kafirin suppression may have on the overall protein and mineral composition of these protein-biofortified grains.

4.2 Materials and methods

4.2.1 Plant material

As reported in section 3.2.1 in Chapter 3.

4.2.2 Protein extraction

The procedure followed for the sequential extraction of proteins from the sorghum wholegrain flour samples was essentially as described by Cremer *et al.*, (2014). Only samples from the three transgenic lines 44-3, 44-2 and 42-1 were used in the present analysis, along with the WT. In brief, 100 mg of wholegrain sorghum flour from each genotype was mixed with 1 mL of extracting solvent (50 mM Tris-HCl pH 7.8, 100 mM KCl, 5 mM EDTA) and allowed to shake for 1 hour at room temperature. Next, the samples were centrifuged (15 000 x *g* for 5 minutes) and the clear supernatant removed to a fresh tube. This extraction process was repeated an additional two times and the supernatants pooled and labelled as the albumin/globulin fraction. The pellet remaining after the extraction of the albumin/globulin fraction was then washed with 1 mL distilled water before proceeding to the kafirin extraction step. For kafirin extraction, the retained pellet was mixed with 1 mL of 60% (v/v) tert-butanol solution with 0.5% (w/v) sodium acetate and 2% (v/v) β -mercaptoethanol, and allowed to shake for 4 hours at room temperature. After this first round of extraction, the samples were centrifuged as before and the supernatant transferred to a fresh tube. This process was repeated once more and the supernatants pooled, and labelled the kafirin fraction. For the final fraction, the pellet retained from the kafirin extraction was washed with 1 mL distilled water, before 1 mL of a sodium borate buffer (125 mM pH 10, containing 1 %SDS (w/v) and 1% (v/v) β -mercaptoethanol) was added. The samples were allowed to shake for the extraction of the glutelins/residual proteins for 1 hour at room temperature. Next, the samples were centrifuged, as before, and the supernatant transferred to a fresh tube. The extraction of glutelins/residual proteins was repeated two more times, and the supernatants pooled. After the collection of the three major fractions, the proteins were precipitated overnight by incubating the samples with 5 x volume of ice-cold methanol containing 0.1 M ammonium acetate, at -20°C. The precipitated proteins were then recovered after centrifugation as before, and solubilised in 250 μ L of Bio-Rad's IEF sample buffer. The protein concentration of each

extract was then determined using the Bio-Rad Bradford Protein Assay solution, with bovine serum albumin (BSA) as the protein standard (Bradford, 1976). 5 µg of the extracted protein was then used for 1D SDS-PAGE analysis.

4.2.3 One dimensional sodium dodecyl sulphate polyacrylamide gel electrophoresis (1D SDS-PAGE)

An aliquot of each protein extract equating to 5 µg of solubilised protein was resuspended in loading buffer (10% (v/v) glycerol, 5% (v/v) β-ME, 2% (w/v) SDS, 0.01% (w/v) bromophenol blue in 0.125 M Tris-HCl, pH 6.8) and heated at 95°C for 5 minutes, before separation by 1D SDS-PAGE. The electrophoretic separation was performed using pre-cast anykD (10 – 250 kDa range) gradient gel (Bio-Rad), with 5 µL of a broad range protein marker of known molecular weight standards (PageRuler™ unstained Protein Ladder, Thermo Scientific) added to the first well. Gels were run in SDS buffer (25 mM Tris, 200 mM glycine, 0.1 % SDS (w/v)) at 100 V until the loading dye front reached the bottom of the gel. After electrophoresis, gels were stained with Coomassie Blue R250 for six hours to visualise the polypeptide bands. Destaining was achieved by gently shaking the gels in an aqueous solution containing 40% (v/v) methanol and 10% (v/v) acetic acid until the bands were visible against the background. Variability between the WT and transgenic protein profiles were investigated by visually assessing differences in the protein banding pattern that were evident in the electrophoretic profiles. On this basis, a total of five bands were identified as potential candidates that were indicative of differential protein expression between the WT and transgenic samples. These bands of interest were then numbered and submitted for mass fingerprinting for possible protein identification.

4.2.4 Mass fingerprinting for protein identification of isolated protein bands

Protein bands of interest were manually excised from the 1D gel and in-gel trypsin digested using standard methods. In brief, the excised gel slices were destained in 200 µL of 50% acetonitrile/25 mM ammonium bicarbonate solution until made clear. Then the samples were dehydrated with 100 µL acetonitrile (100%) before reduction in 100 µL 2 mM Tris (2-carboxyethyl)phosphine (TCEP) in 25 mM ammonium bicarbonate for a period of 15 minutes with agitation at room temperature. Cysteine residues were then carbamidomethylated in 100 µL 20 mM iodoacetamide in 25 mM ammonium bicarbonate for 30 minutes at room temperature in the dark. The gel pieces were then washed in 25 mM ammonium bicarbonate, and allowed to dry. Proteins were then digested in 10 µL

trypsin (10 ng/ μ L) (sequencing-grade modified trypsin, Promega) by incubating the samples at 37°C overnight. Peptides were then extracted from the gel pieces with 10 μ L 30% acetonitrile (ACN) with 0.1 % trifluoroacetic acid (TFA). Samples were then dried using a SpeedVac and redissolved in 0.1% TFA. A C₁₈ ZipTip® sample clean-up step was then followed, according to the manufacturer's instructions to remove acrylamide contamination and the purified samples were eluted in 80% ACN:0.1% TFA. Lastly, the samples were lyophilised once more before resuspension in 15 μ L 0.1% TFA.

The digested peptides were run on a Thermo Scientific Easy-nanoLC II system connected to a Proteineer FC II protein spotter. The liquid chromatography separation of the peptides was performed in a EASY column (2 cm, ID 100 μ m, 5 μ m, C18) pre-column followed by an analytical column (15 cm, 75 μ m, 3 μ m C18) with a flow rate of 100 μ L/h using a 70 minute gradient run.

MALDI-TOF MS was performed using an UltrafleXtreme MALDI TOF/TOF system (Bruker Daltonics, Germany). Peptides were ionised with a 337 nm laser and spectra acquired in reflector positive mode at 28 kV using 500 laser shots per spectrum, with a scan range of $m/z = 700 - 4000$. Spectra were internally calibrated using the peptide calibration standard II (Bruker Daltonics, Germany). This calibration method provided a mass accuracy of 50 ppm across the mass range of 700 Da to 4000 Da. Peptide spectra of accumulated shots were automatically processed using WARP LC 3.2 software (Bruker Daltonics, Germany). Protein identification was performed using the Mascot algorithm on the SwissProt database on a ProteinScape 3.0 workstation. Trypsin was specified as the proteolytic enzyme. Carbamidomethyl cysteine was set as a fixed modification and oxidised methionine as a variable modification. Candidate protein matches with a molecular weight search (MOWSE) score greater than 50 and at least 2 unique peptides were considered as identified proteins.

4.2.5 Bulk mineral analysis using ICP-AES/MS

4.2.5.1 Sample preparation for ICP-AES/MS

Equal quantities of grain from three biological individuals per genotype were mixed to form a composite sample of approximately 5 g. For bulk element concentration analysis, four subsamples (each of approximately 1 g) from the composite were rapidly rinsed three times with Milli-Q water to remove surface contaminants and then ground to a fine powder

using liquid nitrogen. The resultant flour was then freeze-dried to a constant dry weight before acid digestion.

Acid digestion of the samples was carried out using a closed vessel microwave digestion system (MARS Xpress CEM-USA). An aliquot of 0.5 g of each flour sample was carefully weighed and transferred to Teflon digestion vessels along with 10 mL of HNO₃: HCl, 4:1, for the destruction of organic matter. Samples were allowed to pre-digest at room temperature for 20 minutes, before microwave heating in four successive stages: (i) 4 min ramping from 25°C to 90°C; (ii) 10 min holding at 90°C; (iii) 6 min ramping from 90°C to 200°C; and (iv) 200°C for 25 min. After cooling to room temperature, the sample digests were transferred into a volumetric flask and brought to a final volume of 50 mL with ultrapure water and thoroughly mixed before ICP-AES/MS analysis at the Central Analytical Facility, Stellenbosch University. The above procedure was also applied for the digestion of the certified reference material NIST-SRM # 1547 peach leaves and true sample blanks.

All six of the transgenic lines were used along with the WT sample for the comparison of the bulk mineral content by ICP-AES/MS analysis.

4.2.5.2 ICP-AES/MS Analytical Procedure

All digests were diluted 10-fold in Milli-Q water before the analysis. The concentrations of the major elements (Ca, K, Mg, Na, P and S) were determined using a Thermo ICap 6200 ICP-AES instrument (Thermo Fischer Scientific), whereas the trace elements (Cr, Mn, Fe, Co, Ni, Cu, Zn, Se, Mo, Cd, Ba and Pb) were analysed on an Agilent 7700 quadrupole ICP-MS system (Agilent Technologies), according to standard manufacturer protocols. For the measurement of all elements, an external calibration was performed using aqueous multi-element calibration standards from the National Institute of Standards and Technology (NIST, Gaithersburg, USA). For ICP-AES, the calibration concentration ranged from 0 to 10 mg/L, whereas for ICP-MS it ranged from 0 to 1 mg/L.

To control variation within samples, each sample was measured thrice and the mean of triplicate observation was used to determine the concentration of elements detected within each sample. Before sample measurement, the accuracy and precision of the chosen ICP-AES/MS procedure was evaluated to expose any systematic errors. For accuracy, a comparison was made between the measured concentration values of the prepared

reference sample and the certified values. The accuracy of the ICP-AES/MS measurements was 96 – 105% of the certified values for the reference sample, and was therefore within the limits of standard deviation uncertainty outlined by Szymczycha-Madeja (2014). As a further quality assurance measure, a spiked recovery assay was also included, which resulted in spike recoveries in the range of 84.6 - 99.7%. To measure the precision of the technique, the relative standard deviation (RSD) for six independently prepared multi-element standards was analysed. In all cases, the precision was good and varied from 0.2% (for P) to 7.9% (for Ca). A variation in analytical precision below 10% is regarded as acceptable (Velu *et al.*, 2007).

4.2.6 Micro-PIXE analysis

4.2.6.1 Sample preparation for micro-PIXE

Sorghum grains (randomly selected from at least three biological replicates) were first embedded in commercial resin (EpoFix, Struers) and then longitudinally sectioned with a rotating diamond-coated blade to produce a flat sample surface in preparation for micro-PIXE analysis. The samples were photographed at this stage using a stereomicroscope to provide a pictorial reference for sample identification and to aid subsequent interpretation of the elemental maps generated. To handle the samples, no metallic implements were used, so as to avoid any inadvertent risk of extraneous contamination. To avoid charge build-up during PIXE measurements, the cut surfaces of the samples were then coated with carbon using a Balzers sputter coater. Following this, the samples were immediately taken to the nuclear microprobe for analysis at the Materials Research Department iThemba LABS.

4.2.6.2 Micro-PIXE Analytical Procedure

Measurements were carried out using a proton beam of 3.0 MeV energy and a current of ~100 pA, focused to a 3 x 3 μm^2 spot and raster scanned over a sample area of 2 mm^2 using square scan patterns with a variable number of pixels. Both micro-PIXE and proton backscattering (BS) spectra were collected simultaneously in event-by-event mode. The X-ray spectra were detected with a high purity Si(Li) detector using an external 125 μm Be absorber to shield the detector from backscattered protons and to attenuate X-rays from major light elements. Elemental maps were obtained using the Dynamic Analysis method, as part of the data processing by GeoPIXE II software, as noted by Ryan (2000).

4.2.7 Statistical Analysis

To evaluate differences between the means at the 5% significance level, one way analysis of variance (ANOVA) and the Tukey mean separation test was performed using *Statistica* for Windows Version 12.6 (Statsoft Inc., USA).

4.3 Results and discussion

4.3.1 1D SDS-PAGE and protein identification

In the current study, protein profiles derived from transgenic and non-transgenic sorghum grain samples were analysed using 1D SDS-PAGE in order to highlight important changes in protein expression levels that may be associated with genetically engineered kafirin suppression. The transgenic lines were originally produced using a RNAi strategy that sought to improve the nutritional value of sorghum through the silencing of certain kafirin subclasses (Grootboom *et al.*, 2014). The kafirins are the dominant storage proteins in sorghum grain, but are of low nutritional value because they are deficient in essential amino acid content, and are furthermore highly resistant to digestion. By silencing the nutritionally inferior kafirins, it is hypothesised that a compensatory mechanism driving the synthesis of other types of grain proteins will occur. To visualise and assess the extent of these possible changes, a 1D SDS-PAGE strategy was adopted in order to compare the protein profiles of the transgenic grains against that of their wild type progenitor.

The result of the 1D SDS-PAGE analysis of the three major protein fractions of the sorghum grain is depicted in Figure 4.1. Given a constant protein loading of 5 µg per lane, the difference in the band intensity may be indicative of a differential expression of the proteins between the WT and transgenic samples. In the albumin/globulin fraction, 2 bands with an estimated molecular weight of ~50 – 55 kDa were observed to have a higher intensity in the transgenic samples in comparison to the WT. One of the bands was chosen as a candidate for protein identification, marked 1 (Figure 4.1).

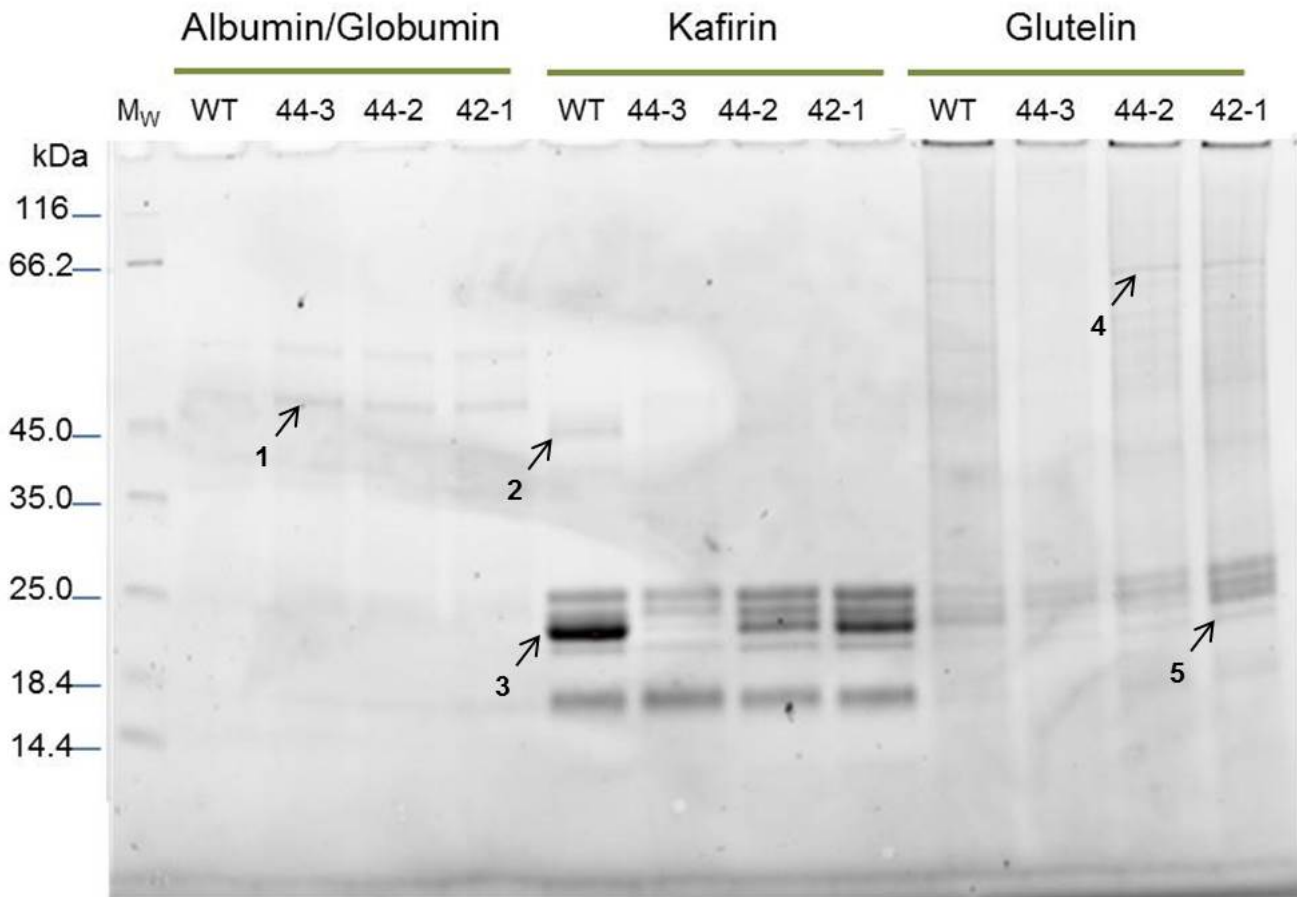


Figure 4.1 Main fractions of sorghum grain proteins separated by 1D SDS-PAGE. 5 µg of extracted protein loaded onto each lane. Bands identified as differentially expressed between the transgenic lines and WT were numbered 1-5 and excised from the gel to submit for protein identification by mass fingerprinting.

In the kafirin fraction, a similar electrophoretic pattern was observed as was found previously (Chapter 3), however the gradient gel allowed a better resolution of the protein bands in the 14 – 25 kDa range. Interestingly, for sample 44-3 evidence of almost complete silencing of the band of ~20 kDa was observed. The bands labelled 2 and 3 were observed to have a higher intensity in the WT compared to the transgenic samples, and may be indicative of the kafirins that were targeted for suppression by RNAi. In the glutelin fraction two bands were observed to have a higher intensity in the transgenic samples in comparison to WT. These were labelled as protein band 4 and 5. The selected protein bands of interest, labelled 1-5 (Figure 4.1) were prepared as detailed in section 4.2.4. Table 4.1 shows the proteins that were positively identified using MALDI TOF mass spectrometry. The MOWSE score gives a measure of confidence for the MS-based identification (Thiede *et al.*, 2005; Pappin *et al.*, 1993). Only scores above 50 were deemed to be acceptable for confident protein identification. Additionally, it is conventionally accepted that the identification should be based on at least 2 matching

Table 4.1 List of proteins identified from bands 1-5 in Figure 4.1.

Band No.	Protein	Positive ID	No. of Peptides	MOWSE score	Mw (kDa)	Accession No.
1	Globulin-1 S allele	NO	1	47.99	65	GLB1_MAIZE
2	Outer dynein arm protein 1	NO	1	45.93	62.20	ODA1_CHLRE
3	Putative cytochrome c oxidase subunit	NO	1	46.71	1.70	PS17_PINST
4	Pyruvate phosphate dikinase 2	YES	9	290.37	96.00	PPDK2_MAIZE
	Pyruvate phosphate dikinase 1	YES	7	254.25	102.60	PPDK1_MAIZE
	Uncharacterised protein	YES	2	78.89	51.5	tr C5WY16 C5WY16_SORBI
5	Glyceraldehyde-3-phosphate dehydrogenase 1	YES	4	103.88	36.50	G3PC1_HORVU
	Endochitinase A	YES	2	66.51	29.10	CHIA_MAIZE
	40S ribosomal protein S7	YES	2	70.58	22.20	RS7_SECCE
	Putative uncharacterised protein	YES	4	127.38	18.90	tr C5XRL7 C5XRL7_SORBI
	Putative uncharacterised protein	YES	2	70.58	22.10	tr C5YW90 C5YW90_SORBI
	Putative uncharacterised protein	YES	2	64.93	18.90	tr C5X7S1 C5X7S1_SORBI
	Chitinase B (fragment)	YES	2	66.51	27.40	tr Q941I5 Q941I5_SORBI
	Glyceraldehyde-3-phosphate dehydrogenase	YES	3	83.75	36.30	tr C5XX52 C5XX52_SORBI
	Putative uncharacterised protein	YES	2	71.38	25.70	tr C5XRZ8 C5XRZ8_SORBI
	Putative uncharacterised protein	YES	2	64.61	28.30	tr C5YBE8 C5YBE8_SORBI
	Gamma kafirin protein (fragment)	YES	2	59.26	19.60	tr Q6Q299 Q6Q299_SORBI
	Uncharacterised protein	YES	2	71.28	25.70	tr C5XRZ8 C5XRZ8_SORBI
	Gamma kafirin	YES	2	59.26	22.00	tr C5XDL2 C5XDL2_SORBI
	Uncharacterised protein	YES	2	70.58	22.20	tr A0A1B6QNT2 A0A1B6QNT2_SORBI
	Uncharacterised protein		2	68.51	28.50	tr C5YBE9 C5YBE9_SORBI

peptides. Accordingly, a definitive protein identity could not be determined for bands 1 to 3. It is noted however, that for protein band 1, a globulin was retrieved from the analysis as a possible candidate. No confident identity was established from the analysis of peptides from bands 2 and 3. This was a somewhat surprising result, but it may be due to the multitude of proteins that may migrate within a single zone of the gel during 1D SDS-PAGE separations. It has been demonstrated in other studies utilising this kind of profiling technique, that as many as 300 unique gene products may be identified from a single gel slice from SDS-PAGE (Roux Dalvai *et al.*, 2008).

For bands 4 and 5, some definitive protein identities were derived from the analysis. For band no.4 pyruvate phosphate dikinase 1 and 2 were positively identified. These are enzymes implicated in pyruvate metabolism. Pyruvate is a metabolic precursor for several amino acids. It may be speculated that the enzymes of this type are upregulated in the transgenic lines, as a part of the compensatory response to the imposed kafirin suppression. For band no.5 glyceraldehyde-3-phosphate dehydrogenase was positively identified in two instances. This enzyme is also implicated in the subpathway that synthesises pyruvate (Dhar-Chowdhury *et al.*, 2005). Interestingly, two positive identities for gamma kafirin were also found amongst the peptides in this band. It is not entirely clear why these kafirins are extracted in this fraction, but the result gives an indication that the sequential extraction process may include some overlap from other protein fractions. The remaining proteins that were positively identified in this band include a chitinase, endochitinase and the 40S ribosomal protein. The two former proteins are classed as chitinases, which are pathogenesis-related proteins, likely expressed in the grain to ward off fungal pathogens (Hamid *et al.*, 2013). Unfortunately, the plant chitinases are also known to act as food allergenic proteins (Volpicella *et al.*, 2014). The possibility that these potentially allergenic proteins may be more expressed in the transgenic grain may constitute a cause for concern. The 40S ribosomal protein is the other protein that was positively identified in band no.5. This protein is implicated in genetic information processing (Yan *et al.*, 2012). Its possible upregulation in the transgenic sorghum may be related to the possible genetic perturbations in the system that may be due to the targeted suppression of certain kafirins by RNAi. All other proteins identified (a total of 9) were classed as uncharacterised proteins.

4.3.2 Grain mineral composition by ICP-AES/MS

The objective of this part of the study was to analyse the mineral composition of the wild-type and transgenic sorghum grains in order to highlight differences that may be of biological or nutritional significance. The three major categories of mineral elements that were evaluated were the essential major elements (K, P, Mg, S and Ca); the essential trace and ultra-trace elements (Fe, Zn, Mn, Cu, Se, Mo, Ni, Cr and Co); and, finally, the non-essential potentially toxic elements (Al, Ba, Cd and Pb). The bulk content of the essential major elements was determined using ICP-AES and is presented in Table 4.2 below. The remaining elements were determined using ICP-MS and are presented in Table 4.3 (essential trace and ultra-trace elements) and Table 4.4 (the non-essential, potentially toxic elements).

According to the statistical analysis of the data, few significant differences were found. Out of a total of 18 elements analysed, the content of only four elements was identified as significantly different from the wild-type in one or more of the transgenic lines. These elements were P, S, Zn and Mn. Notably, these significant differences in mineral content were only detected in grain from transgenic lines 42-1, 44-2 or 44-3. In the sections that follow, a more detailed discussion of the results obtained for each of the three major categories of elements will be presented. As will be shown, most differences tended to fall within the known range of variation for sorghum grain and therefore would not immediately raise a cause for concern at a nutritional or toxicological level.

4.3.2.1 Bulk analysis of the essential major elements

The bulk concentrations of five essential major elements found in the tested sorghum grain are presented in Table 4.2. For K, Mg and Ca, no significant difference was found between the transgenic grain and the wild-type. However, in the case of P and S, instances of significant difference were observed. For P, a reduction of 10.6% was found in grain from line 44-3, while the grain of line 44-2 was reduced in S by 15.8%. Although these differences serve to statistically differentiate the transgenic grain from the wild-type in these specific cases, it is further observed from the literature that the reduced levels of P and S do not exceed the natural range of variation that has been documented for food-grade sorghum grain. The primary source of information on the natural levels of variation that may be expected for sorghum grain is the 2010 Consensus Document on Compositional Consideration for New Varieties of Grain Sorghum, produced by the Organisation for Economic Co-operation and Development (OECD).

Table 4.2 Essential major elements found in sorghum whole grain samples (mg/kg dry weight basis). Values represent the mean of three independent determinations \pm SD. Means followed by the same superscript in the row are not significantly different at $p < 0.05$.

	WT	42-1	42-2	42-4	44-1	44-2	44-3	Reference range
K	4953 ^a \pm 313	4555 ^a \pm 308	4549 ^a \pm 256	4855 ^a \pm 104	4675 ^a \pm 74	4716 ^a \pm 155	4503 ^a \pm 191	2400 – 4700 ^{S1} 2910 - 6840 ^{S2}
P	4652 ^b \pm 332	4583 ^b \pm 69	4559 ^b \pm 61	4796 ^b \pm 32	4741 ^b \pm 84	4491 ^{bc} \pm 47	4159 ^c \pm 31	3200 – 3600 ^{S1} 2010 - 4600 ^{S2}
Mg	1932 ^{de} \pm 92	2100 ^e \pm 27	1982 ^{de} \pm 64	2044 ^{de} \pm 58	2005 ^{de} \pm 84	2057 ^{de} \pm 63	1885 ^d \pm 99	1400 – 1900 ^{S1} 1110 - 2180 ^{S2}
S	1328 ^{fg} \pm 52	1278 ^{gh} \pm 21	1410 ^{fg} \pm 23	1329 ^{gh} \pm 105	1398 ^g \pm 165	1118 ^h \pm 50	1248 ^{gh} \pm 7	900 – 1700 ^{S1} 1160 - 2650 ^{S2}
Ca	251 ⁱ \pm 35	217 ⁱ \pm 28.7	253 ⁱ \pm 33.2	210 ⁱ \pm 12.9	240 ⁱ \pm 31	212 ⁱ \pm 9.6	239 ⁱ \pm 27.1	300 – 700 ^{S1} 50 - 380 ^{S2}

^{S1/S2} Literature range sources, S1: OECD, 2010; S2: Ng'uni *et al.* 2011.

Table 4.3 Essential trace and ultra-trace elements found in sorghum whole grain samples (mg/kg dry weight basis). Values represent the mean of three independent determinations \pm SD. Means followed by the same superscript in the row are not significantly different at $p < 0.05$.

	WT	42-1	42-2	42-4	44-1	44-2	44-3	Reference range
Fe	51.9 ^a \pm 1.9	49.0 ^a \pm 2.9	60.0 ^a \pm 4.7	52.3 ^a \pm 0.26	53.0 ^a \pm 0.51	45.0 ^a \pm 5.1	49.9 ^a \pm 4.0	10.6 – 89 ^{S1} 27.9 – 80.3 ^{S2}
Zn	42.6 ^b \pm 1.92	39.2 ^{bc} \pm 1.8	44.6 ^b \pm 2.49	40.8 ^b \pm 0.17	43.2 ^b \pm 2.5	34.5 ^c \pm 4.5	33.6 ^c \pm 2.1	16.9– 47.1 ^{S1}
Mn	14.0 ^d \pm 0.55	12.7 ^e \pm 0.46	13.6 ^{de} \pm 0.63	13.0 ^{de} \pm 0.26	13.8 ^{de} \pm 0.48	13.3 ^{de} \pm 0.41	13.4 ^{de} \pm 0.29	10.9 – 21.0 ^{S1} 9.6 – 38.7 ^{S2}
Cu	4.74 ^f \pm 0.16	4.48 ^f \pm 1.06	3.44 ^f \pm 0.75	2.98 ^f \pm 0.09	4.13 ^f \pm 1.1	4.86 ^f \pm 0.58	4.31 ^f \pm 0.93	0.20 – 11.5 ^{S1} 3.1 – 8.0 ^{S2}
Se	1.53 ^g \pm 0.42	1.05 ^g \pm 0.24	1.58 ^g \pm 0.40	1.84 ^g \pm 0.62	1.72 ^g \pm 0.61	1.37 ^g \pm 0.21	1.99 ^g \pm 0.73	0.23 – 0.46 ^{S1} 0.1 – 3.6 ^{S2}
Mo	1.31 ^{hi} \pm 0.11	2.20 ^h \pm 0.96	1.28 ^{hi} \pm 0.14	1.17 ^{hi} \pm 0.26	1.39 ^{hi} \pm 0.13	0.91 ^h \pm 0.14	1.21 ^{hi} \pm 0.28	1.0 ^{S1}
Ni	0.22 ^j \pm 0.03	0.25 ^j \pm 0.11	0.21 ^j \pm 0.02	0.23 ^j \pm 0.05	0.19 ^j \pm 0.08	0.25 ^j \pm 0.10	0.25 ^j \pm 0.11	0.46 – 1.27 ^{S1}
Cr	0.18 ^k \pm 0.08	0.23 ^k \pm 0.10	0.15 ^k \pm 0.02	0.14 ^k \pm 0.01	0.20 ^k \pm 0.03	0.28 ^k \pm 0.11	0.20 ^k \pm 0.10	0.8 ^{S1}
Co	0.023 ^l \pm 0.02	0.030 ^l \pm 0.01	0.020 ^l \pm 0.01	0.017 ^l \pm 0.01	0.020 ^l \pm 0.01	0.020 ^l \pm 0.01	0.023 ^l \pm 0.01	0.007 - 0.015 ^{S3}

^{S1/S2/S3} Literature range sources, S1: OECD, 2010; S2: Ng'uni *et al.*, 2011; S3: Pontieri *et al.*, 2014

Table 4.4 Non-essential trace and ultra-trace elements found in sorghum whole grain samples (mg/kg dry weight basis). Values represent the mean of three independent determinations \pm SD. Means followed by the same superscript in the row are not significantly different at $p < 0.05$.

	WT	42-1	42-2	42-4	44-1	44-2	44-3	Reference range
Al	5.06 ^a \pm 0.10	3.47 ^a \pm 0.49	2.96 ^a \pm 1.18	3.96 ^a \pm 1.39	4.73 ^a \pm 1.42	3.72 ^a \pm 0.66	3.51 ^a \pm 0.40	9.33 – 54.9 ^{S3}
Ba	0.26 ^b \pm 0.11	0.34 ^b \pm 0.14	0.21 ^b \pm 0.10	0.16 ^b \pm 0.06	0.22 ^b \pm 0.11	0.27 ^b \pm 0.05	0.25 ^b \pm 0.09	0.35 – 0.71 ^{S3}
Cd	0.02 ^c \pm 0.01	0.04 ^c \pm 0.02	0.02 ^c \pm 0.01	0.04 ^c \pm 0.03	0.03 ^c \pm 0.02	0.02 ^c \pm 0.01	0.02 ^c \pm 0.01	0.009 – 0.06 ^{S3}
Pb	0.06 ^d \pm 0.01	0.05 ^d \pm 0.03	0.02 ^d \pm 0.02	0.04 ^d \pm 0.01	0.04 ^d \pm 0.02	0.05 ^d \pm 0.03	0.04 ^d \pm 0.03	0.09 – 0.30 ^{S3}

^{S3} Literature range source, S3: Pontieri *et al.*, 2014.

According to this reference, the average sulphur content (1118 mg/kg) of transgenic grain from line 44-2 is within the acceptable known range of variation for sorghum, which is listed as 900 – 1700 mg/kg. The acceptable range for P, however, is listed as 3200-3600 mg/kg (OECD, 2010), which is far below the average values obtained in this study, which range from 4159 – 4796 mg/kg.

Another study, which focused on the determination of the mineral contents of 40 different Southern African sorghum varieties, found that the grain P content ranged from 2010 – 4600 mg/kg (Ng'uni *et al.*, 2011), whilst a much older study found sorghum grain P to range from 3880 – 7560 mg/kg (Deosthale and Belvady, 1978). It is therefore evident that although the mean P values for the sorghum samples in this study are much higher than the OECD values, they are within the range of other reports found within the literature. The reduced level of P in transgenic line 44-3, compared to WT, is therefore within the limits of known variation for sorghum grain types. The finding that grain from transgenic lines 44-2 and 44-3 is significantly lower in S and P, respectively, in comparison to the wild-type, would therefore seem to not carry much nutritional significance. It may be speculated that the reduced S and P levels may in some way be associated with the induced kafirin suppression, but this effect is not evident across all the transgenic lines, and therefore it is difficult to objectively conclude that this is in fact the case. On the available evidence, it therefore seems that the average grain content of P, K, S, Mg and Ca in the transgenic lines is within the acceptable known range of variation for food grade sorghums, and therefore the two instances of significant difference from the wild-type do not warrant much concern. This is especially the case because neither P nor S are critically limiting elements in the human diet, so the reduced levels found in the two transgenic lines is not likely to have a significant impact on nutrition.

4.3.2.2 Bulk Analysis of the Essential Trace and Ultra-trace Elements

The results for a total of nine different trace and ultra-trace essential elements were quantified using ICP-MS for all of the sorghum grain samples (see Table 4.3). For seven of these elements (Fe, Cu, Se, Mo, Ni, Cr and Co), no significant difference in the bulk content of the transgenic *versus* the wild-type grain could be determined. This is an important finding that serves to emphasise the lack of an obvious impact on the accumulation of these specific minerals within the transgenic grain.

However, in the case of Zn, a significant difference in comparison to wild-type was observed in grain from transgenic lines 44-2 and 44-3 and, in the case of Mn, only for grain from transgenic line 42-1. Grain from transgenic lines 44-2 and 44-3 were found to have an average bulk Zn content of 34.5 and 33.6 mg/kg, respectively. In comparison to wild-type grain (with an average bulk Zn content of 42.6 mg/kg), transgenic grain from lines 44-2 and 44-3 was reduced in bulk Zn content by 19 and 21 %, respectively. In spite of this reduction, the Zn content of grain from transgenic lines 44-2 and 44-3 is still within the acceptable range of variation for sorghum, according to the OECD reference range of 16.9 – 47.1 mg/kg (OECD, 2010). In a more recent study on 22 sorghum cultivars from Ethiopia and South Africa, the average bulk Zn was determined to be 26.04 mg/kg, with a range from 20 to 33.42 mg/kg (Gerrano *et al.*, 2016). Moreover, in the Ng'uni *et al.* (2011) study, the average Zn content of 40 different Southern African sorghum varieties was 29.7 mg/kg, with a range from 20.4 to 55.1 mg/kg. It is therefore evident that sorghum exhibits a wide range of variation for grain Zn content, which is inclusive of the average Zn levels found in the transgenic grain of lines 44-2 and 44-3. Zinc, however, is a mineral that is often critically limited in the diet, so the observation that the zinc content has been significantly reduced in two of the transgenic lines in comparison to the wild-type is a noteworthy concern.

The remaining case of significant difference revealed by the data involves Mn, which was found to be reduced by 9.3% in transgenic line 42-1 in comparison to the wild-type. Interestingly, all other transgenic grains were observed to have a lower average Mn content in comparison to the wild-type, but only grain of line 42-1 was determined to be significantly lower. This finding may be indicative of a subtle effect that kafirin suppression may have on Mn accumulation in the grain. However, more intensive investigation would be needed in order to refute or corroborate this. It is clear from the reference range data of the OECD and Nguni *et al.*, (2011) that levels of Mn across the transgenic lines, including line 42-1, are within the known range of variation for sorghum grain. The trend is therefore noted, but would not be highlighted by the regulatory authorities as a major cause for concern.

4.3.2.3 The Non-essential or Potentially Toxic Elements

The final category of elements to be considered included the non-essential or potentially toxic elements present within sorghum grain. In this study, four elements (Al, Ba, Cd and Pb) were assigned to this category, as listed in Table 4.4. A fifth element, Arsenic (As),

was often below the detection limit in the majority of the samples and therefore was excluded from this report. In this category of elements, no significant differences from the wild-type were detected in any of the transgenic grain samples. Furthermore, all the elements in this category were found at levels that were below or within the range of previous reports on food-grade sorghum. On the available evidence, it therefore seems clear that the transgenic grains do not differ significantly from the wild-type in terms of these investigated non-essential or potentially toxic elements.

4.3.3 Micro-PIXE analysis

Micro-PIXE offers the investigator a unique opportunity to gain both a quantitative as well as a spatial comprehension of the elemental composition of a particular sample. In the present study, quantification and localisation of elements within the basal portion of the grain, which includes the endosperm region and the surrounding pericarp, but excludes the embryo, was prioritised. This particular region of the grain was chosen as the main area of focus because of the central importance of the endosperm for nutrient storage, and because of its relatively simple morphology, which facilitates comparison between different sample elemental maps. Figure 4.2 below illustrates the region of the sorghum grain chosen for micro-PIXE analysis.



Figure 4.2 A halved sorghum grain prepared for micro-PIXE analysis. The proton beam was scanned over an area of approximately $2.3 \times 2.3 \text{ mm}^2$ as demarcated by the red box and elemental maps produced using the Dynamic Analysis method in GeoPIXE. The three major morphological features of the grain are pointed out: P = pericarp; En = endosperm; and Em = embryo.

Elemental maps depicting the distribution of several elements found in the basal portion of the sorghum grain were produced using micro-PIXE. The elemental maps presented here include P, S, K, Ca, Fe and Zn. Mn was identified as an element of interest in the ICP-based analysis, but it was not consistently detected across all sample replicates in both the wild-type and the transgenic lots, and therefore could not be reported on further.

The immediate utility of the elemental maps was to compare the general distribution pattern of elements located within the grain tissue. As shown in Figure 4.3, the general spatial distribution of elements was conserved across the different genotypes. For each element, a clear dichotomy in the general spatial distribution pattern was evident, with relatively high concentration levels confined to the outer grain layers, while the converse was found in the bulk of the endosperm tissue. This pattern is well-known amongst cereal grains, and has been explored in much depth in studies focused on different millet (Minnis-Ndimba *et al.*, 2015; Kruger *et al.*, 2014), rice (Kryiacou *et al.*, 2014) and buckwheat (Pongrac *et al.*, 2013).

Although useful for providing a general overview of elemental distribution patterns in the grain, it is admitted that a direct comparison of concentration values, as represented by the colour concentration scales in the micro-PIXE maps, is not the most precise way to proceed due to discrepancies that relate to the amount of surrounding resin that is also included in the analyses. To retrieve more accurate quantitative data relating directly to within tissue elemental concentrations, region selection analysis tools provided within the GeoPIXE II software package were used to extract representative concentration data from the two main regions of difference that were apparent from the elemental distribution maps.

The two main regions of difference are perhaps best exemplified in the S distribution maps (Figure 4.4). As shown, these regions can be easily demarcated into an area including outer grain tissue layers, which we shall refer to as the grain periphery, and an inner core, comprising endosperm tissue (Figure 4.4). The outer grain tissue layers encompass tissues belonging to the peripheral endosperm, the aleurone layer

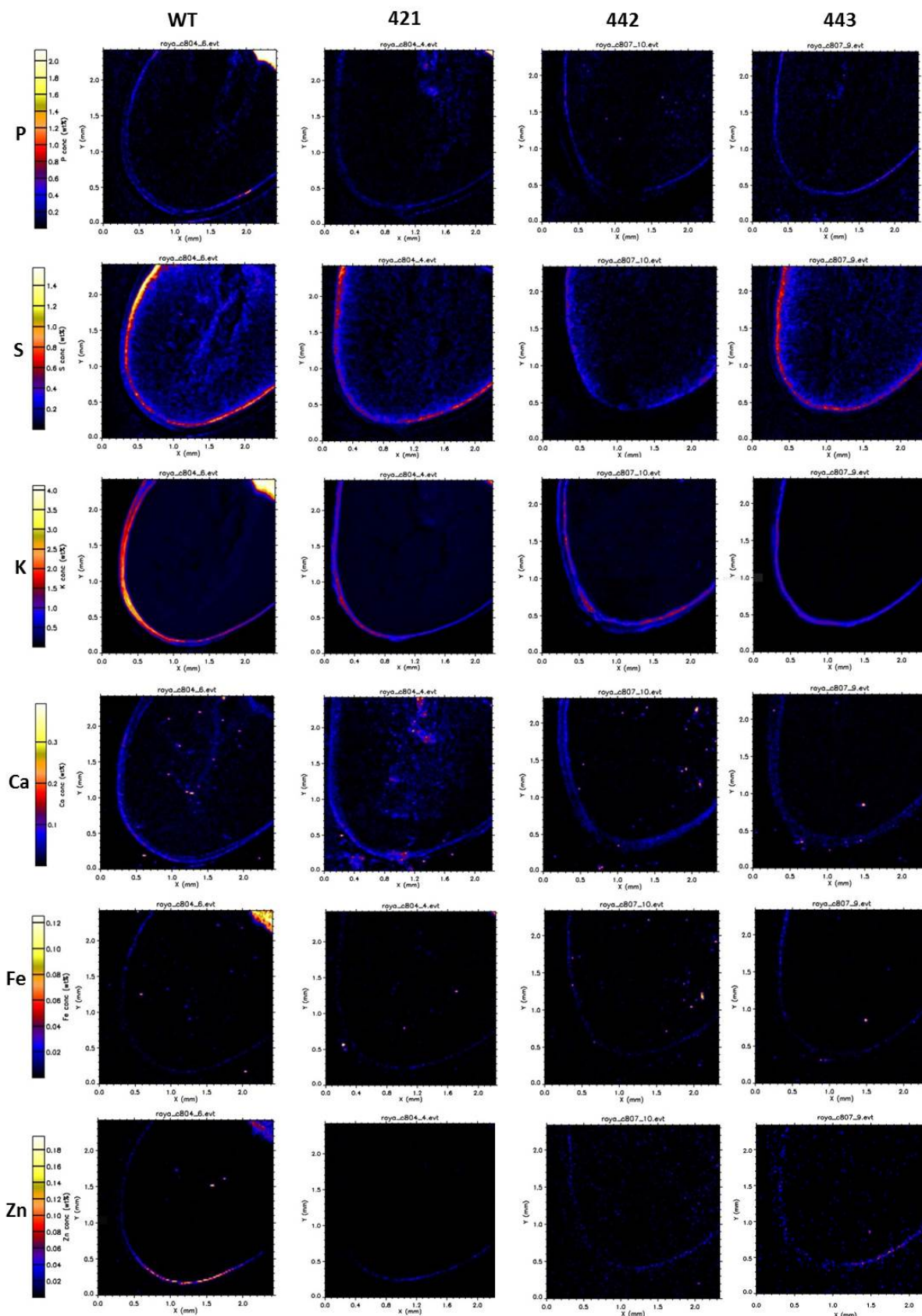


Figure 4.3 Representative micro-PIXE element maps of wild-type and transgenic sorghum grains.

and parts of the pericarp (depending on its state of intactness). These tissues are commonly referred to as the bran layer, and are typically removed from the grain along with the germ during decortication or milling processes. The inner core, in contrast, is morphologically homogenous and is only composed of starchy endosperm tissue. The rationale informing the use of the sulphur maps as a guide to region selection was based on the understanding of sulphur as a key indicator of the presence of protein (Garman and Grime, 2005). Given that proteins were the principal targets of the genetic modification, it seems logical that any differences in local elemental concentrations may be most apparent where protein levels may be highest. To explore this possibility, GeoPIXE region selection analysis was used to extract elemental concentration data specific to the peripheral and inner core endosperm regions of the wild-type and selected transgenic grains. The results of this analysis are shown in Table 4.5.

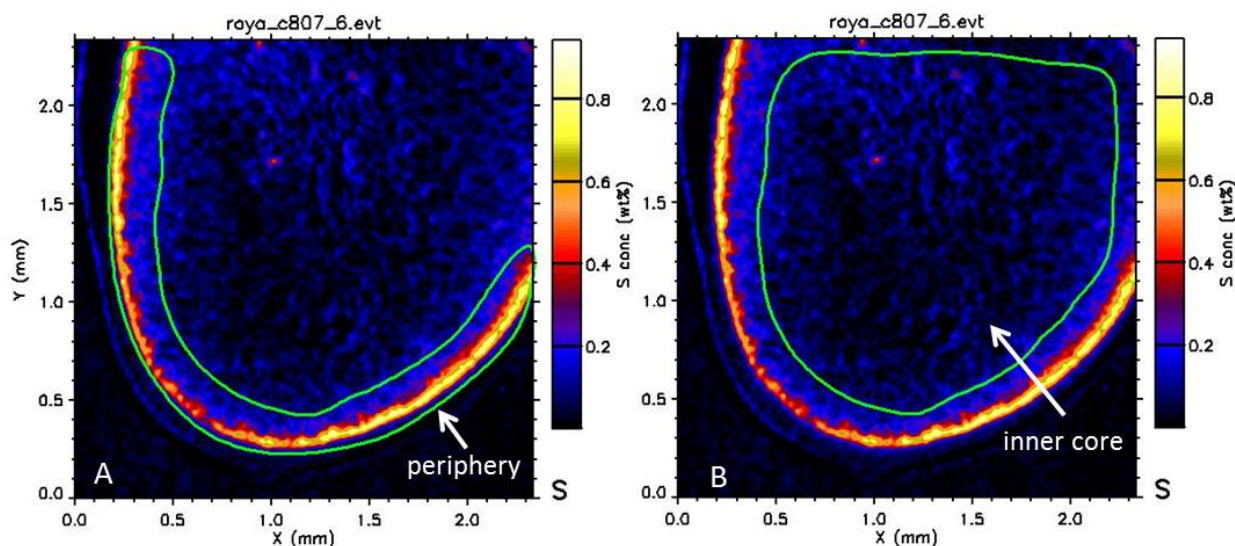


Figure 4.4 Typical S distribution maps of the scanned area of the grain samples used for micro-PIXE analysis. Two main regions of interest were highlighted for region selection analysis, as demarcated by the green encircling. Panel A highlights grain peripheral layers, which feature high levels of S, whilst panel B highlights the inner core of the endosperm, which features comparatively low S concentration levels.

Region selection analysis has been helpful for zooming in on the area of the grain where significant differences in elemental composition are most apparent. This area includes the peripheral grain layers and not the core of the central endosperm tissue. Amongst the elements that could be quantified by micro-PIXE, no significant differences could be detected within the core of the endosperm that could serve to differentiate the transgenic grains from their wild-type counterpart. On the other hand, in the peripheral grain layers, a

consistent trend could be detected amongst all three transgenic lines (42-1, 44-2 and 44-3), which serves to differentiate grains of these genotypes from the wild-type. This consistent trend was characterised by a significant depletion in the average levels of the essential elements K and Zn (Table 4.5). In the case of K, the average concentration in comparison to the wild-type was reduced by 37.2% in grain from line 42-1, and by 64.3% and 63.6% in grain from lines 44-2 and 44-3 respectively. In the case of Zn, the average concentration was reduced by 78.3%, 76.1% and 75.2% in transgenic grain of lines 42-1, 44-2 and 44-3, respectively.

The localised depletion of K and Zn in the peripheral grain layers of the selected transgenic grains may be an unintended consequence of the targeted silencing of certain kafirins within the grain. The peripheral grain layers, in particular the aleurone and sub-aleurone layers, are known to contain the highest concentrations of protein in comparison to the rest of the endosperm (Kent and Evers, 1969).

To determine more precisely where the greatest diminution in K and Zn may be in the transgenic grains in comparison to wild-type, the linear traverse tool in the GeoPIXE software package was used. The linear traverse offers an alternative form of quantitative image exploration in the region selection analysis toolbox. In essence, it allows the user to extract concentration data along a line projection rectangle that is sizeable, rotatable and movable. In the present study, a line projection rectangle of ~100 μm (width) and ~300 μm (length) was used to assess the concentration data of each of three independent replicate micro-PIXE scans for the wild-type and the transgenic samples of interest 42-1, 44-2 and 44-3. The projection rectangle was always chosen to span across the pericarp-aleurone-outer endosperm region, found at the most distal end of the grain away from the embryo (see Figure 4.5). The results of the linear traverse analysis were then averaged across the three replicates and presented as x-y plots for the two elements of most interest, K and Zn, in Figure 4.6 A and B.

Table 4.5 Average concentrations (mg/kg) of P, K, S, Ca, Fe and Zn, as determined by region selection analysis of micro-PIXE data using GeoPIXE. Results are presented as the mean \pm SE of three replicates, with the minimum detection limit indicated in brackets. Means highlighted in bold are significantly different from the wild-type, at $p < 0.05$.

	Peripheral Layers				Inner Endosperm			
	WT	42-1	44-2	44-3	WT	42-1	44-2	44-3
P	1092 \pm 97 (30)	861 \pm 111 (22)	775 \pm 81 (28)	1232 \pm 280 (32)	656 \pm 66 (12)	632 \pm 97 (17)	462 \pm 55 (16)	567 \pm 163 (18)
K	4833 \pm 365 (6)	3033 \pm 283 (4)	1724 \pm 129 (5)	1758 \pm 192 (5)	1498 \pm 138 (2)	1413 \pm 226 (3)	777 \pm 97 (3)	1197 \pm 349 (3)
S	3521 \pm 555 (18)	2230 \pm 158 (13)	2470 \pm 321 (16)	4321 \pm 907 (19)	954 \pm 152 (7)	706 \pm 16 (10)	577 \pm 85 (10)	744 \pm 51 (10)
Ca	228 \pm 29 (4)	185 \pm 17 (3)	128 \pm 13 (4)	147 \pm 58 (4)	99 \pm 25 (2)	115 \pm 35 (2)	118 \pm 37 (2)	91 \pm 39 (2)
Fe	19 \pm 1.6 (1)	15.8 \pm 6.1 (1)	17.6 \pm 5 (1)	19.5 \pm 7.3 (1)	3.2 \pm 0.8 (0.4)	3.5 \pm 1.2 (0.6)	4.6 \pm 1.7 (0.5)	5.8 \pm 3.2 (0.6)
Zn	114 \pm 11.5 (1)	24.7 \pm 3.9 (1)	27.3 \pm 14.9 (1)	28.3 \pm 7.2 (1)	3.3 \pm 2.0 (0.6)	2.3 \pm 0.4 (0.8)	2.4 \pm 0.4 (0.6)	4.2 \pm 2.8 (0.8)

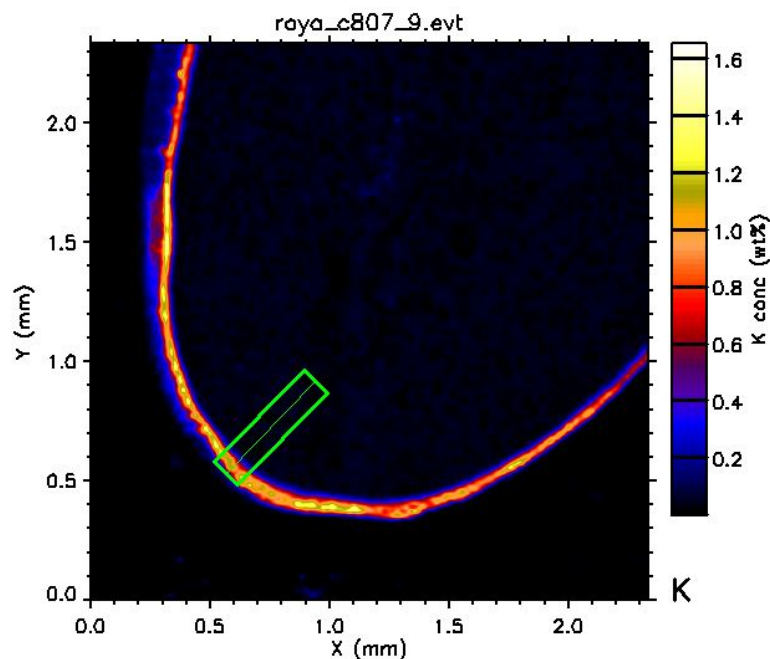


Figure 4.5 An example of the linear traverse projection rectangle used to extract concentration data spanning the regions of the grain demarcated in green.

The dimensions of the linear traverse were so chosen in an attempt to visualise more precisely where the most difference in K and Zn accumulation occurred between the wild-type and transgenic grains. An understanding of the precise tissue layers involved in the area of analysis was provided by considering the general schema of cereal grain outer layers in conjunction with semi-thin resin-embedded sections of sorghum grain (see Figure 4.7).

To improve the precise localisation of the elements by linear traverse analysis, thinner samples are required for micro-PIXE analysis. However, the results obtained thus far have been useful in pinpointing that the areas showing the biggest mineral loss in the transgenic grains are the aleurone and subaleurone layers, which are the most concentrated in protein. In the case of potassium, peak concentration levels seem to be localised precisely in what is likely to be the aleurone layer. For zinc, peak concentration levels for the wild-type sample are clearly in the zone just adjacent to the aleurone layer, namely the subaleurone layer. The peak levels of zinc for the transgenic grains are also more or less within this zone, and differences in the precise centre of the peak are likely attributable to variations in the morphology of the individual grains analysed. The clear message to be

derived from this analysis is that the reduction in K and Zn in the transgenic grains is localised within the aleurone and subaleurone region of the grain tissue.

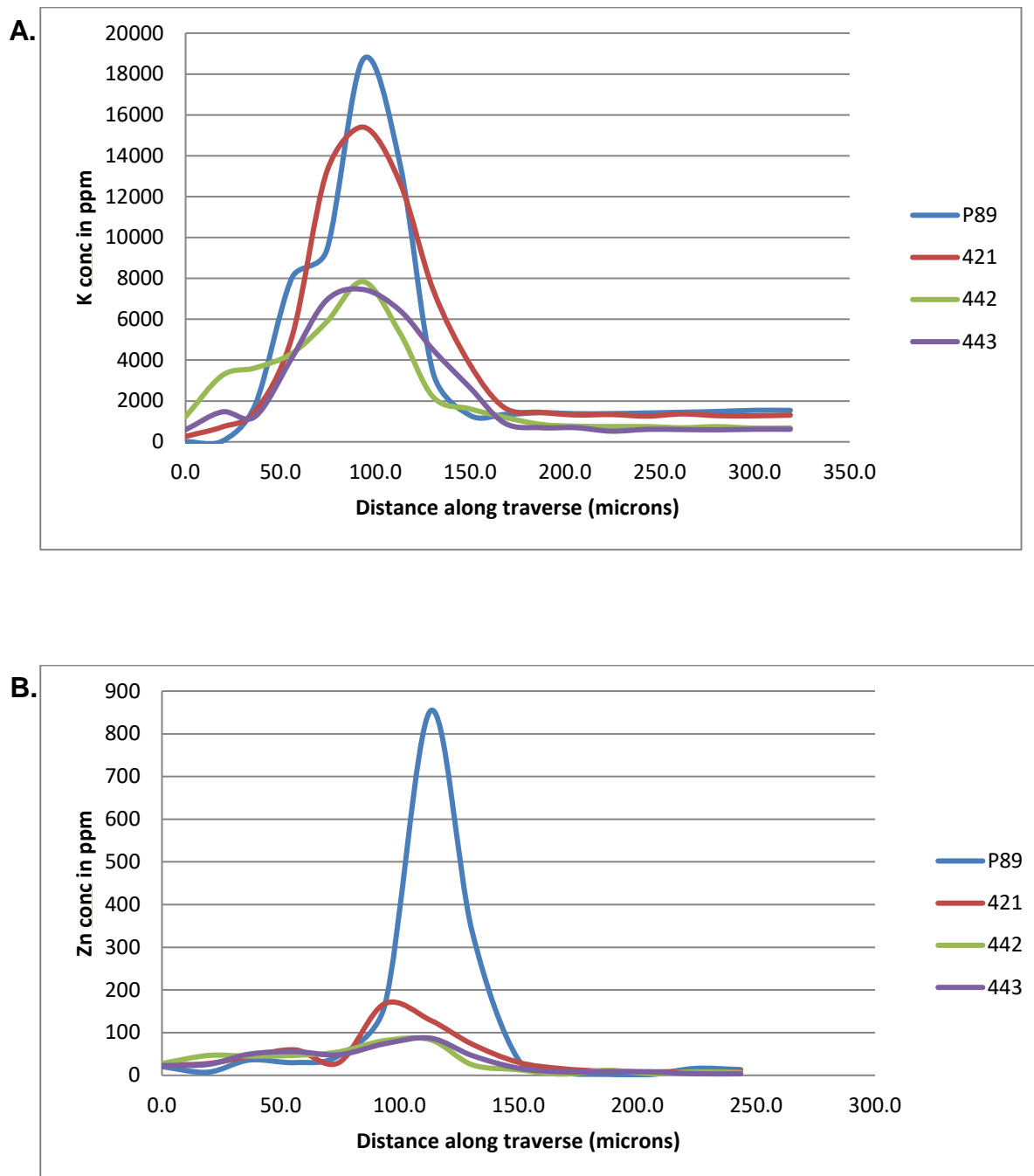


Figure 4.6 X-Y plots of average potassium (A) and zinc (B) concentration data as determined from the applied quantitative linear traverse tool in GeoPIXE.

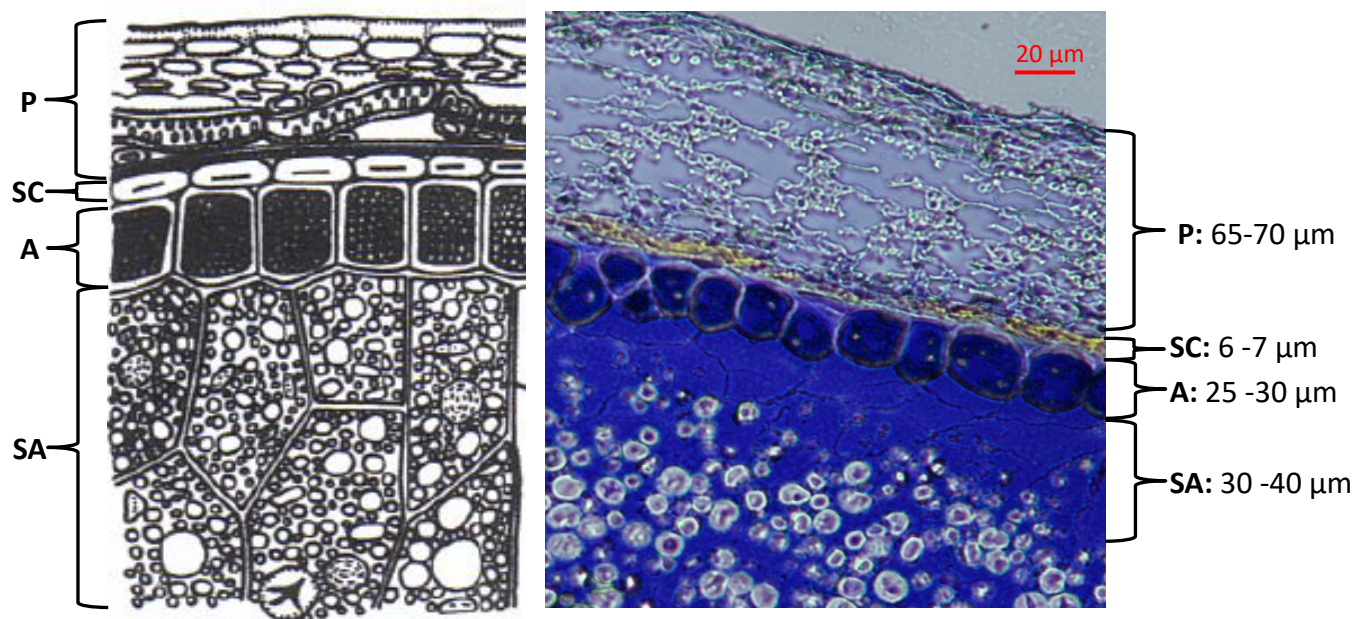


Figure 4.7 Schematic of typical cereal grain outer layers (left) (from Jacomet 2006) and semi-thin resin-embedded section of sorghum (right) stained with Coomassie brilliant blue (specific for protein). The section was prepared as part of the TEM analysis completed in Chapter 3. Specific tissue layer thicknesses in microns are shown. P, pericarp; SC seed coat; A aleurone and SA sub-aleurone.

It may be speculated that the reason for the diminished levels of K and Z in the aleurone and subaleurone layer of the transgenic grain is likely related to the targeted suppression of certain kafirin subclasses using RNAi. In the case of Zn, it is well-established that cysteine and histidine moieties have a high affinity for this particular element, in comparison to other types of amino acids (Trzaskowski *et al.*, 2008). Amongst the different kafirin subclasses, the gamma kafirins are particularly renowned for their high cysteine content, which facilitates extensive cross-linking (Rooney and Serna-Saldivar, 2000; Shull *et al.*, 1992). It therefore seems plausible that the suppression of the gamma-kafirins in the transgenic grains may have led to a paucity of cysteine residues, which most favourably bind zinc. The dramatic decrease in Zn is most clearly visualised in the subaleurone area of the grain tissue, which is the main storage compartment of the kafirin proteins. The association of Zn with other prolamin proteins in cereals was also recently examined in the study of Uddin *et al.*, (2014) on barley grain. In this study, the relative amounts of certain subclasses of hordeins (which are functionally similar to kafirins in sorghum), was

identified as one of the key factors for zinc biofortification in this cereal grain. Moreover, it was revealed that Zn distribution was not limited to the embryo and aleurone layer, but was also present in the sub-aleurone layers of the endosperm, which are known to be rich in proteins, such as the hordeins (Uddin *et al.*, 2014).

In the case of K, the immediate link with kafirin suppression is not so obvious. However, an answer may be related to the association of protein bodies with phytate (myo-inositol hexakisphosphate), the major storage compound for phosphorus in seeds. Phytate primarily accumulates in the grain as mixed salts of several mineral cations, particularly of potassium and magnesium (Raboy, 2007). These salts are known to be deposited as discrete globular inclusions (globoids) with protein storage vacuoles (PSV) localised in the aleurone cells or cereal germ tissues (Raboy, 2007). The proteins that make up the PSV also include kafirins (Reyes *et al.*, 2011) and it may thus be that the targeted suppression of certain subclasses of kafirins by RNAi has caused some changes to the PSV that may, in turn, have affected the ability of the globoids to accumulate K.

The unintended consequences of targeted kafirin suppression on K and Zn accumulation in the specific area of the aleurone and subaleurone layers is a finding that clearly warrants further study and corroboration. However, the initial work done here has been helpful for pinpointing this subtle change in the grain that may have important corollary effects on the integrity and functioning of these specific grain layers. Given the critical role that the aleurone and subaleurone tissues play in germination, future work aimed at investigating the effects of the localised depletion of Zn and K may focus on how the transgenic grains differ from their WT counterpart in terms of the important process of germination.

4.4 Conclusion

As a result of this study important differences in the protein and mineral element profile of transgenic sorghum grains were highlighted. Of note, the sequential extraction and electrophoretic separation of grain proteins revealed instances of differential protein expression between the transgenic and wild-type sample. An attempt to identify proteins from selected bands of interest, led to the finding that the transgenic sorghum grains may have upregulated levels of globulins and enzymes related to pyruvate metabolism. Additionally, some chitinase proteins were identified as potentially expressed at higher

levels in the transgenic grains, which could be allergenic. In terms of the bulk mineral content as assessed by ICP-AES/MS, few significant differences between the WT and transgenic sorghum grains could be found. However, using micro-PIXE analysis, mineral concentration differences peculiar to Zn and K were found to be significantly reduced in the subaleurone parts of the transgenic grain, in comparison to WT. The questions that remain to be addressed relate to how these changes in the protein and mineral composition may affect the biology or nutritional value of the grain.

References

- Bradford MM. 1976. A rapid and sensitive method for the quantitation of microgram quantities of protein utilizing the principle of protein-dye binding. *Analytical Biochemistry* 72: 248–254.
- Cremer JE, Bean SR, Tilley MM, Ioerger BP, Ohm JB, Kaufman RC, Wilson JD, Innes DJ, Gilding EK, Godwin ID. 2014. Grain sorghum proteomics: integrated approach toward characterisation of endosperm storage proteins in kafirin allelic variants. *Journal of Agricultural and Food Chemistry* 62: 9819-9831.
- Deosthale YG, Belvady B. 1978. Mineral and trace element composition of sorghum grain: effect of variety, location and application of nitrogen fertiliser. *Indian Journal of Nutrition and Diet* 15: 302- 308.
- Dhar-Chowdhury P, Harrell MD, Han SY, Jankowska D, Parachuru L, Morrissey A, Srivastava S, Liu W, Malester B, Yoshida H, Coetzee WA. 2005. The glycolytic enzymes, glyceraldehyde-3-phosphate dehydrogenase, triose-phosphate isomerase, and pyruvate kinase are components of the K_{ATP} channel macromolecular complex and regulate its function. *The Journal of Biological Chemistry* 280: 38464-38470.
- Distelfeld A, Uauy C, Fahima T, Dubcovsky J. 2007. Multiple QTL-effects of wheat GPC-B1 locus on grain protein and micronutrient concentrations. *Physiologia Plantarum* 129(3):635 – 643.
- Garman EF, Grime GW. 2005. Elemental analysis of proteins by micro-PIXE. *Progress in Biophysics and Molecular Biology* 89(2): 173-205.
- Gerrano AS, Labuschagne MT, Van Biljon A, Shargie NG. 2016. Quantification of mineral composition and total protein content in sorghum (*Sorghum bicolor* (L.) Moench) genotypes. *Cereal Research Communications* 44(2): 272-285.
- Grootboom AW, Mkhonza NL, Mbambo Z, O’Kennedy MM, da Silva LS, Taylor J, Taylor JRN, Chikwamba R, Mehlo L. 2014. Co-suppression of synthesis of major α -kafirin sub-class together with γ -kafirin-1 and γ -kafirin-2 required for substantially improved protein digestibility in transgenic sorghum. *Plant Cell Reports* 33: 521-537.
- Hamid R, Khan MA, Ahmad M, Ahmad MM, Abdin MZ, Musarrat J, Javed S. 2013. Chitinases: an update. *Journal of Pharmacy and Bioallied Sciences* 5(1): 21–29.
- Jacomet S. 2006. Identification of cereal remains from archaeological sites. 2nd edition. Basel.
- Kent NL, Evers AD. 1969. Variation in Protein Composition within the endosperm of hard wheat. *Cereal Chemistry* 46: 293 - 300.

- Kruger J, Pineda-Vargas CA, Minnis-Ndimba R, Taylor JRN. 2014. Visualisation of the distribution of minerals in red non-tannin finger millet using PIXE microanalysis. *Journal of Cereal Science* 60: 1-3.
- Kyriacou B, Moore KL, Paterson D, de Jonge MD, Howard DL, Stangoulis J, Tester M, Lombi E, Johnson AAT. 2014. Localization of iron in rice grain using synchrotron X-ray fluorescence microscopy and high resolution secondary ion mass spectrometry. *Journal of Cereal Science* 59: 173-180.
- Minnis-Ndimba R, Kruger J, Taylor JRN, Mtshali C, Pineda-Vargas CA. 2015. Micro-PIXE mapping of mineral distribution in mature grain of two pearl millet cultivars. *Nuclear Instruments and Methods in Physics Research B* 363: 177-182.
- Ng'uni D, Geleta M, Johansson E, Fatih M, Bryngelsson T. 2011. Characterization of the Southern African sorghum varieties for mineral contents: Prospects for breeding for grain mineral dense lines. *African Journal of Food Science* 5(7): 436 – 445.
- Organization for Economic Co-operation and Development, 2010. Consensus Document on compositional consideration for new varieties of grain sorghum. Series on the Safety of Novel Foods and Feeds No. 19. <<http://www.oecd.org/science/biotrack/46815316.pdf>> (accessed 21 February 2015).
- Pappin DJ, Hojrup P, Bleasby AJ. 1993. Rapid identification of proteins by peptide-mass fingerprinting. *Current Biology* 3(6): 327-332.
- Pongrac P, Vogel-Mikuš K, Jeromel L, Vavpetič P, Pelicon P, Kaulich B, Gianonceli A, Eichert D, Regvar M, Kreft I. 2013. Spatially resolved distributions of the mineral elements in the grain of tartary buckwheat (*Fagopyrum tataricum*). *Food Research International* 54: 125-131.
- Pontieri P, Troisi J, Di Fiore R, Di Maro A, Bean SR, Tuinstra MR, Roemer E, Boffa A, Del Giudice A, Pizzolante G, Alifano P, Del Giudice L. 2014. Mineral contents in grains of seven food-grade sorghum hybrids grown in a Mediterranean environment. *Australian Journal of Crop Science* 8(11):1550-1559.
- Raboy V. 2007. The ABCs of low-phytate crops. *Nature Biotechnology*. 25(8):874–875.
- Reyes FC, Chung T, Holding D, Jung R, Vierstra R, Otegui MS. 2011. Delivery of prolamins to the protein storage vacuole in maize aleurone cells. *The Plant Cell Online* 23(2) DOI: <https://doi.org/10.1105/tpc.110.082156>.
- Rooney LW, Serna-Saldivar SO. 2000. Sorghum. In: Kulp K, Ponte JG (Eds) *Handbook of Cereal Science and Technology*, 2nd Ed. Marcel Dekker: New York, pp 149-175.
- Roux Dalvai F, Gonzalez de Peredo A, Simo C, Guerrier L, Bouyssié D, Zanella A, Citterio A, Buret-Schiltz O, Boschetti E, Righetti PG, Monsarrat B. 2008. Extensive analysis of the cytoplasmic proteome of human erythrocytes using the peptide ligand library technology and advanced mass spectrometry. *Molecular and Cellular Proteomics* 7: 2254-2269.
- Ryan CG. 2000. Quantitative Trace Element Imaging using PIXE and the Nuclear Microprobe. *International Journal of Imaging Systems and Technology* 11: 219-230.
- Shull JM, Watterson JJ, Kirleis AW. 1992. Purification and immunocytochemical localization of kafirins in Sorghum bicolor (L. Moench) endosperm. *Protoplasma* 171:64- 74.
- Syltje PW, Dahnke WC. 1983. Mineral and protein content, test weight and yield variations of hard red spring wheat grain as influenced by fertilisation and cultivar. *Plant Foods for Human Nutrition* 32(1): 37-49.

- Szymczycha-Madeja A. 2014. A simple and rapid method for the multielement analysis of wheat crispbread products by Inductively Coupled Plasma-Optical Emission Spectrometry. *Journal of the AOAC International* 97(6): 1656-1661.
- Thiede B, Höhenwarter W, Krah A, Mattow J, Schmid M, Schmidt F, Jungblut PR. 2005. Peptide mass fingerprinting. *Methods* 35(3): 237-247.
- Trzaskowski B, Adamowicz L, Deymier PA. 2008. A theoretical study of zinc (II) interactions with amino acid models and peptide fragments. *Journal of Biological and Inorganic Chemistry* 13(1): 133-137.
- Uddin MN, Kaczmarczyk A, Vincze E. 2014. Effects of Zn fertilisation on hordein transcripts at early developmental stage of barley grain and correlation with increased Zn concentration in the mature grain. *PLoS ONE* 9(9): e108546. Doi:10.1371/journal.pone.0108546
- Velu G, Rai KN, Muralidharan V, Kulkarni VN, Longvah T, Raveendran TS. 2007. Prospects of breeding bio fortified pearl millet with high grain iron and zinc content. *Plant Breeding* 126: 182-185.
- Volpicella M, Leoni C, Fanizza I, Placido A, Pastorello EA, Ceci LR. 2014. Overview of plant chitinases identified as food allergens. *Journal of Agricultural and Food Chemistry* 62(25): 5734–5742.
- Yan L, Liu S, Zhao S, Kang Y, Wang D. 2012. Identification of differentially expressed genes in sorghum (*Sorghum bicolor*) brown midrib mutants. *Physiologia Plantarum* 146: 375-387.

CHAPTER 5

A preliminary report of the use of RNA-seq to examine changes in the gene expression profile of wild-type versus transgenic sorghum grains.

5.1 Introduction

The use of transgenesis to improve the quality of a plant or plant products may lead to unintended effects that go beyond the intention of the original genetic modification (Ricroch *et al.*, 2011). This is possible because the integration of transgenes is essentially an uncontrolled process which could lead to the inactivation or alteration of endogenous gene activities (Gregersen *et al.*, 2005). The potential changes in gene expression could in turn lead to changes in metabolic activities that may not be detected during conventional health and safety risk evaluations (Gregersen *et al.*, 2005). In theory, however such changes could constitute a potential risk to consumers of the transgenic food product and therefore ought to be investigated.

The emergence of global profiling techniques, such as transcriptomics, proteomics and metabolomics, presents researchers with an opportunity to carry out a more holistic search for unintended alterations in transgenic crops (Ricroch *et al.*, 2011; Simó *et al.*, 2014). Such approaches are viewed as more unbiased, and can remarkably extend the breadth of comparative analyses between transgenic and non-transgenic crops, whilst reducing levels of uncertainty (Jiao *et al.*, 2010; Simó *et al.*, 2014). Whilst proteomics and metabolomics studies are focused on the primary and secondary products of cellular metabolism, transcriptomics instead looks at dynamics of gene expression through the analysis of RNA transcripts. Although it is understood that RNAs are not the final products of the transcription-translation process, their relative abundance can provide valuable insight into the genetic variables involved in the manifestation of a particular phenotype (Finotello and Di Camillo, 2015). Comparative transcript profiling can therefore be a powerful tool for identifying and assessing similarities and differences between a transgenic line and its non-transgenic counterpart based on differences in gene expression (Gregersen *et al.*, 2005). Currently, the most sought after technology for transcript profiling and

differential gene expression analysis is high throughput RNA sequencing, or RNA-seq.

5.1.1 Background to RNA-Seq

RNA-seq is a relatively new approach to whole transcriptome analysis based on next-generation sequencing (NGS) (Shendure and Ji, 2008). The sequencing framework of RNA-seq allows one to characterise all RNAs present in a sample and to quantify their abundances at the same time (Finotello and Di Camillo, 2015). The standard workflow of a typical RNA-seq experiment is depicted in Figure 5.1. Firstly, messenger RNA (mRNA) must be extracted from the sample of interest, and reverse transcribed into complementary DNAs (cDNA). Next, the sample cDNA is amplified and fragmented into segments that are subjected to the NGS process. With several different NGS technologies on the market, the specifics of the sequencing process can vary from one platform to another. However in essence, cDNA fragments of a

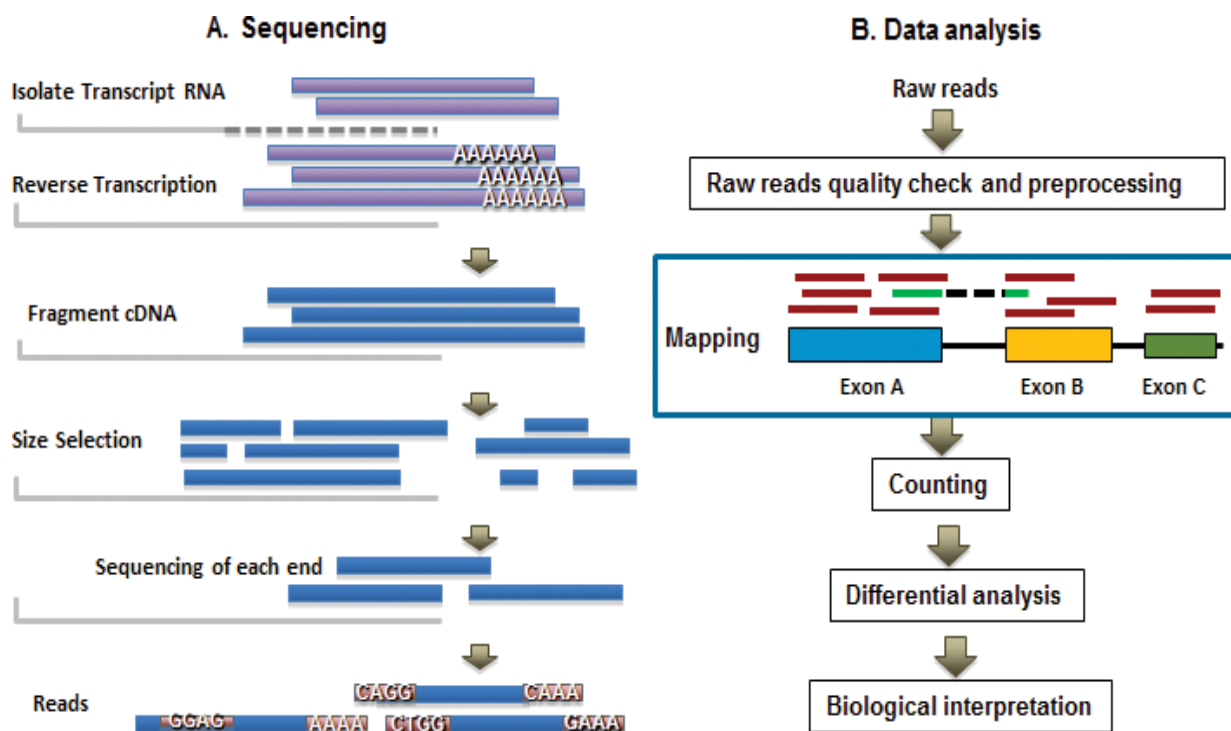


Figure 5.1 An overview of the laboratory processes involved in RNA-seq analysis (A) and the subsequent data analysis pipeline (B) (From Zhao *et al.*, 2016).

certain length are ligated with sequencing adaptors and the ends sequenced to produce millions of short genetic reads. These reads are then computationally mapped to a reference genome to reveal a transcriptional map, where the number of reads aligned to each gene gives a measure of its level of expression (Finotello and Di Camillo, 2015).

In this chapter, a preliminary report is given of the use of RNA seq analysis to assess differences in gene expression that serve to differentiate the transgenic sorghum grain (featuring kafirin suppression) from its wild-type non-transgenic counterpart.

5.2 Materials and methods

5.2.1 Plant tissue collection

Three independent plants for each genotype (wild-type P898012 and Transgenic Line 44-3) were grown in a containment glasshouse, under identical conditions, as described previously (Chapter 3, section 3.2.1). Plants were visually monitored and tagged at the onset of anthesis and immature kernels harvested at 15 days post-anthesis from the middle part of the sorghum panicle. The glumes were quickly removed from the immature grains and discarded before the grains were immediately frozen in liquid nitrogen.

5.2.2 Total RNA Extraction

The frozen grains of each sample were ground in liquid nitrogen using an oven-baked RNase-free mortar and pestle. Approximately 0.1 g of the grain powder was then transferred to pre-chilled 2 mL RNase-free eppendorf tubes and subjected to the RNA extraction protocol as prescribed by the TRIzol® Plus RNA purification kit (Invitrogen). In brief, 1 mL TRIzol® reagent was added to 0.1 g of ground seed powder and vigorously mixed to aid RNA extraction in the buffer. Samples were then allowed to incubate at room temperature for 5 minutes before centrifugation at 12,000 x *g* for 10 minutes, at 4°C. The supernatant was carefully transferred into another 2.0 mL RNase-free tube, to which 200 µL of chloroform was added, and mixed by shaking vigorously by hand for ~15 seconds. Next, the samples were allowed to incubate at room temperature for 3 minutes, before centrifuging at 12,000 x *g* for 15 minutes at 4°C. After centrifugation the upper colourless aqueous phase

(~600 μ l) was transferred to a fresh RNase-free tube and mixed with an equal volume of 70% ethanol (prepared in RNase-free water). The supernatant-ethanol mixture was then loaded onto the prescribed RNA binding column, according to the kit protocol and treated to series of steps to wash and desalt the samples. Finally, the RNA from each column was eluted using 50 μ l RNase-free water.

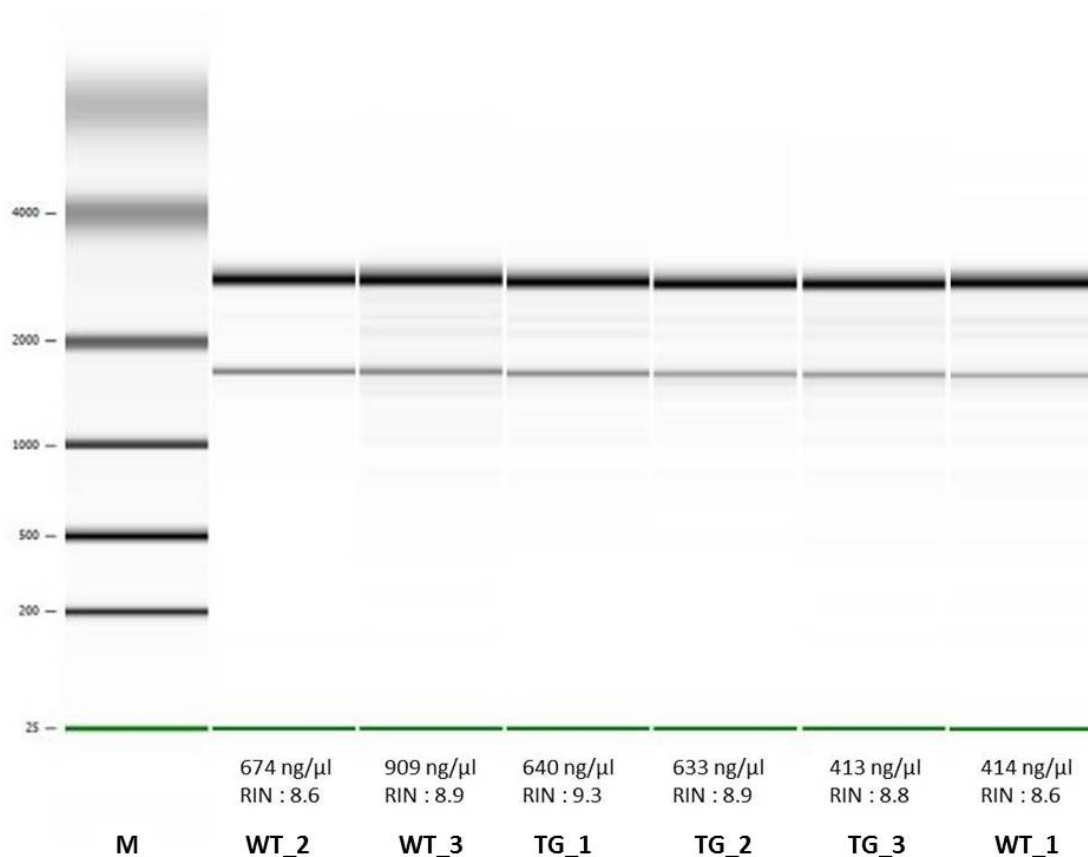


Figure 5.2 Electrophoretic trace of total RNA extracted from the immature sorghum grain samples, M: Marker; WT_1,2,3: wild-type RNA extracts; TG_1,2,3: transgenic RNA extracts.

All RNA samples were quantified and quality checked using microfluidic capillary electrophoresis with the Agilent 2100 Bioanalyser and associated software (Agilent Technologies, USA). RNA samples with a RNA integrity number (RIN) above 8.0 were deemed acceptable for subsequent RNA-seq analysis. The results of the Bioanalyser electrophoretic trace is shown in Figure 5.2; whilst, the data relating to RNA yield and quality are listed in Table 5.1.

Table 5.1 RNA yield and quality as assessed by the Agilent 2100 Bioanalyser.

Sample	28S:18S	RNA integrity Number (RIN)	RNA yield (ng/μl)
WT_1	4.6	8.60	414
WT_2	3.7	9.6	674
WT_3	3.9	8.9	909
TG_1	3.4	9.3	640
TG_2	3.7	8.9	633
TG_3	3.4	8.8	413

5.2.3 Library Construction and Sequencing

cDNA libraries for each sample were generated using the Ambion® Ion Torrent RNA-Seq Kit v2, according to the manufacturer's protocol. The kit is specifically designed to convert expressed RNA transcripts into representative cDNA libraries for RNA sequencing. In brief, two rounds of mRNA enrichment was performed on the RNA extracts using the protocol of Dynabeads® *mRNA DIRECT*[™] kit (Ambion, Life Technologies), allowing for the purification of poly-A mRNA from ~10 mg of total RNA extract, using poly-T oligo-attached magnetic beads. Next, the cDNA libraries generated for each sample were subjected to sequencing using the Ion Torrent Proton[™] Semiconductor Sequencer (Life Technologies, Thermo Fischer Scientific), at the DNA sequencing unit of the Central Analytical Facility of Stellenbosch University.

5.3 Results and discussion

According to the results obtained from the RNA sequencing run (Table 5.2), more than 10 million clean reads were found in each sample, which on average mapped to about 80% of the *S. bicolor* reference genome (Ensembl Plant Genome release 36) using Partek Flow Software[™]. Mismatches of no more than two bases were allowed in the alignment and sequences mapping to multiple gene locations were discarded. After alignment, gene expression levels were calculated as reads per kilobase of

exon model per million mapped reads (RPKM). The differentially expressed genes (DEGs) were identified using the number of mapped read counts per gene and normalised to the number of transcripts per million reads for each sample. Only genes with a false discovery rate (FDR) < 0.05 and fold change ≥ 2 or ≤ -2 were considered as differentially expressed. In total 1,742 genes were identified as differentially expressed between the transgenic samples and the wild-type (WT) (Appendix B). The vast majority of the DEGs (91%) were upregulated in the transgenic samples in comparison to WT, whilst the remaining 8% were downregulated (Figure 5.3).

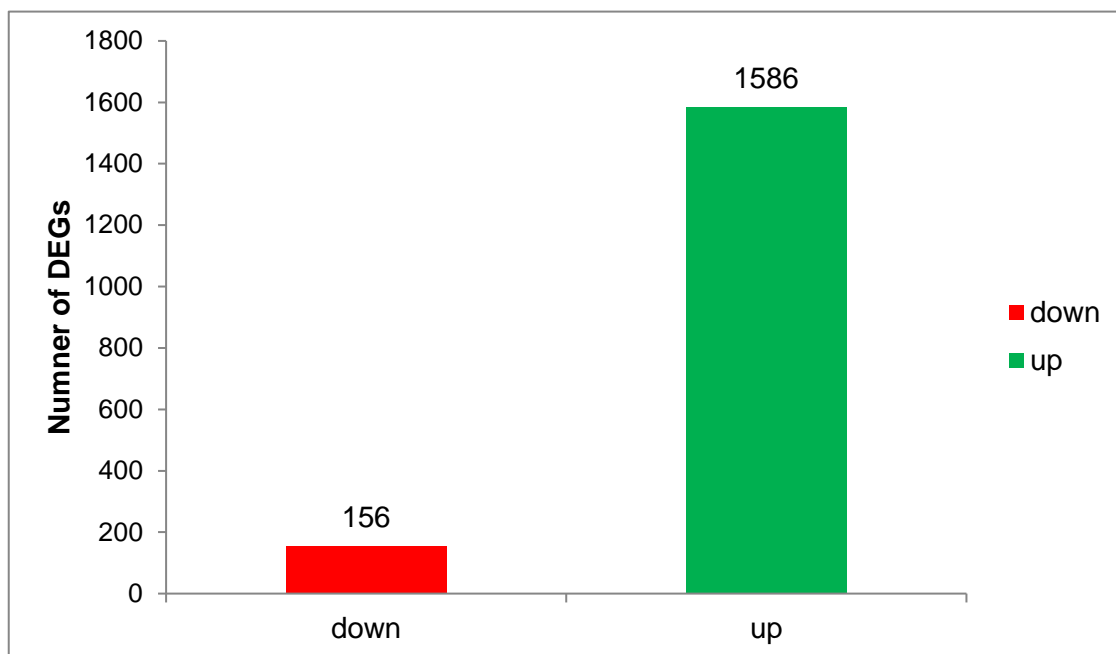


Figure 5.3 Bar chart showing the total number of differentially expressed transcripts with a false discovery rate (FDR) < 0.05 and fold change ≥ 2 or ≤ -2 , identified using RNA seq analysis. Transcripts identified as significantly downregulated were 156 in total; whilst 1586 were found to be significantly upregulated in the transgenic sample in comparison to the WT.

Table 5.2 Total number of reads and percentage of aligned reads for each sample for the RNA seq experiment.

Sample	Total Reads	Total aligned to <i>S.bicolor</i> genome	% Aligned reads
WT_1	23 009 853	20 147 427	87.56
WT_2	18 251 406	15 924 352	87.25
WT_3	10 394 266	8 727 026	83.96
443_1	13 381 761	9 990 823	74.66
443_2	16 801 243	12 075 053	71.87
443_3	15 947 023	12 497 682	78.37

Table 5.3 RNA seq analysis data pertaining to the three kafirin genes targeted for suppression by RNAi in the transgenic line 44-3. Importantly, all three of the targeted genes were detected to have a significant negative fold change (i.e. decreased mRNA expression) in comparison to the WT.

Gene ID	Gene Name	Total counts	P-value (Transgenic vs WT)	FDR set up (Transgenic vs WT)	Fold change (Transgenic vs WT)
Sb02g025510	γ –kafirin 1	19219.10	5.21×10^{-5}	0.00816	-17.4114
Sb02g025490	γ –kafirin 2	2302.32	9.72×10^{-4}	0.02231	-7.97009
Sb05g024310	α A1–kafirin	6713.31	0.00236	0.03190	-12.57487

On the basis of fold-change, the top 20 differentially expressed genes, identified as a result of the RNA-seq analysis, were further characterised in terms of their functional annotation, using the Morokoshi transcriptome database for *Sorghum bicolor*. The Morokoshi transcriptome database represents a large-scale collection of experimentally validated data sets of transcriptional units, transcription start sites and expression profiles for *S. bicolor* (Makita *et al.*, 2015). Using the search tool available on the Morokoshi website (<http://sorghum.riken.jp/morokoshi/Search.html>), a functional description could be appended to the top differentially expressed genes that serve to differentiate the transgenic grain from the wild-type (Tables 5.4 and 5.5)

Table 5.4 Top 20 up-regulated genes in transgenic sorghum versus wild-type, identified by RNA-seq analysis, and assigned functional descriptions from the Morokoshi transcriptome database.

	Gene ID	Functional description	P-value (Transgenic vs WT)	FDR set up (Transgenic vs WT)	Fold change (Transgenic vs WT)
1	Sb03g041830	Heat shock protein (Hsp 70) family protein	0.004	0.04	69.13
2	Sb01g045972	Thioredoxin 4	2.85×10^{-6}	0.005	27.65
3	Sb09g001080	Serine protease inhibitor	3.11×10^{-7}	0.002	23.14
4	Sb03g027040	Photosystem II light harvesting complex gene	4.36×10^{-4}	0.017	21.81
5	Sb04g031630	Oxidative stress 3	1.31×10^{-6}	0.004	21.57
6	Sb09g004130	Alpha/beta-Hydrolases superfamily protein	0.003	0.037	21.47
7	Sb08g007150	Lipase/Acylhydrolase superfamily protein	1.30×10^{-5}	0.006	20.61
8	Sb02g028520	Auxin efflux carrier family protein	8.04×10^{-8}	0.001	18.96
9	Sb05g007280	Nuclear factor Y	6.58×10^{-6}	0.005	17.27
10	Sb06g026500	Homeodomain-like superfamily protein	0.001	0.02	15.93
11	Sb01g019910	Zinc finger (C3HC4-type RING finger) family protein	0.003	0.03	15.87
12	Sb05g011660	Seed storage 2S albumin superfamily protein	2.88×10^{-5}	0.007	15.81
13	Sb07g000330	Seed storage 2S albumin superfamily protein	5.01×10^{-5}	0.008	14.42
14	Sb05g005880	Glycosyltransferase superfamily protein	7.72×10^{-4}	0.02	13.46

Table 5.4 Continued.

	Gene ID	Functional description	P-value (Transgenic vs WT)	FDR set up (Transgenic vs WT)	Fold change (Transgenic vs WT)
15	Sb02g002860	Hydrolase-type esterase superfamily protein	1.80×10^{-4}	0.01	13.39
16	Sb08g006540	Serine carboxypeptidase-like 20	0.002	0.03	13.32
17	Sb01g041190	3-ketoacyl-CoA synthase 1	7.25×10^{-4}	0.02	12.95
18	Sb04g030950	Phosphoribulokinase	0.003	0.04	12.76
19	Sb06g025300	Monocopper oxidase	2.77×10^{-4}	0.01	12.06
20	Sb06g015670	Alpha/beta-Hydrolases	4.68×10^{-5}	0.008	11.97

Table 5.5 Top 20 down-regulated genes in transgenic sorghum versus wild-type, identified by RNA-seq analysis, and assigned functional descriptions from the Morokoshi transcriptome database.

	Gene ID	Functional description	P-value (Transgenic vs WT)	FDR set up (Transgenic vs WT)	Fold change (Transgenic vs WT)
1	Sb02g025510	Prolamin precursor, expressed	5.21×10^{-5}	0.008	-17.41
2	Sb01g007420	Cytochrome P450 family	4.38×10^{-5}	0.008	-15.99
3	Sb05g024320	Zein seed storage protein	6.86×10^{-4}	0.02	-15.28
4	Sb05g024310	Zein seed storage protein	0.002	0.03	-12.57
5	Sb02g025490	Prolamin precursor, expressed	9.72×10^{-4}	0.02	-7.97

Table 5.5 Continued.

	Gene ID	Functional description	P-value (Transgenic vs WT)	FDR set up (Transgenic vs WT)	Fold change (Transgenic vs WT)
6	Sb08g004070	HSP20-like chaperones superfamily protein	0.004	0.04	-7.87
7	Sb03g001170	Late embryogenesis abundant protein	1.64×10^{-4}	0.012	-7.77
8	Sb01g046120	Tetratricopeptide repeat (TPR)-like protein	0.002	0.03	-7.50
9	Sb02g012500	Histone superfamily protein	0.003	0.03	-6.60
10	Sb02g025840	Cytochrome P450 superfamily protein	0.003	0.03	-6.46
11	Sb08g002990	Phytosulfokine precursor	7.54×10^{-4}	0.02	-6.30
12	Sb10g002830	Early nodulin-related	0.001	0.03	-6.07
13	Sb01g033920	Unknown expressed protein	4.17×10^{-5}	0.008	-5.84
14	Sb09g016810	Small hydrophilic plant seed protein	2.91×10^{-5}	0.007	-5.78
15	Sb01g043130	Disease resistance protein	2.64×10^{-4}	0.01	-5.77
16	Sb10g027000	Phosphatidylinositol transfer family protein	0.004	0.04	-5.48
17	Sb08g023190	Unknown expressed protein	2.75×10^{-4}	0.01	-5.46
18	Sb10g012265	Late embryogenesis abundant protein	8.75×10^{-4}	0.02	-5.30
19	Sb10g017780	Oleosin family protein	1.03×10^{-4}	0.01	-5.17
20	Sb01g014470	Plant thionin	0.006	0.05	-5.11

A survey of the genes listed in Table 5.4 gives an indication of the genes that were significantly up-regulated in the transgenic grain samples in comparison to WT. Notably, this gene list includes a number of enzymes belonging to the hydrolase protein family, such as alpha/beta hydrolases, lipase and serine carboxypeptidase. Enzymes of this type are known to be involved in a multitude of biochemical processes, particularly involving metabolism and the catalysis of important organic compounds (Holmquist, 2000). Importantly, the list of top up-regulated genes, also indicates that gene expression for two types of albumin proteins, was significantly increased in the transgenic grain samples in comparison to the WT. This result lends further support to the hypothesis that the suppression of kafirins, leads to an increased expression of other grain storage proteins. Lastly, the list of top up-regulated genes in the transgenic samples, also includes a heat shock protein and oxidative stress protein. This result may indicate that the transgenic samples are exhibiting more signs of stress in comparison to the wild-type samples.

In Table 5.5, the top-most down-regulated genes in the transgenic samples in comparison to WT are listed. Importantly, this list includes the three genes that were targeted for silencing in the original transformation. Although definitive validation is needed by means of quantitative PCR, the fact that the RNA-seq experiment was able to confirm a significant decrease in expression for the three targeted kafirins, is a good preliminary indicator that the analysis was credible. Importantly, amongst the list of down-regulated genes, there are a number of candidates that are known to play an important role in defence or disease resistance. Notably, these include the late embryogenesis abundant proteins (Olvera-Carillo *et al.*, 2011), the phytosulfokines (Sauter, 2015) and thionins (Stec, 2006). It may be speculated that a decreased expression of these defence-related genes in the transgenic grains may mean that these grains would be more susceptible to disease and predatory attack.

5.4 Conclusion

The preliminary use of RNA-seq was useful for highlighting some of the changes in gene expression that differentiate the transgenic sorghum grain from the wild-type. Importantly, even though only three genes were targeted for silencing in the original transformation, over 1700 genes were found to have an altered expression pattern in

the transgenic grains in comparison to the wild-type. Of note, many of the differentially upregulated genes seemed to indicate major changes in metabolism, whilst, some of the differentially downregulated genes were known to play a role in plant protection or defence. The results of this preliminary study however require further validation, using a follow-up technique, such as real-time PCR.

References

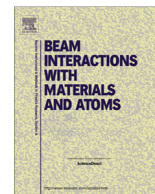
- Finotello F, Di Camillo B. 2015. Measuring differential gene expression with RNA-seq challenges and strategies for data analysis. *Briefings in Functional Genomics* 14(2): 13-142.
- Gregersen PL, Brinch-Pedersen H, Holm PB. 2005. A microarray-based comparative analysis of gene expression profiles during grain development in transgenic and wild type wheat. *Transgenic Research* 14(6): 887-905.
- Holmquist M. 2000. Alpha/Beta-hydrolase fold enzymes: structures, functions and mechanisms. *Current Protein and Peptide Science* 1(2): 209-235.
- Jiao Z, Si XX, Li GK, Zhang ZM, Xu XP. 2010. Unintended compositional changes in transgenic rice seeds (*Oryza sativa* L.) studied by spectral and chromatographic analysis coupled with chemometrics methods. *Journal of Agricultural and Food Chemistry* 58: 1746-1754.
- Makita Y, Shimada S, Kawashima M, Kondou-Kuriyama T, Toyoda T, Matsui M. 2015. Morokoshi: transcriptome database in Sorghum bicolor. *Plant Cell Physiology* 56(1): e6 1-8.
- Olvera-Carrillo Y, Reyes JL, Covarrubias AA. 2011. Late embryogenesis abundant proteins. *Plant signalling and Behaviour* 6(4): 586-589.
- Ricroch AE, Bergé JB, Kuntz M. 2011. Evaluation of genetically engineered crops using transcriptomic, proteomic and metabolomics profiling techniques. *Plant Physiology* 155(4): 1752-1761.
- Sauter M. 2015. Phytosulfokine peptide signalling. *Journal of Experimental Botany* 66(17): 5161-5169.
- Shendure J, Ji H. 2008. Next-generation DNA sequencing. *Nature Biotechnology* 26(10): 1135-1145.
- Simó C, Ibáñez C, Valdés A, Cifuentes A, García-Cañas V. 2014. Metabolomics of genetically modified crops. *International Journal of Molecular Sciences* 15: 18941-18966.
- Stec B. 2006. Plant thionins – the structural perspective. *Cellular and Molecular Life Sciences* 63(12): 1370-1385.
- Zhao S, Zhang B, Zhang Y, Gordon W, Du S, Paradis T, Vincent M, von Schack D. 2016. Bioinformatics for RNA-seq data analysis. In: Abdurakhmonov IY (Ed.) *Bioinformatics*

– updated features and applications. Open Access <[http: www.rna-seqblog.com/bioinformatics-for-rna-seq-data-analysis/](http://www.rna-seqblog.com/bioinformatics-for-rna-seq-data-analysis/)>, accessed 19 November 2017.

CHAPTER 6

Micro-PIXE mapping of mineral distribution in mature grain of two pearl millet cultivars

This research has been accepted and published in the Nuclear Instruments and Methods in Physics Research B Journal



Micro-PIXE mapping of mineral distribution in mature grain of two pearl millet cultivars



R. Minnis-Ndimba^{a,*}, J. Kruger^b, J.R.N. Taylor^b, C. Mtshali^a, C.A. Pineda-Vargas^{a,c}

^a iThemba LABS, National Research Foundation, South Africa

^b Department of Food Science and Institute for Food, Nutrition and Well-being, University of Pretoria, South Africa

^c Faculty of Health and Wellness Sciences, CPUT, Bellville, South Africa

ARTICLE INFO

Article history:

Received 19 March 2015

Received in revised form 3 September 2015

Accepted 3 September 2015

Available online 14 September 2015

Keywords:

Pearl millet

Micro-PIXE

Scutellum

Mineral distribution in grains

ABSTRACT

Micro-proton-induced X-ray emission (micro-PIXE) was used to map the distribution of several nutritionally important minerals found in the grain tissue of two cultivars of pearl millet (*Pennisetum glaucum* (L.) R. Br.). The distribution maps revealed that the predominant localisation of minerals was within the germ (consisting of the scutellum and embryo) and the outer grain layers (specifically the pericarp and aleurone); whilst the bulk of the endosperm tissue featured relatively low concentrations of the surveyed minerals. Within the germ, the scutellum was revealed as a major storage tissue for P and K, whilst Ca, Mn and Zn were more prominent within the embryo. Fe was revealed to have a distinctive distribution pattern, confined to the dorsal end of the scutellum; but was also highly concentrated in the outer grain layers. Interestingly, the hilar region was also revealed as a site of high accumulation of minerals, particularly for S, Ca, Mn, Fe and Zn, which may be part of a defensive strategy against infection or damage. Differences between the two cultivars, in terms of the bulk Fe and P content obtained via inductively coupled plasma optical emission spectrometry (ICP-OES), concurred with the average concentration data determined from the analysis of micro-PIXE spectra specifically extracted from the endosperm tissue.

© 2015 Elsevier B.V. All rights reserved.

1. Introduction

Mineral deficiencies adversely affect the health of more than 3 billion people worldwide [1]. This problem is particularly widespread in sub-Saharan Africa, where unfavourable socio-economic conditions often force people to subsist on monotonous cereal-based diets that are deficient in several important micronutrients. Pearl millet (*Pennisetum glaucum* (L.) R. Br.) is one of the major African food security crops, which is relied upon by 90 million people as a source of food and income [2]. In terms of its overall nutritional quality (protein, starch, fat, mineral and fibre content) and anti-oxidant profile (total phenolic content and radical scavenging capacity), pearl millet grain compares well to other major cereals [3]. However, there are concerns that the amount and/or bioavailability of minerals supplied by the grain is insufficient to meet the nutritional needs of those who are most dependent on it. As a result, there is much interest in the bioforti-

fication of pearl millet, with research efforts focused on increasing the overall grain mineral content, particularly for key mineral nutrients, such as iron (Fe) and zinc (Zn), which are often the most limiting in the human diet [4].

The potential to breed high Fe and Zn biofortified pearl millet grains has been widely evaluated and confirmed [4–7]. To support this drive for biofortification, there is a need to understand the spatial distribution of minerals in different tissues within the grain. The mapping of minerals in seed tissues has been achieved in several notable studies, which include work on important cereals, such as wheat [8,9], barley [10] and rice [11,12]; as well as certain pseudocereals [13–15] and legumes [16,17]. To our knowledge, the only studies reporting on the spatial distribution of mineral elements in millet, include a recent study using micro-proton-induced X-ray emission (micro-PIXE) for finger millet [18] and a much earlier study on pearl millet, using energy dispersive X-ray analysis (EDX) [19]. With a view to complement the previous work done on mineral distribution in millet grains, the present study was initiated, which seeks to interrogate differences in the mineral concentration of two cultivars of pearl millet, at the level of the main grain tissues, using micro-PIXE.

* Corresponding author at: Materials Research Dept, NRF: iThemba LABS, P.O. Box 7129, Somerset West, South Africa. Tel.: +27 21 843 1165; fax +27 21 843 3543.
E-mail address: rminnis@tlabs.ac.za (R. Minnis-Ndimba).

2. Materials and methods

2.1. Plant material

Mature, dried pearl millet grains of two cultivars, namely ICMH 1201 and ICMH 1301, were kindly supplied by the International Crops Research Institute for the Semi-Arid Tropics (ICRISAT). The pearl millet cultivars were grown according to standard methods at the ICRISAT facility in India, and harvested in 2013. The cultivars were chosen because of their current use in the ICRISAT breeding programme to develop high Fe and Zn pearl millet grains.

2.2. Analysis of the bulk mineral content

Grain samples (~3 g) of each cultivar were separately milled to fine (wholegrain) flour and subjected to nitric-perchloric acid digestion, according to [20], before bulk mineral content analysis by inductively coupled plasma optical emission spectrometry (ICP-OES, SPECTRO Analytical Instruments, Kleve, Germany) [21]. For each cultivar, three independent determinations of the calcium (Ca), iron (Fe), zinc (Zn) and phosphorus (P) content, were made, and the mean value (\pm SD) reported. To evaluate differences between the means, the Student's *t*-test was performed using *Statistica* for Windows Version 12.6 (Statsoft Inc., USA); and differences were considered significant at $p < 0.05$.

2.3. Sample preparation for micro-PIXE analysis

Dry whole kernels from the two cultivars of pearl millet were embedded in a commercial resin (Struers EpoFix™) and longitudinally sectioned through the median, using a diamond-coated rotating blade operated at a low speed (~100 rpm), which cleanly cut the sample into half. Due to the low moisture content of the grains, no elaborate fixation procedure was deemed necessary [14]. A Nikon SMZ1500 stereomicroscope fitted with a digital camera (Nikon DS Fi2) was used to visually inspect and photograph each half-grain sample, to ensure that major anatomical features (i.e. the scutellum, embryonic axis, endosperm etc.) were clearly distinguishable in all samples selected for micro-PIXE analysis. Finally, the selected samples were coated with a thin layer of carbon before mounting in the nuclear microprobe for micro-PIXE analysis.

2.4. Micro-PIXE analysis

Micro-PIXE analysis was performed using the nuclear microprobe situated at the Materials Research Department, iThemba LABS [22–24]. A proton beam of 3.0 MeV energy, a current of ~100 pA and a spot size of $3 \times 3 \mu\text{m}^2$ was raster scanned, in two separate irradiation events, across a square-shaped area of ~2 mm² over the surface of the grain ($n = 2$ per cultivar). The first scanning event covered the upper half of the grain, whilst the second scanning event was used to cover the basal half that included the entire germ tissue. Scanned areas were analysed in a square modality, using a data matrix of up to 128×128 pixels, with a total dwell time of 10 ms pixel⁻¹. X-ray spectra were detected with a PGT Si(Li) detector. Proton backscattered spectra (BS) were collected simultaneously with a surface barrier detector. A 125 μm Be filter was interposed between the target and the Si(Li) detector to prevent scattered protons from reaching the detector. Following data collection, quantitative elemental maps were generated, using the Dynamic Analysis method, as part of GeoPIXE II software [25]. Additionally, micro-PIXE spectra were extracted from selected regions of interest from each sample, to obtain representative concentration data, along with the estimate of uncertainty [26], and the minimum detection limit for each element, using the Currie

formula [27]. Regions of interest were selected on the basis of the major morphological features of the grain tissue [28,29], which were readily distinguishable in the light micrographs and correlating micro-PIXE distribution maps. For data processing, each sample was treated as 'infinitely thick', and the main constituent of the biological matrix was assumed to be cellulose, following the approach of [30–32].

3. Results and discussion

The bulk mineral content of the two pearl millet cultivars, as determined by ICP-OES, for Ca, Fe, P and Zn is shown in Table 1. The average content for all the minerals analysed was slightly higher in ICMH1301, however only Fe and P emerged as significantly higher ($p < 0.05$) at 10% and 14%, respectively. A recent study evaluating the mineral content of 225 accessions of pearl millet, found the following mean values (and ranges) for Ca = 229.1 (73.5–603.5); Fe = 42.9 (19.7–86.4); P = 4023.5 (626.7–5705.5); Zn = 40.3 (13.5–82.4) $\mu\text{g}\cdot\text{g}^{-1}$, respectively [7]. A comparison of these mean values with the results obtained in this study, indicate that the Fe content was above average in both cultivars but levels of Zn and Ca were below average, with Ca distinctly at the lowest level of the range. A large variation in the grain mineral content of different varieties of pearl millet, is a typical observation, which may be due to the influence of both genetic and agronomic factors [7,19]. However, the high maximum levels of Fe and Zn observed for some varieties [7] is demonstrative of the potential that exists within the germplasm to boost the concentration of these minerals even further.

Using micro-PIXE, the spatial distribution of several minerals within the grain tissues of the two pearl millet cultivars was investigated. Quantitative elemental maps (Figs. 1 and 2) were obtained, which were further supplemented with average concentration data (Table 2), for selected grain tissues by means of the region selection analysis tools available in the GeoPIXE software (Fig. 3). The micro-PIXE maps (Figs. 1 and 2) provided a clear visual demonstration of the non-homogenous distribution of minerals within and amongst the major grain tissues of pearl millet, which was mirrored across the two individual cultivars. This morphological distribution was mainly characterised by relatively low concentrations of the surveyed minerals in the bulk of the endosperm, whilst the outer grain layers and the germ tissue, featured high mineral concentrations. This finding confirms the well-known pattern of mineral distribution in cereal grains, which is typified by high concentrations of several important minerals within the so-called cereal 'bran' layers; whilst much lower concentrations are localised within the starchy endosperm [33,34].

In line with the above proposition, the most striking features of the micro-PIXE maps, were localised within the germ area of the pearl millet grains. The germ of pearl millet occupies a relatively large percentage of the total kernel (>17%), and thus contributes significantly to the overall nutritional and mineral content of the grain [3,35]. Within the germ, a clear distinction in terms of the mineral concentration was observed between the two main tissue types: the scutellum and the embryo. The scutellum in particular was revealed as a major site of mineral accumulation, with the

Table 1

Total mineral contents (mg/kg) of the pearl millet grains, as determined by ICP-OES. Values in the same column with different superscripts differ significantly ($p < 0.05$).

Cultivars	Ca	Fe	P	Zn
1201	72 ^a (2)	50 ^a (1)	3264 ^a (102)	31 ^a (1)
1301	74 ^a (2)	55 ^b (1)	3731 ^b (135)	32 ^a (1)

() – values in parentheses are 1 standard deviation of 3 analyses.

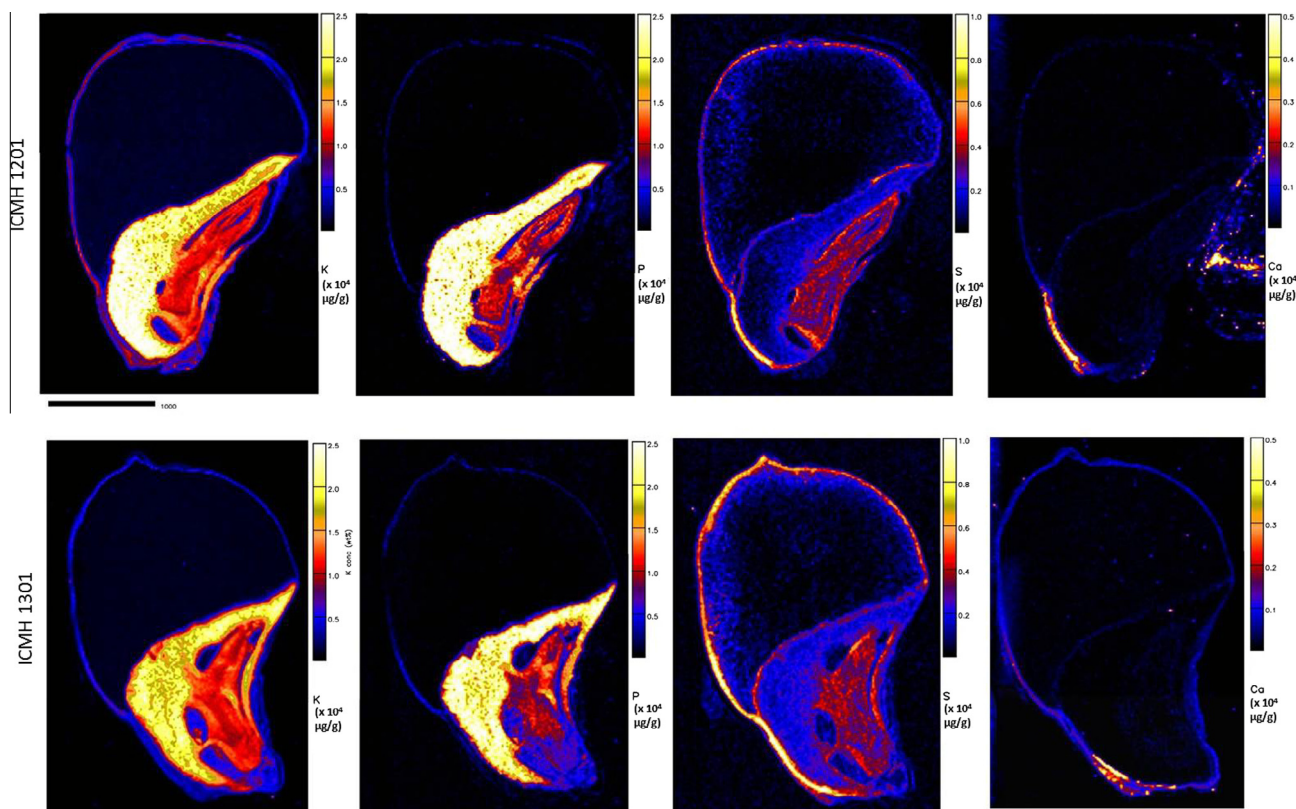


Fig. 1. Quantitative spatial distribution maps of K, P, S and Ca in two cultivars of pearl millet grain, cross-sectioned longitudinally. Top row, ICMH 1201; bottom row, ICMH 1301. Colour scales represent concentrations ($\times 10^4 \mu\text{g}\cdot\text{g}^{-1}$). Scale bar = 1 mm. Note a small piece of parafilm (ICMH 1201), which is rich in Ca that was used to securely place the grain. (For interpretation of the references to colour in this figure legend, the reader is referred to the web version of this article.)

highest concentration of P and K, for both cultivars, at an average of $>2.0 \times 10^4 \mu\text{g}\cdot\text{g}^{-1}$ for P, and $>1.8 \times 10^4 \mu\text{g}\cdot\text{g}^{-1}$ for K. In mature seeds, P is principally stored as phytic acid, which accounts for up to 80% of the total seed P content, and can contribute as much as 1.5% of the seed total dry weight [36]. At physiological pH, phytic acid exists in its anionic form, and as such is able to strongly chelate cationic minerals, such as K, Mg, Ca, Fe, Zn and Mn, to form phytate [36,37]. The most common form of phytate is as a mixed salt of K^+ and Mg^{2+} [38], and therefore the strong co-localisation of P and K in the scutellum is likely indicative of the pervasive presence of the phytate molecule. Although certain major cereals grains like barley, wheat and rice, store most of their phytate reserves in the aleurone with little in the germ, maize exhibits a different pattern, with about 88% of its phytate stored in the germ, 2% in the endosperm and 10% in the aleurone/outer grain layers [38]. Given the dominant levels of P and K in the germ tissues, it is clear that pearl millet is more aligned to the strategy of maize, when it comes to the preferred accumulation pattern of phytate reserves within its grain tissues.

The next highest concentration of P and K were found within the embryo. Interestingly, although the concentration of P and K were significantly reduced ($\sim 57\%$ for P; and $\sim 39\%$ for K) in the embryo in comparison to the scutellum, the levels of the majority of the other minerals were not. In fact a $>50\%$ increase in S, Ca, Mn, and Zn concentration was found for the pearl millet embryo tissues in comparison to the scutellum, which likely reflects the great importance of these minerals for the embryo's survival. Fe is the only mineral that demonstrates a reversal of this trend, with an average concentration that is 15% higher in the scutellum than in the embryo. Limited levels of Fe within the embryo may be a biological strategy aimed at protecting the embryo from Fe excess, which is linked to the production of toxic reactive oxygen species

(ROS) that can lead to tissue damage by means of oxidative stress [37,39].

In terms of the spatial distribution of the minerals within the germ, varying patterns of accumulation were observed in the micro-PIXE maps, which often coincided with basic aspects of the grain tissue morphology (Fig. 4). In the scutellum, fairly uniform distributions of P, K and S were observed throughout this tissue, which was a pattern mirrored closely by Zn. Interestingly, the scutellar epithelial layer, which borders the scutellum and the starchy endosperm, was found to feature relatively higher concentrations of S, Ca, Mn and Zn, which may be related to the secretory functions of this important cell layer [40]. Within the scutellum, Fe is distinguished by a unique distribution pattern, which is characterised by higher concentrations of this mineral accumulating specifically at the dorsal end of the scutellum, in the region closest to the border with the starchy endosperm. For the embryo tissue, a very specific distribution of the various minerals was observed, which seemed to follow a clear demarcation of the different tissue types found in the embryonic region, such as the plumule, coleoptile, embryonic root, root cap and coleorhiza (root sheath), particularly for P, K and S. For Fe and Zn, there appears to be some common hotspots, such as at the apex of the plumule and in the tissues surrounding the shoot apical meristem and the embryonic root. Mn however has the most distinctive pattern of distribution in the embryo that is conspicuously localised in the tissues surrounding the embryonic root, extending upwards and around what is most likely the shoot apical meristem. Interestingly, this distribution pattern for Mn, was also observed in similar studies done on mature wheat [9] and barley grains [10]. It is speculated that this very specific localisation of Mn may be related to its known ability to inhibit the growth hormone auxin [41]. In line with the very specific localisation of Mn, it is further noted that the most

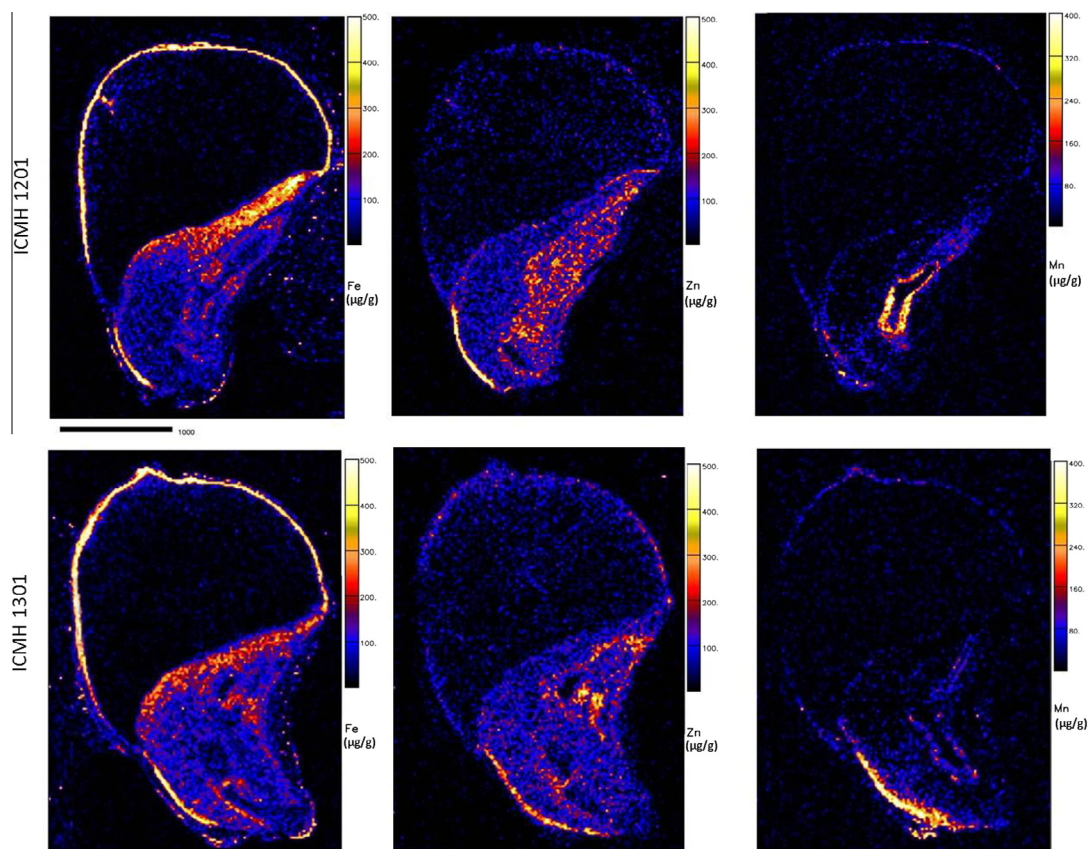


Fig. 2. Quantitative spatial distribution maps of Fe, Zn and Mn in two cultivars of pearl millet grain, cross-sectioned longitudinally. Top row, ICMH 1201; bottom row, ICMH 1301. Colour scales represent concentrations ($\times 10^4 \mu\text{g}\cdot\text{g}^{-1}$). Scale bar = 1 mm. Note a small piece of parafilm (ICMH 1201) that was used to securely place the grain, contains some Fe. (For interpretation of the references to colour in this figure legend, the reader is referred to the web version of this article.)

Table 2
Concentrations of mineral elements in different tissues of the mature pearl millet grain, presented as average of two representative measured samples from each cultivar. Results are reported in $\mu\text{g}\cdot\text{g}^{-1} \pm 1\sigma$ uncertainty, followed by the minimum detection limit in brackets. The concentration data are based on the extraction of X-ray spectra from the encircled regions, as depicted in Fig. 3, using GeoPIXE software.

Grain tissue	Cultivar	P	K	S	Ca	Mn	Fe	Zn
Scutellum	1201	23,081 \pm 40 (28)	18,451 \pm 13 (4)	1737 \pm 12 (16)	70.5 \pm 3 (3)	8.65 \pm 1 (1)	99.5 \pm 2 (1)	84 \pm 2 (1)
	1301	20,578 \pm 30 (19)	18,685 \pm 10 (3)	1998 \pm 9 (12)	60 \pm 3 (3)	<1	142 \pm 2 (1)	72 \pm 1 (1)
Embryo	1201	8791 \pm 35 (36)	10,811 \pm 13 (6)	3500 \pm 17 (21)	144.5 \pm 3 (4)	65 \pm 2 (1)	84 \pm 2 (1)	144.5 \pm 3 (2)
	1301	9710 \pm 33 (28)	11,767 \pm 12 (5)	3331 \pm 15 (17)	94 \pm 3 (4)	20 \pm 1 (1)	120.5 \pm 2 (1)	117.5 \pm 3 (1)
Inner endosperm	1201	<29	1046 \pm 4 (5)	352 \pm 8 (17)	93.2 \pm 2 (4)	<1	6.2 \pm 1 (2)	18 \pm 1 (4)
	1301	163 \pm 6 (13)	1268 \pm 2 (2)	479 \pm 4 (8)	73.7 \pm 1 (2)	<1	10.5 \pm 0.4 (1)	18.1 \pm 1 (1)
Outer grain layer	1201	531 \pm 26 (54)	2350 \pm 11 (10)	1999 \pm 22 (32)	185 \pm 5 (7)	4.8 \pm 2 (3)	188 \pm 4 (3)	37.5 \pm 3 (7)
	1301	1005 \pm 15 (26)	2184 \pm 6 (4)	2926 \pm 14 (16)	216 \pm 2 (3)	9.7 \pm 1 (1)	191 \pm 2 (1)	53 \pm 2 (1)
Hilar region	1201	4285 \pm 95 (104)	7329 \pm 37 (16)	6109 \pm 65 (59)	2405 \pm 20 (11)	48.5 \pm 5 (4)	256.5 \pm 9 (4)	329.5 \pm 14 (5)
	1301	2762 \pm 47 (62)	6700 \pm 20 (10)	6798 \pm 39 (37)	3251 \pm 13 (7)	85 \pm 4 (3)	196.5 \pm 5 (2)	243 \pm 7 (3)

* Note: The germ collectively denotes both the embryo and the scutellum tissue.

pronounced difference in concentration between the scutellum and the embryonic tissues, was observed for Mn. In cultivar 1301, Mn was below the detection limit ($<1 \mu\text{g}\cdot\text{g}^{-1}$) in the scutellum, but was found at an average concentration of $20 \mu\text{g}\cdot\text{g}^{-1}$ in the embryo; whereas in cultivar 1201, the average concentration of Mn in the embryo ($65 \mu\text{g}\cdot\text{g}^{-1}$) was more than 7-fold greater in the scutellum of the same cultivar.

The relatively high concentrations of S, Ca, Mn, Fe and Zn found in the germ tissues are in most cases exceeded by >2 -fold in the grain hilar region. This region is easily identified, by its distinctive black colouration, which surrounds the outer basal region of the scutellum. During grain development, specialist transfer cells located within this region facilitate the transport of nutrients from

the mother plant to the grain basal endosperm [29]. At grain maturity, darkly pigmented material accumulates to form a pigment strand, which creates an impermeable seal at this area of the grain, signalling the end of nutrient transfer from the maternal tissues [29,42]. It is suggested that the pigmented material is mainly composed of phenolic compounds which carry out a protective function against disease and insect predation [29]. The high concentration of minerals in the hilar region may be reflective of this protective function or may be indicative of structural limitations at the maternal–filial interface, which serve as a bottleneck for mineral transport into the grain [29,43]. Certainly, the high concentration of Ca (2405 – $3251 \mu\text{g}\cdot\text{g}^{-1}$) is likely to play a role in maintaining cell wall integrity around this critical entry point into

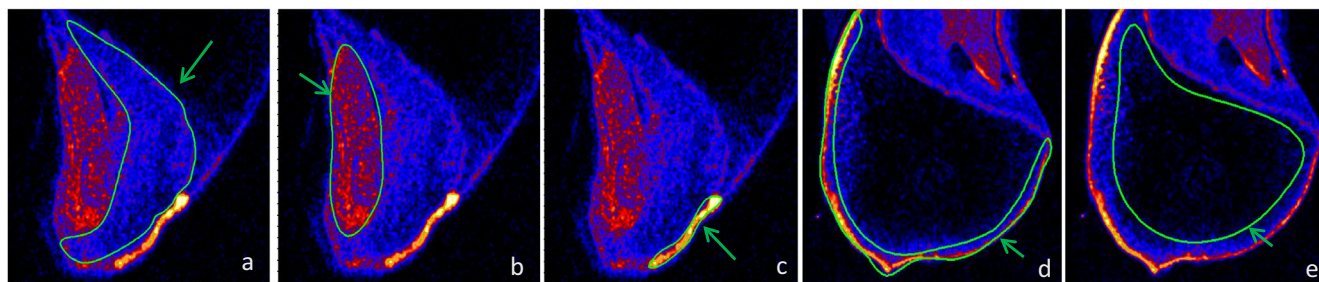


Fig. 3. Examples of the regions selected for elemental quantification, based on micro-PIXE S distribution maps. The encircled regions are pointed out by the green arrow and correspond to the scutellum (a), the embryo (b), the hilar region (c), the outer grain layers (d) and the inner endosperm (e). Scale bar = 0.5 mm.

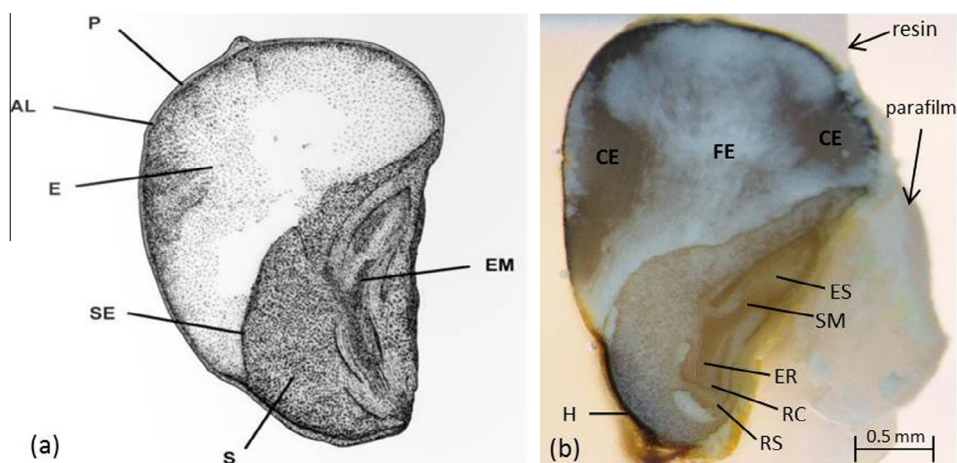


Fig. 4. (a) Schematic diagram of a longitudinal median section of a pearl millet grain depicting major morphological features such as the pericarp (P), aleurone (AL), the starchy endosperm (E), scutellar epithelial cells (SE), scutellum (S) and embryo (EM) [28]. (b) Light micrograph of the dissected pearl millet grain (ICMH 1201) used for micro-PIXE analysis. Finer anatomical features such as the hilar region (H), root cap (RC), root sheath (RS), embryonic root (ER), embryonic shoot (ES) and shoot apical meristem (SM) are pointed out, including a differentiation between the outer, more dense corneous endosperm (CE) and the inner, less dense floury endosperm (FE). Black arrows point to the outline of the embedding resin and to a small piece of parafilm, which was used to secure the position of the grain during resin polymerisation.

the grain [44]; whilst the high concentration of sulphur ($>6100 \mu\text{g}\cdot\text{g}^{-1}$) is likely reflective of sulphur-rich proteins like defensins which are known to be localised around the hilar region, to protect the grain against attack by pathogenic micro-organisms and viruses [45].

Due to the low level of resolution of the micro-PIXE maps, it was not possible to definitively distinguish all the constituent layers of the outer grain tissues, (which include the pericarp, seed coat and the aleurone); therefore these structures are broadly referred to as the outer grain layers. The multi-layered nature and variable thickness of the outer grain layers were perhaps most aptly reflected in the K distribution maps, where the presence of K is likely indicative of its contribution to the fortification of cell walls [13,19]. The cell walls of the aleurone layer are known to be particularly thick [46], and therefore regions of elevated K ($>2000 \mu\text{g}\cdot\text{g}^{-1}$) are probably associated with the cells of this layer. As may be expected, Ca was also prominently featured within these peripheral layers, where it is likely to function in cell wall maintenance and rigidity, but also as a key regulator of certain cell-to-cell signalling processes, which are vital to the process of seed germination and growth [44]. S and Fe were also noted to be present at relatively high levels in the outer grain layers. It therefore seems plausible that Fe and S may be closely linked, particularly as part of a metalloprotein complex [8,47].

Given the nutritional importance of Fe and Zn, it is interesting to note that these two elements do not share the same pattern of distribution within the pearl millet grain. Apart from the hilar

region, Fe was most concentrated ($188\text{--}191 \mu\text{g}\cdot\text{g}^{-1}$) in the outer grain layers. However for Zn, the highest concentration of this mineral was found in the embryonic tissues ($118\text{--}145 \mu\text{g}\cdot\text{g}^{-1}$). In all of the grain tissues investigated (apart from the hilar region), Fe was found to accumulate to higher levels in the grain of ICMH 1301 in comparison to that of ICMH 1201. This difference was most pronounced in the endosperm, where ICMH 1301 was found to have an average concentration of $11 \mu\text{g}\cdot\text{g}^{-1}$, which was 69% higher than the average concentration of Fe in the ICMH 1201 grain. This result confirms the average higher Fe content for ICMH 1301 that is supported by bulk analyses (Table 1), and highlights the major contribution that the endosperm tissue (which comprises 75% of the grain [35]) makes towards the overall mineral content. A similar scenario was also evident for the concentration of P found in the grain endosperm by micro-PIXE (Table 2). Whereas undetectable levels of P were found in the endosperm of ICMH 1201, cultivar ICMH 1301 was found to have an average P concentration of $163 \mu\text{g}\cdot\text{g}^{-1}$. The low concentration of P in the endosperm of ICMH 1201 is therefore likely to be the main cause of the finding supported by bulk analyses, which showed that the bulk wholegrain P content of ICMH 1201 was significantly lower than that of ICMH 1301.

4. Conclusion

In this study, differences in the spatial distribution and concentration of several minerals were investigated in two cultivars of

pearl millet. Using micro-PIXE, quantitative elemental mapping of P, K, S, Ca, Zn, Fe and Mn in major parts of the grain was obtained. Of note, the germ and outer grain layers were found to feature relatively high concentrations of the surveyed minerals, whilst the bulk of the endosperm tissue featured lower concentrations. Although restricted by the low level of resolution of the micro-PIXE maps, a broad partitioning of the grain into its major constituent parts such as the scutellum, embryo, endosperm and outer grain layers allowed a preliminary investigation of the differential accumulation of minerals within these structures. In future, more detailed and precise elemental mapping may proceed on thin sections of the grain to reveal the exact cellular locations of minerals that were found to accumulate to high concentrations in areas of the embryo, hilum and outer grain layers. However, the information obtained from the present study, has provided valuable basic information on the preferential storage pattern of the investigated minerals, which will be of benefit to on-going research initiatives focused on the mineral biofortification of pearl millet grain.

Acknowledgements

Financial and technical support for this study was provided by NRF: iThemba LABS and the University of Pretoria. The pearl millet grains analysed were kindly supplied by the International Crops Research Institute for the Semi-Arid Tropics (ICRISAT). The digital stitching of the micro-PIXE maps was done using Photoshop software by Dr. M. Khenfouch.

References

- [1] R. Welch, R. Graham, *J. Exp. Bot.* 55 (2004) 353–364.
- [2] ICRISAT, Pearl millet, a dependable and nutritious source of food for millions in marginal agricultural areas. Available from: <http://exploreit.icrisat.org/page/pearl_millet/680>, 2015 (11.03.15).
- [3] V.S. Nambiar, J.J. Dhaduk, N. Sareen, T. Shahu, R. Desai, *J. Appl. Pharm. Sci.* 1 (2011) 62–67.
- [4] K.N. Rai, M. Govindaraj, A.S. Rao, *Qual. Assur. Saf. Crops Foods* 4 (2012) 119–125.
- [5] G. Velu, K.N. Rai, V. Muralidharan, V.N. Kulkarni, T. Longvah, T.S. Raveendran, *Plant Breed.* 126 (2) (2007) 182–185.
- [6] M. Govindaraj, K.N. Rai, P. Sahnugasundaram, S.L. Dwivedi, K.L. Sahtrawat, A. R. Muthaiah, A.S. Rao, *Crop Sci.* 53 (2013) 507–517.
- [7] E.M.A. Bashir, A.M. Ali, A. Ali, A.E. Melchinger, H.K. Parzies, B.I.G. Haussmann, *Plant Genet. Resources* 12 (1) (2014) 35–47.
- [8] S.P. Singh, K. Vogel-Mikuš, I. Arçon, P. Vavpetič, L. Jeromel, P. Pelicon, J. Kumar, R. Tuli, *J. Exp. Bot.* 64 (2013) 3249–3260.
- [9] A.P. Mazzolini, C.K. Pallaghy, G.J.F. Legge, *New Phytol.* 100 (1985) 483–509.
- [10] E. Lombi, E. Smith, T.H. Hansen, D. Paterson, M.D. de Jonge, D.L. Howard, D.P. Persson, S. Husted, C. Ryan, J.K. Schjoerring, *J. Exp. Bot.* 62 (2011) 273–282.
- [11] L. Lu, S. Tian, H. Liao, J. Zhang, X. Yang, J.M. Labavitch, W. Chen, *PLoS ONE* 8 (2) (2013) e57360, <http://dx.doi.org/10.1371/journal.pone.0057360>.
- [12] E. Lombi, K.G. Scheckel, J. Pallon, A.M. Carey, Y.G. Zhu, A.A. Meharg, *New Phytol.* 184 (2009) 193–201.
- [13] Y. Konishi, S. Hirano, H. Tsuboi, M. Wada, *Biosci. Biotechnol. Biochem.* 68 (1) (2004) 231–234.
- [14] K. Vogel-Mikuš, P. Pelicon, P. Vavpetič, I. Kreft, M. Regvar, *Nucl. Instr. Meth. Phys. Res. B* 267 (2009) 2884–2889.
- [15] P. Pongrac, K. Vogel-Mikuš, L. Jeromel, P. Vavpetič, P. Pelicon, B. Kaulich, A. Gianoncelli, D. Eichert, M. Regvar, I. Kreft, *Food Res. Int.* 54 (2013) 125–131.
- [16] C. Cvitanich, W.J. Przybyłowicz, D.F. Urbanski, A.M. Jurkiewicz, J. Mesjasz-Przybyłowicz, M.W. Blair, C. Astudillo, E.Ø. Jensen, J. Stugaard, *BMC Plant Biol.* 10 (2010) 26–39.
- [17] C. Cvitanich, W.J. Przybyłowicz, J. Mesjasz-Przybyłowicz, M.W. Blair, C. Astudillo, E. Orłowska, J. Stugaard, *Nucl. Instr. Meth. B* 269 (2011) 2297–2302.
- [18] J. Kruger, C.A. Pineda-Vargas, R. Minnis-Ndimba, J.R.N. Taylor, *J. Cereal Sci.* 60 (2014) 1–3.
- [19] E. Varriano-Marston, R.C. Hosney, *Cereal Chem.* 57 (2) (1980) 150–152.
- [20] R.J. Zasoski, R.G. Bureau, *Commun. Soil Sci. Plant Anal.* 8 (1977) 425–436.
- [21] J. Kruger, J.R.N. Taylor, A. Oelofse, *Food Chem.* 131 (2012) 220–224.
- [22] V.M. Prozesky, W.J. Przybyłowicz, E. van Achterbergh, C.L. Churms, C.A. Pineda, K.A. Springhorn, J.V. Pilcher, C.G. Ryan, J. Kritzing, H. Schmitt, T. Swart, *Nucl. Instr. Meth. B* 104 (1995) 36–42.
- [23] W.J. Przybyłowicz, J. Mesjasz-Przybyłowicz, C.A. Pineda, C.L. Churms, K.A. Springhorn, V.M. Prozesky, *X-ray Spectrom.* 28 (1999) 237–243.
- [24] W.J. Przybyłowicz, J. Mesjasz-Przybyłowicz, C.A. Pineda, C.L. Churms, C.G. Ryan, V.M. Prozesky, R. Frei, J.P. Slabbert, J. Padayachee, W.U. Reimold, *X-ray Spectrom.* 30 (2001) 156–163.
- [25] C.G. Ryan, *J. Imaging Syst. Technol.* 11 (2000) 219–230.
- [26] C.G. Ryan, D.R. Cousins, S.H. Sie, W.L. Griffin, G.F. Suter, E. Clayton, *Nucl. Instr. Meth. Phys. Res. B* 47 (1990) 55–71.
- [27] L.A. Currie, *Anal. Chem.* 40 (1968) 586–593.
- [28] J.A. Delcour, R.C. Hosney, *Principles of Cereal Science and Technology*, 3rd ed., AACC International, St Paul, MN, 2010.
- [29] L.K. Fussell, D.M. Dwarde, *J. Exp. Bot.* 31 (121) (1980) 645–654.
- [30] E.T.F. Witkowski, I.M. Weiersbye-Witkowski, W.J. Przybyłowicz, J. Mesjasz-Przybyłowicz, *Nucl. Instr. Meth. Phys. Res. B* 130 (1997) 381–387.
- [31] W.J. Przybyłowicz, C.A. Pineda, A.D. Barnabas, J. Mesjasz-Przybyłowicz, *Nucl. Instr. Meth. Phys. Res. B* 150 (1999) 282–290.
- [32] C.A. Pineda, M. Peisach, *Nucl. Instr. Meth. Phys. Res. B* 35 (1988) 344–348.
- [33] B. Kryiacou, K.L. Moore, D. Paterson, M.D. de Jonge, D.L. Howard, J. Stangoulis, M. Tester, E. Lombi, A.T. Johnson, *J. Cereal Sci.* 59 (2014) 173–180.
- [34] P. Pongrac, I. Kreft, K. Vogel-Mikuš, M. Regvar, M. Germ, P. Vavpetič, N. Grlj, L. Jeromel, D. Eichert, B. Budič, P. Pelicon, *J. R. Soc. Interface* 10 (2013) 20130296, <http://dx.doi.org/10.1098/rsif.2013.0296>.
- [35] A. Abdelrahman, R.C. Hosney, E. Varriano-Maston, *J. Cereal Sci.* 2 (1984) 127–133.
- [36] L. Bohn, A.S. Meyer, S.K. Rasmussen, *J. Zhejiang Univ. Sci. B* 9 (3) (2008) 165–191.
- [37] I. Kranner, L. Colville, *Environ. Exp. Bot.* 72 (2011) 93–105.
- [38] J.C. Liu, I. Ockenden, M. Truax, J.N.A. Lott, *Seed Sci. Res.* 14 (2004) 109–116.
- [39] H. Roschztardt, G. Conéjéro, F. Divol, C. Alcon, J.-L. Verdeil, C. Curie, S. Mari, *Front. Plant Sci.* 4 (2013) 1–11 (article 350).
- [40] H. Tnani, N. García-Muniz, C.M. Vicient, I. López-Ribera, *J. Plant Physiol.* 169 (14) (2012) 1430–1433.
- [41] C.D. Foy, R.L. Chaney, M.C. White, *Annu. Rev. Plant Physiol.* 29 (1) (1978) 511–566.
- [42] N. Aoki, T. Hirose, S. Takahashi, K. Ono, K. Ishimaru, R. Ohsugi, *Plant Cell Physiol.* 40 (1999) 1072–1078.
- [43] S.Y. Zee, T.P. O'Brien, *Aust. J. Biol. Sci.* 24 (1971) 391–395.
- [44] P.K. Hepler, *Plant Cell* 17 (2005) 2142–2155.
- [45] M. Balandin, J. Royo, E. Gómez, L.M. Muniz, A. Molina, G. Hueros, *Plant Mol. Biol.* 58 (2005) 269–282.
- [46] L. Taiz, E. Zeiger, *Plant Physiology*, Sinauer Associates Inc, Sunderland, MA, 2002.
- [47] D. Steinfurth, C. Zörb, F. Braukmann, K.H. Mühling, *J. Plant Physiol.* 169 (2012) 72–77.

CHAPTER 7

A comparative study of tissue-specific differences in the mineral content of biofortified and conventional pearl millet grain using micro-PIXE analysis

7.1 Introduction

Pearl millet (*Pennisetum glaucum* (L.) R. Br) is an indigenous African cereal that is currently ranked as the world's sixth most important grain producing crop (Pattanashetti *et al.*, 2016). It is cultivated across 31 million hectares of the world's most marginal arid and semi-arid environments in Africa and Asia (Shivhare and Lata, 2017); where it is known to contribute up to 75% of the total cereal production in these areas (Lestienne *et al.*, 2005). As a crop, pearl millet exhibits remarkable stress tolerance characteristics, which enable it to thrive in low moisture nutrient-deprived soils and at high ambient temperatures in excess of 40 °C (Manwaring *et al.*, 2016). Under these extreme conditions, most other crops, such as rice, wheat, maize and even sorghum would tend to fail (Vadez *et al.*, 2012). Pearl millet therefore serves as an important lifesaver crop for more than 90 million people who depend on this species for food and economic survival (Shivhare and Lata, 2017).

It is estimated that nearly 37 African countries are dependent on pearl millet for baseline subsistence (Kumara Charyulu *et al.*, 2014). The crop is mainly cultivated for its grain; but it is also relied on in marginal environments as a source of hay, bird feed, fuel and forage material (Shivhare and Lata, 2017). In terms of food security, pearl millet grain is valued as a good basic nutritional source. In comparison to other major cereals it has an equivalent or superior nutritional profile that is generally rich in metabolizable energy, protein and essential micronutrients (Manwaring *et al.*, 2016). Given that the crop is also relatively inexpensive to grow, research is driven to develop highly nutritious pearl millet varieties that will address the lingering problem of malnutrition that plague many of the world's poorest people (Manwaring *et al.*, 2016).

Various reports indicate that about half of the world's population suffers from Fe and/or Zn deficiencies (Cakmak 2008; Goudia and Hash, 2015). The consequences of Fe and Zn deficiency include: poor growth and compromised psychomotor development in children, reduced immunity, muscle wasting, sterility, increased morbidity and in acute cases even death (Rawat *et al.*, 2013). It is currently estimated that children require up to 10 mg of Fe

and Zn per day to be healthy, whilst adults require about 8 mg (Manwaring *et al.*, 2016). Even though pearl millet has relatively high concentrations levels of both Fe and Zn, the bioavailability of the minerals is low due to high contents of inhibitors such as phytate. Extensive variability for Fe and Zn density however has been reported within the pearl millet germplasm, which indicates that there is potential to develop cultivars with higher levels of these specific mineral nutrients using biofortification methods (Rai *et al.*, 2015).

Biofortification is regarded as the most cost-effective and sustainable approach for improving the Fe and Zn content in staple foods (Velu *et al.*, 2007). It is defined as the process of increasing the concentration and/or bioavailability of essential micronutrients in the edible part of a plant by traditional plant breeding or genetic engineering (White and Broadley, 2005). For pearl millet, most biofortification efforts at International Crops Research Institute for the Semi-Arid Tropics (ICRISAT) under the HarvestPlus programme (www.harvestplus.org) have been achieved using traditional plant breeding approaches which exploit the large genetic variability available within the pearl millet germplasm. In recent evaluations of an Indian collection of pearl millet landraces, significant variability in grain Fe (51-121 mg/kg) and Zn (46-87 mg/kg) content were found with positive correlation (Rai *et al.*, 2015; Upadhyaya *et al.*, 2016). Selected candidates within this group could therefore serve as valuable genetic resources for breeding the high Fe and Zn trait into other elite pearl millet lines.

However, in any attempt to increase the Fe and Zn concentration in pearl millet, it is important to have a thorough understanding of how these minerals may be distributed and stored within the grain tissues. This knowledge is particularly valuable because pearl millet is often consumed decorticated, and therefore it is vital that an increased concentration of essential minerals is not only limited to the bran layers, but is also evident within the bulk of the starchy endosperm. In the present study, micro proton induced X-ray emission (micro-PIXE) was utilised to carry out elemental mapping of Fe and Zn in the grain tissues of two contrasting pearl millet varieties. One variety, known as Dhanashakti, is a high Fe/Zn variety that was developed by the HarvestPlus programme. The other variety, ICMB 92111 serves as a control, and has moderate Fe and Zn levels. Micro-PIXE mapping of elements in the grains of these two contrasting varieties can provide valuable information about the spatial distribution of key mineral nutrients that are present within pearl millet grains.

7.2 Materials and methods

7.2.1 Plant material

Mature, dried pearl millet grains of two varieties, namely Dhanashakti and ICMB 92111, were kindly supplied by the International Crops Research Institute for the Semi-Arid Tropics (ICRISAT). Both varieties were grown according to standard cultivation methods at the ICRISAT facility in India, and hand-harvested in 2014. The cultivars were selected for this particular study because of their prominent role in the biofortification programme of HarvestPlus.

7.2.2 Analysis of the bulk mineral content

Grain samples (~3 g) of each variety were rinsed thoroughly with milli-Q water to remove surface contaminants before being ground to a fine powder using liquid nitrogen. The resultant flour was then allowed to freeze-dry to a constant weight, before nitric-perchloric acid digestion, and bulk mineral content analysis by inductively coupled plasma-mass spectrometry (ICP-MS Laboratory, Central Analytical Facility, Stellenbosch University). For each variety, two independent determinations of the iron (Fe) and zinc (Zn) content were made and reported as the mean \pm standard deviation.

7.2.3 Sample preparation for micro-PIXE analysis

A minimum of three seed specimens for each variety were prepared. The selected seeds were embedded in EpoFix™ (Struers) commercial resin and longitudinally sectioned through the median using a rotating diamond-coated blade, operated at a low speed (~100 rpm), which cleanly sectioned the specimens in half. Photomicrographs were then made of each half-seed using a Nikon SMZ1500 stereomicroscope fitted with a digital camera. The specimens determined to have the best preserved morphology of the seed were then subjected to a light coating of carbon, before micro-PIXE analysis.

7.2.4 Micro-PIXE analysis

The distribution and concentration of Fe, Zn and other nutritionally important elements in the seed of pearl millet was determined using the nuclear microprobe facility, situated at the Materials Research Department (MRD), iThemba LABS. A proton beam of 3.0 MeV energy with a current of 100 pA was focused to a 3 x 3 μm^2 spot size and raster scanned over a 2 mm^2 area of the specimens, using a square area divided into 128 x 128 pixels and scanned with a dwell time of 10 ms per pixel. Samples were irradiated with a total accumulated charge of 1.6 to 3 μC . Both micro-PIXE and proton backscattering spectrometry (BS) were collected simultaneously in event-by-event mode. Micro-PIXE

spectra were recorded using a Si(Li) detector, whilst proton BS spectra were recorded using an annular Si surface barrier detector. From the micro-PIXE measurements, elemental distribution maps were generated using the Dynamic Analysis method of GeoPIXE II software package (Ryan, 2000). Additionally, micro-PIXE spectra were extracted from the bran and the endosperm regions of each sample to obtain average concentration values for particular mineral elements of interest (Figure 7.2). For data processing, each sample was treated as “infinitely thick”, and the main constituent of the biological matrix was assumed to be cellulose (Witowski *et al.*, 1997; Przybylowicz *et al.*, 1999). The concentrations of the elements in the different parts of the pearl millet seed were then presented as the mean \pm standard deviation of three representative measured samples. A statistical comparison of the means was performed using the Fisher’s least square difference (LSD) test available in the *Statistica* software package (Version 13.0, Statsoft Inc., USA). A significant difference between the means was accepted at $p < 0.05$.

7.3 Results and discussion

Bulk concentrations of P, S, Fe and Zn were determined in the ground wholegrain samples of the Dhanashakti and ICMB 92111 varieties using ICP-MS analysis. The results (Table 7.1) confirmed the comparatively high Fe and Zn contents of the Dhanashakti grain. In comparison to the levels found in ICMB 92111, Dhanashakti contained nearly three times the amount of Fe and, nearly two times the amount of Zn. The high iron content of Dhanashakti grain is particularly notable given that iron is reported to range from 29 to 73 mg/kg in wheat (Shahzad *et al.*, 2014); and from 4 to 24 mg/kg in brown rice (Laenoi *et al.*, 2015). Bulk concentrations of P and S were comparable for both pearl millet varieties. However, beyond establishing the bulk content, it is vital to determine if the high levels of iron and zinc found in Dhanashakti grain are also localised within the dominant edible part of the grain – the endosperm. It is suggested that more than 75 % of the nutrients located in seedy parts other than the endosperm can be lost after common post-harvest processing practices such as milling or polishing of the grains (Ozturk *et al.*, 2006). Accordingly, agencies involved in the mineral biofortification of cereal grains, typically aim to increase the concentration of iron and zinc within the grain endosperm to 8 and 30 mg/kg respectively (Shahzad *et al.*, 2014).

Table 7.1. Concentrations of the indicated minerals in wholegrain samples of two varieties of pearl millet. Data represents the mean \pm standard deviation (SD) of two representative samples.

Variety	Bulk mineral concentration (mg/kg on dry mass basis)			
	P	S	Fe	Zn
Dhanashakti	3640 \pm 46	1176 \pm 18	87.9 \pm 0.9	42.3 \pm 1.4
ICMB 92111	3685 \pm 14	1167 \pm 8	31.9 \pm 0.1	22.8 \pm 1.7

Routinely, conventional bulk chemical techniques are used to assess the mineral content of the various parts of a cereal grain, following fractionation by grain milling. However, the precision involved in this approach is greatly hampered by the possibility that individual fractions may be contaminated by others due to the destructive manner of the various mechanical and chemical processing steps at play (Pongrac *et al.*, 2013). Micro-PIXE can provide a quantitative approach to assess the concentrations and spatial distributions of minerals with grain tissues without chemical destruction or milling of the grain (Pongrac *et al.*, 2013). Hence, it was used within this study to interrogate more precisely the concentration levels of key mineral elements like Fe and Zn as found within the grain tissues, such as the endosperm and bran of pearl millet.

Micro-PIXE elemental distribution maps of P, S, Fe and Zn of both Dhanashakti and ICMB 92111 pearl millet grains are shown in Figure 7.3. The three major anatomical parts (i.e. the germ, bran and the endosperm) of the grain are pointed out in Figure 7.1. The elemental maps provided unique spatial information about the general pattern of mineral localisation within the grain tissues. Of note, elements tend to be most highly concentrated within the germ and the bran layers of the grain, which include the pericarp and aleurone, whilst the endosperm features the lowest concentration of mineral elements (Figure 7.3). It is the main interest of this study to evaluate the concentration of Fe and Zn within the endosperm tissue of the Dhanashakti and ICMB 92111 grains.

The results of the region selection analysis, as it pertained to concentrations of P, S, Fe and Zn are shown in Figure 7.4. In the bran (Figure 7.4 A), the average concentrations of P, S and Zn were not found to be significantly different between the two varieties. However, for Fe, the Dhanashakti grain was determined to have significantly higher Fe versus the ICMB 92111. In fact, the average Fe concentration of the Dhanashakti bran layer was more than three times higher than that of ICMB 92111. It is therefore evident

that the Dhanashakti variety has a superior capacity to accumulate Fe in the bran layers compared to ICMB 92111.

The elemental distribution in the endosperm was different compared to that of the bran (Figure 7.4 B). The first noticeable difference pertained to the absence of P concentration data, which could not be reported here due to the measurement being below the minimum detection limit. Minimum detection limits (MDLs) are calculated using the Currie equation (Currie 1968) during data processing of micro-PIXE spectra, and are defined as the concentration values that result in X-ray peak intensities that are discernible above the background threshold (Campbell *et al.*, 1995). Importantly, the MDL values are not absolute, and can be decreased by accumulating more counts in the spectrum, by virtue of longer irradiation times or an increased beam current (Campbell *et al.*, 1995). For the present study, operational constraints did not allow this particular concern to be addressed immediately. However, in future experiments, it would be advantageous to carry out the micro-PIXE measurements for longer irradiation periods. In the current study, the average accumulated charge for all measured samples was 2.2 μC . This is far below what was reported for micro-PIXE mapping of *Burkea africana* seeds (12.6 μC) (Witkowski *et al.*, 1997); but within the range of 200 nC to 3 μC stipulated for micro-PIXE mapping of soybean seeds (Malan *et al.*, 2012).

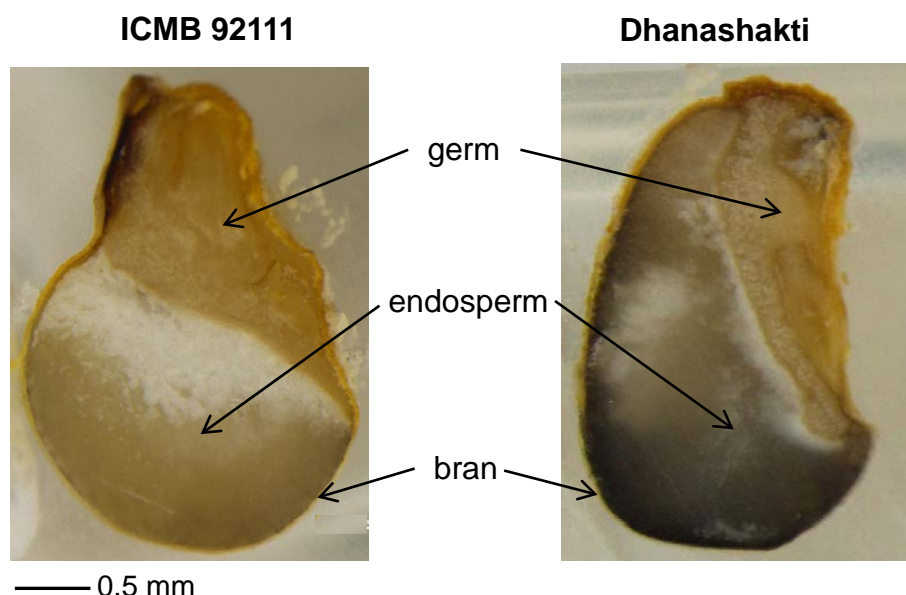


Figure 7.1. Optical micrographs showing the basic morphology of bi-sectioned pearl millet grains prepared for micro-PIXE analysis.

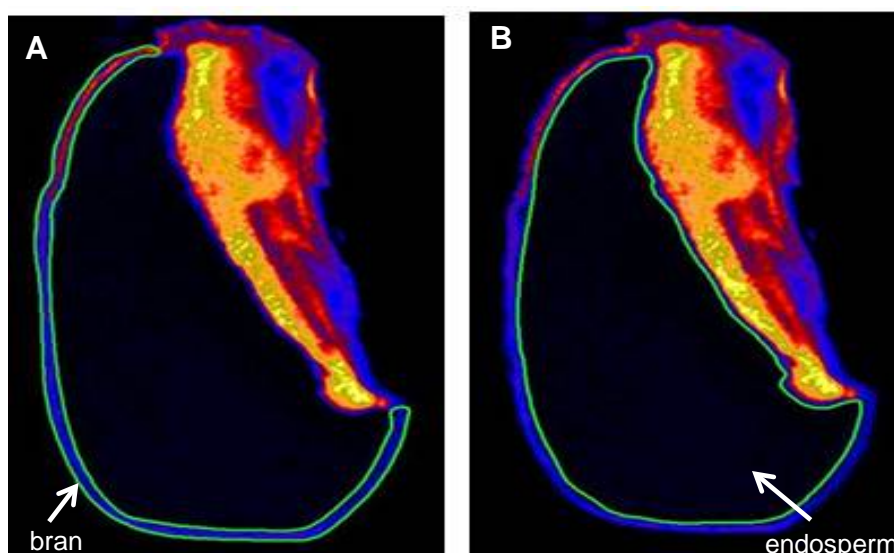


Figure 7.2. The areas encircled in green represent the regions chosen for region selection analysis using GeoPIXE software. In panel (A) the outer parts of the grain are encircled in green, to represent the bran region. This region notably includes the grain pericarp and the aleurone. In panel (B) as much of the inner core of the grain endosperm is encircled, to extract concentration data specific to the endosperm tissue.

Low P concentration in the grain endosperm has been previously reported. Other studies, focused on rice (Lombi *et al.*, 2009; Kyriacou *et al.*, 2014), wheat (Singh *et al.*, 2013; Regvar *et al.*, 2011) and finger millet (Kruger *et al.*, 2014), have similarly reported quite low levels of P specific to the grain endosperm. Moreover, in an earlier report involving the quantitative mapping of minerals in two other cultivars of pearl millet, levels of P above the minimum detection limit of micro-PIXE (i.e. 13 mg/kg), could not be established in the endosperm tissue of the ICMH 1201 cultivar (Minnis-Ndimba *et al.*, 2015)

From a nutritional point of view, low levels of P in the grain endosperm can be construed as a desirable trait, because of the association of P with phytic acid or phytate. In mature seeds, salts of phytic acid can account for 60 - 90% of the total P content (Nielsen *et al.*, 2013), contributing up to 1.5 % of the total seed dry weight (Bohn *et al.*, 2008). At physiologically relevant pH values (pH ~1.5 – 7), phytic acid is negatively charged and can strongly chelate mineral cations such as K, Mg, Ca, Fe, Zn and Mn (Nielsen *et al.*, 2013). The resultant mineral-phytate complex is an important survival stratagem for the seed, as it helps to preserve important nutrients until needed for germination, whilst safeguarding the surrounding tissues against possible metal toxicity stress (Kranmer and Colville, 2011).

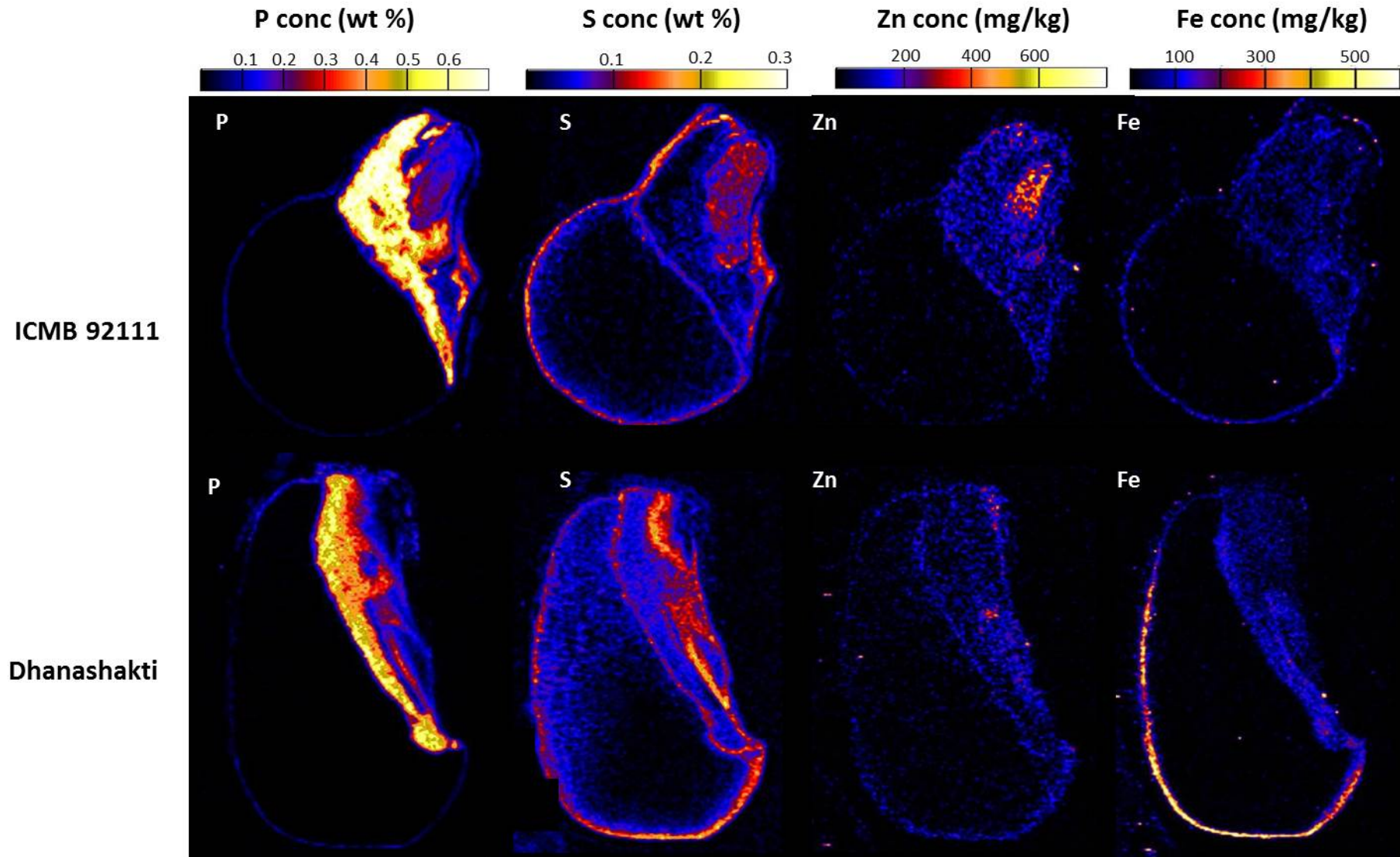


Figure 7.3. Micro-PIXE elemental maps of P, S, Zn and Fe distribution in pearl millet grain. Maps in the top row refer to the ICMB 92111 variety, whilst maps in the bottom row refer to the Dhanashakti variety. Colour scales above the maps indicate concentration values in % wt or mg/kg on a dry mass basis.

However, in the diet, phytate is generally construed as an anti-nutritional compound, because mineral nutrients bound within the insoluble phytate complex cannot be readily absorbed by the gut; and thus have limited bioavailability (Kryiaccou *et al.*, 2014; Nielsen *et al.*, 2013). In this study, the finding that P is highly concentrated in the bran but is below the limit of detection (13 mg/kg) in the endosperm, may lead to the speculation that Fe and Zn may be more bioavailable in the endosperm tissue. However, to confirm this hypothesis, further study investigating the bioavailability of Fe and Zn, resulting from the endosperm flour would be needed.

According to the statistical comparison of the average S, Fe and Zn concentrations in the endosperm of two varieties, a significant difference at $p < 0.05$ could only be established for Zn. The finding that the Dhanashakti endosperm featured a significantly higher average Zn concentration in comparison to the ICMB 92111 grain, is an important one, as it confirms that the intended result of breeding a higher density of this mineral into the most nutritionally relevant portion of the grain has succeeded. It is notable however, that the reported mean concentration of Zn in the endosperm of the Dhanashakti grain at 24 mg/kg is still below the cited biofortification target of 30 mg/kg Zn in the grain endosperm (Shazhad *et al.*, 2014). However, in the case of Fe, the Dhanashakti grain endosperm featured an average concentration of 12 mg/kg, which exceeds the cited biofortification target level of 8 mg/kg Fe in the grain endosperm (Shazhad *et al.*, 2014) by 50%. But nonetheless, this average value of 12 mg/kg Fe in the Dhanashakti endosperm was not determined to be statistically different from the average value of 5 mg/kg Fe found in the endosperm of the comparator variety, ICMB 92111. This is likely due to the relatively small sample size ($n=3$) used for the statistical comparisons.

As such, the results must be treated with caution, and need to be further verified with a larger number of sample replicates. However, as a preliminary study, some valuable information about the extent of the potential Fe and Zn enrichment of the bran and endosperm components of Dhanashakti grain have been highlighted.

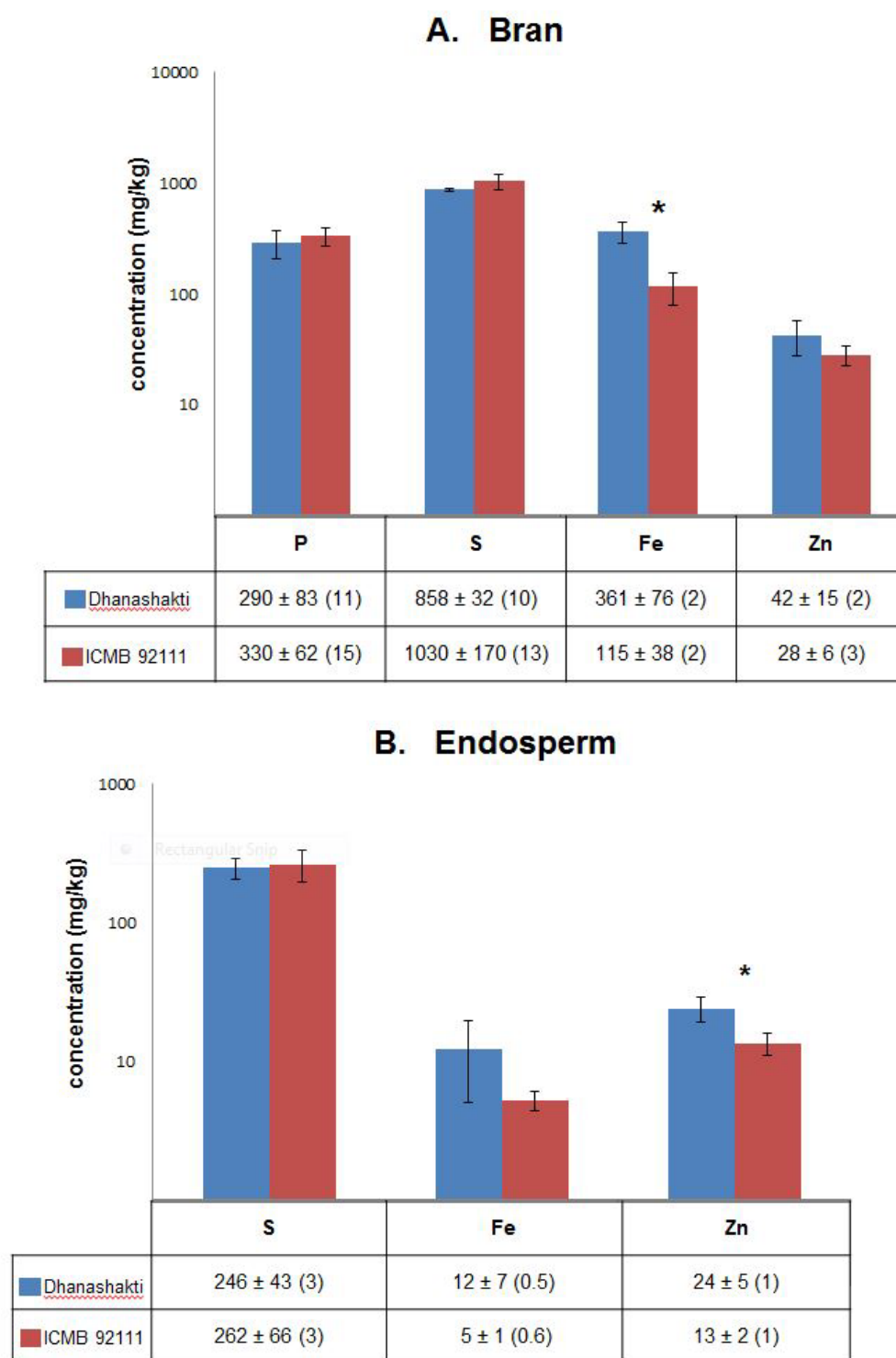


Figure 7.4. Mineral element concentrations derived from region selection analysis of micro-PIXE mapping data of the grain bran layers (A) and endosperm tissue (B) of two pearl millet varieties. Instances of significant statistical difference ($p < 0.05$) are marked with an asterisk. Results below the bar charts represent the mean concentration \pm SD, followed by the minimum detection limit in brackets. P was below the detection limit of the micro-PIXE analysis in the endosperm tissue.

7.4 Conclusion

This report provides important preliminary evidence that the bran and endosperm compartments of Dhanashakti grain are enriched to different extents in Fe and Zn in comparison to ICMB 92111. Of note, the Fe concentration in the bran layer of Dhanashakti was found to be significantly higher than that of the comparator variety ICMB 92111; whilst in the Dhanashakti endosperm tissue, Zn was determined to be significantly higher. The micro-PIXE technique along with region selection analysis, proved to be valuable for extracting information on tissue-specific concentrations of nutritionally important mineral elements such as P, S, Fe and Zn. However, more work is needed to validate these preliminary results and to investigate whether phytate or other ligating macromolecules may play a decisive role in the enhanced concentrations of Fe and Zn found in the various parts of the Dhanashakti pearl millet grain.

References

- Bohn L, Meyer AS, Rasmussen SK. 2008. Phytate: impact on environment and human nutrition. A challenge for molecular breeding. *Journal of Zhejiang University Science B* 9(3): 165-191.
- Cakmak I. 2008. Enrichment of cereal grains with zinc: agronomic or genetic biofortification? *Plant Soil* 302:1-17.
- Campbell JL, Teesdale WJ, Halden NM. 1995. Theory, practice and application of micro-PIXE analysis and element-distribution maps. *The Canadian Mineralogist* 33: 279-292.
- Currie LA. 1968. Limits for qualitative detection and quantitative determination: application to radiochemistry. *Analytical chemistry* 40: 586-593.
- Goudia BD, Hash CT. 2015. Breeding for high grain Fe and Zn levels in cereals. *International Journal of Innovation and Applied Studies* 12 (2): 342-354.
- Kranner I, Colville L. 2011. Metals and seeds: biochemical and molecular implications and their significance for seed germination. *Environmental and Experimental Botany* 72: 93-105.
- Kruger J, Pineda-Vargas CA, Minnis-Ndimba R, Taylor JRN. 2014. Visualisation of the distribution of minerals in red non-tannin finger millet using PIXE microanalysis. *Journal of Cereal Science* 60: 1-3.
- Kumara Charyulu D, Bantilan C, Rajalaxmi A, Rai KN, Yadav OP, Gupta SK, Singh NP and Moses Shyam D. 2014. Development and Diffusion of Pearl Millet Improved Cultivars in India: Impact on Growth and Yield Stability. Working Paper Series No. 52. Patancheru 502 324, Telangana, India: International Crops Research Institute for the Semi-Arid Tropics. 76 pp.
- Kyriacou B, Moore KL, Paterson D, de Jonge MD, Howard DL, Stangoulis J, Tester M, Lombi E, Johnson A. 2014. Localisation of iron in rice grain using synchrotron X-ray fluorescence microscopy and high resolution secondary ion mass spectrometry. *Journal of Cereal Science* 59: 173-180.

- Laenoi S, Phattarakul N, Jamjod S, Yimyam N, Dell B, Rerkasem B. 2015. Genotypic variation in adaptation to soil acidity in local upland rice varieties. *Plant Genetic Resources*. 13: 206-212.
- Lestienne I, Besancon P, Caporiccio B, Lullien-Pellerin V, Treche S. 2005. Iron and zinc in vitro availability in pearl millet flours (*Pennisetum glaucum*) with varying phytate, tannin and fiber contents. *Journal of Agricultural and Food Chemistry* 53: 3240-3247.
- Lombi E, Scheckel KG, Pallon J, Carey AM, Zhu YG, Meharg AA. 2009. Speciation and distribution of arsenic and localisation of nutrients in rice grains. *New Phytologist* 184: 193-201.
- Malan HL, Mesjasz-Przybylowicz J, Przybylowicz WJ, Farrant JM, Linder PW. 2012. Distribution patterns of the metal pollutants Cd and Ni in soybean seeds. *Nuclear Instruments and Methods in Physics Research B* 273: 157-160.
- Manwaring HR, Bligh HFJ, Yadav R. 2016. The challenges and opportunities associated with biofortification of pearl millet (*Pennisetum glaucum*) with elevated levels of grain iron and zinc. *Frontiers in Plant Science* 7: 1944, doi: 10.3389/fpls.2016.01944.
- Minnis-Ndimba R, Kruger J, Taylor JRN, Mtshali C, Pineda-Vargas C. 2015. Micro-PIXE mapping of mineral distribution in mature grain of two pearl millet cultivars. *Nuclear Instruments and Methods in Physics Research B* 363: 177-182.
- Nielsen A, Tetens I, Meyer AS. 2013. Potential of phytase-mediated iron release from cereal-based foods: a quantitative view. *Nutrients* 5: 3074-3098.
- Ozturk L, Yazici MA, Yucel C, *et al.*,. 2006. Concentration and localization of zinc during seed development and germination in wheat. *Physiologia Plantarum* 128:144–152.
- Pattanashetti SK, Upadhyaya HD, Dwivedi SL, Vetriventhan M, Narsimha Reddy K. 2016. *Pearl millet*. In: *Genetic and Genomic Resources for Grain Cereals Improvement* (eds. Singh, M. and Upadhyaya H.D.). Academic Press, Elsevier, USA, pp. 253-289. ISBN 978-0-12-802000-5.
- Pongrac P, Vogel-Mikus K, Jeromel L, Vavpetic P, Pelicon P, Kaulich B, Gianoncelli A, Eichert D, Regvar M, Kerft I. 2013. Spatially resolved distributions of the mineral elements in the grain of tartary buckwheat (*Fagopyrum tataricum*). *Food Research International* 54: 125-131.
- Rai KN, Velu G, Govindaraj M, Upadhyaya HD, Rao AS, Shivade H, *et al.*,. 2015. India pearl millet germplasm as a valuable genetic resource for high grain iron and zinc densities. *Plant Genetic Resources* 13:75–82.
- Rawat N, Neelam K, Tiwari VK, Dhaliwal HS. 2013. Biofortification of cereals to overcome hidden hunger. *Plant Breeding* 132: 437-445.
- Regvar M, Eichert D, Kaulich B, Gianoncelli A, Pongrac P, Vogel-Mikus K, Kerft I. 2011. New insights in to globoids of protein storage vacuoles in wheat aleurone using synchrotron soft X-ray microscopy. *Journal of Experimental Botany* 62(11): 3929-3939.
- Ryan CG. 2000. Quantitative trace element imaging using PIXE and the nuclear microprobe. *Int. J. Imaging Syst Technol* 11 (4): 219-230.
- Shahzad Z, Rouached H, Rakha A. 2014. Combating mineral malnutrition through iron and zinc biofortification of cereals. *Comprehensive reviews in Food Science and Food Safety* 13(3): 329-346.

- Shivhare R, Lata C . 2017. Exploration of Genetic and Genomic Resources for Abiotic and Biotic Stress Tolerance in Pearl Millet. *Front. Plant Sci.* 7:2069. doi: 10.3389/fpls.2016.02069
- Singh SP, Vogel-Mikus K, Arcon I, Vavpetic P, Jeromel L, Pelicon P, Kumar J, Tuli R. 2013. Pattern of iron distribution in maternal and filial tissues in wheat grains with contrasting levels of iron. *Journal of Experimental Botany* 64(11): 3249-3260.
- Upadhyaya HD, Reddy KN, Ahmed MI, Kumar V, Gumma MK, Ramachandran S. 2016. Geographical distribution of traits and diversity in the world collection of pearl millet [*Pennisetum glaucum* (L.) R. Br., synonym: *Cenchrus americanus* (L.) Morrone] landraces conserved at the ICRISAT genebank. *Genetic Resources and Crop Evolution*. 01-17. ISSN 0925-9864.
- Vadez V, Hash T, Bidinger FR, Kholova J. 2012. Phenotyping pearl millet for adaptation to drought. *Frontiers in Physiology* 3: 386. doi: 10.2135/cropsci2010.06.0336
- Velu G, Rai KN, Muralidharan V, Kulkarni VN, Longvah T, Raveendran TS. 2007. Prospects of breeding biofortified pearl millet with high grain iron and zinc content. *Plant Breeding* 126: 182- 185.
- White PJ, Broadley MR. 2005. Biofortifying crops with essential mineral elements. *Trends in Plant Science* 10:586–593.
- Witkowski ETF, Weiersbye-Witkowski IM, Przybylowicz WJ, Mesjasz-Przybylowicz J. 1997. Nuclear microprobe studies of elemental distributions in dormant seeds of *Burkea africana*. *Nuclear Instruments and Methods in Physics Research B* 130: 381-387.

CHAPTER 8

Summary and Future Work

The work presented in this dissertation has brought new knowledge to the fore about some of the intended and unintended changes that may occur in food grains as a result of biofortification. Two important millets were used in the study: (1) pearl millet varieties involved in a mineral biofortification programme at ICRISAT; and (2) transgenic sorghum originally developed as part of the African Biofortified Sorghum project to produce protein-biofortified sorghum grains using RNAi technology to target the suppression of certain kafirins.

In this general discussion, a review of the main findings of this research will be made, alongside a critical examination of some of the experimental methodologies that have been applied. Lastly, an overview of some of the directions for future research efforts will be considered.

8.1 Biofortified Pearl Millet

In the case of the pearl millet grains, the aim of the research work was to provide important baseline data on mineral concentration and distribution patterns as found within the intact grain tissues. Using micro-PIXE analysis elemental maps were produced for the first time to document the distribution of several important minerals within the grain of two varieties of pearl millet. The distribution maps revealed that the predominant localisation of minerals was within the germ (consisting of the scutellum and embryo) and the outer grain layers (specifically the pericarp and aleurone); whilst the bulk of the endosperm tissue featured relatively low concentrations of the surveyed minerals. Within the germ, the scutellum was revealed as a major storage tissue for P and K, whilst Ca, Mn and Zn were more prominent within the embryo. Fe was revealed to have a distinctive distribution pattern, confined to the dorsal end of the scutellum; but was also highly concentrated in the outer grain layers. Interestingly, the hilar region was also revealed as a site of high accumulation of minerals, particularly for S, Ca, Mn, Fe and Zn, which may be part of a defensive strategy against infection or damage. Differences between the two cultivars, in terms of the bulk Fe and P content obtained via inductively coupled plasma optical emission spectrometry (ICP-OES), concurred with the average concentration data determined from the analysis of micro-PIXE spectra specifically extracted from the

endosperm tissue. These results have therefore been instructive for understanding in detail how minerals are differentially distributed throughout the grain tissues, and what may be the potential targets for future research efforts to boost the overall mineral content of pearl millet grains.

Due to the successful first run of micro-PIXE mapping of minerals in pearl millet grains (Chapter 6), a second investigation was devised to interrogate if mineral enrichment in biofortified pearl millet grains was targeted to most nutritionally relevant tissue, i.e. the endosperm (Chapter 7). The results obtained from the study clearly indicated that the mineral biofortified grains (Dhanashakti) exhibited enhanced levels of Zn in the endosperm, that was significantly increased in comparison to the normal variety (ICMB 92111). The results for Fe however, indicated that a significant increase in Fe concentration seemed to be mostly due to the bran portion of the grain. The statistical analysis of the results however was based on only 3 replicate samples for each variety; therefore it would be useful to repeat this analysis with several more grains to achieve more weighty statistical analyses. Unfortunately, constraints on access to the nuclear microprobe facility, did not allow for more samples measurements to be completed on this research material at the time. Therefore the minimum number of three replicates per variety had to be taken as the sample size. In future, it would be advisable to complete such analyses with a minimum of 5 replicates per variety, in order to produce more robust statistical comparisons of the differences in the mean concentrations found for key minerals such as Fe and Zn in the grain tissues. Nevertheless, the study has provided some important preliminary results which confirm the Fe/Zn biofortified status of the Dhanashakti variety of pearl millet.

8.2 Protein Biofortified Sorghum

The main objective of the research work presented on the transgenic biofortified sorghum, was to interrogate aspects of significant difference between the wild-type (WT) and the transgenic grains in order to reveal any unexpected changes that could potentially result from the genetic engineering process. Several important findings were made in this regard. In Chapter 3, a comparative study of several physico-biochemical traits of the grains revealed that the transgenic grains tended to be less dense and characterised by a prominent floury-type endosperm texture. Additionally, protein bodies of some of the transgenic lines had dramatically changed protein body morphologies which were suggestive of a high digestibility phenotype, described previously in other kafirin

suppressed mutant or transgenic lines (Da Silva *et al.*, 2011; Oria *et al.*, 2000). Importantly, a significant increase in lysine (of up to 50 %) was found in some of the lines, specifically lines 42-1, 44-2, 44-3 and 42-4; and these lines were also observed to have protein body morphologies that were most different to WT.

Using 1D SDS-PAGE the electrophoretic profile of the alcohol soluble proteins (kafirins) and other major protein fractions of the grain were studied. The separation of the alcohol soluble proteins on a 12% resolving gel provided some confirmatory evidence of the intended suppression of certain kafirins in the transgenic lines, but could not provide definitive information on the specific protein involved in the differential banding patterns observed. The electrophoretic pattern of sorghum kafirins by SDS-PAGE however is well documented in the literature (El Nour *et al.*, 1989) and is known to conform to a distinctive pattern that was also observed in the results presented in this study. The use of either 70 % ethanol or a 60 % tert butanol extracting solvent yielded similar results, with reduced band intensities in regions of the gel that most likely correspond to the kafirins targeted for suppression. Interestingly, the alcohol extracts also revealed an increased expression of some low molecular weight protein species in a number of the transgenic lines. From the literature, it is noted that an overexpression of low molecular weight alcohol soluble proteins was also present in other types of transgenic sorghum lines featuring kafirin suppression (Da Silva *et al.*, 2011). Due to limitations of time and project resources, it was not possible to submit some of these low molecular weight bands that were distinctly expressed in the transgenic lines for protein identification by mass spectrometry analysis. However, for future research it would be worthwhile to attempt to identify what these proteins are and if their expression in the transgenic grains warrant some concern from a nutritional point of view.

The fractionation of the major grain proteins into an albumin/globulin fraction, a kafirin fraction and a glutelin/residual fraction, followed by separation by 1D SDS-PAGE was insightful for providing some direct evidence of the compensatory biological response to kafirin suppression. Several protein bands upregulated in the transgenic lines relative to WT were excised from 1D gel and processed for protein identification using mass spectrometry. Some evidence of a protein identification for globulin was found, but was based only on 1 matching peptide and a relatively low MOWSE score. More convincing identities were found instead for certain chitinases, a 40S ribosomal protein, and enzymes likely involved in the metabolism of pyruvate, such as pyruvate phosphate dikinase and

glyceraldehyde-3 phosphate dehydrogenase. Additionally, some evidence of an upregulation of gamma kafirins was also detected, but unexpectedly not in the kafirin fraction, but in the glutelin/residual protein extracts. These results have been useful for pinpointing some of the possible changes in the overall protein profile for the transgenic grains in comparison to the WT. The upregulation of enzymes involved in pyruvate metabolism may be expected as pyruvate plays a central role in certain pathways of amino acid synthesis. The possibility that there may be an upregulation of some potentially allergenic proteins, in the form of the chitinases however may be a cause for concern. Future work is therefore needed to corroborate this initial finding and to characterise more precisely the expression levels of these particular proteins. The use of two-dimensional polyacrylamide gel electrophoresis (2D PAGE) would have been particularly helpful in this regard, and was attempted several times during the study period. All of the attempts however to obtain well resolved protein spots in a 2D PAGE format were not successful and had to be abandoned due to time and resource limitations. The reasons behind the unsuccessful 2D PAGE gel attempts are not known, but it may be due to a need to carry out extensive post-extraction clean-up of the protein extracts, to avoid interfering substances such as phenols and lipids which greatly hamper the successful resolution of well-defined protein spots by 2D PAGE.

In Chapter 4, the mineral profile of all of the transgenic lines was investigated using ICP-based analyses. Few significant differences were found in comparison to the WT, and all minerals were determined to be within the normal range of variation that is known for sorghum. At the level of bulk mineral concentrations, there was therefore no compelling evidence to support the view that the genetic intervention aimed at suppressing kafirins had a detrimental effect on the grain capacity to retain the normal levels of mineral nutrients. However, using micro-PIXE, a targeted analysis of mineral concentration levels in the peripheral endosperm tissue, revealed some significant changes in the potassium and zinc content – that may be related to the suppression of kafirins. Using micro-PIXE, it was evident that there was a significant decrease in K and Zn confined to the peripheral endosperm layer, where most kafirins are located. It is speculated that this change to the elemental composition of the grain, may lead to biological consequences that may negatively impact on the grain's ability to withstand various environmental stresses, such as weathering and pathogen attack. Further studies are therefore needed to test the survivability of the transgenic lines in comparison to the WT under field conditions.

As a means to probe the molecular mechanisms that may underpin many of the changes that were discussed above, an RNA-seq experiment was embarked upon, which sought to gather more evidence at the level of the transcriptome, of the changes that may arise in the transgenic samples in response to kafirin suppression. According to the results obtained from the RNA sequencing run a total of 1,742 genes were identified as differentially expressed between the transgenic samples and the WT. The vast majority of the differentially expressed genes (91%) were upregulated in the transgenic samples in comparison to WT, whilst the remaining 8% were downregulated. Importantly, the results gave a clear indication that the three kafirins that were targeted for silencing by RNAi were amongst those genes identified in the RNA-seq analysis as significantly downregulated in the transgenic grain (derived from line 44-3) in comparison to WT.

Continuing work on the results obtained from RNA-seq analysis will be of great benefit for unravelling in more depth what unexpected effects kafirin suppression may have had on the sorghum grain. However, based on the results obtained thus far in this study, it is clear that beyond the intended effect of reducing the expression of certain kafirins, there are a number of corollary changes in the grain composition, that may have improved grain lysine and protein digestibility, but may have also led to a softer, more vulnerable grain, that may be compromised in terms of its resistance to the stresses and strain found outside the temperature-controlled greenhouse environment. An important part of studying these transgenic grains in the future will therefore necessitate an evaluation of the performance of these transgenic plants and their grain quality characteristics under a variety of different field conditions, in much larger scale multiyear trials.

References

- Da Silva LS, Taylor J, Taylor JRN. 2011. Transgenic sorghum with altered kafirin synthesis: kafirin solubility, polymerisation and protein digestion. *Journal of Agricultural and Food Chemistry* 59: 9265-9270.
- El Nour INA, Peruffo ADB, Curioni A. 1998. Characterisation of sorghum kafirins in relation to their cross-linking behaviour. *Journal of Cereal Science* 28: 197 – 208.
- Oria MP, Hamaker BR, Axtell JD, Huang CP. 2000. A highly digestible sorghum mutant cultivar exhibits a unique folded structure of endosperm protein bodies. *Proceedings of the National Academy of Sciences* 97: 5065 – 5070.

APPENDIX A.

List of Peer-Reviewed published Research outputs produced during the study period.

- Ndimba R**, Kruger J, Mehlo L, Barnabas AD, Kossmann J, Ndimba BK. 2017. A comparative study of selected physical and biochemical traits of wild-type and transgenic sorghum to reveal differences relevant to grain quality. *Frontiers in Plant Science* 8:952. doi: 10.3389/fpls.2017.00952.
- Minnis-Ndimba R**, Kruger J, Taylor JRN, Mtshali C, Pineda-Vargas CA. 2015. Micro-PIXE mapping of mineral distribution in mature grain of two pearl millet cultivars. *Nuclear Instruments and Methods in Physics Research B* 363: 177-182.
- Ndimba R**, Grootboom AW, Mehlo L, Mkhonza NL, Kossmann J, Barnabas AD, Mtshali C, Pineda-Vargas C. 2015. Detecting changes in the nutritional value and elemental composition of transgenic sorghum grain. *Nuclear Instruments and Methods in Physics Research B* 363: 183-187.
- Ndimba R**, Cloete K, Mehlo L, Kossmann J, Mtshali C, Pineda-Vargas C. 2017. Using ICP and micro-PIXE to investigate possible differences in the mineral composition of genetically modified versus wild-type sorghum grain. *Nuclear Instruments and Methods in Physics Research B* 404: 121-124.
- Kruger J, Pineda-Vargas CA, **Minnis-Ndimba R**, Taylor JRN. 2014. Visualisation of the distribution of minerals in red non-tannin finger millet using PIXE microanalysis. *Journal of Cereal Science* 60: 1-3.
- Kruger J, **Minnis-Ndimba R**, Mtshali C, Minnaar A. 2015. Novel in situ evaluation of the role minerals play in the development of the hard-to-cook (HTC) defect of cowpeas and its effect on the in vitro mineral bioaccessibility. *Food Chemistry* 174: 365-371.
- Mbambo Z, **Minnis-Ndimba R**, Pineda C, Ndimba B, Bado S, Lin J, Chikwamba R, Mehlo L. 2014. Proton-induced X-ray emission and electron microscopy analysis of induced mutants of sorghum. In: Tomlekova N, Kozgar I, Wani R (Eds.) *Mutagenesis: exploring novel genes and pathways*. Wageningen Academic Publishers, Netherlands, pp 181-196.

APPENDIX B.

RNA-seq list of differentially expressed genes

Gene ID	Total counts	P-value (Mut vs. WT)	FDR step up (Mut vs. WT)	Ratio (Mut vs. WT)	Fold change (Mut vs. WT)	LSMean(Mut) (Mut vs. WT)	LSMean(WT) (Mut vs. WT)
Sb0010s016100	25.117580831050873E0	0.00106302910888065E0	0.023050654614317753E0	4.742456978798265E0	4.742456978798265E0	6.914522647857666E0	1.4580042958259583E0
Sb0010s021250	228.078008078125E0	3.278974852629816E-4	0.014916355761841811E0	3.0776301708416742E0	3.0776301708416742E0	57.37953567504882E0	18.444064585367836E0
Sb0012s012030	202.82690642042363E0	9.1007253219752954E-4	0.02193075290519822E0	2.55226498959203455E0	2.55226498959203455E0	48.57632097225156E0	19.032636642456055E0
Sb016s002040	8802.87841796875E0	4.766340982256347E-4	0.01694804189458247E0	24.93179583971427E0	24.93179583971427E0	2821.1335899297134E0	113.1542460123701E0
Sb0019s004610	216.93977165222168E0	6.193985723368349E-4	0.019104004967157005E0	2.6461551659255194E0	2.6461551659255194E0	52.48051452636719E0	19.83274269104004E0
Sb0067s000240	65.88489633798599E0	0.003871977119973E-4	0.02072016687845007E0	7.318513424983208E0	7.318513424983208E0	19.32154115041097E0	2.6400939072251026E0
Sb0073s0002050	35.36554005445566E0	0.005436499411972616E0	0.04739201088590727E0	9.292033246765785E0	9.292033246765785E0	36.321587244669894E0	3.007249632472636E0
Sb0088s0002010	445.07161172646484E0	0.0043893963951404E0	0.042701297447410864E0	2.378458868566252E0	2.378458868566252E0	104.44451904296874E0	43.91268866585286E0
Sb019g000240	278.71016120910645E0	0.004273493617485664E0	0.04222886452339475E0	2.3725962405637597E0	2.3725962405637597E0	65.35683822631836E0	27.54654884338379E0
Sb019g000510	101.1072473526001E0	1.7315975014506316E-4	0.01212822798451459E0	1.9031862822149143E0	1.9031862822149143E0	-5.254346404999343E0	5.388639132181801E0
Sb019g001140	60.36240315437317E0	9.006932955975566E-5	0.0107255905742378E0	5.797342810909748E0	5.797342810909748E0	17.16070302127474E0	2.9600980281829834E0
Sb019g001180	264.46488094329834E0	0.0038917729583037024	0.04042285842247165E0	6.005243230603046E0	6.005243230603046E0	75.5708204905192E0	12.584139823913574E0
Sb019g001200	123.35409307479858E0	0.00548100321095226E0	0.04749759604882219E0	4.462740391239755E0	4.462740391239755E0	33.591033935546875E0	7.526997089385986E0
Sb019g001220	119.51805591583252E0	0.0022217848599616692	0.031249316583516E0	5.24369253970323E0	5.24369253970323E0	33.45861625671386E0	6.380735715230031E0
Sb019g001270	101.01144647598267E0	3.240754042999804E-4	0.014916355761841811E0	3.41588706214555E0	3.41588706214555E0	26.4587072790853E0	7.624851385752361E0
Sb019g001320	13.929219245910645E0	0.004771625231560794E0	0.04433454132575016E0	5.2015286807292345E0	5.2015286807292345E0	8.8943749268849692E0	1.7446981550852456E0
Sb019g001390	63.23318529129208E0	6.903109809054794E-4	0.0196111419318368392E0	3.485988778194774E0	3.485988778194774E0	16.379158291585285E0	4.6985691388448085E0
Sb019g001510	151.15742426515781E0	0.005326932404870647E0	0.046900574361293045E0	5.282552355991949E0	5.282552355991949E0	36.321587244669894E0	14.06221064249676E0
Sb019g001700	173.37682628631592E0	0.002318868175733296E0	0.03174006343987432E0	4.2327195073091693E0	4.2327195073091693E0	-3.2625472898380413E0	10.60523733780924E0
Sb019g002020	128.0106258392334E0	6.994431976496187E-4	0.01965150311697767E0	3.1809866326910488E0	3.1809866326910488E0	32.46443376043945E0	10.202774943033855E0
Sb019g002200	270.0542583465576E0	7.837231506979965E-4	0.020436688291011625E0	2.5060596729562734E0	2.5060596729562734E0	64.34308497111002E0	25.67500114440918E0
Sb019g002430	140.1724655151367E0	8.62038053500214E-4	0.021535880788377284E0	3.0712893132010115E0	3.0712893132010115E0	352.475992385417E0	114.7648289983725E0
Sb019g002660	62.54165363117767E0	0.0034352716479081804	0.0220235941259937E0	2.4758095607388255E0	2.4758095607388255E0	14.84941579171377E0	5.998702098592123E0
Sb019g002810	255.88030815124512E0	9.75326654580615E-4	0.03820596526129930E0	2.5145592323261234E0	2.5145592323261234E0	61.02483945506976E0	24.88801099650063E0
Sb019g003110	29.357438802719116E0	0.0026913886652580035	0.03361883219102873E0	4.8973394064413815E0	4.8973394064413815E0	8.126452287038166E0	1.659360647201538E0
Sb019g003430	94.7341320514679E0	1.3972242004242595E-4	0.011896419993609695E0	4.226328702353129E0	4.226328702353129E0	25.53593571980794E0	6.0421082973480225E0
Sb019g003470	287.4103667190552E0	4.651282015651704E-5	0.0081633599330531E0	4.460676652244635E0	4.460676652244635E0	78.26048914591472E0	17.544533093770347E0
Sb019g003480	90.52388453483582E0	0.0010803125830732745	0.023214535655974575E0	3.217512252359843E0	3.217512252359843E0	23.20020641751302E0	7.154603560765858E0
Sb019g003570	194.84263515472124E0	3.305703392384375E-4	0.014916355761841811E0	3.3231105196982154E0	3.3231105196982154E0	49.92420832316081E0	10.60523733780924E0
Sb019g003640	203.23904418945312E0	0.00152237077476318010	0.026676389229457087E0	2.433018696257088E0	2.433018696257088E0	40.01259358723958E0	19.73324475911406E0
Sb019g003700	131.52421188354492E0	0.0019362962313643646	0.0297020942811662E0	2.3874730157831876E0	2.3874730157831876E0	39.89188995361328E0	12.94221496582031E0
Sb019g003900	455.9360771179199E0	1.4279416298363867E-4	0.011896419993609695E0	3.166697850426234E0	3.166697850426234E0	115.50470189124269E0	36.474613189697266E0
Sb019g004000	108.29667285104492E0	0.001564609390425545	0.0269339066025127E0	2.6127595628986593E0	2.6127595628986593E0	26.10683618969726E0	9.992054621378582E0
Sb019g004375	46.92156434059143E0	0.0017536124046215E-4	0.01580781689178915E0	3.693646004273762E0	3.693646004273762E0	12.30824597676595E0	3.332275470078585E0
Sb019g004480	151.17696762089496E0	3.069621996660931E-4	0.014847800502898957E0	3.6945852769162113E0	3.6945852769162113E0	39.65815327039493E0	10.73413721703777E0
Sb019g004670	48.03748750686645E0	0.0020625715275818606	0.03032552575715648E0	4.2527233581210515E0	4.2527233581210515E0	12.964077949523926E0	3.0484178660982265E0
Sb019g004730	565.2617454528809E0	0.0012797609697499206	0.02509693249886681E0	3.8745083994188412E0	3.8745083994188412E0	-2.6423511215766506E0	13.69099908040363E0
Sb019g004740	148.3809366219652E0	0.001684341378530672410	0.0280854585008088E0	2.45967349593587E0	2.45967349593587E0	15.16407521567552E0	14.2962336991882324E0
Sb019g005340	80.47859787940979E0	4.930512337856769E-4	0.017184449852419653E0	3.4300820101717452E0	3.4300820101717452E0	20.770736055853062E0	6.058623425333063E0
Sb019g005370	16.9125060815911E0	0.004899312382499417E0	0.04484189451296578E0	4.137730529109392E0	4.137730529109392E0	4.542521079381307E0	1.97429148380637E0
Sb019g005610	60.49242353439331E0	0.00150300988026665710	0.026611572667805452E0	2.7863756171389467E0	2.7863756171389467E0	14.93869457244873E0	5.325446606682375E0
Sb019g005680	57.24283170700073E0	0.002619953758212208E0	0.0324967958702172E0	3.6678470018957654E0	3.6678470018957654E0	14.993204116821289E0	10.0773978512289E0
Sb019g005780	53.074999040094E0	7.946103386324851E-4	0.0206795233948859E0	4.079215875802586E0	4.079215875802586E0	14.208517233503682E0	3.48314913113912E0
Sb019g005910	98.9554934501648E0	0.00114105457807536E0	0.02382071034709788E0	3.0498668672055531E0	3.0498668672055531E0	24.84041513180696E0	8.144791645812999E0
Sb019g006050	17.966015100479126E0	6.61070803884307E-4	0.019428283869416807E0	5.537365911432687E0	5.537365911432687E0	5.072603702545165E0	0.916067997614542E0
Sb019g006320	158.8673505783081E0	0.0025516281568444914	0.03308778383058782E0	2.262292826343325E0	2.262292826343325E0	36.7230949018555E0	16.23268585917153E0
Sb019g006480	474.9120979309082E0	6.68947999040912E-4	0.019428283869416807E0	2.6454493213135404E0	2.6454493213135404E0	14.87892401952056E0	43.251085917155E0
Sb019g006640	295.08331298828125E0	0.001774477206710426	0.028652293201569718E0	2.413437779725754E0	2.413437779725754E0	59.54525629679361E0	28.815848032633454E0
Sb019g007070	260.352201461792E0	0.002598512785708394E0	0.03314758396281515E0	2.08351467747362E0	2.08351467747362E0	59.36016691389976E0	27.04805056254068E0
Sb019g007170	73.13554573059082E0	3.768809093245538E-4	0.02002640620352137E0	3.3793390335952793E0	3.3793390335952793E0	18.811804135640465E0	5.566711107889812E0
Sb019g007420	217.94335481254467E0	4.376430379324736E-5	0.00812508446252593E0	0.6253525184019364E0	0.6253525184019364E0	31.993980616108502E0	12.76171376043294E0
Sb019g007430	19.73700749874115E0	4.085061853140777E-4	0.016260594395928054E0	6.060445123644772E0	6.060445123644772E0	5.647191206614177E0	0.931811292962066E0
Sb019g007520	157.05499070843262E0	0.002170130568388526	0.03091930079588447E0	2.4346112586952944E0	2.4346112586952944E0	37.10927510288822E0	15.242388407389324E0
Sb019g007570	44.0560188293457E0	0.001231649227940484	0.02458137914130859E0	3.4322571134282422E0	3.4322571134282422E0	11.37205269525146E0	3.312869042567557E0
Sb019g007610	110.96230363845825E0	5.07080997957363E-5	0.0081633599330531E0	6.4357189333418425E0	6.4357189333418425E0	32.01313429364583E0	4.97429145206913E0
Sb019g007740	81.26900243759155E0	0.004707316897111169E0	0.043919908192231606E0	2.2287489846544983E0	2.2287489846544983E0	18.6995239257125E0	8.300143553415835E0
Sb019g008150	101.2655463218689E0	0.001283260640066786E0	0.02512026650212972E0	2.738075444900242E0	2.738075444900242E0	24.72508557637532E0	9.030096530914357E0
Sb019g008210	80.02687919139846E0	0.0022540040976805694	0.031477263123627E0	2.512483871108195E0	2.512483871108195E0	-3.9801250527388445E0	21.319209410773506E0
Sb019g008220	219.88307094573975E0	0.0013031688565864554	0.025168839605047753E0	2.594354516001724E0	2.594354516001724E0	52.9039077758789E0	20.90449206013434E0
Sb019g008740	51.27573323249817E0	0.003583921295705183	0.03884778925044758E0				

Sb01g014850	48.75502610206604E0	0.004063697543147797E0	0.041273633767159396E0	2.8995106766613055E0	2.8995106766613055E0	12.08405621846517E0	4.167619148890177E0
Sb01g015090	636.855167388916E0	0.001480117696777016E0	0.02645498630941633E0	2.434386871435259E0	2.434386871435259E0	4.743424275571613E0	61.811631520589177E0
Sb01g015510	34.564183592796326E0	0.004384704902091037E0	0.04270129744410864E0	3.677049429932079E0	3.677049429932079E0	0.150085015055338E0	2.46338951573671E0
Sb01g015770	154.39320659637445E0	0.00172900810310616781E0	0.0283995454354556E0	2.74389780174685E0	2.74389780174685E0	37.71819365419922E0	13.746209144592285E0
Sb01g017120	103.01261363861084E0	0.0049343494344523675E0	0.0450127572860556E0	2.3954551842349776E0	2.3954551842349776E0	24.29667675781246E0	10.13682030755959E0
Sb01g017160	61.149128675460815E0	5.255626561680117E-5	0.00816335908330531E0	5.728192931466057E0	5.728192931466057E0	17.353545506795246E0	3.0294973850250244E0
Sb01g017770	147.5172285003662E0	6.198424601558098E-4	0.019104004967157005E0	2.8484960704797957E0	2.8484960704797957E0	36.4086977640797957E0	12.781728519266766E0
Sb01g018190	201.212149635069615E0	4.0180976849930426E-4	0.016083645915520358E0	0.354713374667145137E0	0.354713374667145137E0	-2.819177599202779E0	49.50915654500325E0
Sb01g018430	2299.269302368166E0	0.002645864046122235E0	0.033253647510190616E0	0.391147060703776E0	-2.564025088577345E0	155.5016255669607E0	550.9179382324219E0
Sb01g018450	660.6331596374512E0	0.0014336657246770822E0	0.026054287142056428E0	2.3826881453924647E0	2.3826881453924647E0	155.11162821451822E0	65.09942499796549E0
Sb01g019130	92.85544061660767E0	1.9051681583496624E-4	0.012265348051354766E0	3.6972883198102826E0	3.6972883198102826E0	24.36251958211263E0	6.589293669756592E0
Sb01g019210	82.06289482116699E0	0.0026977321041708247	0.0336444770050523E0	3.960279461645916E0	3.960279461645916E0	20.86995182802932E0	6.36734945719402E0
Sb01g019280	2117.6682739257812E0	5.211366403147301E-4	0.01756379693626165E0	3.2859261192707443E0	3.2859261192707443E0	54.1.900329589844E0	164.69939168294275E0
Sb01g019310	56.479576587677E0	0.0029809169454630643	0.03534265831372578E0	2.797383701088464E0	2.797383701088464E0	13.86876328786214E0	4.957762241363525E0
Sb01g019320	176.87221813201094E0	8.867499229557432E-4	0.021794018774009933E0	2.5479902488022343E0	2.5479902488022343E0	42.34027862548828E0	16.617127418518066E0
Sb01g019330	082.066490111023E0	0.0019596864690119026	0.029848452180022362E0	2.50416698053252E0	2.50416698053252E0	19.534678141276043E0	7.800868829091391E0
Sb01g019490	203.57136726379395E0	0.002181511902089323E0	0.03098787781397259E0	2.226539086444957E0	2.226539086444957E0	46.82619094848633E0	21.03093147277832E0
Sb01g019610	503.0979461669922E0	0.0014384353126135766	0.02605823730090818E0	2.417628797106686E0	2.417628797106686E0	18.63040669759113E0	49.0689069140625E0
Sb01g019910	19.349443435668945E0	0.0028797181653144543	0.03485476596757248E0	15.87250386132303E0	15.87250386132303E0	6.067546705404917E0	0.382275371513977E0
Sb01g019920	24.69467538591598E0	0.0017845649163103845	0.028733944855430625E0	5.176292273569971E0	5.176292273569971E0	6.898791472111055E0	1.362766989868928E0
Sb01g020150	95.00502109527586E0	0.003315574008974332E0	0.03737190672160142E0	2.263091847794987E0	2.263091847794987E0	21.96332995068422E0	9.705010414123535E0
Sb01g020230	76.49966325296631E0	2.080372082747677E-4	0.01246740873140653E0	3.485615541615591E0	3.485615541615591E0	19.815074284871418E0	5.684813499450684E0
Sb01g020340	25.07966928482056E0	3.72319114015389045E-4	0.01565947301784307E0	0.22136081382898424E0	0.22136081382898424E0	-4.517511308228948E0	28.732887585957844E0
Sb01g020950	18.952620714904885E0	0.00169725045780213974	0.028128845621104333E0	4.943578411688063E0	4.943578411688063E0	5.2546216646803235E0	1.0629185736179352E0
Sb01g021140	13.29550766942878E0	0.0029729573047338974	0.03514679807806233E0	6.835080868967175E0	6.835080868967175E0	6.368508958692442E0	0.7467463811363208E0
Sb01g021760	131.2980718612671E0	0.0013499053409633543	0.025482361059929105E0	2.922380063725709E0	2.922380063725709E0	32.60799662272135E0	11.58027331034344E0
Sb01g021890	443.8591728210449E0	1.78233940045773E-4	0.012265348501354766E0	3.0373926237815168E0	3.0373926237815168E0	111.30736287434894E0	36.645694732666016E0
Sb01g021970	74.09375E0	0.002724643728117807E0	0.03376856797467776E0	3.00999110289335E0	3.00999110289335E0	16.538821538289387E0	6.150995128372729E0
Sb01g022040	70.080389213562E0	3.670247471510805E-4	0.019263301080138164E0	3.1445444758273973E0	3.1445444758273973E0	17.7257080078125E0	15.66971632639568E0
Sb01g022180	123.49194420570068E0	0.0024172155098336383	0.03234270565123847E0	6.2901339780256803E0	6.2901339780256803E0	30.00835474650063E0	11.155145327520164E0
Sb01g023290	22.42775058746338E0	0.005185944648504193E0	0.0460865346462992E0	2.54392360959233E0	2.54392360959233E0	52.9822654724121E0	20.62984724309092E0
Sb01g025210	136.50605535507202E0	0.005860808085320155E0	0.049085966435653584E0	2.761894229911611E0	2.761894229911611E0	33.40651130672695E0	12.09507144927979E0
Sb01g026190	213.92118191719055E0	7.839276371163432E-5	0.009932416156830517E0	8.573626064807266E0	8.573626064807266E0	63.85877927144367E0	7.448281367619828E0
Sb01g026390	34.993316039443016E0	1.1648270340879895E-4	0.011418140219586082E0	11.637678895373922E0	11.637678895373922E0	10.741449679054014E0	0.9229989858437995E0
Sb01g026455	12.86195595562458E0	0.003109511374038168E0	0.036125949215451564E0	5.5234574505566147E0	5.5234574505566147E0	6.363010295232137E0	0.8572156995534897E0
Sb01g026830	83.24203681945801E0	0.0024491781605769004	0.0325283995903545E0	3.2045778304932653E0	3.2045778304932653E0	21.14802718695063E0	6.599317869580619E0
Sb01g027330	59.812167286872864E0	4.1240674831058816E-5	0.007945053016772329E0	11.023325150133756E0	11.023325150133756E0	18.27916320164983E0	1.6582258939743042E0
Sb01g027420	1327.363334655761E0	0.0054689478305078034E0	0.0474509419026321E0	4.02269399171995836E0	4.02269399171995836E0	-2.3657776537843866E0	30.91967196289060E0
Sb01g027540	198.6701144958499E0	0.004469644750233663E0	0.04294673073604734E0	2.166223653008171E0	2.166223653008171E0	45.13815927083333E0	10.20160855116654E0
Sb01g027600	117.57634925842285E0	0.003973420709404992E0	0.04082382114519792E0	2.45118867624317E0	2.45118867624317E0	27.83599535624186E0	11.356112106322202E0
Sb01g027730	115.82377481460571E0	0.0036109697042094793	0.03978826129270356E0	2.6835329060041953E0	2.6835329060041953E0	28.1267302323291E0	22.6835329060041953E0
Sb01g027760	75.8057876586941E0	0.0037430610215029563	0.0397978735089780E0	2.8587475329908676E0	2.8587475329908676E0	18.7362025777311E0	6.55399046183266E0
Sb01g027800	101.70735359191895E0	0.001681765217578907	0.02808545800808685E0	2.5335512107017597E0	2.5335512107017597E0	24.30800946553458E0	9.594441731770832E0
Sb01g027900	116.5953016281128E0	0.0029044502368899792	0.03493652683935844E0	2.502046404572163E0	2.502046404572163E0	27.767274856567383E0	11.097825686136883E0
Sb01g028085	225.2788810729998E0	0.0059543726099452075	0.0494056289130288E0	0.3567797160537969E0	0.3567797160537969E0	-2.80248499239267557E0	12.66747532848697E0
Sb01g028220	155.83710289001465E0	0.00397645345323158E0	0.04082382114519792E0	2.287924360879411E0	2.287924360879411E0	36.14676662597656E0	15.798934300740562E0
Sb01g028395	330.0967960537666E0	0.002564765134948914E0	0.03314759356288151E0	2.5509162631223417E0	2.5509162631223417E0	79.04525883992513E0	30.98700650370406E0
Sb01g028470	54.1024121455078E0	3.8115229461378904E-4	0.015746746267701945E0	0.353382781274793E0	0.353382781274793E0	-2.829788679585627E0	133.2522557576497E0
Sb01g028510	33.39925169944703E0	0.00271212576453998E0	0.033759823323411424E0	3.0233511939135838E0	3.0233511939135838E0	8.365996796875E0	2.76117102948078E0
Sb01g028690	158.873099327687E0	0.001514741410006162E0	0.026624421585471E0	2.69811807244626E0	2.69811807244626E0	38.637524460969593E0	12.320175488789879E0
Sb01g028700	67.168194890022228E0	6.062524881469115E-4	0.018888363178348537E0	7.1045044705276945E0	7.1045044705276945E0	19.626811345418293E0	2.762586951255799E0
Sb01g028760	47.96131467819181E0	3.193819537865419E-4	0.014849533042052694E0	5.2578484751069245E0	5.2578484751069245E0	13.43237625789389E0	2.5547286669413243E0
Sb01g029030	109.61424636840802E0	0.001057555477640161E0	0.02296726254505687E0	3.0926109947400136E0	3.0926109947400136E0	6.102625096028648E0	8.9278170277409E0
Sb01g029040	232.9270429611206E0	4.14168073775548E-4	0.016384236759404063E0	4.921679044184064E0	4.921679044184064E0	64.53080495198567E0	13.11154207171219E0
Sb01g029120	324.1890525817871E0	0.0014786843895116888	0.02645498630941633E0	2.6701865254519643E0	2.6701865254519643E0	78.61955006917317E0	29.444364758089195E0
Sb01g029180	159.54188246440094E0	3.7161071862009364E-4	0.01565947301784307E0	3.108656050968006E0	3.108656050968006E0	40.263907026570638E0	12.943525950113933E0
Sb01g029270	61.68790817260742E0	0.0013498858202281151	0.025482361059929105E0	3.102781415351844E0	3.102781415351844E0	5.550758997599281E0	5.011877059936523E0
Sb01g029400	20.048746588545947E0	8.528585630190442E-4	0.021456600115391095E0	4.9538806252094005E0	4.9538806252094005E0	15.600468514760335E0	1.1224470138549806E0
Sb01g029590	60.27552103996271E0	2.1124423647399297E-4	0.01247388487278447E0	3.1111602852920766E0	3.1111602852920766E0	5.827014729504395E0	4.264732917194962E0
Sb01g029740	91.56420953252905E0	0.00249013217339369E0	0.03267262838993149E0	3.014760389982714E0	3.014760389982714E0	9.91912587483724E0	7.602304299672445E0
Sb01g029960	14.647209376096725E0	0.0059510033339923965E0	0.0476445713515444E0	4.403837886619643E0	4.403837886619643E0	22.978956384165444E0	0.903506586940304E0
Sb01g030050	23.442742824554443E0	0.00327268960633805E0	0.0319834505869979E0	3.468282669827114E0	3.468282669827114E0	6.06542189915975E0	1.7488257090255065E0
Sb01g030140	49.60815778315369E0	3.0389120382586932E-5	0.00748725052184712E0	8.99612135203034E0	8.99612135203034E0	14.8818057378133E0	1.654246868512427E0
Sb01g030345	1609.554761645508E0	6.756138406011912E-4	0.01945				

Sb01g036930	50.07446336746216E	0.004663336548933003E	0.043731447581215444E	2.5141896933889787E	2.5141896933889787E	11.941747665405273E	4.749740123748779E
Sb01g037300	145.73885107004050E	0.003063913258095053E	0.03588485001526081E	2.512530587457197E	2.512530587457197E	34.74924151102702E	13.30375512441002E
Sb01g037420	517.49860600061035E	0.00566273595753347E	0.0482327831843357E	2.3753509761172396E	2.3753509761172396E	121.39387512207031E	51.10565821329753E
Sb01g037440	463.54052733735E	0.00418523645651131E	0.041898711394925033E	2.142412122039027E	2.142412122039027E	105.34315745035806E	49.17035166422526E
Sb01g037450	176.0407846661379E	0.00381265069800404E	0.040060697542439E	2.449111071104486E	2.449111071104486E	30.168787638346E	16.04732774708852E
Sb01g037483	77.35887205600739E	1.0415764148770346E-4	0.011303471493304145E	5.128889764924403E	5.128889764924403E	21.578955968221027E	4.207334717114765E
Sb01g037720	24.61118194460869E	0.00229884195434999E	0.031648173510648143E	6.44331749999786E	6.44331749999786E	6.75002113978068E	1.453706175088824E
Sb01g037860	47.9226247874756E	0.00183221700278973E	0.02918874767209445E	2.8498379029455365E	2.8498379029455365E	11.09697713978068E	3.89389762356247E
Sb01g037980	56.231077671051025E	0.00153255109599162E	0.02674011618572897E	3.297614726884258E	3.297614726884258E	14.382274945576984E	4.306147611440023E
Sb01g038035	23.706649124622345E	8.575119543522389E-4	0.01854807307542439E	6.88590338917601E	6.88590338917601E	6.90015117327373E	1.0026652016003924E
Sb01g038340	93.82516264915466E	2.0911765162670418E-4	0.012467408874140652E	4.317659447083822E	4.317659447083822E	25.393697102864586E	5.8813571135203055E
Sb01g038460	239.0623340606895E	4.7512704724322804E-4	0.0169480418948623E	3.5599189938001117E	3.5599189938001117E	62.21181742350261E	17.47562763387047E
Sb01g038590	157.8879966735839E	0.005735312577046129E	0.048466952528674855E	2.208295134629068E	2.208295134629068E	36.22518920984375E	16.404143015543617E
Sb01g038700	22.09657597541809E	0.0023137480073484574	0.03173076681862712E	5.491475538391838E	5.491475538391838E	6.230879545211792E	1.134645779927572E
Sb01g038750	33.8082733592987E	8.295509720076004E-4	0.0210930300450228E	4.443295183860315E	4.443295183860315E	9.14479744407998E	2.0581116278966274E
Sb01g039110	76.82169961929321E	5.695584195913483E-4	0.01825173323947533E	3.12896215367809E	3.12896215367809E	19.4053761184473E	6.20185708996338E
Sb01g039250	96.36227941513062E	1.8312831278882854E-4	0.01226534850135476E	3.920155455278669E	3.920155455278669E	25.92535636393229E	6.52840344111248E
Sb01g039350	377.766170501709E	0.003233958764117436	0.03737190672160142E	2.2309905226781E	2.2309905226781E	86.5342915852864E	39.08662767537444E
Sb01g039650	128.7828457061768E	0.00183221700278973E	0.03407057901466409E	2.865499223732053E	2.865499223732053E	29.86601511637369E	13.01660407165527E
Sb01g039680	130.9069869643384E	0.00100413377816753317	0.02281323538948012E	2.9978881066861827E	2.9978881066861827E	25.59316722884417E	8.537066564927166E
Sb01g039720	102.27234077453613E	0.00290884509793171E	0.034959963286319944E	2.547162768424E	2.547162768424E	24.8006248744121E	9.6107177734375E
Sb01g039800	1009.2639846801758E	0.004055474616478084E	0.04124749627270414E	2.198472064293505E	2.198472064293505E	231.23944091796872E	105.1818873067565E
Sb01g039900	411.42243576408905E	0.00577113019044646E	0.0486475810501756E	2.0142937212765139E	2.0142937212765139E	91.62349700927734E	45.51731491088867E
Sb01g039930	358.21648406825293E	0.0013416851261862607	0.02542406402643126E	2.303418723440182E	2.303418723440182E	83.25945790608725E	36.14603678385417E
Sb01g040090	137.7047056958203E	0.003321484206661670E	0.03737190672160142E	3.395196007531448E	3.395196007531448E	32.38200950225586E	13.5195568227539E
Sb01g040200	80.15233325858252E	0.0039599222827087785	0.040817760018177445E	2.397844507051091E	2.397844507051091E	18.854387601216638E	7.863056818644207E
Sb01g040260	85.96670866012573E	0.002033773803724737E	0.03024206831969458E	2.473076170211758E	2.473076170211758E	20.404794692993164E	8.25077486038208E
Sb01g040350	94.010746959587158E	0.00440678373191053E	0.04275250272651923E	2.444554925029464E	2.444554925029464E	9.097522414117206E	6.52840344111248E
Sb01g040400	80.958176612854E	1.996586230063474E-4	0.01232623069606228E	3.621075191951903E	3.621075191951903E	21.14627965291341E	5.839779218037924E
Sb01g040490	133.90784984827042E	0.004013891745798985E	0.041058348638129925E	0.265280824738106E	0.265280824738106E	3.76589594851093E	9.358444598213831E
Sb01g040530	188.08990573883057E	0.004922029606995498E	0.04497174110227983E	2.13636147442822E	2.13636147442822E	43.18707275390625E	19.50962492370605E
Sb01g040560	216.89088344573975E	1.1655251045167559E-5	0.00594840622694443E	3.75708459232023E	3.75708459232023E	63.665218353271484E	8.63174295308433E
Sb01g040620	23.759270429611206E	0.005607159681146546E	0.04810521191281655E	4.693506460710683E	4.693506460710683E	6.528741121292114E	1.391015688572828E
Sb01g040720	148.65438556481143E	0.002092473677371059E	0.030511682499624933E	6.933443228415111E	6.933443228415111E	3.252384322841511E	11.65263017018635E
Sb01g040970	415.8764419555664E	0.004290042212473528E	0.0422886452339475E	2.2503697453686793E	2.2503697453686793E	59.6763830442709E	42.64914194742839E
Sb01g041000	234.29564476013184E	7.1001421715152817E-4	0.019777980389772663E	3.2248179725912207E	3.2248179725912207E	95.6187836318164E	18.48565991719564E
Sb01g041190	14.112246803939342E	7.254068441056773E-4	0.01996610907015655E	12.94886101462359E	12.94886101462359E	4.366844534873961E	0.33723773310581784E
Sb01g041360	16.572978467288E	4.833698103039687E-4	0.01706540710266296E	11.244828866302804E	11.244828866302804E	5.0731704235076895E	0.4411558587352427E
Sb01g041640	537.751136779785E	0.00546459992163761E	0.04745094109263126E	2.188143053139911E	2.188143053139911E	123.0263068954752E	56.22407033119979E
Sb01g041650	544.65005874633379E	0.00184325101173488E	0.029207786698473128E	2.5418647765176994E	2.5418647765176994E	130.29170481363939E	51.258314768447301E
Sb01g041700	48.17676782608033E	0.0010292563994511047	0.022698036710760926E	3.671881212869022E	3.671881212869022E	67.1821565818786621E	3.437356778908023E
Sb01g041770	64.35864925384521E	9.09698919346734E-4	0.021930752925019822E	6.739158401693958E	6.739158401693958E	18.680891354878742E	2.771991972936238E
Sb01g041860	245.62390899658203E	0.0010247106104245042	0.022698036710760926E	2.4092319373354987E	2.4092319373354987E	56.690924218744E	24.01556650795258E
Sb01g041870	14.906561553478241E	0.005743673302311378E	0.044867605498446664E	4.3795747122898988E	4.3795747122898988E	3.8739000956217446E	1.094953755536687E
Sb01g042270	41.14985227584839E	9.795798855808775E-4	0.022308048921512414E	5.937647305570472E	5.937647305570472E	11.420813719431559E	2.2958037058512364E
Sb01g042290	85.43496131896973E	0.0027547705134472146	0.03402066381235834E	2.386922045903175E	2.386922045903175E	20.070001662012785E	8.408318837483723E
Sb01g042440	75.53598403903664E	6.836786274343198E-4	0.0195393517207846E	3.132815339248123E	3.132815339248123E	19.0862662698387E	6.092375119527182E
Sb01g042650	278.30882649633032E	0.00271892206972933E	0.04189871139492503E	2.149181095976506E	2.149181095976506E	63.311346689860024E	29.45826212565104E
Sb01g042750	400.5222856414258E	0.0012974413310071467	0.025168839850472753E	2.6476482938571153E	2.6476482938571153E	96.90648789390988E	36.00095771832033E
Sb01g042830	333.6643581390381E	9.3329802694420974E-4	0.022186681940138973E	2.4900754843392394E	2.4900754843392394E	79.35350308378986E	31.867921829223633E
Sb01g042850	26.92493712902069E	0.001799140590579277E	0.0288225497868102E	4.227839176251057E	4.227839176251057E	7.25821256637532E	1.7126764663117406E
Sb01g042910	67.69418835639954E	0.001765825618966605E	0.028642052321263104E	4.752771108160507E	4.752771108160507E	14.443526280050537E	4.12102031841288E
Sb01g042930	1005.3670272812748E	0.005829387525369482E	0.04894160200618674E	2.54581272013257E	2.54581272013257E	64.01020406087238E	94.51213636994922E
Sb01g042970	21.651091188192368E	2.400584897171474752E-4	0.01332135027666156E	5.98707552920954E	5.98707552920954E	6.5354302075472E	0.681683093306925E
Sb01g042980	137.23143768310547E	2.834195330902418E-4	0.01409127950520428E	3.7367888616249223E	3.7367888616249223E	36.86676915486656E	9.657138654548504E
Sb01g042990	188.4069588500171E	0.001987494833490934E	0.0493125773863397E	2.364856767453736E	2.364856767453736E	44.13813145955404E	18.68418607118324E
Sb01g043020	5057.2801513671875E	5.611754232524719E-4	0.018251783239475343E	5.203484466746585E	5.203484466746585E	14.141059912109375E	271.74405924479174E
Sb01g043060	807.20597176416022E	0.0014156964585218406	0.02605428714205648E	3.257525136907906E	3.257525136907906E	30.8702850341797E	63.19837182750359E
Sb01g043130	50.94215214252472E	2.639216074379076E-4	0.01394885727499626E	1.1732560376826207E	1.1732560376826207E	2.507564890230563E	1.7321057148785596E
Sb01g043150	143.91556549072266E	0.0010230058428014749	0.022698036710760926E	2.933440156409252E	2.933440156409252E	37.57959202128093E	12.9993414293297E
Sb01g043240	158.0789966748047E	7.386266671530728E-4	0.020026040623052137E	3.971239173339397E	3.971239173339397E	45.06286944071452E	15.9542944843546E
Sb01g043370	67.3443454004137E	0.001981075948498915E	0.02989395492131055E	3.598433665739849E	3.598433665739849E	17.56642786618736E	4.88168728351593E
Sb01g043400	58.497273683454794E	1.5787925634559401E-4	0.01212822798451459E	4.392334116375045E</			

Sb01g049690	257.5482978820801E	0.003556172181159644E	0.038644639139750046E	2.130393115640313E	2.130393115640313E	58.42494328816731E	27.42448933919271E
Sb01g049760	48.9262351664623E	0.004285273497543326E	0.04228864352339475E	2.518306697849377E	2.518306697849377E	11.673346201578775E	4.675394970575968E
Sb01g049780	204.05599975589593E	0.0025992415166177065E	0.033147593662881515E	5.228588881895895E	5.228588881895895E	48.74221674601237E	19.276449832974086E
Sb01g049830	1024.6195793151855E	0.001868693319618223E	0.02929876485245603E	2.8266858198128753E	2.8266858198128753E	252.28712998908856E	89.252112987233988E
Sb01g049840	189.8098421096801E	0.002300636226816263E	0.031648173151064813E	2.4392951242010703E	2.4392951242010703E	44.87375122848388E	18.39619647465004E
Sb01g049870	472.59874534606934E	5.7040651782689685E-5	0.008671392701857825E	5.335597203486407E	5.335597203486407E	132.66818491617838E	24.86473019917804E
Sb01g050080	232.371083295956252E	0.003470594441931212E	0.03838740150644387E	3.0095202969869492E	-5.28431600284645E	21.95225429534912E	55.50477345784505E
Sb01g050140	54.273208114326904E	0.0010292441356004759E	0.022698036710760926E	0.3778324617687867E	0.3778324617687867E	1.654626846313475E	4.436444534128824E
Sb01g050280	179.5737599618652E	0.004336979263901113E	0.042451638922104365E	2.2543182007467792E	2.2543182007467792E	41.456232800754545E	18.389694849650063E
Sb01g050460	102.05020427703857E	1.728477486298405E-4	0.01212822798451459E	3.69863493673507E	3.69863493673507E	26.23241766357422E	7.784392992655437E
Sb01g050660	22.417230010032654E	0.004708558387018812E	0.043919908192231606E	3.1154671867893855E	3.1154671867893855E	5.6567206382751465E	1.6158893650690717E
Sb02g000660	122.57681560516357E	0.00138031025222777E	0.0256252123504372E	2.4615619252689873E	2.4615619252689873E	29.055325190226235E	11.803613344828289E
Sb02g000780	61.63781404495239E	2.5296634643877684E-4	0.013649281350587152E	3.66791686011918E	3.66791686011918E	16.144416173299156E	4.401521841684978E
Sb02g000810	120.07730388641357E	0.001423007491360581E	0.026054287142056428E	2.6708610808607824E	2.6708610808607824E	29.122122446695962E	10.30345515441895E
Sb02g000850	20.763809740543365E	0.001896510355287553E	0.029418181691495383E	4.193683983030631E	4.193683983030631E	5.588637826826904E	1.3326320846875515E
Sb02g000920	18.6578414412318E	0.0014576745900481765E	0.026234470896458997E	5.83926898412145E	5.83926898412145E	5.30993175506918E	0.909348716338471E
Sb02g000990	50.120282888412476E	0.001299215132779511E	0.025168839850472753E	3.4062054056306406E	3.4062054056306406E	12.915117263793945E	3.791643699010214E
Sb02g001375	14.693709909915924E	0.00459706067017979E	0.04350463316745757E	5.069257291363662E	5.069257291363662E	4.090901215871175E	0.807002047343133E
Sb02g001550	72.2962517595291E	0.0020119066850408955E	0.030075925628064654E	4.827233784380314E	4.827233784380314E	4.77530018488566E	0.9892415203197363E
Sb02g001640	148.25628185272217E	1.8707550298442037E-4	0.012265348501345766E	3.9295881653845366E	3.9295881653845366E	39.39833796183266E	10.024926821390789E
Sb02g002010	66.86009788513184E	8.834419417601825E-4	0.021794811707409933E	3.2672394714526436E	3.2672394714526436E	17.06393507006836E	5.222743988037109E
Sb02g002660	114.8198471069336E	0.001027859512621263E	0.022698036710760926E	2.568524326226062E	2.568524326226062E	27.5480416615804E	10.72524070739746E
Sb02g002860	16.73826131274484E	1.8045351443529052E-4	0.012265348501345766E	1.392379373239987E	1.392379373239987E	5.191755533218383E	0.3876649091641102E
Sb02g002910	113.23384666442871E	0.0012419890282624687E	0.030793785929447363E	3.609088002804004E	3.609088002804004E	29.55044354841473E	8.189172108968098E
Sb02g003020	45.4352607720510E	0.002514762547327701E	0.024891914832515674E	2.9429844097554207E	2.9429844097554207E	113.31151360515413E	38.501738230337375E
Sb02g003030	104.34831285476685E	0.0012476950149756323E	0.024797721507651995E	3.499818036077478E	3.499818036077478E	27.05295372009277E	7.729817231496174E
Sb02g003395	33.14774262905121E	0.002346447859448891E	0.03179925966671042E	4.062417459769287E	4.062417459769287E	8.866644541422525E	2.1826030015945435E
Sb02g003480	70.2209529876709E	0.005320186664464168E	0.04687143491688839E	2.3678169241842872E	2.3678169241842872E	16.456789334615074E	6.950194994608562E
Sb02g003650	37.489314794540405E	2.2128116071754322E-4	0.012750434592488277E	4.346926770521727E	4.346926770521727E	10.15931288401286E	2.337125380339443E
Sb02g003750	171.1024293899536E	0.0013377173986798474E	0.025407945526896654E	5.0103737914942466E	5.0103737914942466E	47.5448592586655E	9.489283879597977E
Sb02g003880	247.1656455936523E	0.004109878200810667E	0.04147610133445228E	1.326149876257987E	1.326149876257987E	56.08830174073892E	26.300247192382812E
Sb02g003990	423.98931884765625E	5.663849835664168E-4	0.018251783239475343E	7.344194369723676E	7.344194369723676E	103.4845937093099E	37.8451792399086E
Sb02g004100	223.1280479431523E	0.001984139146818851E	0.02990859536713226E	2.3366306405707693E	2.3366306405707693E	52.08526102701823E	22.29075495402108E
Sb02g004180	14.443753838539124E	0.005060862768944793E	0.04559882028261100E	4.793821134961287E	4.793821134961287E	3.98359855016072E	0.830986026856485E
Sb02g004230	35.2329950326416E	0.002433781160182361E	0.032386550374227295E	2.9736009097949603E	2.9736009097949603E	8.788742542266846E	2.955589135487875E
Sb02g004260	212.7785387091846E	6.603730749141445E-4	0.01942828386941287E	2.859961194940882E	2.859961194940882E	52.55135929232050E	18.3748264377793E
Sb02g004436	26.319968819618225E	2.170587644731239E-4	0.012660284844171813E	0.1380577139046804E	0.1380577139046804E	1.064291675885519E	7.70903126398723E
Sb02g004580	144.52570247650146E	6.206335572518611E-4	0.0191044003967157005E	3.2603557294063115E	3.2603557294063115E	36.867437998453774E	11.307796160380417E
Sb02g004590	712.704544067383E	3.187415876999032E-4	0.01484953200525694E	3.404922828607063E	3.404922828607063E	178.66871643066046E	58.5746837158203E
Sb02g004630	23.83465769697383E	8.124326100321969E-4	0.02084886879940746E	4.973053913292865E	4.973053913292865E	6.61476453145345E	1.330211358253659E
Sb02g004730	681.3999633789063E	7.33451029843822E-4	0.020026406230525137E	4.15175597311052E	4.15175597311052E	185.19365618351237E	41.93966929178376E
Sb02g004910	854.325393767578E	0.002651637981164004E	0.0326796858628784E	2.7045480816189233E	2.7045480816189233E	27.90337117513022E	76.87176005405547E
Sb02g004990	69.8490770156886E	0.004691714494088306E	0.0438436129554652E	4.42445547536658E	4.42445547536658E	18.02067756652832E	5.26234303495459E
Sb02g004993	84.71500372886658E	9.970485262688913E-6	0.05625147032420528E	1.625455510656781E	1.625455510656781E	24.2902730958957E	3.948061545688995E
Sb02g005120	28.441334307193756E	6.664370737712272E-4	0.01942828386941287E	4.85975964450759E	4.85975964450759E	8.0187611771050837E	1.46168361170750837E
Sb02g005150	214.939227104187E	3.2005992083959623E-4	0.0148495330252694E	3.235674774990934E	3.235674774990934E	54.73141606648763E	16.9149296824137E
Sb02g005580	73.39054107666016E	0.011468301293845E-4	0.019189549367125327E	3.2763504177906448E	3.2763504177906448E	18.742861429850258E	5.720652262369789E
Sb02g005920	181.82934379577637E	0.002668573054709247E	0.0341692558929398E	2.6897599047863263E	2.6897599047863263E	44.18329741517904E	16.4264839007975E
Sb02g006000	81.34437012672424E	0.004464773987276704E	0.04293541450618042E	3.3483521149139572E	3.3483521149139572E	20.87914276123047E	6.236644728101946E
Sb02g006010	140.40779876708984E	0.005865329893381406E	0.04910109207754786E	2.272125246079059E	2.272125246079059E	32.49917411804199E	14.303452470987957E
Sb02g006200	199.9442434310913E	6.02781020694015E-4	0.01888863178348532E	3.128002823766443E	3.128002823766443E	50.50272369847656E	16.14535744984949E
Sb02g006330	546.2652969360352E	0.004799026024020565E	0.0444565900798171E	2.1528524848565285E	2.1528524848565285E	124.33487559729167E	57.535525742005E
Sb02g006500	1012.5413360595829E	0.0032035661804150094E	0.026785802791592E	3.3316924883481227E	3.3316924883481227E	236.20977782603125E	101.3040058449219E
Sb02g007180	13.503082171082497E	0.00147304806649448E	0.0364586309419231E	3.324455763262089E	3.324455763262089E	4.01831551632089E	0.4827120751142502E
Sb02g007410	191.33359182121338E	0.002197878064127145E	0.031158410256424163E	3.110042208995111E	3.110042208995111E	48.25978215553482E	15.51740423832973E
Sb02g007480	3328.3048931640625E	0.003666587479352015E	0.03936554100671698E	2.940703371616275E	2.940703371616275E	82.82970781168619E	281.5321960449219E
Sb02g007830	61.98201560974121E	0.002455277247270514E	0.03252838959503445E	2.5834150579637E	2.5834150579637E	14.895034472147621E	5.765637397766113E
Sb02g008380	49.2974967956542E	0.001807948671890463E	0.02891018203645739E	4.453021906323363E	4.453021906323363E	4.1319032414754232E	3.0134665711505333E
Sb02g008650	110.6255331039428E	0.005678018325163774E	0.04823952548548772E	1.591980445749814E	1.591980445749814E	25.2085542805989E	11.672322273254395E
Sb02g008800	17.33706483437347E	7.45215579202145E-4	0.020026406230525137E	5.62221246101185E	5.62221246101185E	5.01076158777672E	0.768259826286015E
Sb02g008860	125.4705356674193E	0.004457709899208517E	0.04292566743847015E	3.3949135384556385E	3.3949135384556385E	11.841060642582192E	9.983945846557617E
Sb02g008910	145.34128093719482E	1.0071400861540061E-4	0.01128553057533440E	4.85030603467394E	4.85030603467394E	40.16597239176432E	8.281121253967285E
Sb02g009030	44.18490648269653E	5.58413094					

Sb02g026140	623.8045043945312EC	0.005345995369585224E-0	0.04698294823577666E	2.0904700040622553E	2.0904700040622553E	140.65224202473956E	67.2825927734375E
Sb02g026210	44.42235517051831EC	0.004442280574718289E	0.042834135960621836E	3.1970170654449933E	3.1970170654449933E	11.279356956481934E	3.52809476852417E
Sb02g026300	1626.987159729004E	8.105481174720636E-0	0.00526487845493454E	4.83927262423688E	4.83927262423688E	449.45292154947913E	92.8761316935215E
Sb02g026680	119.2629244711731E	4.9512510677045514E-0	0.00816335908330531E	0.22012437700904366E	0.22012437700904366E	-4.5428862246405745E	32.58217684427897E
Sb02g026990	38.51367437839500E	0.00259067732171257E-0	0.0367262838983149E	3.201526779603415E	3.201526779603415E	7.17231379445396E	3.055532362350464E
Sb02g027340	106.81426811218262E	0.0014410751338559274	0.026067042611140765E	2.5920394113568386E	2.5920394113568386E	25.692627588907875E	9.912128448486328E
Sb02g027620	249.4802532196045E	0.002347671025079041E	0.03179925986671042E	2.739005531090735E	2.739005531090735E	60.918853749756622E	22.24123064679203E
Sb02g027980	270.08828353881836E	0.003240339593507186E	0.03702808129210082E	2.1999446353082557E	2.1999446353082557E	61.894744873046875E	28.134682973225914E
Sb02g028250	97.03578460216522E	0.039450751612154E-E	0.0011488375124053768E	18.955678982409253E	18.955678982409253E	30.72440656026204E	1.6208549737930298E
Sb02g028630	424.9375534057617E	0.003952124263514636E	0.040776791137634764E	2.214800671087598E	2.214800671087598E	97.58531188964844E	44.6053924560547E
Sb02g028910	241.52365970611572E	2.5294630156705448E-0	0.007323983547975973E	4.919488860740385E	4.919488860740385E	66.90740712483723E	13.600479443868004E
Sb02g028920	134.15180015563965E	0.00307323428951112E	0.03588485001526081E	2.521654232956629E	2.521654232956629E	32.01946512858073E	12.69780158996582E
Sb02g029180	142.75661468503876E	9.160013493324673E-4	0.022020678547875344E	2.710639674221796E	2.710639674221796E	34.761458714803505E	12.824079513549805E
Sb02g029200	131.35741901597705E	0.002120325581091251E	0.030645420718365637E	0.3918679292628587E	0.3918679292628587E	-2.551880175244492E	31.4583053588672E
Sb02g029380	768.6105461120605E	0.0018675005680387452E	0.029298764852456603E	2.5238390397396993E	2.5238390397396993E	183.49721735416666E	72.7057901652017E
Sb02g029650	269.1353540020532E	1.0234697189848407E-5	0.005625147032420528E	5.50566640721706E	5.50566640721706E	5.50566640721706E	13.950626219437653E
Sb02g029880	256.373373016162E	0.0012803123692060345E	0.025096932449868634E	2.4542833043864818E	2.4542833043864818E	76.016723126124674E	13.950626219437653E
Sb02g029900	202.6203842163086E	0.0017855665721640272E	0.02873394854306202E	2.3633131355754315E	2.3633131355754315E	47.458700018538688E	20.081472256266274E
Sb02g030150	50.09555125236511E	0.00230893839694397E	0.03169520407226987E	2.7174500987950942E	2.7174500987950942E	12.20658938090066E	4.49192770322164E
Sb02g030170	17.0349495481323E	7.1844949691550776E-4	0.02043686829101162E	2.9725300086241964E	2.9725300086241964E	7.171802625512367E	5.960512638092041E
Sb02g030540	54.57557487487793E	1.1935713751268714E-4	0.011418140219586002E	4.76803597023277E	4.76803597023277E	14.800841825052898E	3.3833964657308E
Sb02g030640	1411.5233192443848E	1.329352971202258E-4	0.011799039728621856E	2.1812754271623567E	2.1812754271623567E	-4.571941210659336E	386.0654296875E
Sb02g030820	291.9195308685303E	8.905657110021102E-5	0.02182878903982874E	2.486146142478435E	2.486146142478435E	69.39416631285807E	27.91234978881836E
Sb02g030920	139.6916017532486E	6.937129273058033E-4	0.019630015301666595E	2.8969637407720414E	2.8969637407720414E	34.61511166890462E	11.94875558217366E
Sb02g031240	160.1080379486304E	4.292712895477668E-4	0.01659609176017736E	2.759376490002625E	2.759376490002625E	39.17301686604817E	14.196329116821289E
Sb02g031250	49.87065744000244E	0.004464074552523409E	0.04293514150618042E	3.4271327310377044E	3.4271327310377044E	12.86862720326332E	3.75492525100708E
Sb02g031370	24.572588980197906E	4.4117700294851625E-4	0.01670586387998329E	5.248146844464031E	5.248146844464031E	6.879936218261719E	1.3109267751375837E
Sb02g031620	132.90898990631104E	5.31057528603842E-4	0.017689312956584824E	2.967939290373748E	2.967939290373748E	33.1377560760905E	11.16524155934652E
Sb02g031920	169.9925365447998E	0.006033598682650097E	0.0498094162627954E	2.4546441032366886E	2.4546441032366886E	26.0485862223308E	16.4023202260378E
Sb02g032250	3371.2095947265625E	0.003815616920635374E	0.0400625758904593E	2.626810765805193E	2.626810765805193E	813.895019531253E	309.8415120442033E
Sb02g032390	217.9131446838333E	3.1077961323308184E-4	0.0148495333052052694E	0.6088807370329916E	0.6088807370329916E	54.79026291590169E	17.8530227355957E
Sb02g032400	141.4298076629964E	0.0031394490945896897E	0.03638501829204924E	3.4684352406812335E	3.4684352406812335E	8.058151245117188E	2.3232814470926924E
Sb02g032410	382.0506413015498E	0.0011747341103554656E	0.02410855462974272E	4.599782024438591E	4.599782024438591E	10.60821914672852E	22.74199657788086E
Sb02g032420	1240.5006713867188E	9.068653946935147E-4	0.02192742219418837E	2.592308701136E	2.592308701136E	298.39312744140625E	115.10709635416669E
Sb02g032530	96.26134826660156E	0.0036816297642685365E	0.03949736436291095E	2.2683236547290333E	2.2683236547290333E	75.7402005859375E	33.27305603027344E
Sb02g032980	323.923147758484E	8.86957417185703E-4	0.021794011774009933E	6.4673471791392485E	6.4673471791392485E	76.7420289459228E	2.5887344879938738E
Sb02g033260	17.478886306285858E	0.002893615773302791E	0.034927445578855194E	6.377201714345591E	6.377201714345591E	5.036525050799052E	0.789770384629567E
Sb02g033370	72.96423411369324E	0.002833748738989457E	0.03456942173246444E	3.065199676047741E	3.065199676047741E	18.33857822418213E	5.98233110473895E
Sb02g033390	94.36461067199707E	0.00126852466461131807E	0.025035745997286E	3.1271473907890655E	3.1271473907890655E	23.833414713541668E	7.21455510457566E
Sb02g033430	389.57840838623094E	5.558913026980875E-4	0.01821854591523017E	2.7412360113652854E	2.7412360113652854E	95.14866892496745E	34.710133870442704E
Sb02g033710	2792.05809020061E	0.003248540669744744E	0.03702808129210082E	2.9353840021960407E	2.9353840021960407E	694.1942942122395E	236.4917957747323E
Sb02g033850	33.36709343780544E	3.0471162906200316E-4	0.014810643073289201E	6.925013118296611E	6.925013118296611E	9.71891387303670E	1.403450608253479E
Sb02g033940	96.79850769042969E	0.005072900744690005E	0.0405296455693476E	2.5429395839126205E	2.5429395839126205E	23.158994674682617E	9.107174555460613E
Sb02g033970	96.96812319755554E	0.002014912859319399E	0.030075925656064654E	3.571832982427727E	3.571832982427727E	25.252740859985348E	7.069966872533161E
Sb02g034260	100.4266667360278E	1.4141967505250885E-4	0.011896419993069695E	3.452903255706587E	3.452903255706587E	25.95786348978678E	7.517692089080105E
Sb02g034330	201.4537868499756E	0.004628747372496794E	0.04367978455479936E	2.1896332618548535E	2.1896332618548535E	46.08289489746094E	21.0529727935917E
Sb02g034880	162.1306257279248E	0.00129670414369053E	0.025168839850472753E	2.5825844656322836E	2.5825844656322836E	38.9584706624349E	15.085071245829266E
Sb02g034920	69.87764310836792E	0.001431955408310228E	0.026054287142056428E	3.3263020668381E	3.3263020668381E	17.708065303467613E	5.511628629321697E
Sb02g034960	37.200966119766235E	0.006031036190983833E	0.0498094162627954E	2.858970183406994E	2.858970183406994E	9.186946074167887E	3.213375895371919E
Sb02g035080	93.29704189300537E	0.002794668309464312E	0.0342796653815023E	2.470581978998995E	2.470581978998995E	12.138264973958332E	8.960749690567697E
Sb02g035160	31.06981909275055E	6.4272858346934236E-4	0.01928755883385955E	4.522542499358135E	4.522542499358135E	8.481273333201607E	1.8733302010185738E
Sb02g035390	113.9208122957764E	0.001180964807224976E	0.02410855462974272E	2.7619848504418543E	2.7619848504418543E	27.795925776163735E	10.65350760288090E
Sb02g035600	32.14119214564564E	0.002045067158362188E	0.0302529360617046E	7.448691525678105E	7.448691525678105E	9.445637226104736E	1.268904891104698E
Sb02g035640	102.103385925293E	0.0026026312090659943E	0.03147593562881515E	2.5302162143203115E	2.5302162143203115E	26.73910033836352E	5.267911148071289E
Sb02g035880	320.488588331299E	9.50570490121262E-4	0.02228029648934363E	2.775911810465894E	2.775911810465894E	78.57315006510416E	28.29237937927246E
Sb02g036110	627.5259094238281E	0.001202953854384126E	0.024348740197095133E	5.8774000469648855E	5.8774000469648855E	50.83029638329292E	58.30382963423292E
Sb02g036180	100.69118165969849E	2.75511779408957E-4	0.014027248659543077E	4.50017038195691E	4.50017038195691E	46.146135012308756E	6.102370968119315E
Sb02g036420	177.24828910827637E	5.860453392882748E-4	0.01854807305742394E	3.065682703838012E	3.065682703838012E	44.55068959822591E	14.53206443780811E
Sb02g036420	557.8379554784835E	1.5085021066682568E-4	0.012087379665330687E	3.3339666611412992E	3.3339666611412992E	143.04164737848306E	42.9034313980144E
Sb02g036510	300.32978439431055E	8.096927399520916E-4	0.0208486879940746E	2.7360650751107585E	2.7360650751107585E	73.31437555948894E	26.79552571614586E
Sb02g036640	45.36186635442322E	0.0015228135328820174E	0.026766398229457087E	3.366873191837489E	3.366873191837489E	11.65804793977863E	3.4625714243362427E
Sb02g036685	428.1200585229492E	0.0049971160018680175E	0.045158033295808078E	2.168870258079307E	2.168870258079307E	97.2727523803711E	45.03390460611984E
Sb02g036710	173.4372908706665E	0.0016835156					

Sb02g043230	585.0834197998047E	8.836121399588974E-4	0.021794018774099335E	3.9690899084028795E	3.9690899084028795E	155.77961222330728E	39.24819437662761E
Sb02g043250	89.94251251220703E	0.0011036690548470445	0.023399748952175202E	4.862757182178357E	4.862757182178357E	24.8670597076416E	5.1137779642741E
Sb02g043280	40.478270903396606E	0.0012642792041172358	0.02502922917832823E	3.425052402500516E	3.425052402500516E	10.443698565165201E	3.04920402633667E
Sb02g043290	157.9673557281494E	0.0005338344635796E	0.0386282038902047E	2.5898565659217154E	2.5898565659217154E	37.9878495534261E	14.6793568929036E
Sb02g043336	30.8639640827179E	0.0024883732034697062	0.0326726283983149E	3.35748500236491E	3.35748500236491E	8.31339065236836E	1.907841483751933E
Sb02g043440	222.3696575164795E	0.003030158673575812E	0.0357268708295366E	2.1872016673454193E	2.1872016673454193E	50.86669921874999E	23.25651995340983E
Sb02g043450	19.611834049224854E	0.0011418527650197893	0.023920710347079798E	5.535799231496487E	5.535799231496487E	5.53705175717671E	1.000226259215674E
Sb02g043680	57.29878199235233E	0.00197592665020753E	0.02987810588594805E	2.7926152973823024E	2.7926152973823024E	15.45208691914875E	4.063782181163534E
Sb02g043690	88.23871612548828E	0.00720597505999581E-4	0.0194282836869416807E	3.328348189590305E	3.328348189590305E	22.61749426523844E	6.795411109924316E
Sb02g043820	54.27911591529846E	0.0016232250914993542	0.027416621215311663E	2.8562360943607357E	2.8562360943607357E	13.401147842407227E	4.691890796025595E
Sb02g043920	35.57699775695801E	5.887985223608559E-4	0.01854807305424399E	3.88618039732615E	3.88618039732615E	41.931950251261394E	5.12470490010579433E
Sb02g043970	55.48066568374634E	0.003209580693259318E	0.03675072764957985E	2.6087771546383336E	2.6087771546383336E	13.3689908436811033E	5.12460403104417E
Sb02g044000	142.55416584014897E	1.3385105343689658E-4	0.011806984898847236E	3.699606255679428E	3.699606255679428E	37.406983693440705E	10.111071586608887E
Sb02g044010	86.90525436401363E	0.002176124245710065E	0.03094210496464506E	2.535105037430073E	2.535105037430073E	20.77391815185547E	8.194499964824222E
Sb02g044050	25.987054467201233E	0.00556811066947246E	0.0479936871276321E	3.055038591887062E	3.055038591887062E	6.526156902313232E	2.136194586753845E
Sb034s002010	5666.416133886015E	2.45017062846196E-5	0.0073298357975973E	0.05694539780863612E	-17.56068183323008E	101.763792673482E	1787.0415852864583E
Sb035s002020	18006.396541499805E	6.5042804266477253E-4	0.018888363178348532E	0.10954693730809038E	-9.128507145641095E	592.5979105635153E	5409.534261087708E
Sb03g000170	59.2137778053284E	0.004037979948718788E	0.04117570474334912E	2.8183883840704818E	2.8183883840704818E	14.568748792012531E	5.16917713483174E
Sb03g000310	47.7305447281311E	1.6444193708665373E-4	0.01212822798445159E	1.0286809702582537E	-7.7711606275285945E	1.81391986211411E	14.09626261932291E
Sb03g001640	27.70780384540565E	0.0038532202436605675	0.04205037813005810E	3.641872735149066E	3.641872735149066E	5.938618342081705E	1.630649603686199E
Sb03g001720	45.35891580581668E	0.002867198369796345	0.03147726312397627E	2.8754344021354283E	2.8754344021354283E	11.27823744303385E	3.901408576368196E
Sb03g002210	84.499167120275981E	0.00434319776957774E	0.0245163892104365E	2.55445323639646E	2.55445323639646E	20.24213409423828E	7.92425314585368E
Sb03g002590	11.24713435768018E	0.0016174756933196675	0.02735352385507461E	6.8867187716326885E	6.8867187716326885E	32.7362991663148E	4.0753617942333214E
Sb03g002780	185.7927703857422E	0.002063423748900568	0.0300759256560645E	2.635851799828182E	2.635851799828182E	44.8975217285652E	17.03340148925781E
Sb03g003005	66.7558826318386E	0.002352874647267305	0.03137746325754086E	3.164446287356934E	3.164446287356934E	16.90684276885983E	5.343317985534668E
Sb03g003070	14.508354783058167E	9.890645709105428E-4	0.022317798435197114E	7.205514234106096E	7.205514234106096E	4.26474076410929E	0.5893741846084595E
Sb03g003160	423.1224555969238E	0.005065517688930933E	0.0456029545693476E	2.5011853852807553E	2.5011853852807553E	10.750785164388E	40.28373336791992E
Sb03g003190	1000.7224044799805E	0.00232723168359882E	0.031758885615915146E	3.5055230032046114E	3.5055230032046114E	259.537417039128E	74.3067177327407E
Sb03g003200	23.95125150680542E	0.0041803291239902E	0.04189871139492503E	3.84348131467673E	3.84348131467673E	6.335400899251302E	1.64834960301771E
Sb03g003240	89.52473121288452E	2.2576025129091734E-4	0.01285304788634297E	3.9406670473888917E	3.9406670473888917E	23.1963356730143E	6.6452438036600715E
Sb03g003300	88.20152378082275E	2.561098234620429E-4	0.013756357225425805E	4.286671934703778E	4.286671934703778E	23.8925724029541E	5.561250686645508E
Sb03g003680	1017.6401405334473E	4.4470597946315984E-4	0.01670586387998329E	3.3907280140197316E	3.3907280140197316E	-2.9492191525397318E	85.8937848409167E
Sb03g003750	45.61668252944946E	0.0011552416603585738	0.02397350158313839E	2.9901182911278337E	2.9901182911278337E	11.394756317138672E	3.018045262111494E
Sb03g003820	109.28100395202637E	0.0022749810364097707	0.03147726312397627E	2.407052308720788E	2.407052308720788E	25.735354105631508E	6.8109647211710613E
Sb03g004000	348.6400382385254E	4.43896546407173E-5	0.00812508484852593E	3.961034704751004E	3.961034704751004E	52.7785415694124E	23.422804514567062E
Sb03g004040	224.57117630859375E	5.104615439400310E-4	0.0174305993948652307E	2.7103542545513037E	2.7103542545513037E	64.68201192220052E	17.210522884730727E
Sb03g004310	107.7137885093689E	0.005728232202044756E	0.048435762229124005E	2.9327234679401344E	2.9327234679401344E	26.77489344278971E	9.12970272699992E
Sb03g004420	145.70599042011709E	0.0034619930829799988	0.03835029546960014E	2.3555289768369305E	2.3555289768369305E	34.09435017903646E	14.4741799036618E
Sb03g004450	131.8567950713051E	6.966312581791397E-4	0.01963485368713985E	2.672034877122982E	2.672034877122982E	31.982798894246818E	11.969454129536945E
Sb03g004470	68.46829867362976E	2.6865817942119276E-4	0.0140141060510689214E	2.68959739719380205E	-7.092277357623726E	4.8463925520579E	9.17623762748533E
Sb03g004640	92.38246822357178E	0.0015648388521251617	0.0269393068752127E	2.7819437965195584E	2.7819437965195584E	22.65174102783203E	11.4245036691895E
Sb03g004750	124.92239761352539E	0.002247248979374446E	0.03147726312397627E	3.503516805060533E	3.503516805060533E	32.409682515442635E	9.15111668904622E
Sb03g005100	180.46832847595215E	0.0010360663874035404	0.0227752103999476E	2.5066140716812244E	2.5066140716812244E	43.8862140716812244E	17.155041376749672E
Sb03g005130	29.22323212291718E	6.618484407153839E-4	0.01952055334273131E	6.8562260834152955E	6.8562260834152955E	8.500894228617395E	1.238979508813221E
Sb03g005260	117.55673050880432E	4.76774864450907E-4	0.01694804189448622E	0.2232766531484889E	0.2232766531484889E	17.152285973230995E	32.03329086303711E
Sb03g005270	130.20843172073364E	5.701686329694005E-4	0.018251783239475343E	3.276224780817676E	3.276224780817676E	33.253014426622726E	10.14979632695516E
Sb03g005300	517.7645111083984E	0.001141557069321184	0.023820713047097988E	2.8743680299753518E	2.8743680299753518E	128.04202270507812E	44.54614766438803E
Sb03g005520	40.348594863204956E	0.005224734636275372E	0.04628732669807108E	7.136082930699152E	7.136082930699152E	92.07836036682129E	3.6216855843861904E
Sb03g006050	64.18631792068481E	0.001606598962634998	0.02729182542700562E	2.858745016089181E	2.858745016089181E	15.85077667236328E	5.54462634531686E
Sb03g006530	14.596180364489555E	0.003821270506240689E	0.04009247836557052E	5.380668114487661E	5.380668114487661E	4.102872451146434E	5.0622510036364306E
Sb03g006670	87.52095222473145E	0.0015509249429091416	0.0269393068752127E	2.7025608778566514E	2.7025608778566514E	21.2943337538322E	7.8793169657389353E
Sb03g006680	101.010555863380432E	0.003733820268100472E	0.03977363157128064E	3.2759154872556344E	3.2759154872556344E	7.919392585745824E	2.417496529057495E
Sb03g006910	11.909521088004112E	0.002893918514021312E	0.04427445578955194E	8.1081520477503E	8.1081520477503E	35.33984621368586E	0.43855713021722E
Sb03g007080	689.327579498291E	9.747291664448861E-4	0.03293059625129933E	2.5950330543413878E	2.5950330543413878E	165.86104838053387E	63.91481145222983E
Sb03g007306	85.886699626516E	6.37616613792408E-4	0.01926330108013816E	3.9075390336576645E	3.9075390336576645E	15.62217649932613E	3.997840166091919E
Sb03g007470	9.246152465975104E	0.004328299037417559E	0.04422080414744115E	6.31650396472745E	6.31650396472745E	6.242060661315914E	0.4578475406019016E
Sb03g007840	14.872424572706223E	0.0033181681249492257	0.03731906721601442E	5.138542575042825E	5.138542575042825E	4.149876832962038E	0.8075980246067047E
Sb03g008260	789.0233993530721E	9.02859938093072E-4	0.02918603788110684E	0.37890983924872335E	-2.6391502579683124E	17.22717615763346E	190.7360328000778E
Sb03g008300	34.17732810974173E	0.00376240161390028E	0.03984795890476985E	2.769244668632755E	2.769244668632755E	6.38999690508952E	3.0224736631575527E
Sb03g008320	298.5779438018799E	4.83659138958212E-4	0.010654072701606296E	2.8889343017806404E	2.8889343017806404E	9.937868493855794E	25.59209632873535E
Sb03g008440	20.42931824922516E	0.00139828000359046913	0.02583260270605606E	7.088461715362688E	7.088461715362688E	5.96380778172811E	0.8419119715690613E
Sb03g008585	52.15089964866381E	1.19624430205361293E-4	0.01141814219586002E	6.0609344540572E	6.0609344540572E	14.92168807938394E	2.4619451368811435E
Sb03g008590	14.03202718429565E	1.1153180409768259E-4	0.0113034714930415				

Sb03g025730	19.144218146800995EC	0.0014220007628543605	0.026054287142056428E	7.3320697566351125E0	7.3320697566351125E0	5.615521192550658E0	0.7658848563830052E0
Sb03g025740	54.15802812576294EC	0.005300951435947063E	0.046759627172644154E	2.6353314451277003E0	2.6353314451277003E0	13.086780548095703E0	4.965899438525277E0
Sb03g026000	24.193860590457916EC	0.004479743672292226E	0.04296344770272209E	5.8981957007145E0	5.8981957007145E0	6.895528952280681E0	1.1690912445386248E0
Sb03g026110	63.66431951522827EC	0.002929229479028687E	0.0351200427809631E	2.7096062373867285E0	2.7096062373867285E0	5.100768025716146E0	5.720671812693277E0
Sb03g026200	26.232936059188842EC	1.9931006126529342E-4	0.012326232069066226E	3.8048517890399927E0	3.8048517890399927E0	55.29955546061197E0	14.008313197016113E0
Sb03g026270	128.80415630340576E0	0.003736447824858696E5	0.039773631577128064E	2.2699216935993487E0	2.2699216935993487E0	29.804520924886067E0	13.130197842915852E0
Sb03g026290	449.19543075561523E0	0.001470950712961465	0.025960791824286336E	2.609442990446342E0	2.609442990446342E0	108.2485377604186E0	41.483356472583008E0
Sb03g026470	70.16090911587828EC	0.0021077231184193686E0	0.0365309625852266E0	2.914378002346795E0	2.914378002346795E0	17.41233730136162E0	5.974653242719310E0
Sb03g026680	44.74259006977081EC	0.00329725652068126E0	0.03729149013093729E	5.094520837668501E0	5.094520837668501E0	12.467048327128092E0	2.44714483627955113E0
Sb03g026700	117.89237117767334EC	2.812480505677631E-4	0.0140912795505204248E	3.2987758693877693E0	3.2987758693877693E0	30.1559911127726235E0	9.141545931498212E0
Sb03g026810	405.631473541259777E	7.688931944813185E-4	0.020267542727598113E	3.0532046046972856E0	3.0532046046972856E0	101.85158030192058E0	33.358910878499344E0
Sb03g027000	59.746452803803613E0	0.003527737201133566E0	0.0386282038902467E0	2.832258846118638E0	2.832258846118638E0	14.718683878580729E0	5.19680039079313E0
Sb03g027040	70.62297010059364E	4.36334361588659E-4	0.01669427553422531E0	2.1813856639837788E0	2.1813856639837788E0	10.907503854497273E0	1.0318718155225142E0
Sb03g027246	41.486206531524666E0	0.004720655903524742E0	0.04397534084834978E0	3.8450690664002925E0	3.8450690664002925E0	22.524518021952312E0	2.854187488559082E0
Sb03g027380	177.052906036377EC	0.0035446997515620263	0.038629238498006035E	2.760720315009522E0	2.760720315009522E0	175.4612909552799E0	63.56634350179046E0
Sb03g027440	115.3011794090271E0	0.00493457091861099E0	0.04278018492700348E0	2.5309061508603788E0	2.5309061508603788E0	27.546281814575195E0	10.87444665100506E0
Sb03g027460	19.160160660743713E0	0.0046340785681143735	0.04367978454579936E0	4.020248526967701E0	4.020248526967701E0	5.114528179168701E0	1.2721920410792036E0
Sb03g027730	199.90004539489746E0	0.005646672948796474E0	0.048209007463216906E0	3.1279194178693266E0	3.1279194178693266E0	49.19233825683594E0	16.14211463922227E0
Sb03g027890	154.0555667871973E0	9.98150604491167E-4	0.022427000217262225E0	3.4086625941725153E0	3.4086625941725153E0	30.703911463419594E0	11.44479413248698E0
Sb03g027900	153.4449872970581E0	0.001953750161915019E0	0.029828087407869266E0	2.554158569516101E0	2.554158569516101E0	36.575207234700516E0	14.109121864318848E0
Sb03g027920	81.28076362609863E0	0.004005393470539317E0	0.0100168405469203E0	3.2422083939964127E0	3.2422083939964127E0	18.987095197401832E0	8.38692678324383E0
Sb03g027980	223.02260303497314E0	5.033111387927682E-4	0.01724090689078566E0	3.177040580708581E0	3.177040580708581E0	56.54337064477864E0	17.797497113545738E0
Sb03g028590	55.11711263636013E0	0.004634583599336178E0	0.04367978454579936E0	0.3907287886088919E0	0.3907287886088919E0	22.559319991650197E0	11.032606570122077E0
Sb03g028820	51.391390800476074E0	1.958069238740496E-4	0.012326270869368437E0	4.544359274472837E0	4.544359274472837E0	14.607533654562988E0	3.089710235595703E0
Sb03g028830	69.91147375106812E0	0.003976680128349581E0	0.0482382115194932E0	3.097938318964713E0	3.097938318964713E0	17.41705755654549E0	5.686718281140282E0
Sb03g028880	214.5105495452881E0	7.63712000578719E-5	0.00992131317115454E0	3.7123783930844017E0	3.7123783930844017E0	56.32996495664778E0	15.173551559448242E0
Sb03g029110	50.590909361839294E0	8.966764612538059E-4	0.02188788553325817E0	4.545928752939584E0	4.545928752939584E0	13.8229128519694E0	3.04072360197703E0
Sb03g029120	234.60549163981836E0	3.4498874790525076E-4	0.015262814884105365E0	4.157805715094664E0	4.157805715094664E0	63.03998947143554E0	15.161840174625649E0
Sb03g029490	314.9169101715088E0	0.0014952212067127605	0.02668066053041762E0	2.358268607088194E0	2.358268607088194E0	73.7143939208984E0	31.257863998413086E0
Sb03g029520	165.81935119628903E0	0.0014695754850449958	0.026382203117202248E0	2.5788873174758984E0	2.5788873174758984E0	38.8289874762056E0	15.444218317667444E0
Sb03g029880	46.962260723114014E0	0.0046544680093290215E0	0.04371761335662161E0	3.32898682002335E0	3.32898682002335E0	11.0339796175944E0	3.6161071459452036E0
Sb03g030110	524.7491264343262E0	0.00562779311662538E0	0.0481563854112376E0	2.1753266711255788E0	2.1753266711255788E0	129.87027140299478E0	55.8616047511394E0
Sb03g030370	216.81759452819824E0	0.002217962105425095E0	0.031233076559539337E0	2.5598791816104263E0	2.5598791816104263E0	51.5079696105957E0	20.3019618980371E0
Sb03g030400	15.824635237455368E0	0.0025844846621130768	0.03314759336815515E0	7.883460125469402E0	7.883460125469402E0	4.681091944376628E0	0.593786608104948E0
Sb03g030450	76.87147951126099E0	0.002921183677090647	0.03507875189400906E0	2.456087012048635E0	2.456087012048635E0	18.2097117061198E0	7.4141147931416835E0
Sb03g030770	231.0523490057617E0	5.52422723783419E-4	0.018218549925123017E0	2.778472787517606E0	2.778472787517606E0	56.3429112413489E0	20.38319784423828E0
Sb03g030785	203.1865873336792E0	1.0934556023113342E-4	0.011303471493304145E0	0.2817202212857536E0	-3.549620951723127E0	14.86670444885247E0	52.84215799967448E0
Sb03g030710	16.552214488387103E0	0.0021209461924747105	0.030645452071836563E0	10.273630898443899E0	10.273630898443899E0	5.027996857961019E0	0.489079715013504E0
Sb03g031060	92.7853527069092E0	3.3114854981525015E-4	0.014916355761841811E0	3.3379327172403808E0	3.3379327172403808E0	33.793927172403808E0	7.199227604675293E0
Sb03g031470	1106.1750106811523E0	0.0012177069573891539	0.0244053750644643773E0	3.0658082180948063E0	3.0658082180948063E0	278.03577174740885E0	90.6892768629554E0
Sb03g031610	99.46943712334497E0	1.7395725823831824E-4	0.01212822798445159E0	6.37459216252661E0	6.37459216252661E0	26.006771087646484E0	10.149079953135174E0
Sb03g031750	109.64505863189697E0	0.001372829489052269E0	0.0259526254205366E0	2.489700178119491E0	2.489700178119491E0	26.075145721435547E0	10.47320715586344E0
Sb03g031880	114.51209497451782EC	4.6004362121151496E-4	0.01681335861157414E0	2.9893441908501424E0	2.9893441908501424E0	28.602534612019856E0	9.568163712819416E0
Sb03g031920	61.495939016342146E0	1.707783370862043E-4	0.011212822798451459E0	4.641610429222757E0	4.641610429222757E0	16.865172068277992E0	3.633474270502727E0
Sb03g032090	124.0784158706665E0	0.0024297000902177954	0.032386550374227295E0	2.446366326916162E0	2.446366326916162E0	29.35952059427897E0	11.999951362609863E0
Sb03g032470	49.964383363723755E0	0.00361141857208915E0	0.03897822612927035E0	3.1128308618926512E0	3.1128308618926512E0	12.06532240046713E0	4.00472252527872E0
Sb03g032560	151.09348583221436E0	0.00374143893583046E0	0.039811662631511E0	2.291636316961678E0	2.291636316961678E0	35.06374804178874E0	15.30074273561605E0
Sb03g032630	292.7076557232636E0	0.0065499729165129E0	0.0498537639464567E0	2.086315458084846E0	2.086315458084846E0	65.9574824015299E0	31.3135069529154E0
Sb03g032720	29.538044647216987E0	0.001795401497022951	0.028794935364182826E0	3.7276989482702705E0	3.7276989482702705E0	7.763486358524879E0	2.082648436228345E0
Sb03g032930	127.195950547509929E0	0.004304060322624512E0	0.042451163892210436E0	3.4030246508319605E0	3.4030246508319605E0	7.0097255257715E0	2.0435482630739325E0
Sb03g033270	96.35003471374512E0	0.0010208087107936644	0.02269803610709226E0	4.683028142282074E0	4.683028142282074E0	26.6543633636474E0	5.6513319052093E0
Sb03g033390	131.48472380638123EC	1.0180414983630771E-4	0.01128553057535344E0	0.22295570039243012E0	0.22295570039243012E0	9.992078164546648E0	3.537963104258029E0
Sb03g033490	429.65807590155273E0	0.004541104896212519E0	0.042303987328147064E0	4.04022352985062177E0	4.04022352985062177E0	2.4738787481509146E0	11.09014822268157E0
Sb03g033560	115.14779901504515E0	3.143324275996327E0	0.0348042035025694E0	3.183998999232244E0	3.183998999232244E0	29.20893796284993E0	9.17366170883167E0
Sb03g033760	71.428495045993046E0	2.3183613684491225E-0	0.007630856113533163E0	11.369612154272227E0	11.369612154272227E0	22.01395924868066E0	19.351052842907232E0
Sb03g033850	50.41438335433962E0	0.00512638372033701E0	0.0457284200785727E0	2.5842512479672237E0	2.5842512479672237E0	12.118680318196613E0	4.68943579916586E0
Sb03g034050	112.87939167022705E0	0.0026450126964473607	0.033253647510190616E0	2.510110278662955E0	2.510110278662955E0	26.907010396321617E0	10.71945348375407E0
Sb03g034090	47.36405396461487E0	0.0013207521165240562	0.025336621134401022E0	2.961488525129555E0	2.961488525129555E0	18.80624822625625E0	3.98537516593937E0
Sb03g034200	3643.1099243164062E0	0.004090592742505847E0	0.04139842088555846E0	9.2216609071796238E0	9.2216609071796238E0	954.3799845377604E0	326.656696904163E0
Sb03g034350	59.501975059502903E0	0.005941246706102664E0	0.049375112304529603E0	2.5332547540708625E0	2.5332547540708625E0	14.220427971598305E0	5.613510714907845E0
Sb03g034380	54.83978748321533E0	6.50967					

Sb03g043820	357.24827861785899E2	2.0397347389510562E-4	0.0124563288117994E2	7.049761165530519E2	7.049761165530519E2	104.289431254069E2	14.793328285217285E2
Sb03g043900	322.17893409729004E2	4.1038001069266314E-0	0.00794505301677329E2	3.946624515333317E2	3.946624515333317E2	85.6862227376302E2	21.71035578666992E2
Sb03g044010	130.2400665283203E2	0.003048377161166877E3	0.03579400955881239E2	2.451862123282841E2	2.451862123282841E2	30.836562475868684E2	12.576793034871418E2
Sb03g044190	22.19848356861134E2	0.00166885061453288E6	0.0279604367625293E2	4.048281156381371E2	4.048281156381371E2	5.933749198913574E2	1.465745329856726E2
Sb03g044350	185.128924386812E2	7.01348256790309E-4	0.01965150311697761E2	2.6682350315220282E2	2.6682350315220282E2	48.88693491187839E2	18.62270654004562E2
Sb03g044500	624.3630714416504E2	0.003170129570769917E3	0.03653318674701784E2	2.393973814319376E2	2.393973814319376E2	146.8002726236979E2	61.32075119018555E2
Sb03g044660	206.42678833007812E2	4.4117265711576386E-0	0.0052648784539454E2	5.264820261447366E2	5.264820261447366E2	57.82554499308269E2	10.98338450276695E2
Sb03g044830	67.97948122024536E2	0.00111323727745203E3	0.02353358458162566E2	4.1808769261447366E2	4.1808769261447366E2	18.28603539328984E2	4.373743534088135E2
Sb03g044980	144.06697273254395E2	0.002231223052058761E4	0.03135120689676205E2	2.411276427680751E2	2.411276427680751E2	33.944800694783524E2	14.07752549397782E2
Sb03g045030	131.85494995117188E2	0.00420729826614508E0	0.0419895569033332E2	2.353978512694933E2	2.353978512694933E2	30.84731737726235E2	11.04332050997723E2
Sb03g045420	287.75689125061035E2	0.002150978489227354E0	0.03086092631632418E2	4.3423577582677997E2	-3.2028963887059593E2	29.040863672892257E2	11.76810007731119E2
Sb03g045910	198.18336391448975E2	7.412249721792781E-0	0.00986244982166241E2	3.39280538590891E2	3.39280538590891E2	52.122600139973954E2	13.939061164855957E2
Sb03g046030	241.36288738250732E2	7.05053230651847E-4	0.01971665492370822E2	2.8191582126778822E2	2.8191582126778822E2	59.3883196512858E2	21.0659761428833E2
Sb03g046050	87.97127546386719E2	0.001333912980424403E2	0.0253816464584084E2	2.810233635849795E2	2.810233635849795E2	61.627816518417785E2	7.690091969807943E2
Sb03g046340	26.0857675075531E2	2.8505647800849217E-4	0.01409500716519491E2	7.0831383502119225E2	7.0831383502119225E2	6.1795281346638986E2	1.0757277011871338E2
Sb03g046550	66.9556488907837E2	0.003760631536963245E0	0.03984798590476985E2	3.044208857801949E2	3.044208857801949E2	9.27257368775164E2	3.045972665150961E2
Sb03g046620	46.63759136199951E2	0.003804577430610196E0	0.04002760684483091E2	2.9134012083250846E2	2.9134012083250846E2	9.1257395093282063E2	3.972468690511056E2
Sb03g046860	60.52548170089722E2	0.001564047323985742E0	0.02693390680725127E2	4.148018505121751E2	4.148018505121751E2	16.25614579518636E2	3.91901477179739E2
Sb03g046900	142.53015613395350E2	0.001811669151286340E4	0.028919094035881239E2	2.680498233293777E2	2.680498233293777E2	34.60145905317383E2	12.06892542012535E2
Sb03g046930	9.8387011885643E2	0.002937652737812473E0	0.0351200427809631E2	6.009308630744981E2	6.009308630744981E2	2.8116796811421714E2	0.4678873817125955E2
Sb03g047010	103.94234466527343E0	0.001756514381199503E0	0.02863749505899517E2	2.6445109826091686E2	2.6445109826091686E2	25.144070022379555E2	9.50674819946289E2
Sb03g047100	19.950827538967133E2	0.002272005776653765E0	0.03147726312397627E2	4.763897487215071E2	4.763897487215071E2	5.496494770050409E2	1.153781076272393E2
Sb03g047490	34.9343016147135E2	0.00480653825565523E0	0.0444565990798171E2	2.912071603699636E2	2.912071603699636E2	8.668142954508463E2	2.9766242504119873E2
Sb04g000320	21.408456563945985E2	0.00529978801149629E0	0.04675962712644154E2	4.48474070163038E2	4.48474070163038E2	5.8356019901766E2	1.3010919888814287E2
Sb04g000340	164.67957305908203E2	2.8380712283099284E-0	0.01409127950520428E2	3.214236897258056E2	3.214236897258056E2	8.16250318802628E2	1.026538391113328E2
Sb04g000540	67.58002853393555E2	0.0024963391436117056E0	0.03267262839893149E2	2.980936303318973E2	2.980936303318973E2	16.86803849538167E2	5.658637682596844E2
Sb04g000560	241.3826560974121E2	0.0019270152581704711E0	0.02962859671340667E2	2.649458037413669E2	2.649458037413669E2	58.41353532864583E2	22.047351837158203E2
Sb04g000570	65.0290869474411E2	6.54368921096990174E-0	0.009451339687407967E2	6.939502501902308E2	6.939502501902308E2	18.946170806884762E2	3.7301915089289324E2
Sb04g000740	31.174825429916382E2	0.0029917412360195403E0	0.035403128504883974E2	3.3191201971571638E2	3.3191201971571638E2	7.98553559368682E2	2.4059549172719317E2
Sb04g001123	26.964933395385742E2	0.0014319951721550844E0	0.026054287142056428E2	4.115918654185477E2	4.115918654185477E2	12.231381098429361E2	1.756930033658857E2
Sb04g001130	194.08698749542236E2	0.001183164567371509E0	0.02411900380561892E2	2.68967834225345E2	2.68967834225345E2	47.16134713583984E2	17.534226324890137E2
Sb04g001140	23831.797607421875E2	1.8895879874599266E-4	0.01226534850154766E2	6.76338887355718E2	6.76338887355718E2	69.20767578124989E2	1023.255779947911E2
Sb04g001370	172.1926336288452E2	0.0018923748125725293E0	0.0294181691495383E2	2.7200117947884004E2	2.7200117947884004E2	41.968146006266274E2	15.423998536682129E2
Sb04g001460	207.12150835990906E2	7.310696162771681E-0	0.00986244982146813E2	5.69475351783446E2	5.69475351783446E2	58.727847189589375E2	3.101262803077697E2
Sb04g001700	121.7969913482666E2	5.89289078043574E-4	0.0185480730254239E2	2.9050567137955E2	2.9050567137955E2	30.203673044804963E2	10.395324071248371E2
Sb04g001860	138.62291526794433E0	0.0032493501707693793E0	0.037208081292100829E2	2.274647151820598E2	2.274647151820598E2	32.09691562947586E2	14.110722859700516E2
Sb04g002070	237.46587753295898E2	0.0018495516474368399E0	0.029236828586142082E2	2.5041257886502364E2	2.5041257886502364E2	56.5661226903659E2	22.589169820149742E2
Sb04g002250	18.96503448486328E2	0.002592656487999196E0	0.033147593895815151E2	4.367750586929188E2	4.367750586929188E2	5.14396357536319E2	1.1777145862579346E2
Sb04g002640	15.879228591918945E2	0.0013099442621811322E0	0.025193947499498935E2	6.410970682171474E2	6.410970682171474E2	5.4788544813791905E2	0.714221715927124E2
Sb04g002740	127.7165508720264E2	9.8063387392302129E-4	0.022308084921512414E2	2.7877049083939536E2	2.7877049083939536E2	44.83924178282032E2	16.0846399735657E2
Sb04g002750	142.59117794036865E2	0.0017021322004738151E0	0.028128845621104334E2	5.583791219359963E2	5.583791219359963E2	34.26779174806875E2	12.628600987427261E2
Sb04g003020	216.23785400390625E2	0.005074086617582908E0	0.0456029549845476E2	2.65619875456361E2	2.65619875456361E2	50.00721458292644E2	22.07216008504232E2
Sb04g003090	59.117809414863586E2	1.2837273326440327E-4	0.01153798480178129E2	6.55266652579628E2	6.55266652579628E2	17.09679950463864E2	2.609136621157326E2
Sb04g003170	253.12456512451172E2	7.13591865728347E-4	0.01983229614390544E2	2.682302832791815E2	2.682302832791815E2	61.46124394734701E2	22.9136110941569E2
Sb04g003240	49.39255046444824E2	8.876230825453332E-4	0.021794018774099335E2	6.88892442852655E2	6.88892442852655E2	12.952891349792479E2	3.511292139698127E2
Sb04g003420	36.21465766429901E2	0.0014299546062103033E0	0.026054287142056428E2	3.847076095633964E2	3.847076095633964E2	9.581072117854817E2	2.490481386911518E2
Sb04g004160	235.60545921325684E2	0.0017643675825935905E0	0.028642052321263104E2	2.3247669132639708E2	2.3247669132639708E2	54.9139022871484E2	23.621250788070766E2
Sb04g004300	76.11274317785855E2	5.27138525916379E-0	0.017641240129613715E2	3.2365778216812044E2	3.2365778216812044E2	19.3823746348877E2	5.98859995739746E2
Sb04g004490	95.21452951431274E2	1.8579880425215108E-4	0.012265348501354766E2	3.9089470895720835E2	3.9089470895720835E2	25.2728029868881E2	6.465373516082764E2
Sb04g004540	384.73317337306193E2	0.001303354897785153E0	0.025168839890427753E2	5.283402650277678E2	5.283402650277678E2	91.89744858771094E2	36.34694544472484E2
Sb04g004590	47.43930011304653E2	0.0045281030838003125E0	0.04313727871167097E2	3.2178447048504903E2	3.2178447048504903E2	12.064005374908447E2	3.749094963073305E2
Sb04g004700	25.68418049812317E2	0.0019158132707588398E0	0.029532871239637347E2	3.749248672747553E2	3.749248672747553E2	6.690019925435385E2	1.8713137539390586E2
Sb04g004750	465.57439395751953E2	0.001511442625073214E0	0.0266244215854711E2	2.822756540611642E2	2.822756540611642E2	114.59450022379566E2	40.596664428271094E2
Sb04g004910	44.487954939192809E2	0.001051054965720515177E3	0.02925836152051034E2	3.3889956302214075E2	3.3889956302214075E2	15.48056819915771E2	3.378749767939251E2
Sb04g004940	48.6700484752655E2	7.11543528094252E-4	0.01965150311697761E2	4.35861240773567E2	4.35861240773567E2	14.504020531972246E2	1.719328959782917E2
Sb04g004960	132.290132522583E2	4.022828403319712E-0	0.01694804189448622E2	2.980311337148308E2	2.980311337148308E2	32.35531855171854E2	33.97199249567578E2
Sb04g005115	90.68400955200195E2	0.003898019517576342E0	0.04402285842247165E2	2.306659424331742E2	2.306659424331742E2	21.08644994099348E2	9.1415523001301E2
Sb04g005260	72.72401285171509E2	0.0012160506252935775E0	0.02440537506443775E2	3.200646837653053E2	3.200646837653053E2	18.470479329427082E2	5.770858287811279E2
Sb04g005330	186.2518701553447E2	5.868342775858667E-0	0.0052648784539454E2	5.707620322485642E2	5.707620322485642E2	52.8282136389974E2	9.255735079447426E2
Sb04g005420	467.6847801208496E2	0.006070754397874167E0	0.04987508885721045E2	4.8091246110062035E2	4.8091246110062035E2	22.0793805128513236E2	10.625418345133454E2
Sb04g005430	425.532169342041E2	9.376694024872861E-0					

Sb04g023520	64.845376968383799E	3.44821408044247E-4	0.015262814884105365E	4.287171224108179E	4.287171224108179E	17.526904424031578E	4.088221232096355E
Sb04g023575	33.63739654421806E	1.707520357869319E-E	0.00604932594970895E	0.0429094549798431E	-23.304887010794108E	0.4613255560398102E	10.751139958690943E
Sb04g023640	125.583250625261353E	7.470668389597408E-E	0.02026406230525137E	3.1977113022581194E	3.1977113022581194E	8.1888724644978844E	9.972358862559002E
Sb04g023690	29.38091814517975E	0.0059485859814701566E	0.049375123045296030E	2.719299669158669E	2.719299669158669E	7.160044489526432E	2.633194486300151E
Sb04g024120	19.27700304985046E	0.004827846368947125E	0.042288643239475E	4.3055178979251E	4.3055178979251E	5.21472708384106E	1.2117117318917222E
Sb04g024400	24.507028460502625E	0.002593497008330789E	0.033147593562881515E	0.21117103578161606E	-4.735497916646849E	1.4242895046869908E	6.744719982147217E
Sb04g024530	81.96814632413377E	0.00101107147857468914E	0.02260262767328762E	2.805397183965127E	2.805397183965127E	20.14274990844727E	7.17999045054118E
Sb04g024680	46.653912067415771E	2.7732353928380335E-E	0.01402724865934077E	4.184660485687149E	4.184660485687149E	12.55182037113443E	2.99948358535666E
Sb04g024750	144.36029730303696E	0.0058739080432449E-E	0.0174677112037733E	3.0035183086432142E	3.0035183086432142E	36.100646336873375E	12.014942730814617E
Sb04g024780	18.12303031539971E	1.5157501396520361495E	0.048506195765995616E	3.676684345285015E	3.676684345285015E	4.748565150665283E	1.291534900665283E
Sb04g024850	130.8820743560791E	0.0022184445561884134E	0.031233076595939337E	2.406653539328786E	2.406653539328786E	30.820467631022133E	12.08690487670898E
Sb04g024880	93.90237712860107E	1.636296699527865E-E	0.01212822798451459E	5.977891576967745E	5.977891576967745E	26.81509276967745E	4.485709190368652E
Sb04g024940	119.06147956848145E	0.00409488155743694E	0.04140000803847919E	2.5912994280788872E	2.5912994280788872E	28.3624064127604E	11.05091921488441E
Sb04g024930	303.8225631713867E	0.0025299246422553342E	0.03289526422046154E	3.2420086100130684E	3.2420086100130684E	79.9076949243164E	30.30338921363937E
Sb04g025030	117.11439180374146E	0.0017036911023337199E	0.028128845621104334E	0.35241008838668356E	-2.837603131411473E	10.17252937956277E	28.8560121270375E
Sb04g025090	761.9089736938477E	0.0016813801555254344E	0.0280854586080805E	2.5003284068393445E	2.5003284068393445E	181.41370646158858E	75.559514363609E
Sb04g025120	10678.316223144531E	0.0034680901110280275E	0.03835029546960014E	3.0160138042493223E	3.0160138042493223E	2673.1273600260415E	886.3113810221355E
Sb04g025220	26.11625874042511E	0.0058127003848887785E	0.04883215073936845E	2.9054454047917644E	2.9054454047917644E	6.476373036702474E	2.229046543439222E
Sb04g025360	45.46896553039551E	0.005539588944235959E	0.04786250520031026E	2.566360220850927E	2.566360220850927E	10.90682862733365E	4.29478097318036E
Sb04g025400	18.25519460439682E	8.861457096078723E-E	0.02179401787409933E	6.424954409108277E	6.424954409108277E	5.26552248010985E	0.819542388121286E
Sb04g025430	63.822574765014655E	0.0055842437028101434E	0.0480504859480722E	2.4194732935430117E	2.4194732935430117E	15.052710215250649E	6.221482297616504E
Sb04g025270	191.9841766357222E	3.5496426217763339E-E	0.01532459436755676E	4.239037903298045E	4.239037903298045E	51.77974891665998E	12.21497628621622E
Sb04g025140	101.9739351272583E	0.002201147910476244E	0.01316876213791291E	2.460147782583313E	2.460147782583313E	24.167053185831703E	9.82356894317477E
Sb04g025970	179.25842475891113E	0.004575367300502434E	0.03438561866899786E	2.278582630721027E	2.278582630721027E	41.24121229096575E	18.511596043904618E
Sb04g026020	33.83421589794031E	0.001228386176030825E	0.0245614055055754E	2.5790951774048533E	-6.82437606067248E	2.438830713035684E	8.8392411867775E
Sb04g026360	411.6476135253906E	0.002958616669263205E	0.03521073684173913E	2.80370235042128E	2.80370235042128E	101.14157867431639E	36.0742925008138E
Sb04g026400	89.81076431274414E	0.001159013246216135E	0.02400332302070402E	2.723358000982105E	2.723358000982105E	21.8966197675293E	8.04030164082845E
Sb04g026500	172.84402179718018E	0.005108055128205283E	0.0457284207857276E	2.695901619570421E	2.695901619570421E	42.0258731842041E	15.588800748189293E
Sb04g026570	239.79335403442383E	5.674465945087649E-E	0.0052648784394354E	4.678993747238228E	4.678993747238228E	69.24370193481445E	10.68741607660156E
Sb04g026600	42.3526853239828E	0.0011435274526318557E	0.023820710347097988E	5.05055353237518E	5.05055353237518E	11.784293969472248E	2.332678079605103E
Sb04g026870	159.4654607728271E	0.0010285613095627956E	0.02269803617069296E	2.5581154776108312E	2.5581154776108312E	34.21602249145508E	14.939131100972496E
Sb04g026780	181.24488067262953E	6.438184439293915E-E	0.019287558833895955E	2.77365351886975E	2.77365351886975E	40.8026815315755E	10.0697407256262E
Sb04g026890	39.190979155921936E	0.003552051741524138E	0.038629238498006035E	2.9220265091386863E	2.9220265091386863E	9.734485759204102E	3.331502159436544E
Sb04g027100	19.56635844707498E	0.003565615625518706E	0.0387178107926247E	4.149019308652497E	4.149019308652497E	5.2554473022245E	1.2666721741358433E
Sb04g027240	27.00053154222107E	0.0035921003321334704E	0.038901189780483399E	3.6230257290137597E	3.6230257290137597E	7.053361892700195E	1.9488159290450073E
Sb04g027360	32.77762925624447E	6.21473551483058E-E	0.01910400496157005E	4.139544228815865E	4.139544228815865E	8.00031302204428E	2.12584539254503E
Sb04g027660	166.11559772491455E	0.0014236240747433344E	0.026054287142056428E	2.871589850812339E	2.871589850812339E	41.0697657267252E	14.30210018157959E
Sb04g027810	55.05561578273773E	0.0010424802455794616E	0.02281323538980102E	4.69666007282656E	4.69666007282656E	15.3035758336385E	3.22151434415393E
Sb04g027680	117.177358662173193E	0.004946454718831919E	0.0450127572860556E	2.13063498710849E	2.13063498710849E	37.0031649273672E	17.369413699716847E
Sb04g027900	22.4524221127524686E	8.858972254575095E-E	0.01854807307542439E	5.90455367898631E	5.90455367898631E	6.40019782788086E	1.03942712714098E
Sb04g027920	46.485222114733723E	0.004539843765041784E	0.043203987328147064E	2.8601992719215916E	2.8601992719215916E	11.481013139088947E	4.01406057569546E
Sb04g028070	14.31123209996328E	0.003380143577974234E	0.037822899147166314E	4.921704335133319E	4.921704335133319E	3.9648300011952715E	10.865869654701743E
Sb04g028160	182.7062282562256E	8.2603169578396878E-E	0.021049895619880413E	6.2318699682286626E	6.2318699682286626E	44.13328297932942E	7.167687931067019E
Sb04g028330	20.943078219890594E	0.0018953723279609207E	0.029418181691495383E	3.618960025487574E	3.618960025487574E	6.022198473612467E	0.953827599684396E
Sb04g028350	173.6878662190375E	0.001704659237842096E	0.028128845621104334E	0.3761228146556905E	-2.685706042374753E	15.824161529541016E	42.07179387141681E
Sb04g028450	303.51910972585215E	0.004414583289038292E	0.042769081491767588E	2.078412278562764E	2.078412278562764E	68.3070619710287E	32.86533037821452E
Sb04g028690	488.7451591491699E	0.0011388747802163048E	0.023820710347097988E	2.6071149757945977E	2.6071149757945977E	117.75013478597005E	45.16491826375325E
Sb04g028840	81.3077903747559E	4.5460661211345266E-E	0.016725661127861553E	3.0913615148282365E	3.0913615148282365E	20.49411455792016E	6.62947845489884E
Sb04g028900	392.6722640991211E	7.347293402283073E-E	0.020026046203525137E	2.5495442926320266E	2.5495442926320266E	94.03135945468380E	36.875368754069015E
Sb04g029230	50.18217468261719E	9.651899671735256E-E	0.02230596526129933E	3.896494123605809E	3.896494123605809E	13.111193943023682E	3.416197617848715E
Sb04g029465	77.73994994000726E	0.0020109751066655920E	0.030075925656046654E	3.5637406338705993E	3.5637406338705993E	20.235294921875E	5.678007035814922E
Sb04g029500	307.20448112487903E	0.0053673851521804170E	0.04705225840074774E	2.3173929247775518E	2.3173929247775518E	71.33343073527010E	30.88680297302246E
Sb04g029510	460.32018661499023E	6.2164886270208542E-E	0.01910400496157005E	2.711778267109906E	2.711778267109906E	112.1013692220052E	41.3386929821951E
Sb04g029560	24.813441812992096E	6.872544363454264E-E	0.019656321683991064E	8.07410934165099E	8.07410934165099E	7.359632644654133E	0.911510646343231E
Sb04g029630	23.810646653175354E	6.657807070039108E-E	0.019428238369416807E	3.61208356267452E	3.61208356267452E	6.856874899857584E	1.078203717875328E
Sb04g029770	70.54601812362671E	4.553031615632006E-E	0.016725661127861553E	0.25952956372891334E	0.25952956372891334E	8.84540069187442E	18.689938405354817E
Sb04g029850	250.9261131286621E	1.5310117000873707E-E	0.01208739665330678E	3.100006793985968E	3.100006793985968E	63.2415440877788E	20.40093621826172E
Sb04g029940	127.2092857360398E	0.00528226651571566E	0.04665240447966605E	4.164149890661261E	-2.40145053914282E	12.466180165080728E	29.936915079752602E
Sb04g029960	17.504884630441666E	0.0018686421884508296E	0.02929876485256603E	5.64338301004461E	5.64338301004461E	5.0614412014449E	0.773520159336044E
Sb04g030000	141.06824696124268E	7.483625561301906E-E	0.020026046203525137E	3.390194053426343E	3.390194053426343E	36.31894734700516E	10.71086025308017E
Sb04g030010	51.66681146627104E	0.00605591552509131E	0.0498857636846567E	2.846377189216187E	2.846377189216187E	12.744704168253582E	4.47753032454335E
Sb04g030100	129.8673038482666E	0.001731949378950946E	0.028415105195147942E	2.4973083648485317E	2.4973083648485317E	30.91126759447005E	12.7738368428548E
Sb04g030160	295.26627254868084E	2.755027390446712E-E	0.007323938547975978E</				

Sb04g036270	53.79266953468323EC	0.0019451157171612701E-0	0.029767562908398437EC	3.3813561035179487EC	3.3813561035179487EC	13.838346481323242EC	4.092543363571167EC
Sb04g036320	319.911106109619144EC	0.0010940946076229182	0.023075277125600303E	2.535980275061147EC	2.535980275061147EC	76.479334513346363EC	30.157070085662695EC
Sb04g036400	21.4691746830394025EC	7.582666611033831E-4	0.22014057729956558E	5.101640154100515E	5.101640154100515E	6.057127157840708EC	1.0926444015842547EC
Sb04g036510	22.905085135917966EC	3.4397091301964164E-4	0.015262814884105365E	5.606037319762909E	5.606037319762909E	6.4841964935011393E	1.166088700294946EC
Sb04g036540	14.03648185127884EC	0.0010915280825843897	0.023037527175260030E	2.947006408847458EC	2.947006408847458EC	53.26964441352204EC	18.075849530381055EC
Sb04g036630	530.8738403320312EC	4.5210612962892513E-4	0.016725661127861533E	3.1601638077260894E	3.1601638077260894E	134.4216537475586EC	42.536293029785156EC
Sb04g036670	198.9884328842163EC	9.693831701697889E-4	0.02230598526129933E	2.782916625896714EC	2.782916625896714EC	48.795258868733727EC	17.5395175933838EC
Sb04g036730	132.6117300335694025EC	2.3760190130082623E-4	0.013321350287666158E	4.522720031987929E	4.522720031987929E	36.201419830322666EC	8.00434684752417EC
Sb04g036790	270.907797241211E-0	0.001307548948906957E	0.025193947499499833E	2.4835833804825773E	2.4835833804825773E	64.37860107421875E	25.92165883821617E
Sb04g036905	36.902003441005945EC	0.0012674030187816224	0.02503754978597286E	0.0857711903796522E	0.0857711903796522E	-11.658926448072634E	0.971699129790677EC
Sb04g037215	173.97992420195633EC	6.0359728273855605E-0	0.00898479052431215E	5.393090761435237EC	5.393090761435237EC	48.922060648600265EC	9.07124741871052EC
Sb04g037300	25.790138423442848E	0.005183840346174256E	0.0460865346462992E	5.306818927013493EC	5.306818927013493EC	7.23360577723185E	1.363082230091295EC
Sb04g037430	138.42193412780762EC	0.004066423973796889E	0.041273633767159396E	2.58800083731613883E	2.58800083731613883E	33.28096321922196EC	12.8596814473473E
Sb04g037440	33.506447315216064E	0.002063207914877229E	0.03033255257515648E	5.227860722738603E	5.227860722738603E	8.426562468210856E	2.74225330527832EC
Sb04g037570	307.67140960693363EC	0.0013922750856731904	0.02577151680640903E	2.800083639876244EC	2.800083639876244EC	75.56901041666676E	26.88126118977867E
Sb04g037760	37.31165933609009E	0.0030166750658893377	0.035626689591163406E	2.377450688254741E	2.377450688254741E	22.83316548653645E	9.60454292043049E
Sb04g037810	78.89314985275269E	0.0022764133689498625	0.03147726312397627E	2.506575422602493E	2.506575422602493E	18.79817263285319E	7.499543984751039E
Sb04g037840	17.0139037967282EC	0.005050865134204094E	0.04556620124228314E	5.724603576682482E	5.724603576682482E	4.82793537756754E	0.843365887008519E
Sb04g037930	73.61136779781561E	0.00287976080109183E	0.03456942173246444E	2.3186840669909222E	2.3186840669909222E	17.08558664785156E	73.78563944498697E
Sb04g038000	37.2249995470047EC	8.3903969352604E-4	0.021166325537954667E	4.095130975714719E	4.095130975714719E	9.97300163904826E	2.453331543286642E
Sb04g038120	1690.2919540405273E	1.966160237323521E-4	0.01231267889368443E	4.9581687508160375E	4.9581687508160375E	46.86625162760413E	94.56319929123828E
Sb04g038170	53.49796481613161E	0.00187783255223995	0.02937672927064835E	2.859949061664763EC	2.859949061664763EC	5.1212670008341469E	6.41998851886291E
Sb04g038250	24.189102590084476E	0.00242756169013581E	0.02338655034722795E	4.433913730280267E	4.433913730280267E	63.97919637834553E	1.483835518360138E
Sb04g038260	33.75857865810394E	0.0014268837160829016	0.02605428714205642E	4.413091168608249E	4.413091168608249E	9.174036343892414E	2.07882320880899E
Sb04g038310	395.51244163513184E	5.163905031112608E-0	0.017467112037339E	2.914534549903171E	2.914534549903171E	19.51851338704428E	33.67882157199968E
Sb04g038360	76.88284730911255E	0.003228515805373984	0.03690839268707416E	2.506926034090627E	2.506926034090627E	18.31990083058675E	7.3071714393171432E
Sb04g038410	33.019336462020874E	0.002213698249637428E	0.031233076559539337E	4.4276017852169165E	4.4276017852169165E	8.978580156962076E	2.02766530378215E
Sb04g038510	146.12352657318115E	5.101470341647703E-0	0.00816335990330531E	3.7183304209761157E	3.7183304209761157E	38.38473256429036E	10.32310962677002E
Sb05980020295	905998678588877E	0.002979444118925464E	0.03534265831372578E	2.226494438839799E	2.226494438839799E	68.06489690144856E	30.570432027180992E
Sb0505002050	97.52854633331299E	0.00208776011405210578	0.03049499355628417E	2.579930667742612E	2.579930667742612E	23.428496340060508E	9.01046140431152E
Sb0505002070	26.01242744922638E	4.4216916707828384E-4	0.01670586387998329E	8.33345137038166E	8.33345137038166E	7.741805632909139E	0.9290035168329869E
Sb0505004050	644.577209472656E	1.1624870809225513E-4	0.011418140219586082E	3.13687902007508E	3.13687902007508E	165.09628616524375E	49.82262166341147E
Sb0505010340	36.42861890792847E	3.4940898328742555E-4	0.01532219581866534E	4.013880449073507E	4.013880449073507E	9.72102165222168E	2.4218513170878095E
Sb0505016000	227.199819590481934E	2.5702920778087403E-4	0.01375635725425805E	3.246291755282218E	3.246291755282218E	57.1921760542968E	17.835156122843422E
Sb0505023400	161.991426898664934E	0.002723134366056644	0.03376856794677677E	2.2511836243866334E	2.2511836243866334E	37.9900705730307E	16.609071731567383E
Sb0505025400	763.725895778323E	0.0079151581795036E-0	0.012467040873140653E	3.176875627372605E	3.176875627372605E	193.6265747153644E	60.94874318407539E
Sb0505027400	30.732829332351685E	0.0023724591436124405	0.03198343505869979E	3.5309301605661028E	3.5309301605661028E	7.983311017354329E	2.260965426726985E
Sb0505028200	100.61787600285645E	0.002166828656158593	0.03091930879588437E	2.613531632716877E	2.613531632716877E	24.257709503173828E	9.9215825154444988E
Sb0505029300	106.4761400222778E	0.005618446373862199E	0.04810521191281655E	2.7610519977735746E	2.7610519977735746E	28.54329961140985E	13.20820839601643E
Sb0505030300	93.80024051666262E	0.0028436403261316704	0.03456942173246444E	0.395282975801521E	-2.529833211188226E	8.857853889466332E	2.1008929444222E
Sb0505030790	52.02949180220484E	0.0018519889023574968	0.029420307080053732E	5.8478342113093795E	5.8478342113093795E	6.554191112518310E	1.428784881566371E
Sb0505042200	29.69985681802368E	0.004603548633297329E	0.0435372005904764E	2.7668994839627854E	2.7668994839627854E	7.271811008453396E	2.6281442642211914E
Sb0505045000	32.8388919830322EC	1.3512801769211932E-0	0.00386195874564077E	9.884001464313288E	9.884001464313288E	97.7250292154947E	9.887261072794587E
Sb0505052400	97.935771465301541E	0.00138205594762903E	0.02562521235047125E	3.184483646711835E	3.184483646711835E	14.69679673512776E	6.415127088639404E
Sb0505053900	188.68973350524902E	2.531182335833167E-4	0.01364928135058717E	3.8104737463419176E	3.8104737463419176E	42.92165400187175E	13.074923833211265E
Sb0505054600	154.16293048858643E	1.43549203342194E-4	0.01189641999306965E	4.9833915744512005E	4.9833915744512005E	42.7992630018828E	8.588380495670199E
Sb0505057500	24.824036717414856E	0.00240437887125809E	0.03223130775823461E	4.817928325354556E	4.817928325354556E	6.852406501470019E	1.422272404039322E
Sb0505058800	45.546312734484877E	7.15565600989064E-0	0.020267542727598113E	13.45957800668548E	13.45957800668548E	14.13213555018107E	1.049968894647152E
Sb0505059600	24.330214977264404E	0.0067010985997011E-4	0.01888363178348532E	6.4582854275697445E	6.4582854275697445E	6.673599402109782E	1.4364722500783107E
Sb0505060900	389.30996113189967E	0.0025862979145305134	0.033147593868281515E	2.6978670206628355E	2.6978670206628355E	49.67678705851237E	57.38925604781082E
Sb0505061500	14835.050659179688E	0.0013561550654033663	0.02549928405807265E	4.018532796657613E	4.018532796657613E	399.6617714843475E	985.36111149085051E
Sb0505064700	4496.4610595703125E	0.0038039721164129479E	0.04002760684483071E	2.872959698044852E	2.872959698044852E	111.824239095044852E	98.99311014085052E
Sb0505065200	350.80836296801543E	0.003617750457770654	0.03898774702862312E	2.4349936771331E	2.4349936771331E	82.8935205522461E	34.04260063171387E
Sb0505071600	62.52490520477295E	0.003224025609088405	0.03684511810786645E	4.2336574725021665E	4.2336574725021665E	14.7127896931966E	6.06980609893798E
Sb0505072800	50.8616826534271E	6.5812371224644126E-0	0.0052648784933454E	17.268737493558337E	17.268737493558337E	57.90554674275716E	9.211760123570741E
Sb0505075000	247.86410522460938E	0.003841674566882892E	0.04015912915929351E	2.1573162871343527E	2.1573162871343527E	156.4531415303586E	26.168228677848305E
Sb0505086700	278.9213237762451E	0.0018926154773435237	0.029418181691495383E	2.460846502081464E	2.460846502081464E	66.10931396484375E	28.6464062723796E
Sb0505093500	76.01543760299883E	0.002008580077068060E	0.030462679345604895E	2.860458395838386E	2.860458395838386E	18.77488851339518E	6.5635938760337E
Sb0505103600	15.661751940846443E	0.005110587953004526E	0.04572842070872757E	5.894040043600851E	5.894040043600851E	4.463323513666788E	0.757260466153584E
Sb0505106100	244.65811431407926E	2.880008745312512E-0	0.0074163309139203955E	15.80933855347778E	15.80933855347778E	76.70107396443684E	4.876638069229151E
Sb0505109600	57.969610035419484E	0.00270286699673163E	0.03367390534030471E	6.795796370541504E	6.795796370541504E	16.844533571342365E	2.48685653979455E
Sb0505131900	191.9850254005838E	9.7918119412173735E-0	0.011193999441199704E	8.855741387700159E	8.855741387700159E	51.05176283772787E	13.17924663090063E
Sb0505138300	57.884762293930054E	0.00211891776220747	0.030645420718365637E	2.79090693714932E	2.79090693714932E	14.205131848653156E	5.0897958265686E
Sb0505144700	601.6928825378418E	0.0012744451776910259	0.02508515370413878E	2.656711348094008E	2.656711348094008E	194.1513972736303E	37.0795885718424E
Sb0505160000	645.5226821899414E	3.438990739743847E-0	0.00706232567128601E	5.22352455407616E	5.22352455407616E	180.59989162259766E	34.57343857210495E
Sb0505167300	109.99172782897949E	0.0015232983632776057	0.026676389225490787E	3.737166765276619			

Sb05g027870	39.08126139640808E0	0.005094437624102235E-0	0.04572833771885736E0	9.05096040722657E0	9.05096040722657E0	11.73098341623942E0	1.2961037158966064E0
Sb06g000280	31.0516605377197272E0	0.002414176062053151E-0	0.03233271084104542E0	3.3535202715974077E0	3.3535202715974077E0	7.973039944666634E0	2.3775135670660684E0
Sb06g000400	36.2267141161346444E0	0.002497600494582952E0	0.0326726283984149E0	3.196697942196088E0	3.196697942196088E0	9.198036034901936E0	2.8773553371429443E0
Sb06g000410	76.199373278045654E0	0.00537637901479663E0	0.0470522583407747E0	2.355183730687725E0	2.355183730687725E0	17.8295681267194824E0	7.5703487396242035E0
Sb06g000440	149.60350894927979E0	0.00283198967703608E0	0.0345694217324644E0	2.2298662595919353E0	2.2298662595919353E0	44.2584120627574E0	15.439024289449058E0
Sb06g000850	86.35411834716797E0	0.002829279150161421E-0	0.0345694217324644E0	2.5648965029163624E0	2.5648965029163624E0	20.710220336914062E0	8.074485778808594E0
Sb06g001240	308.549716796875E0	0.002264026809868444E0	0.03147726312597627E0	2.344784755482087E0	2.344784755482087E0	72.02995314982097E0	30.7196040767415E0
Sb06g001690	378.4104995030293E0	0.001007405838154551E-0	0.02259141891210387E0	3.870945206547323E0	3.870945206547323E0	100.268502506543040E0	25.90842790039062E0
Sb06g001710	17.31741075217724E0	0.0010674156098551247E0	0.023050654614317753E0	7.9851783401144773E0	7.9851783401144773E0	5.130026658370685E0	0.624435924396876E0
Sb06g001720	76.48192739486694E0	9.7559330219111883E-4	0.02230565626129933E0	3.4440942920277923E0	3.4440942920277923E0	45.28540484110515E0	13.541492490517174E0
Sb06g001810	47.4532051086426E0	1.7264153230066358E-0	0.01212822798451459E0	0.2977369915137942E0	-3.3586723722751843E0	33.45462163289386E0	112.36311340332031E0
Sb06g001960	973.8639755249023E0	0.003537254381894017E0	0.03862923849006036E0	2.850668960382451E0	2.850668960382451E0	240.31874593098956E0	84.3025924397787E0
Sb06g002080	84.43966364860535E0	3.648022304641822E-4	0.015591555447884785E0	4.748624834246368E0	4.748624834246368E0	23.25033067096352E0	4.896223942438759E0
Sb06g002790	232.012275695890078E0	0.00254437430934391E0	0.03302460287415353E0	2.687385778308637E0	2.687385778308637E0	56.36314489746094E0	20.9735107421875E0
Sb06g002880	43.93865746673584E0	0.005650506661198123E0	0.048209907463216906E0	2.7955717222446377E0	2.7955717222446377E0	10.787012100219727E0	3.8586068163381348E0
Sb06g003290	409.44108390808105E0	1.1097853701759988E-4	0.011303471493304145E0	3.7402229018310456E0	3.7402229018310456E0	107.6883906028623E0	28.79197110286348E0
Sb06g003310	15.92153513431549E0	0.002518052708649033E0	0.02538164645840842E0	5.740170435688781E0	5.740170435688781E0	4.519783099492391E0	0.787395278612727E0
Sb06g003340	91.83953189849854E0	0.001694372577331463E0	0.02128845621104334E0	2.9993684534197955E0	2.9993684534197955E0	22.95867443084718E0	7.654502868652344E0
Sb06g003780	63.97434200424194E0	0.003405838428567426E0	0.03579072744186396E0	6.2809452938767E0	6.2809452938767E0	15.53149067170611E0	5.793289105097452E0
Sb06g004040	59.39917039871216E0	1.9628292215019585E-4	0.012312670869368433E0	4.085912580537916E0	4.085912580537916E0	15.906671206156412E0	3.8930522608099727E0
Sb06g004980	76.3374490737916E0	0.005855154455628747E0	0.048050485662129933E0	2.3676553011648050E0	2.3676553011648050E0	17.3897611915181477E0	7.55949427492032E0
Sb06g013250	394.37179946899441E0	2.77796457008445E-4	0.014027248659543077E0	0.3480160906248099E0	-8.73430358362612E0	33.93820175862625E0	97.51906331380208E0
Sb06g013760	234.77312183380127E0	3.19384977092859E-4	0.014916355761341811E0	0.31618653780806787E0	0.31618653780806787E0	18.79979228973388E0	59.45791498819987E0
Sb06g013910	126.1054562338989E0	0.0038648545267182874E0	0.04030912171372578E0	2.499603634908594E0	2.499603634908594E0	30.0237483978271E0	12.011403719584148E0
Sb06g013930	288.6415562493036E0	0.0549312397538347E-4	0.016725661127861533E0	4.142748672770693E0	4.142748672770693E0	77.505205720181E0	18.708642959594727E0
Sb06g013980	539.3198661804199E0	0.001069772624929022E0	0.02305739187064212E0	0.34689953991640263E0	-2.8827133551205137E0	46.30094273885092E0	133.47234589795572E0
Sb06g013990	785.7378902435030E0	0.005118943667714588E0	0.04572842007857276E0	0.31042185503485825E0	-3.221422666544232E0	62.04368782043457E0	199.8689422607422E0
Sb06g014420	221.55124473517177E0	0.002518052708649033E0	0.03281249418014317E0	2.3160409215101994E0	2.3160409215101994E0	51.57975641886392E0	7.2670658493041992E0
Sb06g014670	53.3253398187256E0	3.092261675113392E-0	0.00526487845394354E0	6.082475122074302E0	6.082475122074302E0	65.9907395426433E0	10.850035985310875E0
Sb06g015600	59.839091062545776E0	0.0011974638690619255E0	0.024271998140276477E0	5.530994056999378E0	5.530994056999378E0	16.892255306243896E0	8.4501038812713623E0
Sb06g015670	42.31147086620341E0	4.681426509962367E-0	0.008163359083053121E0	11.971461161140073E0	11.971461161140073E0	13.01652717590331E0	1.087296446104479E0
Sb06g016340	482.9938163757324E0	9.8322747685595070E-4	0.02330804921512414E0	4.032759660353591E0	4.032759660353591E0	129.00794728597003E0	31.989991565400736E0
Sb06g016430	59.99667205810055E0	0.0059346071256517925E0	0.04936294285539239E0	2.359777753515188E0	2.359777753515188E0	22.934358598601754E0	9.71886380513509E0
Sb06g016540	37.25043718333024E0	1.8881338790470805E-0	0.012265248551354766E0	11.635711697026917E0	11.635711697026917E0	11.434135189593138E0	0.98276040973536E0
Sb06g017050	73.19849872589111E0	0.0016325799818072E-0	0.017231561461398921E0	0.28104598213386384E0	-3.58136616675396E0	5.352954864051953E0	19.046544710795088E0
Sb06g017280	32.803354635238167E0	0.005713659826652938E0	0.048342892369489713E0	2.70275465406084E0	2.70275465406084E0	7.90076828002938E0	2.9377719561258955E0
Sb06g017290	90.79740810394287E0	0.004184869004401563E0	0.04189871139492503E0	3.2229631952303005E0	3.2229631952303005E0	21.57726287841797E0	9.108076413472492E0
Sb06g017690	110.2783465305347E0	0.0041640809736866748E0	0.03091930087998481E0	2.7593040234552015E0	2.7593040234552015E0	26.9811897277832E0	9.7825911839803E0
Sb06g017930	52.85271239280701E0	0.0054321085583513475E0	0.047390006897949186E0	3.06268122065474E0	3.06268122065474E0	13.281131426493324E0	4.336439371109009E0
Sb06g018000	1252.1789093017578E0	7.1629494126745696E-4	0.019832269143905444E0	8.292937617775871E0	8.292937617775871E0	38.385691323486975E0	109.0972728428281E0
Sb06g018040	24.870406985282898E0	0.003967520550401981E0	0.0408177601817445E0	0.9799969701714E0	0.9799969701714E0	6.267164382923985E0	0.20292772468567E0
Sb06g018190	149.068823239476E0	6.959881565677577E-4	0.019634833687139856E0	3.6929201873999E0	3.6929201873999E0	31.616623433403988E0	6.330636177368164E0
Sb06g018375	197.4440221786499002E0	0.004802190963875186E0	0.0444565900798171E0	2.287664910004939E0	2.287664910004939E0	45.79512405395508E0	10.01828320821265E0
Sb06g018610	135.36134719848633E0	6.611024290915237E-4	0.019428283869416807E0	3.5389226734727355E0	3.5389226734727355E0	35.17966524795929E0	9.940783818562828E0
Sb06g018790	59.76353430747986E0	0.005472589323429503E0	0.0474534590667936E0	2.9379144937095294E0	2.9379144937095294E0	14.86236381530761E0	5.05881142818569E0
Sb06g019100	2320.1943969726526E0	0.00428725092581838E0	0.024228864352339475E0	2.48934287719391E0	2.48934287719391E0	55.1752498535156E0	221.64578247070312E0
Sb06g019130	247.17796897888184E0	0.0017687871053014473E0	0.028735713267710114E0	4.029925209471577E0	-2.3259859576178457E0	27.72400538126632E0	57.62052587816731E0
Sb06g019430	111.60403394969097E0	0.003547098862140204E0	0.03862923849006035E0	2.878528795170095E0	2.878528795170095E0	27.60973230997721E0	9.591612339019775E0
Sb06g019520	20.76558437943546E0	7.175155427851023E-4	0.019832269143905444E0	10.181775838848575E0	10.181775838848575E0	6.30283805505167E0	0.61930630407598515E0
Sb06g019700	267.1608533859253E0	1.8116011890946844E-4	0.012265448501354766E0	4.590895786114604E0	4.590895786114604E0	13.7252848037916E0	15.928332964579255E0
Sb06g020045	79.249089241027891E0	0.00497115737964480919E0	0.04395818364985231E0	0.4483434303313695E0	-2.2304330158401386E0	8.17734432220459E0	18.2390187813802E0
Sb06g020420	51.17830562591553E0	8.099911273990979E-0	0.00526487845394354E0	9.194146685432038E0	9.194146685432038E0	15.89598124186197E0	1.673458967755296E0
Sb06g020460	21.90722754592899E0	0.0046400055167519815E0	0.0367947845479936E0	4.811193027294888E0	4.811193027294888E0	6.0457982223917E0	1.256611029307107E0
Sb06g020560	1646.2135620117188E0	0.0021170276792417857E0	0.03064542071836537E0	6.239748527788821E0	6.239748527788821E0	39.79528076171875E0	15.266735232421875E0
Sb06g020950	50.678553342819214E0	0.003394963163961881E0	0.03783849117136447E0	0.6019378616683198E0	0.6019378616683198E0	12.68449815114339E0	4.875019629796347E0
Sb06g021120	62.56885954093933E0	0.0031259325896844033E0	0.03625387395015434E0	2.629105379566407E0	2.629105379566407E0	14.61139061116539E0	5.55755519196537E0
Sb06g021410	144.0378698686609E0	6.639929617775749E-4	0.019428283869416807E0	0.285618829306012E0	-3.5011697317683645E0	10.66664309641525E0	37.34587224325444E0
Sb06g021600	805.0754699707031E0	0.00338432777979221E0	0.037822899147166314E0	2.435387006787701E0	2.435387006787701E0	190.2425486246745E0	78.1159413655599E0
Sb06g021690	16.88054019212722E0	0.0016345976153458604E0	0.02754528298240787E0	5.161931153550135E0	5.161931153550135E0	4.70665508670044E0	0.919991672039032E0
Sb06g021740	128.58432388305664E0	7.435479086504125E-4	0.02002840620352167E0	2.867312182266468E0	2.867312182266468E0	31.778436023498373E0	11.083005269368488E0
Sb06g021780	137.68712520509365E0	3.714758365100034E-0	0.009726449821406513E0	5.26236184046658E0	5.26236184046658E0	35.5578053792317E0	1.079978640745707E0
Sb06g021840	375.062198638916E0	0.0015806528496798416E0	0.027115881418877432E0	7.173802016009355E0	7.173802016009355E0	31.36920878092425E0	33.66381201054622E0
Sb06g021850	2952.9468841552734E0	0.004852583445736973E0	0.04471069406853063E0	2.4055433093612635E0	2.4055433093612635E0	695.282672526024E0	49.0333607991537E0
Sb06g022050	595.4347229003906E0	0.004509293941610001E0	0.0430828092570685E0	2.4084370737095983E0	2.4084370737095		

Sb06g029580	180.77094650268555E	0.003929375796576828E	0.04068897111092962E	2.7806590740508415E	2.7806590740508415E	44.318760553995766E	15.938221613566082E
Sb06g029660	70.46693110466003E	9.3408866921768875E-4	0.022186681490138973E	0.30390972968909524E	-3.2904500745160803E	5.474711656570435E	18.014265378316242E
Sb06g030050	126.00321435928345E	0.005498706044658547E	0.04760058942941569E	2.3097964614774897E	2.3097964614774897E	29.31102416981656E	12.69002930323283E
Sb06g030070	44.382150650022444E	0.0015640329591207387E	0.02693390680275127E	3.94548080996969E	3.94548080996969E	11.50317859646852E	3.2908716201782227E
Sb06g030160	112.20790886878617E	1.1444547489719567E-5	0.00594834062269444E	4.83578173469599E	4.83578173469599E	33.43872133890787E	9.3693149056886753E
Sb06g030920	286.3475497930908E	0.005616121134000205E	0.048105211912816555E	2.3443555124874345E	2.3443555124874345E	66.90878041585286E	28.540372848510742E
Sb06g031080	208.74373817443848E	0.002434096299454242E	0.03286550374227295E	2.295751247472404E	2.295751247472404E	48.4668377380371E	21.112408320109474E
Sb06g031410	524.5711364764094E	0.0023011801335028930E	0.031648173751064813E	0.4491664549924047E	-2.22635557038619E	54.19646199544269E	120.66058349680375E
Sb06g031530	93.85164411781311E	3.126825972768416E-4	0.014849533340252694E	3.2183093868919888E	3.2183093868919888E	23.86766751607259E	7.4162128766377755E
Sb06g031600	288.060481033325E	4.1621138939801254E-4	0.00794505306772329E	4.820149222168155E	4.820149222168155E	79.52215449015299E	16.49786154429117E
Sb06g031680	472.3957691192627E	2.2514504835355738E-4	0.012853047388634297E	3.8735410871454032E	3.8735410871454032E	125.15502166748047E	32.3102407056071E
Sb06g031756	87.29788208007812E	0.004787891682150155E	0.0443990734185111E	2.2462195660035884E	2.2462195660035884E	20.13523801167806E	8.96456015014648E
Sb06g031820	68.2924735546112E	0.003205304355828002E	0.03675072764957985E	2.735376119615958E	2.735376119615958E	16.66959014733805E	6.094207684199013E
Sb06g031830	16.140704691410065E	0.0059787577367118E	0.04962920949705624E	3.82504820975208E	3.82504820975208E	4.26517148389869E	11.55043447469993E
Sb06g031980	426.30118560791016E	4.2397906401345074E-4	0.01658075441846592E	2.947579552954552E	2.947579552954552E	106.10355377197286E	35.9684143066400E
Sb06g032260	14.986514568328857E	0.003298561478341829E	0.007291490113098729E	4.6519723590324525E	4.6519723590324525E	4.111662348469035E	8.838516076405845E
Sb06g032280	180.49888467786969E	2.643017320631515E-4	0.032732983547975973E	4.935533487087376E	4.935533487087376E	5.100296690063476E	10.16627991994224E
Sb06g032390	34.21982383728027E	0.00499354093039985E	0.045228171453769415E	0.294724590869796E	-3.392998178566585E	2.5965428352355957E	8.180065110524494E
Sb06g032480	573.0328559875488E	7.461226747134928E-4	0.020026406230525137E	2.555361784393121E	2.555361784393121E	37.28619384765625E	53.72475814819336E
Sb06g032670	120.87157622628784E	0.004669602161839722E	0.04373144578215444E	2.5662620489903347E	2.5662620489903347E	28.96106566392415E	11.32949591036852E
Sb06g032740	53.05464166242352E	0.0016617683299266742E	0.0279114549374927187E	7.610156192097153E	7.610156192097153E	15.63092470160967E	2.0539585331171666E
Sb06g032770	118.06093978881836E	4.292175716684785E-4	0.016596091736717763E	4.044514559289082E	4.044514559289082E	31.552371342976883E	7.80127525328989E
Sb06g032800	407.0291290283203E	4.8817762773135295E-4	0.017098183684643886E	2.8904979381137323E	2.8904979381137323E	20.8904979381137323E	34.8731840006515E
Sb06g033000	100.541267764893E	0.0026309994254537085E	0.03253647510919661E	2.5878516756886074E	2.5878516756886074E	23.68547821044922E	9.15256404876709E
Sb06g033080	903.6215629577637E	2.26737065668098E-5	0.003732983547975973E	5.176158357591586E	5.176158357591586E	280.374097833923E	54.16644159952796E
Sb06g033120	84.59130382537842E	2.450221789447682E-4	0.013321350227666156E	3.3760996502836678E	3.3760996502836678E	23.75366910298652E	6.44332172139486E
Sb06g033230	99.32871198654175E	0.002602172114158586E	0.033147593562881515E	2.461252736523141E	2.461252736523141E	25.34379399671513E	9.56577666005451E
Sb06g033275	42.56566643714905E	8.233270133063153E-5	0.010142537086333833E	5.394163745330312E	5.394163745330312E	11.9995701599121E	2.2189853191375732E
Sb06g033280	108.27852821350098E	0.0012142711256401444E	0.024405375064643773E	2.7106373118548404E	2.7106373118548404E	26.36598495879557E	9.726858139038082E
Sb06g033410	146.3060064315796E	0.002004159102322022E	0.03007592565064654E	2.31435332242783E	2.31435332242783E	34.054284413655594E	7.14138439687036E
Sb06g033440	215.8662807647705E	0.001543127722180361E	0.02689182336506542E	2.67736132184913E	2.67736132184913E	52.38827387491862E	15.5671286817240395E
Sb06g033600	167.92992877920245E	0.001693369234839598E	0.028128845621104334E	2.5948653493076095E	2.5948653493076095E	40.405366291800125E	15.571276664733867E
Sb06g033610	15.78802469372493E	0.005371963419710466E	0.04570225834077474E	4.7842270179676465E	4.7842270179676465E	4.35284287242635E	9.09832010665287E
Sb06g033720	658.6140747070312E	9.4804705015946002E-5	0.01101430796083056E	3.4444470529942683E	3.4444470529942683E	17.104199829011562E	49.39602661132612E
Sb06g033780	52.2576751708984E	0.002377330203996187E	0.03198812012146021E	2.7834131782815024E	2.7834131782815024E	129.2991180419922E	46.4534034807296E
Sb06g033820	228.1678978686213E	0.00148661047052895E	0.02652142626120936E	6.851926873267818E	6.851926873267818E	90.5665620422363E	16.34934211999105E
Sb06g034050	66.99332642555237E	1.9311038472025527E-4	0.012312670869368433E	3.9661251301730487E	3.9661251301730487E	17.8344221151123E	4.49668669700622E
Sb07g000099	157.4093284606933E	0.0044909191014426515E	0.03402873601871603E	2.2562896620471613E	2.2562896620471613E	36.35641332356125E	16.11336263028336E
Sb07g000330	108.538413119965E	0.010064191388862E-5	0.00816335908330513E	14.420226651534854E	14.420226651534854E	33.832113907174086E	2.346116575292461E
Sb07g000500	73.68014907836914E	2.7411457929870633E-4	0.01402724865943077E	8.9012497821534E	8.9012497821534E	21.99907084362175E	2.560972849527924E
Sb07g000510	184.45411562919617E	3.480389124370156E-6	0.00526487845934356E	7.969508223234675E	7.969508223234675E	54.6298472685587E	6.854858001073197E
Sb07g000970	65.23025107383278E	0.0022684951942998667E	0.03147726312397627E	2.755307846351964E	2.755307846351964E	15.953367869059246E	5.79004915555318E
Sb07g001320	504.3011474609375E	0.0013086450512721E	0.025199647499499835E	2.4075696470327563E	2.4075696470327563E	11.7869234415699E	49.331459045410156E
Sb07g001580	138.26377201408322E	0.002641737191047695E	0.03253647510919661E	2.330752671383829E	2.330752671383829E	32.25083414713542E	13.83702895646566E
Sb07g001930	53.11621746420866E	9.706735662121783E-4	0.02235095626129936E	5.193557749374061E	5.193557749374061E	14.82158152623697E	2.88382499791769E
Sb07g002070	125.1872493286133E	7.201212322789574E-4	0.019865892681981273E	2.7484630454128487E	2.7484630454128487E	30.59677124023475E	11.13232404052734E
Sb07g002350	54.25039291381836E	0.0065084445863938E	0.0498537638464567E	2.4127564157096435E	2.4127564157096435E	12.78467877058918E	5.198785527547201E
Sb07g003000	4253.7049711313477E	9.0282242415116089E-4	0.02189035678110884E	4.745206212570199E	4.745206212570199E	1171.104390820312E	4.745206212570199E
Sb07g003350	155.65249729156494E	0.0020163293259877436E	0.03007592565064654E	2.3808147310486643E	2.3808147310486643E	36.53750200973894E	54.3664657311605E
Sb07g003500	470.4431953403107E	0.0043069314729132947E	0.03848310936779088E	2.495623931621024E	2.495623931621024E	11.95419565865688E	14.84020278930616E
Sb07g003505	35.97500133514404E	0.0024420144665059593E	0.03235106904181626E	3.1888141601764457E	3.1888141601764457E	9.12888383665356E	2.86278327360117E
Sb07g003740	24.361822962760925E	0.003886805061872474E	0.04031723963104133E	3.4963397152593845E	3.4963397152593845E	3.1455914179484E	8.16031455912458801E
Sb07g003750	120.69205856327242E	0.005596422892278779E	0.04806396587498945E	3.4038231043469233E	3.4038231043469233E	31.095286051423293E	9.135400136311848E
Sb07g004110	315.25293502193727E	0.0031249114109488100E	0.036253837395015434E	2.81851359590322E	2.81851359590322E	77.54662097163992E	27.519690196719406E
Sb07g004180	437.9268684387207E	0.004498775293575824E	0.04305927591774851E	2.512458928978141E	2.512458928978141E	10.41624609213867E	41.559382120768234E
Sb07g004330	294.4051170399112E	0.002598637075704711E	0.033147593568288155E	0.41630833090681133E	0.41630833090681133E	28.845702926920563E	69.2893180847168E
Sb07g004600	21.23763942718506E	4.829701893079775E-5	0.00816335908330531E	4.883319656417458E	4.883319656417458E	58.44438044230143E	11.988166033426918E
Sb07g004650	22.8547326924167E	0.002598429573160996E	0.033147593568288155E	4.152472108011014E	4.152472108011014E	6.139683246612549E	1.4785609841208994E
Sb07g004970	58.55946489306846E	0.00400448459495065E	0.04115750474334912E	2.7119631721366977E	2.7119631721366977E	20.260119677257485E	5.258624791359878E
Sb07g005020	181.61950778961182E	0.002722886210778821E	0.0337685679474677E	2.346631871219403E	2.346631871219403E	42.4500554026693E	18.08978040963016E
Sb07g005390	1648.1836547581562E	1.0262104067203888E-4	0.01128530557535344E	3.7150718094962873E	3.7150718094962873E	432.87542594401E	15.61890090650767E
Sb07g005596	85.66471576809674E	0.001117368729979024E	0.02355044126254062E	3.63289370873512E	3.63289370873512E	12.21824099228188E	6.436664263407387E
Sb07g006090	83.15027618408203E	0.0011423308817733					

Sb07g024770	13.880233347415924E0	0.003879063915105314E0	0.040422036055794E0	4.2337862738597485E0	4.2337862738597485E0	3.742729663848877E0	0.8840147852897644E0
Sb07g024810	17.58850407600403E0	0.0028631051562384895	0.0347155575776516E0	4.464218813676602E0	4.464218813676602E0	4.78988448777883E0	0.1729502042134604E0
Sb07g024970	53.90496349374171E0	0.00257674497412852670	0.0314759366288151E0	2.676784753072988E0	2.676784753072988E0	13.081355412801106E0	4.886965751647949E0
Sb07g024990	42.48131073158264E0	0.00137705547340471220	0.0256225197799252E0	0.251654522383785E0	0.251654522383785E0	-9.373032582997616E0	2.8470947345097866E0
Sb07g025220	1720.1088562011719E0	3.81218277364082E-4	0.015746746627701945E0	3.811932822753936E0	3.811932822753936E0	454.2383669992121E0	11.131500623209635E0
Sb07g025350	473.04634857177734E0	0.00389319485620296E0	0.04042285842247165E0	2.1816654089460013E0	2.1816654089460013E0	108.12250010172525E0	49.5596160886719E0
Sb07g025680	558.3889617919922E0	0.004567867227180176E0	0.04334146777981120E0	2.3092714563439722E0	2.3092714563439722E0	129.88475036621094E0	56.24490356453215E0
Sb07g025830	44.902358293532680E0	0.000331064801064032260	0.0371970621760142E0	3.0194654764148487E0	3.0194654764148487E0	11.24371067682901E0	3.723472086880502E0
Sb07g026010	171.93205928802429E0	0.002077263918919461E0	0.030462679345604895E0	2.825378431863698E0	2.825378431863698E0	42.328982671101188E0	14.98077358239746E0
Sb07g026190	130.58894062042336E0	0.00025852243678738E0	0.04539329477049379E0	2.6793677704547307E0	2.6793677704547307E0	31.69890549482422E0	11.310740928649902E0
Sb07g026200	288.22655296325684E0	0.00454553432011926E0	0.04321735557844237E0	3.1168413949577882E0	3.1168413949577882E0	72.33832575480144E0	23.337191899617515E0
Sb07g026240	178.98047828674316E0	0.004852901903129639E0	0.044671069409666336E0	2.541468722999325E-4	2.541468722999325E-4	18.851232526886523E0	40.80982690022786E0
Sb07g026250	62.87512016296387E0	0.003459819478741856E0	0.03835029546960014E0	2.495545772383536E0	2.495545772383536E0	14.962636311848957E0	5.99573705805664E0
Sb07g026270	244.19256496429443E0	7.659095592595367E-6	0.00526487845394354E0	6.928457147273493E0	6.928457147273493E0	71.13101959229251E0	10.66250262479645E0
Sb07g026890	34.6141035567932E0	0.0011795832707093870	0.0241085546977492724E0	4.66358574290083E0	4.66358574290083E0	9.500803120270133E0	2.037213658396406E0
Sb07g026900	39.96809720993042E0	0.0021039828517461444	0.03061072133549124E0	4.87232624684349E0	4.87232624684349E0	11.053975825316977E0	2.26872698465983E0
Sb07g026920	1995.5748901367188E0	5.563614434167396E-4	0.018218545921523017E0	3.1669185110633857E0	3.1669185110633857E0	505.5552876790364E0	159.63632436653644E0
Sb07g027080	61.369590528488159E0	0.0016899434805386840	0.028128845621104334E0	2.774161614431044E0	2.774161614431044E0	15.03547509513119E0	5.41982666514078E0
Sb07g027190	35.47410464268604E0	0.00353175211357367170	0.0386280389024674E0	3.6121076133796923E0	3.6121076133796923E0	9.260862509409588E0	2.5638390382130947E0
Sb07g027200	162.63014888766374E0	0.002859682675675420	0.034719479691453E0	3.878643793627195E0	3.878643793627195E0	43.09834402856445E0	11.1170482635498E0
Sb07g027420	254.2485809326132E0	0.004841081123635605E0	0.044671069409666336E0	2.446451276987202E0	2.446451276987202E0	83.2064056396448E0	34.2622194690755E0
Sb07g027460	76.45480680465699E0	0.004868089719417812E0	0.04470584891054333E0	2.416958823462542E0	2.416958823462542E0	18.026572002237953E0	7.458365599314369E0
Sb07g028080	51.244556188583374E0	0.0029417566726314E-4	0.02227128095972276E0	3.4104687768779796E0	3.4104687768779796E0	13.2085016245524E0	3.8729486707255E0
Sb07g028140	265.096643447876E0	0.002518915753367184E0	0.03281249418014317E0	2.3008375198718922E0	2.3008375198718922E0	61.59490303139972E0	26.770644505818687E0
Sb07g028230	54.21910572005200E0	0.00654612458883753E0	0.0498537638465467E0	2.3766320163010985E0	2.3766320163010985E0	12.7206500312972E0	5.352385203043619E0
Sb07g028610	171.13289833068848E0	0.0011558952127909273	0.02397350158313839E0	2.59872640844137E0	2.59872640844137E0	41.19305292765299E0	15.85124651509832E0
Sb07g028620	38.11944472087644E0	7.743118206212207E-4	0.020302598012251823E0	6.609294998227543E0	6.609294998227543E0	11.03661839167277E0	1.66986318429311E0
Sb07g028710	296.1382722854614E0	6.71751131932355E-4	0.019431829302253747E0	3.0014934339613583E0	-3.316821818839901E0	22.86699835459391E0	75.84575907389322E0
Sb07g028760	80.23943422424854E0	0.00588841506027895E0	0.04926548665772026E0	2.930049150636366E0	2.930049150636366E0	19.94084358215332E0	8.00636498596191E0
Sb07g029020	95.66543626785278E0	0.003147105917704839E0	0.03641469141494102E0	2.751928782866729E0	2.751928782866729E0	14.5791076133796923E0	5.808687875417074E0
Sb07g029085	24.88324018977356E0	0.00164013047290351550	0.02760596203523247E0	3.854421328483124E0	3.854421328483124E0	6.5857828458105225E0	1.7062307605107262E0
Sb07g029110	384.68520164489746E0	0.00259208923666418580	0.03314759366288151E0	2.339268539423583E0	2.339268539423583E0	83.5826350982022E0	38.9257489217128E0
Sb08g000260	41.41921269893461E0	0.0029458248779961930	0.035138428656251524E0	2.9340862422370195E0	2.9340862422370195E0	10.2969732845459E0	3.509431050424231E0
Sb08g000280	55.4252939399696E0	0.00494217272843173660	0.03512418403449417E0	2.9141220120806692E0	2.9141220120806692E0	39.07510206021985E0	13.40809663645508E0
Sb08g000480	227.7780246734619E0	4.299389122481382E-4	0.016596091736717763E0	2.7768809301919295E0	2.7768809301919295E0	55.823147492514976E0	20.1028342697233E0
Sb08g000540	367.098735809326E0	0.001961799574862116E0	0.02984845218022362E0	2.6253329783071628E0	2.6253329783071628E0	88.61314016021117E0	33.7510516357422E0
Sb08g000910	57.28657126426697E0	0.002756887926039955E0	0.03402066361235834E0	3.5153132159846057E0	3.5153132159846057E0	14.86646525065104E0	4.229058504104614E0
Sb08g001160	1187.208377831348E0	6.287015703882647E-4	0.00526487845394354E0	6.538209088789273E0	6.538209088789273E0	343.23875935872394E0	52.97366587320926E0
Sb08g001550	116.9746742824352E0	0.005712587835342784E0	0.04834289236898713E0	2.333582176197707E0	2.333582176197707E0	22.9496336669929E0	11.6965942382125E0
Sb08g001630	53.25479028298247E0	0.00184567051312324940	0.029207786869473128E0	3.5996572931039736E0	3.5996572931039736E0	13.982266591389975E0	3.85933036528477E0
Sb08g001860	17.7855562932129E0	0.004834302017229565E0	0.0446555758411861E0	2.1189113955412675E0	2.1189113955412675E0	37.9964487467448E0	17.32006405639648E0
Sb08g002660	1034.6836417557617E0	0.00124635493271827810	0.024797721507651995E0	5.08480293445265E0	5.08480293445265E0	56.7652943929037E0	11.46258799235028E0
Sb08g002670	1243.2781125713935E0	0.00180865954849878150	0.02891018203624539E0	5.289498567185035E0	5.289498567185035E0	376.56778971354163E0	17.1915854077148E0
Sb08g002700	1236.88990316162E0	0.00110109538769332430	0.02337987086201724E0	8.086313951214914E0	8.086313951214914E0	366.92109711549475E0	45.3755683899258E0
Sb08g002740	62.2371590137481E0	0.00373663938939522740	0.03977363157128064E0	2.627994896765999E0	2.627994896765999E0	15.0274868601147461E0	5.718232870101929E0
Sb08g002890	534.4709587097168E0	0.001928243173090847E0	0.02962859671340667E0	2.548061887373809E0	2.548061887373809E0	127.944506327311E0	50.21247990262106E0
Sb08g002990	16.8638495206832E0	7.54081541155858E-4	0.020066713637082536E0	0.158680012750556E0	-6.301990922904145E0	0.7698288361231489E0	4.851445307347617E0
Sb08g003130	48.10077867507935E0	9.392409457392936E-4	0.02221445553997524E0	4.073534869269552E0	4.073534869269552E0	42.106194953826747E0	26.19495952826747E0
Sb08g003250	250.57517890903107E0	0.001901747732064093E0	0.02987810858394805E0	4.3171665173362095E0	4.3171665173362095E0	59.11540476881198E0	24.30965487162227E0
Sb08g003320	19.2667311699136047E0	4.650975931171245E-4	0.01686863708884206E0	4.331305689901725E0	4.331305689901725E0	1.868824988012695E0	7.8167327644200796E0
Sb08g003440	160.20135116577148E0	1.6038192283730104E-4	0.01212822798451459E0	3.260198967022171E0	3.260198967022171E0	40.865718841552734E0	12.53473154037762E0
Sb08g003510	112.4551682472299E0	0.00462872962278089E0	0.0436797845479936E0	2.7697735352111734E0	2.7697735352111734E0	25.54141700780234E0	9.94358011627197E0
Sb08g003960	160.3203935623169E0	8.212377559120401E-0	0.01421253708633833E0	7.3149791637994145E0	7.3149791637994145E0	42.106012980143234E0	11.334118207295738E0
Sb08g003963	50.99310636520836E0	0.004901552121011375E0	0.0448418451296578E0	2.8534142420774167E0	2.8534142420774167E0	12.866263147274788E0	4.411071950986734E0
Sb08g004010	15.571193143725395E0	0.00419063330158761950	0.0419063330158761950	0.1271204959094499E0	0.1271204959094499E0	-7.866530181459684E0	0.5853922118743258E0
Sb08g004070	155.2361356287881E0	4.87313633286087E-6	0.00526487845394354E0	7.54168566342748E0	7.54168566342748E0	45.68739638739095E0	6.05798212687170E0
Sb08g004400	19.545610070228577E0	0.005098329954984241E0	0.04932756930374224E0	3.576715470033582E0	3.576715470033582E0	5.09164897600898E0	1.4235543807347617E0
Sb08g005180	173.38299889700317E0	2.4447841513474784E-4	0.013321350287666156E0	3.943936393037044E0	3.943936393037044E0	40.1643841004110805E0	11.689949194590248E0
Sb08g005280	31.847634315490723E0	0.00350054629975181980	0.038509851421973E0	3.510938073538924E0	3.510938073538924E0	8.262513319651287E0	2.353364785512289E0
Sb08g005340	11.27650284767151E0	0.01472060805986472330	0.02840343087839529E0	5.50563986912049E0	5.50563986912049E0	31.42729825887047E0	5.66243879000346E0
Sb08g006190	106.7801062740935E0	0.00226851674944740420	0.03147726				

Sb08g022210	613.5702209472656E0	0.0025726698070579067	0.033147593562881515E0	2.2582354720707225E0	2.2582354720707225E0	141.75218963623047E0	62.771217346191406E0
Sb08g022260	86.650158821211411E0	0.002933619810640715E0	0.03215343678083363E0	2.4234105026969406E0	2.423410526969406E0	20.446356246545312E0	8.437020937601726E0
Sb08g022730	23.76249923121869E0	5.009720194573464E-4	0.018251783239475343E0	4.6825056632770415E0	4.6825056632770415E0	6.526993510055447E0	1.39389790517477E0
Sb08g022730	16.6770989388257E0	0.00443320150551325E0	0.0428190889890546E0	2.3159525443694746E0	2.3159525443694746E0	18.198197628698567E0	7.857709316762289E0
Sb08g023070	21.1667015612125397E0	0.0016621923385628438	0.027911549374927187E0	4.932549018468636E0	4.932549018468636E0	6.0049254918468636E0	1.217408948336286E0
Sb08g023070	254.77397346496582E0	0.0024745523573390725	0.03262117452617652E0	2.381387417263556E0	2.381387417263556E0	59.809328715006515E0	25.115329106648765E0
Sb08g023190	110.10697304965271E0	2.746214793622398E-4	0.014027248659340377E0	0.18329920248752302E0	0.455590870118158E0	5.685354789098909E0	31.071969860786133E0
Sb09g000240	82.75449082535596E0	5.64501390649873E-4	0.018251783239475343E0	3.0221674361951707E0	3.0221674361951707E0	20.276629892685027E0	6.858203091133627E0
Sb09g000330	142.19289875030518E0	0.001055336852606669	0.022958361530251034E0	3.935215508790885E0	3.935215508790885E0	37.79366874694824E0	9.603964106820152E0
Sb09g000530	108.13276839256287E0	3.1540433780780764E-4	0.014849533340252694E0	8.93252418543809E0	8.93252418543809E0	32.1658292272542E0	3.8784271128861E0
Sb09g000580	133.39027214050293E0	0.0014453264597434575	0.026110891415592932E0	2.560695325914357E0	2.560695325914357E0	31.97613716125488E0	12.487286885579426E0
Sb09g000680	165.46336936950684E0	7.008995921452775E-5	0.00972413234714578E0	3.4502406477341E0	3.4502406477341E0	47.6086680094401E0	12.935895555827E0
Sb09g000840	36.80981273204088E0	0.004816154499266985967	0.02735163442240553E0	8.662634000186571E0	8.662634000186571E0	11.00103955040088E0	1.269833628464736E0
Sb09g000890	66.64736938476562E0	0.004891071746726166E0	0.04483220991707306E0	2.461947514995864E0	2.461947514995864E0	15.79865280470866E0	6.417136510213217E0
Sb09g001070	975.9683294296265E0	4.478907275605512E-4	0.016711118790705882E0	6.958507212582729E0	6.958507212582729E0	165.8479640622394E0	27.67483743031871E0
Sb09g001080	242.02833652496338E0	3.286218493104947E-7	0.002219824211332348E0	23.1361802699687E0	23.1361802699687E0	77.33357365926106E0	3.32538515726716E0
Sb09g001083	1128.328628540039E0	1.8488264786482813E-5	0.00604932594970985E0	7.7419759077735595E0	7.7419759077735595E0	333.0861409505208E0	43.02340186158816E0
Sb09g001320	2211.7618713378906E0	0.0025002794062637603	0.03267262838983149E0	3.9568796347414708E0	3.9568796347414708E0	588.5204077294921E0	148.73347981770837E0
Sb09g001440	557.54113716935125E0	6.929386907364647E-4	0.019630015931666595E0	5.258103739826351E0	5.258103739826351E0	142.20156001590506E0	8.24590506842425E0
Sb09g001530	38.695945397888E0	6.251135772860804E-4	0.019142029980412797E0	6.3395363575154535E0	6.3395363575154535E0	11.44227881113688E0	1.7574199835459385E0
Sb09g001690	55.387613654136363E0	1.7221097592429863E-4	0.01212822798451459E0	6.062209369266586E0	6.062209369266586E0	15.184286647888184E0	2.614272368240356E0
Sb09g001850	125.29786109924316E0	0.0015911612076168306	0.0271332859668796E0	3.3321995070068E0	3.3321995070068E0	32.12513415018717E0	9.640819549650547E0
Sb09g001860	192.9994354248047E0	2.43482546133738E-5	0.00732398354797597E0	1.0691537112133037E0	1.0691537112133037E0	580.07759187125E0	54.2557255347656E0
Sb09g001870	9311.707824707031E0	1.0897616702347958E-4	0.011303471493304145E0	5.391642707209281E0	5.391642707209281E0	26.18236914062495E0	485.6189116924268E0
Sb09g002000	60.34071898460388E0	0.005211532729695492E0	0.04621059081890412E0	0.3937126839649743E0	0.3937126839649743E0	5.681293254050734E0	14.31648952960285E0
Sb09g002150	136.8587746142676E0	0.003267122775191085	0.037123744323667934E0	4.088561494811688E0	4.088561494811688E0	22.445848011012874E0	32.38697687784305E0
Sb09g002225	396.9848251342734E0	0.002018464286578519E0	0.03007595256506465E0	3.031791458508077E0	3.031791458508077E0	99.50706481933592E0	32.82121022542317E0
Sb09g002260	430.67643547058105E0	0.00145521127426487E0	0.02622388223196102E0	2.466194529328999E0	2.466194529328999E0	102.141794540283203E0	41.41683642069499E0
Sb09g002390	53.21893572807312E0	6.120689174425952E-4	0.019014060191858008E0	4.191393455347702E0	4.191393455347702E0	14.322519302368164E0	3.417125940322878E0
Sb09g002510	575.9235191345215E0	0.0015294496813199816	0.02672687795469149E0	7.273725369173083E0	7.273725369173083E0	40.4705031920573E0	51.50397681616546E0
Sb09g002540	190.84381103515625E0	2.7017598484041154E-4	0.014027248659340377E0	3.130664518368385E0	3.130664518368385E0	48.214029947916664E0	15.4005737046857E0
Sb09g002640	62.520118713378906E0	0.0010733642830210324	0.02309963259594205E0	4.333866657217023E0	4.333866657217023E0	16.139353514432778E0	4.70075425669352E0
Sb09g002960	170.9054718017578E0	3.7247278442956784E-4	0.015659473501478307E0	5.818226042131709E0	5.818226042131709E0	48.611306173299156E0	8.35534247286781E0
Sb09g003150	2888.3162688208984E0	0.0014061645667168996	0.022848702755154988E0	0.2937330085735127E0	0.2937330085735127E0	218.5905624658203E0	744.181437147917E0
Sb09g003300	17.59010368558586E0	1.2053641964497847E-4	0.011481804126186082E0	10.573285896580634E0	10.573285896580634E0	5.356738408406578E0	0.506629486877159E0
Sb09g003440	69.19252794125894E0	0.00345076289089212857	0.03834478257668032E0	2.7818993730883106E0	2.7818993730883106E0	16.95606371561684E0	6.09856939317029E0
Sb09g003460	15.027909517288208E0	0.0014810349228504595	0.02645498630941633E0	6.92675890797399E0	6.92675890797399E0	4.37735470136006E0	0.6319484710693359E0
Sb09g003530	105.1899604797363E0	0.0013331428799719194	0.02538164645804804E0	3.0789934629877652E0	3.0789934629877652E0	94.2582664489741E0	254.13838704427081E0
Sb09g003580	77.69553184509277E0	0.002342892830861883E0	0.03179925966617042E0	7.1419375295337E0	7.1419375295337E0	18.9256204710405E0	6.9728485743204708E0
Sb09g003860	70.124456644058234E0	0.0056745671598080303E0	0.04823952548548772E0	2.4368965815939894E0	2.4368965815939894E0	16.573677698771156E0	6.801141182581581E0
Sb09g003950	433.7120056152534E0	0.00332976964506877E0	0.03737190672161042E0	5.211999736572991E0	5.211999736572991E0	103.40589654072003E0	41.864772033691406E0
Sb09g004020	1202.515510559802E0	0.002331355564107417E0	0.03175888561591541E0	5.207778022337673E0	5.207778022337673E0	286.56715390360406E0	114.27134958901991E0
Sb09g004060	268.5814418792724E0	4.532885997103462E-4	0.016726561127861533E0	3.060188575493876E0	3.060188575493876E0	67.477149633789E0	102.04999732971297E0
Sb09g004130	93.91815302176516E0	0.0032725956667125E0	0.037123744323667934E0	4.17293955182802E0	4.17293955182802E0	29.91299533843994E0	1.3930556774139404E0
Sb09g004200	369.5492115020752E0	0.002768085530862492E0	0.034070579014664090E0	2.278012838528043E0	2.278012838528043E0	85.60448964436848E0	37.57885805632324E0
Sb09g004450	1354.014591217041E0	1.3758222503780919E-4	0.011896419953009695E0	5.266917382110138E0	5.266917382110138E0	379.3190256754557E0	72.01917136989124E0
Sb09g004530	105.2832462044424E0	4.959365298986357E-4	0.0171844498952419653E0	3.015478962317323E0	3.015478962317323E0	26.35643205973307E0	8.73978328704834E0
Sb09g004670	93.51091766357422E0	0.00103288217913795554	0.022741176263988777E0	2.794431332945282E0	2.794431332945282E0	12.95555595994108E0	8.21475029891992E0
Sb09g004730	373.5671730041504E0	0.004072465179549486E0	0.04127380041747683E0	2.197359966395403E0	2.197359966395403E0	85.59720583099192E0	38.94318517049153E0
Sb09g004810	50.822558780643005E0	5.2323744892373305E-4	0.00816335908330531E0	6.3431074623267741E0	6.3431074623267741E0	14.66112168629894E0	2.279731233914694E0
Sb09g004860	45.056512713423231E0	0.005842160365311024E0	0.04894481735250406E0	7.98724282310807E0	7.98724282310807E0	11.06518459320084E0	3.956352979744200E0
Sb09g004990	59.30684733390808E0	0.001318721913839983E0	0.02532867761920378E0	3.17284442958759E0	3.17284442958759E0	15.03142547602419E0	11.725236352284755E0
Sb09g005000	176.4657030195908E0	0.004042653166894249E0	0.041175074432390914E0	2.141837631433858E0	2.141837631433858E0	40.0997682270194E0	18.72213268260293E0
Sb09g005080	95.8694929089078E0	0.0018541263519255347	0.0292444432320943E0	4.2795744228799E0	4.2795744228799E0	202.3287568961456E0	83.3328685030711E0
Sb09g005170	60.72151630773315E0	2.7411358564739574E-4	0.014027248659340377E0	3.720095287603466E0	3.720095287603466E0	19.352349344889324E0	4.28815611203511E0
Sb09g005250	57.35236525535835E0	0.002202970591972851E0	0.03116876213197912E0	2.666792656496112E0	2.666792656496112E0	15.90238284453454E0	5.21367224057155E0
Sb09g005330	125.18661057281494E0	3.99304047628431E-5	0.007945053016772329E0	5.0203317519784125E0	5.0203317519784125E0	34.782542775472E0	6.930327415466309E0
Sb09g005510	76.4292782897949E0	4.6438557111309333E-4	0.01686863786884206E0	3.342531314242062E0	3.342531314242062E0	19.60969066619873E0	5.866718610127767E0
Sb09g005620	270.76076328754425E0	0.002952015276945819E0	0.03518290100713574E0	3.3987400965213447E0	3.3987400965213447E0	7.149897527486979E0	2.10389058027771E0
Sb09g005690	112.99818992614746E0	0.0015762871624699910	0.02863749505899157E0	3.1932841593722183E0	3.1932841593722183E0	28.683589935302734E0	8.982473373413086E0
Sb09g005710	39.96333956718445E0	3.8620752465076647E-4	0.015807816891789155E0	4.419187651401742E0	4.419187651401742E0	10.862974802652994E0	4.258138368404871E0
Sb09g005720	88.37357234954830E0	0.005417281796022421E0	0.0472895271237654E0	2.20413610412563E0	2.20413610412563E0	20.26416105625E0	9.19369729359944E0
Sb09g005780	65.3981654640125E0	2.43273097929787E-4	0.013321350287666156E0	4.795900328101459E0	4.795900328101459E0	18.03821468332715E0	3.76117380401034E0
Sb09g005900	291.24679374694824E0	0.002119648417086055	0.03064542071836563E0	2.212333411318522E0	2.212333411318522E0	66.8603	

Sb09g022920	90.42099237442017E	0.005675642504911914E	0.0482395254854772E	2.302882819422362E	2.302882819422362E	21.01486905415853E	9.125461737314861E
Sb09g023130	101.45724534988403E	0.0010853013437031116E	0.0232518083980771E	2.8579473851052644E	2.8579473851052644E	25.05300132242844E	8.766081651051838E
Sb09g023590	330.1286053080300E	6.433875053830800E-4	0.0192875588385955E	3.292543980637563E	3.292543980637563E	15.59003702799478E	41.18001646830241E
Sb09g023793	103.1889250300518E	0.003099945651699021E	0.03604562601535867E	2.4153189259166683E	2.4153189259166683E	24.35139363660773E	10.071191469828289E
Sb09g024270	2369.049774169922E	0.004844341843982641E	0.04467106940066336E	0.445666034643202E	0.445666034643202E	24.344132791829427E	546.2416788736979E
Sb09g024340	69.4037446975708E	0.0035155433406045215E	0.03861423085106734E	2.8860216351384507E	2.8860216351384507E	17.181299845377605E	5.95328172047933E
Sb09g024390	39.94391471170002E	0.001759352586549838E	0.02663749505899547E	5.0120372318950945E	5.0120372318950945E	11.099974950154623E	2.214663306872049E
Sb09g024400	78.4656388759613E	1.8914277449753357E-4	0.01226534850153476E	3.878437893643236E	3.878437893643236E	20.793821791062174E	5.361390898039241E
Sb09g024600	200.1542568206787E	0.0017386053214858907E	0.02845043087893595E	2.7443208613476107E	2.7443208613476107E	48.899611155192055E	17.818744517000844E
Sb09g025050	172.49628257751465E	9.5108333509448776E-4	0.02228029648934663E	4.846801614543876E	4.846801614543876E	47.66453615824381E	9.83422700927734E
Sb09g025150	12.385270208120346E	0.0033916301899948403E	0.03783849111736447E	5.623129948702624E	5.623129948702624E	3.5050892035166417E	0.6233341991901398E
Sb09g025360	44.3416576385498E	0.00263246623831435E	0.033253647510190616E	2.751213182429664E	2.751213182429664E	34.798719406217939E	12.63489690672008E
Sb09g025410	20.81427949666977E	0.0055776553944267525E	0.04804381891884165E	4.50034199381108E	4.50034199381108E	5.676070115203857E	1.261393053527326E
Sb09g025786	38.64590907096863E	3.2332762667888106E-4	0.014916355761841811E	0.1310409659080275E	0.1310409659080275E	1.4925490020237883E	11.389420668284098E
Sb09g025830	110.4136266780374E	0.0018980800223624033E	0.02941818612691495383E	2.7132782618058076E	2.7132782618058076E	26.892386138916E	9.911603809720867E
Sb09g025850	24.6189706325531E	0.0023582714587558595E	0.031902625291720645E	3.665767411920743E	3.665767411920743E	6.447788184958686E	1.758836825686797E
Sb09g025920	200.31174850463867E	3.45135678307421E-4	0.007706232567728601E	5.656254525742153E	5.656254525742153E	5.673932843439941E	10.03125445048014E
Sb09g026080	271.2357943673828E	6.684184925586373E-4	0.019428283869416807E	2.804582396836973E	2.804582396836973E	66.6479746506031E	23.76395670572915E
Sb09g026090	25.316877541423917E	3.514641873209695E-4	0.015322195818865346E	8.188159292696424E	8.188159292696424E	1.801509811539712E	0.918460259834924E
Sb09g026148	276.1647071838379E	1.78901397281808E-4	0.01226534850153476E	4.4904541303322E	4.4904541303322E	75.28854751568914E	16.766354878743492E
Sb09g026230	43.69230604171753E	0.003767293838862426E	0.0398479859046585E	2.7856534909400494E	2.7856534909400494E	10.71691894531252E	3.847183068593324E
Sb09g026450	420.8941993713379E	0.0038305106992016755E	0.040118929275644926E	2.179224536982009E	2.179224536982009E	96.16841634114581E	44.1296501159668E
Sb09g026780	313.0605792992676E	0.0014634343917769687E	0.02630501387734954E	2.405953239675894E	2.405953239675894E	73.71495946248372E	30.638566970825195E
Sb09g026810	609.4755249023438E	1.72526327141247E-4	0.01212822798451459E	3.22823166729428E	3.22823166729428E	15.0602569580078E	48.0982513427344E
Sb09g027180	29.233445191526817E	0.0030812254001906948E	0.03588485001526081E	3.31679662995486E	3.31679662995486E	7.494895776112874E	2.249584754300765E
Sb09g027280	229.6957340240478E	0.00597653534055666E	0.049509965338814764E	2.2650218619818685E	2.2650218619818685E	53.11509704589844E	23.45014762878418E
Sb09g027440	107.673130989074E	0.0026368921384415257E	0.033256347510190616E	2.566457894706417E	2.566457894706417E	25.827545166015625E	10.063498497009277E
Sb09g027450	167.700956346045E	0.0029368310323025677E	0.0351200427809631E	2.25451822609218E	2.25451822609218E	38.7240994713216E	17.176219304402665E
Sb09g027620	40.86330938339233E	0.0027228635257944183E	0.0337685679474776E	5.202418158023865E	5.202418158023865E	19.29783566792806E	7.65660079320219E
Sb09g027686	44.436875343322754E	0.0015121716288353853E	0.0266244215854711E	3.063499437420609E	3.063499437420609E	11.67085965444445E	6.45205815633137E
Sb09g027720	21.933185577932578E	3.5291687881966065E-4	0.015322195818865346E	7.187832378191745E	7.187832378191745E	6.41814398765564E	0.892917871475219E
Sb09g027750	154.3290205001831E	7.26548403343695E-4	0.01996610907015655E	3.122791965705246E	3.122791965705246E	38.9652957162598E	13.227911041768394E
Sb09g027840	27.04354650770569E	0.0035515181105423834E	0.03629238498006035E	3.64864120637869E	3.64864120637869E	7.07534297303322E	1.939172093452933E
Sb09g027990	17.313626557588577E	4.4658082590298226E-4	0.01670586387998329E	6.6188831968893E	6.6188831968893E	5.229915539423625E	0.541129233105900E
Sb09g028100	151.8850055236816E	0.004449919004717944E	0.042878862801884141E	2.263755367138778E	2.263755367138778E	34.95438321431477E	15.44088363647461E
Sb09g028250	138.9883875848682E	0.0010093128935454705E	0.022602682767328762E	2.98455650624638E	2.98455650624638E	34.70220657958984E	11.62278067206975E
Sb09g028540	48.51998770236969E	2.7019750031328088E-6	0.007323983547975973E	8.56205778157479E	8.56205778157479E	14.481922467549643E	1.6914067665735875E
Sb09g028580	92.2531054019928E	1.082409900471387E-4	0.011303471493004145E	5.427096963185082E	5.427096963185082E	25.96443379725456E	4.78459175427546E
Sb09g028850	39.61876833438873E	5.6745830882110516E-4	0.008671392701857825E	5.91805530319357E	5.91805530319357E	11.202802777893066E	2.003453533569845E
Sb09g029070	23.875334114363861E	0.004652520332709105E	0.04371761335662164E	4.051389735596845E	4.051389735596845E	6.38294406708667E	1.574960770757436E
Sb09g029210	198.57883071893941E	0.00154822689400284E	0.02699390680725127E	3.0136103268398267E	3.0136103268398267E	49.47086246598308E	16.492120130701597E
Sb09g029240	597.9963760375977E	1.246201424705913E-4	0.01153739840781929E	3.192111806932807E	3.192111806932807E	15.178279117376953E	47.54933420817058E
Sb09g029400	627.7432098388672E	0.004946186705617718E	0.045012752860556E	3.1267781340773744E	3.1267781340773744E	158.5428695678711E	50.70486704508446E
Sb09g029740	66.64048099517822E	0.005930530007436968E	0.04936294285539239E	2.64357562886713E	2.64357562886713E	16.116877555847168E	6.09661610921242E
Sb09g029750	37.7724399566654E	0.0020497863329629203E	0.0325293066017046E	2.529683244499427E	2.529683244499427E	16.0961643854777E	6.362916946411133E
Sb09g029900	1233.1474914550781E	0.0020127847255066003E	0.030075925656064654E	0.43126327958462823E	-3.187691172950187E	123.8559601668198E	287.19325764973956E
Sb09g029970	28.5530363254547E	0.001909443936220146E	0.02949179400686875E	3.4664358252519354E	3.4664358252519354E	7.386685933736168E	2.130686104456587E
Sb09g030030	162.5229072570800E	0.0037648661619369777E	0.0398479859046585E	2.309323154928509E	2.309323154928509E	37.0409622192383E	17.630206197102867E
Sb09g030440	595.5106773376465E	0.00138257937166848E	0.02562521350044275E	2.339726725230529E	2.339726725230529E	13.06649271647137E	59.37066396074729E
Sb09g030620	118.59423351287844E	0.0012133790734135418E	0.024405372006443773E	2.6791713157396524E	2.6791713157396524E	28.78670630320195E	10.744650840759277E
Sb09g030650	54.78804850578308E	0.005807879938323273E	0.04638123130027236E	3.6402852135649755E	3.6402852135649755E	14.32700173060099E	3.936581140660304E
Sb09g030700	125.48888966705322E	4.458070364246976E-4	0.01670586387998329E	3.9583929386641783E	3.9583929386641783E	33.393491028239E	8.436125119962183E
Sb09g030730	294.22989462380165E	0.003338511534505874E	0.025470455282968663E	2.46918522392296E	2.46918522392296E	69.805344523112E	18.7970793709312E
Sb10g000210	180.23386571701416E	0.002623551518753842E	0.033256347510190616E	2.357218731596485E	2.357218731596485E	42.1838517784831E	27.89056784283082E
Sb10g000350	234.3378486633008E	4.962037446820539E-4	0.017184449852419653E	3.218239871872624E	3.218239871872624E	59.59473995548052E	18.51782266525E
Sb10g000410	242.57911109924316E	0.002169155896445537E	0.03091930879588437E	2.3675049297437685E	2.3675049297437685E	52.2968317667624E	22.3002052307129E
Sb10g000430	72.85423183441162E	5.254815909410514E-4	0.0176270268891137E	3.594327136674095E	3.594327136674095E	18.9983315633138E	5.258510788472494E
Sb10g000570	181.63415050609292E	3.3999990102494703E-4	0.015183120992077999E	3.7211898038555624E	3.7211898038555624E	47.22087892550658E	12.824307869771324E
Sb10g000930	341.33219146728156E	0.0033961084411265126E	0.03783849111736447E	0.3057962637126295E	-3.2701511386401774E	26.644817352924922E	87.1325093404668E
Sb10g000980	334.3455104827881E	0.004024231975610134E	0.04107591066533487E	3.131371359373463E	3.131371359373463E	84.47235107421875E	16.976152420030494E
Sb10g001106	125.84919881286079E	0.00394597565222756E	0.03783849111736447E	6.25029595608701E	6.25029595608701E	30.377487182671788E	21.57225756785037E
Sb10g001280	52.734829187193919E	0.0038874555255115605E	0.0404228842247165E	2.6451114318448481E	2.6451114318448481E	12.75585524241297E	4.822211533864344E
Sb10g001320	40.34251117706299E	0.003963967168934856E	0.0408177601817445E	3.0510514280701693E	3.0510514280701693E	10.127994419462076E	3.31958024262558E
Sb10g001730	75.714109268188477E	0.005906340124126446E	0.04932756930374244E	2.30536592782583E	2.30536592782583E	18.444575373331703E	7.20245506209883E
Sb10g001830	231.17983657989502E	0.0020451473596395137E	0.03025293066017046E	2.5089761711826142E	2.5089761711826142E	83.8907411739095E	23.34255409240722E
Sb10g002010	421.2104148864746E	0.005115448128258809E	0.04572842007857276E	0.394120765302653E	-2.537293357492125E	39.69234593709304E	100.711126917

Sb10g011070	58.23505353927612EC	0.0017631470269393588	0.028642052321263104EC	2.9898996155767525EC	2.9898996155767525EC	14.546478271484375EC	4.865206241607666EC
Sb10g011810	94.83451890945433EC	0.0051301497363555795	0.04572842007857276EC	2.242213669931746EC	2.242213669931746EC	21.8615531927138672EC	7.949953111012776EC
Sb10g012170	23.344643473625183EC	0.00443723638403859E-4	0.0428190889950546EC	4.550214061702487EC	4.550214061702487EC	6.379521210988362EC	1.400266135533648EC
Sb10g012180	208.63453674316406EC	0.0019757727616946837	0.029878105885394805EC	2.924028988813865EC	2.924028988813865EC	51.822029131736953EC	17.722816467285156EC
Sb10g012265	72.87599471385193EC	8.751989287682021E-4	0.0217050559665671EC	0.1888492314266613EC	-5.300843223359669EC	3.855354229690169EC	20.436628341674805EC
Sb10g013060	32.25921189785004EC	0.00566333655596597E-4	0.048232783184335715EC	2.9725453850771597EC	2.9725453850771597EC	8.046224117279053EC	2.7068465153376264EC
Sb10g013070	29.541205644607544EC	0.0055625203210912895	0.04799368671276321EC	4.252953050083929EC	4.252953050083929EC	7.972490866978964EC	1.8745776812235517EC
Sb10g014850	71.61050176620483EC	0.002668323644995183E-4	0.033418340574742474EC	2.5667430225037526EC	2.5667430225037526EC	17.158924102783203EC	6.711243152618408EC
Sb10g017780	982.4999351501465EC	1.0266752797715936E-4	0.01128553057535344EC	0.1938502853081066EC	-15.165816022460193EC	53.115431467692076EC	274.38454691569007EC
Sb10g019670	63.958125591278076EC	0.0028672943971498766	0.03475282718635905EC	2.5376318908139375EC	2.5376318908139375EC	15.292921384175617EC	6.026453812917074EC
Sb10g020410	29.22622662782669EC	5.16287607341152E-4	0.0174767112037733EC	6.285193667164925EC	6.285193667164925EC	8.404832363128662EC	1.337243179480235EC
Sb10g021760	17.666488587856293EC	0.001858207820592194E-4	0.02927650469268187EC	5.070570774308105EC	5.070570774308105EC	9.9700619180997214EC	0.9700619180997214EC
Sb10g021970	50.725186824798584EC	0.0036900644463935114	0.039558155243033216EC	2.689166289843403EC	2.689166289843403EC	12.325139045715332EC	4.58325662550863EC
Sb10g022120	63.224622726440428EC	3.851670669767391E-4	0.015807816891789155EC	3.6186862629512827EC	3.6186862629512827EC	16.69966294820105EC	4.375206947328766EC
Sb10g022130	109.9237976074218EC	0.005087261873689907E-4	0.04569262864552406EC	2.4368523407793052EC	2.4368523407793052EC	25.979979832967125EC	10.661286036173504EC
Sb10g022160	581.8798789978027EC	0.00502624197711118E-4	0.04539329477049379EC	4.547065499172847EC	4.547065499172847EC	158.9937311808288EC	34.96622848510742EC
Sb10g022260	102.4929676059092EC	9.566129677816067E-4	0.02230586526129933EC	2.7787405382640507EC	2.7787405382640507EC	25.123129526774088EC	9.041193008422852EC
Sb10g022340	82.22508645057678EC	0.0032356859059835884	0.03696079264308991EC	2.427611773416444718EC	-0.038482959931629EC	5.439804474512737EC	21.968557675679524EC
Sb10g022500	849.1766354718785EC	0.005568476736862239E-4	0.04799368671276321EC	2.216119211466638EC	2.216119211466638EC	195.0463205973307EC	88.01255798339844EC
Sb10g022690	20.980221211628148EC	0.00306425606918878EC	0.035884850015260816EC	3.874054996178048EC	3.874054996178048EC	5.539454996891201EC	1.4298854668935146EC
Sb10g023020	36.22456216812134EC	0.001590607298980319E-4	0.02713325898668796EC	3.578179257658069EC	3.578179257658069EC	9.40180303662598EC	2.672349405668114EC
Sb10g023040	999.566355949707EC	2.627749679714645E-4	0.01394885724096646EC	7.329592927381742EC	7.329592927381742EC	284.3887685139974EC	38.800076802571624EC
Sb10g023190	98.06754207611084EC	0.002800618234141114E-4	0.03432318573407289EC	2.343219523848584EC	2.343219523848584EC	22.91142598046057EC	9.777754783630371EC
Sb10g023210	45.64410758018494EC	0.0017399898582679075	0.02845034307893599EC	3.4972850126529633EC	3.4972850126529633EC	11.831616401672363EC	3.38308612505955EC
Sb10g023260	154.33780460357666EC	1.7101277118958995E-4	0.01212822798451459EC	2.850562196576965EC	2.850562196576965EC	39.49114863077999EC	12.021452903747559EC
Sb10g023705	245.04336643218994EC	0.0022942844376821147	0.031646066230190555EC	2.650494182879213EC	2.650494182879213EC	59.30576197306315EC	22.37536017100016EC
Sb10g023770	155.7785587005615EC	0.0047714901897858856	0.04433454132575016EC	2.347458234096369EC	2.347458234096369EC	36.41406186421712EC	15.51212342580159EC
Sb10g023970	91.290039620147705EC	0.002880579328740595E-4	0.0348547659675248EC	3.893016148845319EC	3.893016148845319EC	24.210941632588703EC	6.2190704345703125EC
Sb10g024080	1163.7559127807617EC	5.63373809406728E-4	0.018251783239475343EC	2.3549205288083514EC	-2.8175321482741733EC	101.61502838134766EC	286.30360921223956EC
Sb10g024440	34.040385484695435EC	0.003964966556192643E-4	0.04081776001817445EC	0.938203196020127EC	0.938203196020127EC	8.46558396021525EC	2.8812112013498945EC
Sb10g024620	140.9653434753418EC	0.030050918674112E-4	0.021890356770110864EC	2.6961335870102072EC	2.6961335870102072EC	107.22028350830078EC	39.768164316813156EC
Sb10g024706	14.800621211528778EC	0.003077449975939324	0.035884850015260816EC	4.272168793840617EC	4.272168793840617EC	3.997769832611084EC	3.997769832611084EC
Sb10g025230	38.10433030128479EC	0.0034886014200301656	0.03848310936779308EC	3.1073465130530415EC	3.1073465130530415EC	9.609071413675945EC	3.0923270208085633EC
Sb10g025240	37.9831911956787EC	0.0029396198711710789E-4	0.0351200427809631EC	3.16193862590076EC	3.16193862590076EC	9.618958473206566EC	3.0421078999837246EC
Sb10g025280	1309.7095489501953EC	0.004642079316114164E-4	0.04367978455479936EC	2.2383533314398663EC	2.2383533314398663EC	31.001755310058594EC	134.8122964947919EC
Sb10g025320	45.48090910911566EC	0.005367326606162047E-4	0.04705225834077474EC	2.692581519810256EC	2.692581519810256EC	105.6592109425881EC	4.1056109296460039EC
Sb10g025350	70.67889618873596EC	1.054422036356623E-4	0.011303471493304145EC	8.447702678598096EC	8.447702678598096EC	21.065943082173664EC	2.493688907383196EC
Sb10g025375	68.63008272647858EC	2.0997431114211394E-4	0.012467408873140653EC	5.294167998681149EC	5.294167998681149EC	19.242108345031735EC	3.634585897127785EC
Sb10g025510	201.9632396697998EC	6.702689956348836E-4	0.019428283869416807EC	0.282582254001949174EC	-3.538792162461022EC	14.832377157166829EC	52.48870213262497EC
Sb10g025920	95.30023023605347EC	0.003268416992451611E-4	0.03712374323667934EC	5.513415786477543EC	5.513415786477543EC	26.89803051045738EC	4.878660360972088EC
Sb10g026110	200.68572711944548EC	0.00511294592580058E-4	0.04572842007857276EC	2.1982282540017812EC	2.1982282540017812EC	45.97889836529233EC	20.9163440406856285EC
Sb10g026190	92.40578269958496EC	0.005258254541189601E-4	0.04649780779306894EC	2.2436807728500856EC	2.2436807728500856EC	21.305947621663414EC	9.49597994484691EC
Sb10g026230	61.2465434074401783EC	5.660118411204651E-4	0.018251783239475343EC	3.6340746952166025EC	3.6340746952166025EC	16.009993235270183EC	4.405521233876547EC
Sb10g026250	114.00875186920166EC	0.0021192504166580696	0.030645420718365637EC	2.918717874391923EC	2.918717874391923EC	28.305123647050404EC	9.697793642679851EC
Sb10g026340	61.174920320510864EC	1.8228585932080971E-4	0.012265348501354766EC	6.140925073338263EC	6.140925073338263EC	17.536038080851235EC	2.8556020259857178EC
Sb10g026440	406.2809467315674EC	4.763539743546161E-4	0.01694804189448622EC	3.439889171305425EC	3.439889171305425EC	10.42464828491121EC	30.50233395894368EC
Sb10g026530	42.19368553161621EC	0.0025013194862474213	0.03267262838983149EC	0.356974770497155EC	-2.801318368386378EC	3.699916839596094EC	10.36464500242761EC
Sb10g026680	20.267680860840996EC	0.005241907477929121E-4	0.0463819553102612EC	3.3430210100470665EC	-3.3430210100470665EC	5.200315634409587EC	1.555573712767356EC
Sb10g026970	39.195441961288455EC	0.003697935538670347E-4	0.039612817726836023EC	0.3095949817626677EC	-3.2300265149859233EC	3.088676949047314EC	9.976479371388752EC
Sb10g027000	28.916297674179077EC	0.00354256715347371EC	0.03862923848800035EC	0.18247206759194845EC	-5.480290836821344EC	1.0873971124358311EC	8.151368776957193EC
Sb10g027040	35.726141810417159EC	0.004052228370139332E-4	0.04124383433710189EC	2.631465521196197EC	2.631465521196197EC	9.115304470062256EC	2.7934094667434692EC
Sb10g027180	44.40732121467575EC	0.0029321322321562726	0.0351200427809631EC	2.6929209622129395EC	2.6929209622129395EC	10.794111887613933EC	4.008328517278036EC
Sb10g027240	49.94518518447876EC	0.002056395527361748E-4	0.0302947341092771EC	2.7490122582876086EC	2.7490122582876086EC	12.207653363545736EC	4.440741697947184EC
Sb10g027790	33.27074368047473EC	0.00357280687136449EC-4	0.03876644661488122EC	3.0355458286939188EC	3.0355458286939188EC	8.342107137044271EC	2.7481407324473066EC
Sb10g027960	160.1472635269165EC	0.004855702948076366	0.044671069409666336EC	2.1562801980627344EC	2.1562801980627344EC	36.46934064229329EC	16.91308053345536EC
Sb10g028570	125.29296684265137EC	7.06299165902314E-4	0.019730524429832825EC	3.98926977652963EC	3.98926977652963EC	33.39349365234375EC	8.370828628540039EC
Sb10g028700	37.574859619140625EC	6.088917371164128E-4	0.00526487845394354EC	20.477592629387864EC	20.477592629387864EC	11.941789468129475EC	0.5831637382507324EC
Sb10g028950	359.72362899780273EC	5.755156813601406E-4	0.0183574086755277EC	2.6579521503408645EC	2.6579521503408645EC	87.12782033284505EC	32.78005599975586EC
Sb10g029260	25.499386429786682EC	0.004400709534058537E-4	0.042750604515063156EC	5.379289847106239EC	5.379289847106239EC	7.1673980823664258EC	1.3324046532313032EC
Sb10g029860	2319.9412994384766EC	3.799539671081725E-4	0.015746746627701945EC	3.593203301252641EC	3.593203301252641EC	604.9533182779949EC	186.36044820149743EC
Sb10g029870	5557.640716552734EC	0.004526129963418625E-4	0.04313772871167097EC	2.948308301058014EC	2.948308301058014EC	1383.3467407225652EC	469.200164794219EC
Sb10g029940	48.2446928024292EC	0.0051260284804599135	0.04572842007857276EC	0.4160936673566914EC	-2.4033050418781308EC	4.725278536487678EC	11.35628573099772EC
Sb10g030020	66.63466739654541EC	7.387784780196287E-4	0.00526487845394354EC	10.67690045921127EC	10.67690045921127EC	20.30937671661377EC	1.902179082234703EC
Sb10g030160	826.89628219604494EC	4.8766161306443414E-4	0.017098183684634886EC	3.2648598510475852EC	3.2648598510475852EC	21.00345357259113EC	6.64286409275717EC
Sb10g030240	4450.031341552734EC	9.721997183547858E-4	0.02230596526129933EC	3.68951050948111047EC	3.68951050948111047EC	1167.0327758789062EC	316.3110046386719EC
Sb10g030520	50.09746432						